UNIVERSITY OF SOUTHAMPTON

FACULTY OF ENGINEERING, SCIENCE & MATHEMATICS
SCHOOL OF ENGINEERING SCIENCES
SURFACE ENGINEERING AND TRIBOLOGY RESEARCH GROUP

THE DEVELOPMENT OF A MARINE ANTIFOULING SYSTEM USING ENVIRONMENTALLY ACCEPTABLE AND NATURALLY OCCURRING PRODUCTS

By
Lily D. Chambers

THESIS SUBMITTED FOR THE DEGREE OF
DOCTOR OF PHILOSOPHY

Oct 2008

UNIVERSITY OF SOUTHAMPTON

ABSTRACT

FACULTY OF ENGINEERING, SCIENCE & MATHEMATICS, SCHOOL OF ENGINEERING SCIENCES

Doctor of Philosophy

THE DEVELOPMENT OF A MARINE ANTIFOULING SYSTEM USING ENVIRONMENTALLY ACCEPTABLE AND NATURALLY OCCURRING PRODUCTS

By Lily D. Chambers

Due to legislative pressures and the recent ban of trybutyl tin, alternative environmentally acceptable ship hull antifouling systems are required. This thesis uses a multidisciplinary approach to combine two disparate areas of research namely marine biology and surface engineering, to develop a novel natural product (NP) based antifouling system. The overall objective of this thesis is to transfer a natural marine biological defence mechanism into an engineered antifouling coating system. By combining natural product extraction and incorporation into a trial coating an extensive test programme was able to investigate the antifouling performance and address the issues of bringing this active area of research to the next technological readiness level. By using a stepwise approach to the development of the engineered solution, a suite of techniques were used to fully characterise a NP based system. The biological and surface engineering techniques adapted and developed are described here and their future use to evaluate a novel NP based antifoulant system is critically assessed.

After an extensive literature review, an ethanol extract from the red seaweed *Chondrus crispus* was selected as the natural product source. NP specimens were harvested locally and also purchased as industrially processed dried algae. The industrially processed algae showed good antifoulant activity (≤ 25 $\mu g\ mL^{-1}$) in laboratory bioassays and had a greater efficacy than the locally harvested samples highlighting its potential as an economically viable solution. The direct incorporation of the NP into a commercial control depletion polymer binder, allowed for the rapid development of characterisation techniques to evaluate the effects this had on the performance of the NP-binder matrix. The feasibility of a range of electrochemical techniques to measure corrosion potential, impedance, resistance and water uptake in the NP coating was critically assessed. A combination of open-circuit potential and electrochemical impedance spectroscopy provided a unique and rapid means to non-destructively measure the contribution of incorporated NPs to the degradation and water uptake of the binder film. Studies of biofilm growth were used to successfully measure community viability and structure using fluorescent staining and differential interference contrast microscopy. These techniques were found to be very informative on Southampton water marine biofilm community structure and were cross correlated by fourier transform infrared measurements. Resistance to biofouling was determined through field trials, an important testing platform for an antifouling system, and specifically trials which test the entire coated system including any primers and substrate preparation requirements. An initial NP antifouling performance greater than the booster biocide (Chlorothalonil) control was documented for one field trial over a period of the first 6 weeks.

A key aspect was to determine the potential efficacy of NPs and their viability in a coating system. To achieve this, a range of standard and non-standard techniques were used to assess this novel combination of crude NP extract and commercial binder system. This work has shown that a limited antifoulant activity is achievable. By evaluating the effect of a NP on both the fouling community and a binder system this unique approach helps define key techniques to assess future NP antifoulants and identifies the optimisation required to increase their functionality.

List of Figures

List of Tables

Nomenclature

Symbol		Description	Unit
°C	=	Degrees centigrade	
R_a	=	Average surface roughness	μm
R_t	=	Total surface roughness (trough to peak)	μm
R_p	=	Pore resistance	Ω
R_t	=	Charge transfer resistance at coating/metal interface	Ω
Z_f	=	Electrochemical processes at the coating metal interface	
R_s	=	Electrolyte resistance	Ω
I	=	Current	A
Z	=	Impedance	Ω. cm^2
E	=	Potential	V
C	=	Capacitance	farad
C_t	=	Capacitance at time 't'	farad
C_0	=	Capacitance at time '0'	farad
C_{dl}	=	Double layer capacitance	farad
C_c	=	Coating capacitor	farad
Chl a	=	Chlorophyll a	mg L^{-1}
D	=	Optical density	nm
V	=	volume	L
v	=	volume	L
R	=	Resistance	Ω
A	=	Area	cm
ρe	=	Resistivity	Ω. m
E_m	=	Mixed potential	
b_A	=	Anodic Tafel slope	
E^A_{corr}	=	Corrosion at the anode	
$\frac{Sc}{Sa}$	=	Cathode to anode surface ratio	
Xv	=	Volume fraction	

Abbreviations

Abbreviation		Definition
AC	=	Alternating current
AF	=	Antifouling
CDP	=	Control depletion polymer
CE	=	Counter electrode
CFU	=	Colony forming unit
CNC	=	Computer numerically controlled
CPE	=	Constant phase element
DC	=	Direct current
Dft	=	Dry film thickness
EDIC	=	Episcopic differential interference contrast
EDX	=	Energy dispersive x-rays
EI	=	Electron ionisation
EIS	=	Electrochemical impedance spectroscopy
EPS	=	Extracellular polymeric substances
FR	=	Foul release
FTIR	=	Fourier transform infra-red
GC-MS	=	Gas chromatography – mass spectrometry
LPR	=	Linear polarisation resistance
MIC	=	Microbially induced corrosion
MIC	=	Minimum inhibitory concentration
NP	=	Natural product
OCP	=	Open-circuit potential
ppm	=	parts per million
PVC	=	Pigment volume concentration
SEM	=	Scanning electron microscope
SPC	=	Self polishing copolymer
RE	=	Reference electrode
rpm	=	rotations per minute
TBT	=	Tri-butyl-tin
ZRA	=	Zero resistance ammeter
WE	=	Working electrode

ACKNOWLEDGEMENTS

Thank you to my supervisors Robert Wood and Frank Walsh for their enthusiasm for the research, patience in teaching a marine biologist how to be an engineer, wise words and support. Thank you to my industrial sponsors Keith Stokes and Richard Jones from Dstl for their guidance and financial support for the project.

Thank you to Colin Anderson, Matthew Goodall and Gina Jones of International Paint for the kind provision of the blank topcoat paint. Thank you to Jageth from the MOD for the kind provision of sprayed Envoy TF antifouling system panels. Thank you to the Environmental Health Care Unit and specifically the help from Bill Keevil and Sandra Wilks for their willingness to train me to use their facilities. Thank you to the School of Biological Sciences of Portsmouth and Claire Hellio for her enthusiasm and willingness to share laboratory facilities and expertise. Also thank you to Bob Fletcher for assisting with the macroalgae bioassays and Marie for clambering rocky shores with me in search of spores as well as teaching me microbiolgical techniques. Thank you to those at NOC who supported me with discussions and advice along the way including Debora, Stephen, Duncan, Jenny, and especially Bill Conways very own Bob who always made me smile and was the first to spot that something 'fishy' was happening to my samples and Kevin who caught and sent great photos of the culprit. Thanks to the School of Engineering technicians and secretaries who helped make the research possible.

Thank you Terry and Julian for your help in the Lab and Field, without your guidance I would have truly been lost in jargon, equipment and biofouling. To all from Rm 4061 (Ram, Rakesh, James, Stephane and Shiva) I appreciate everything you guys have helped me with, laughed with me and generally made a second home. Especially James who taught me to never let anyone get me down...(including him), thank you for all the impromptu engineering lessons, coffee, laughter and commiserations. Thanks to Mandar and Mark for keeping the lab cheery and full of chats. To the rest of the Tribology crew Ling, Dan, Jenny, Nick and Fitri and the Materials and Bioengineering groups a big thank you for sharing this time with me. To the Electrochemical Engineering Group, thanks no 1 for the space, no 2 all the smarts and 3 the friends most of all John, Carlos, Richard W., Matt and Dmitiri.

Thank you to my lovely ladies for being great, Catherine for always seeing it like it is, Elena for always saying it like it is, Suk for always giving me a cup of coffee, Lucy for always giving me a cup of tea (properly poured) and Polly for always giving me a hug and suggesting dancing.

Thank you Adrian for the laughter, the roast dinners and being a good friend. Thank you Aoife and Christine for being brilliant, to 'little geek' for helping me get to be a real 'big geek' and the 'modest one' for making sure I don't get 'notions'. You all made a difficult task fun.

Thank you to both my parents for their love and support. Dad for encouraging me to use all '3 brains' my intellect, heart and gut. Mom for nurturing creativity, confidence and the pursuit of perfection. To my wonderful siblings, Eve, Mae, Joe and Will, all I have to say is.... now who doesn't 'know nature'! Thanks to my grandparents for their inspiration. This thesis is dedicated in loving memory to my Grandpa Bill Martin without whom I would never have first sampled the joys of welding, sheet metal working and my first pair of coveralls.

It would take another thesis to express my gratitude fully but most of all thank you Ian for all the energy, support and encouragement.

Chapter 1 Introduction

1.1 Research motivation

This thesis investigates the techniques and procedures involved in the development of an antifouling paint system using environmentally acceptable and naturally occurring products for application to large ship hulls and marine platforms. Fouling in the marine environment can be either inorganic, such as mineral deposits, or organic termed 'biofouling', which is the unwanted growth of organisms on a surface.

Marine biofouling has for centuries afflicted the shipping industry and navies due to its prolific growth on submerged hulls and propellers. This project is sponsored by the defence science and technology laboratory and seeks a solution to the fouling of naval ships hulls. The accumulation of foulers such as algae and barnacles increase the drag on moving vessels, thereby increasing the fuel consumption, emissions and reducing the vessels manoeuvrability. Recently, the use of ship hulls as a key vector for the transportation of alien species between ports has highlighted the environmental requirement for maintaining a clean hull during service. Engineered structures such as ships and marine platforms, as well as offshore rigs and jetties also need to resist the harsh salt-water environment, which is highly corrosive to unprotected surfaces. Biological growth can often increase the corrosion at an unprotected metallic hull through by-products as well as the generation of localised aeration cells. Therefore, protective paint systems are applied to reduce corrosion and resist biofouling.

As mentioned above, marine platforms are typically protected by a variety of coatings and/or cathodic protection to minimise or eliminate corrosion. Methods of protecting marine structures must be capable of expanding and contracting with the underlying surface, resist the ingress of water and control the diffusion of ions to and from the substrate. Protective organic coatings can offer these functions [1.1] and consequently are largely used in the shipping and offshore industries to increase the working life of systems and improve its reliability. Coatings on ships are used for a wide range of functions such as corrosion resistance, ease of maintenance, appearance, non-slip surfaces on decking as well as the prevention of biofouling on the hull.

Antifouling systems were described by the new International Maritime Organisation convention as 'a coating, paint, surface treatment, surface or device that is used on a ship to control or prevent attachment of unwanted organisms'. At present there are two main types of antifouling coating technology, the foul release (FR) and the self-polishing co-polymer (SPC) coatings. The FR coatings are non-biocidal and control fouling through the

coatings surface energy which weakens the adhesive strength of the organisms and removes them as the ship reaches a critical speed. It does not prevent biofouling when the vessel is dockside and is not applicable to certain operational profiles. The SPC coatings control the biofouling by the leaching of biocides and the constant erosion of the leached layer. This is a very effective delivery system for a variety of operational profiles, however, the environmental fate and risks of many present day biocides are being questioned. The most effective biocide to date, tributyltin (TBT) was found to have a large secondary effect on non-target organisms (e.g. *Nucella lapillus*) and has subsequently been banned worldwide. The return to copper based antifoulants has recently come under scrutiny as have the second generation of biocides designed to be environmentally 'safe'. The key modern antifouling technologies and their challenges are listed in Table 1.1.

Antifouling coatings	*Issues*
(1) Self-polishing copolymer TBT based - toxic by interfering with the metabolic functions of the organism.	**Banned due to widespread deformation of marine littoral species.**
(2) Self-polishing copolymer Copper based - toxic either by metal ion overload or through the uncoupling of electron transport in the marine foulers.	**Resistance to copper exhibited by some algal species. Present research focusing on the toxicity of copper.**
(3) Foul release – slippery coatings with low surface tension reduces the mechanical anchoring of organisms.	**If vessel does not reach critical speed to release biofouling, the translocation of marine species becomes an issue.**
(4) Environmentally acceptable solutions - proposed biomimetic approach to reproduce a natural mechanism to deter marine biofouling.	**Mechanisms and ecological relevance not fully understood. Possibly too specific and too transitory for large scale engineering applications.**

Table 1.1 Key generations of antifouling solutions to date

In a plenary lecture given by Dr. Thomas at the 14th ICMCF in Kobe, Japan [1.2] the feasibility of designing a 'safe' biocide was debated. The definition of 'safe' is complicated as it not only includes laboratory environmental acceptability but must also consider its risk and fate in practical applications. Possible introduction to waterways is through hull scrubbing in uncontrolled shipyards and of course, as seen with TBT, its affect on non-target organisms. It was suggested that no biocide could ever be truly 'safe'

beyond doubt but that each successive generation was getting closer to an environmentally acceptable solution and that those with the least risk to the environment when used in a responsible manner should be selected. Antifouling systems, coatings or products with biochemical repellents are deemed non-agricultural pesticides by the Advisory Committee on Pesticides (ACP) for the United Kingdom. The new European REACH programme (Registration, Evaluation and Authorisation of Chemicals REACH, Regulation (EC) No. 1907/2006) as well as the biocide product directive (98/8/EC) will also need to be satisfied. This makes the approval of new compounds expensive and time consuming. An innovative approach to 'safe' biocides being considered by researchers utilises the design philosophy of biomimetics, where natural mechanisms are used as the inspiration for the development of engineered systems.

Some marine organisms have developed antifouling defence mechanisms. Biofilm and biofouling are an inevitable natural process but the growth of organisms on another organism can be harmful to it just as it is to a man made structure. The evolutionary need to defend against fouling health penalties such as parasites or algae being dragged out of the photic water column due to excessive weight has led to the natural adaptation of antifoulant chemicals. Chemical secondary metabolites used in this manner are termed natural products (NP) and have been researched for the last 20 years as possibilities as environmentally acceptable biocides. Although an active area of research, natural product incorporation into a coating system and subsequent testing of efficacy has rarely been addressed and will be the focus of this thesis. The key areas of research within this complex field of natural product antifoulant development are highlighted in Figure 1.1.

Figure 1.1 shows seven main areas of research activity and the type of scientist working in these areas and their skill sets. As can be seen, an initial system approach requires the bridging of at least five of these areas. Therefore, this project incorporates a significant collaboration with three other schools within the University, an external University and industry to cover the five research areas required to improve this technology (Appendix I). To date, each research area has been generating an in-depth understanding but in isolation, therefore this thesis aims to bridge the disciplines from an engineering perspective for the first time. By harnessing cross-discipline techniques, at a preliminary research stage, the design philosophy was to further the understanding of the functionality of NPs in an antifoulant coating. This thesis has used a broad range of multidisciplinary techniques to target the gap in NP coating development. A list of publications, poster and oral

contributions on this research are tabulated in Appendix II. The range of techniques, which includes non-destructive and *in-situ* data collection, were chosen to maximise key attributes of a NP-based coating system. With the September 2008 worldwide ban on TBT in place [1.3] there is a need to develop 'safe' antifouling solutions to meet with environmental legislative requirements and prevent a repeat of the ecological damage inflicted by this once regulated TBT antifoulant. Natural products have the potential for being a broad spectrum, biodegradable and thereby possible biocompatible solution to meet this challenge.

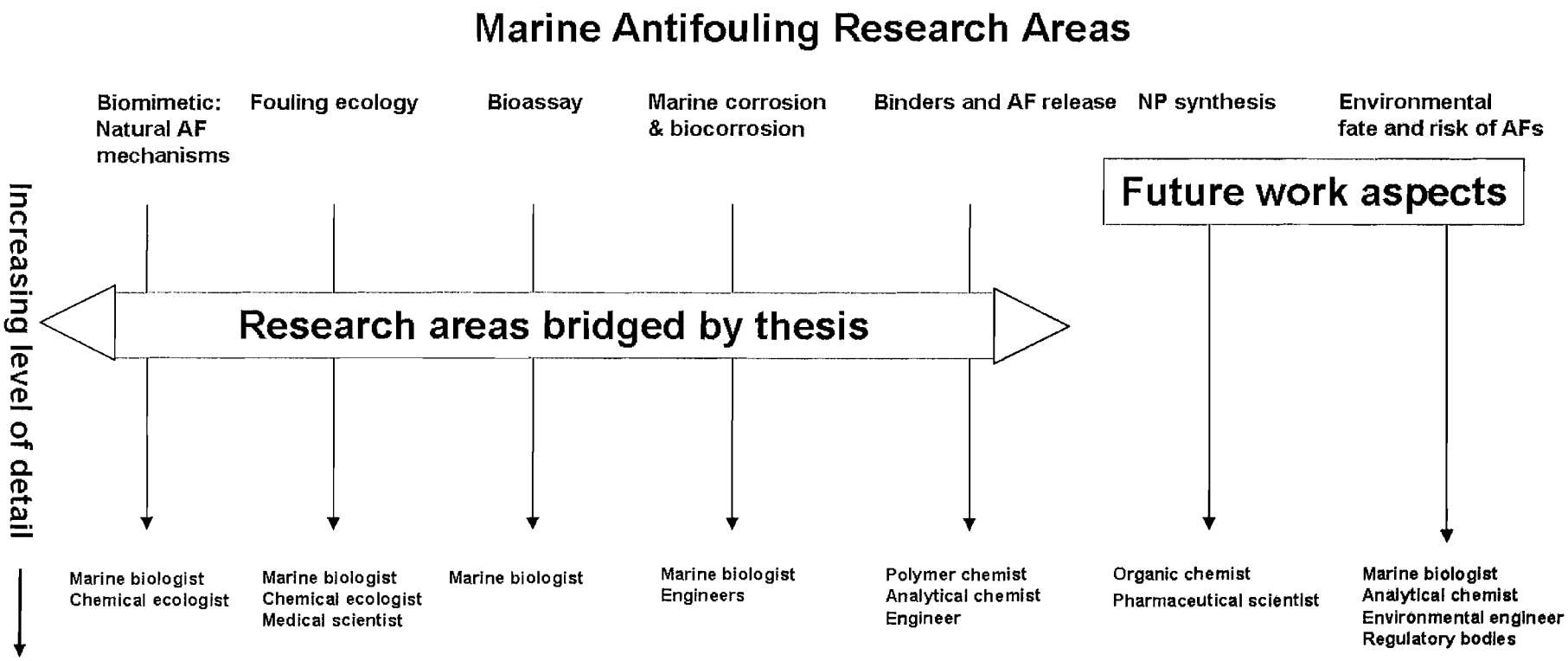

Figure 1.1 Thesis in context of world-wide research areas

The design, build and testing of an antifouling coating system is a complex process, as is the marine fouling environment. Marine fouling is a highly reactive, dynamic community which can not be simplified to a single laboratory test. Figure 1.2 highlights the complexity along with the key interfaces and interactive processes that control the functionality of an antifouling system. The interfaces between the coating/environment and the coating/substrate are of equal importance and this duality of required function is addressed in the present work. Figure 1.3 clearly illustrates how these parameters interact with the different layers in an antifouling coating system, i.e. the substrate, a primer and a topcoat. In this thesis a better understanding of a NP antifouling system has been achieved by using electrochemical techniques to probe the substrate and coating integrity while bioassays, biofilm growth and field trials are used to assess the coating and environment interface.

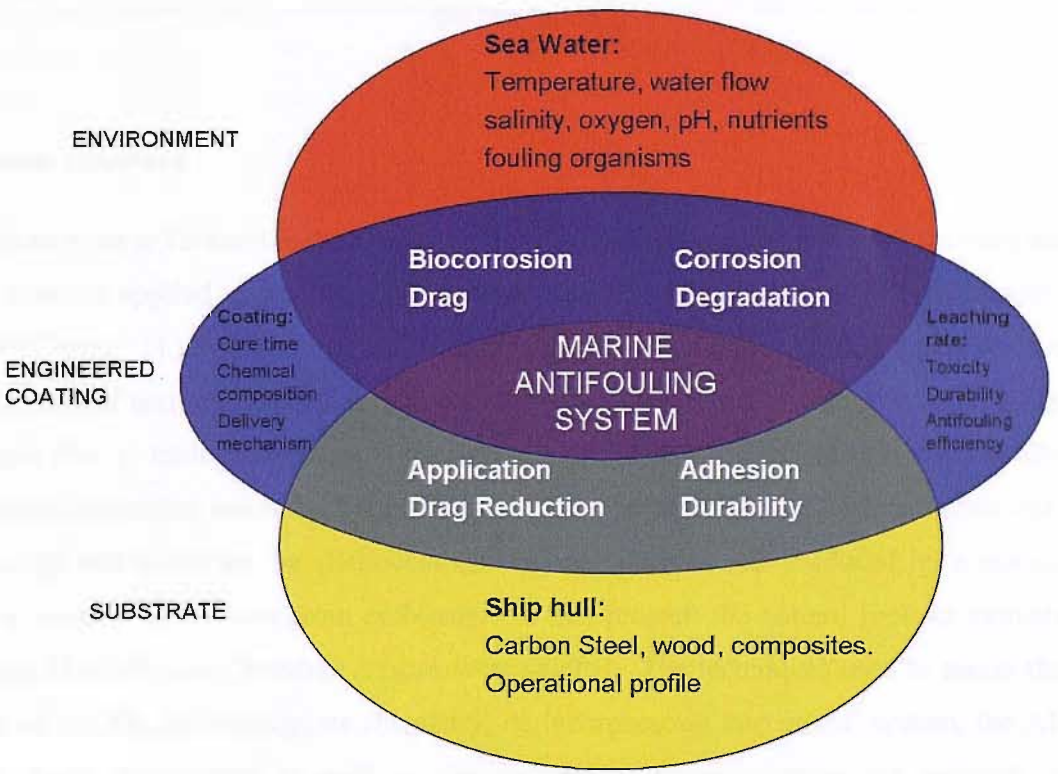

Figure 1.2 Key interactive parameters affecting an antifouling coating system

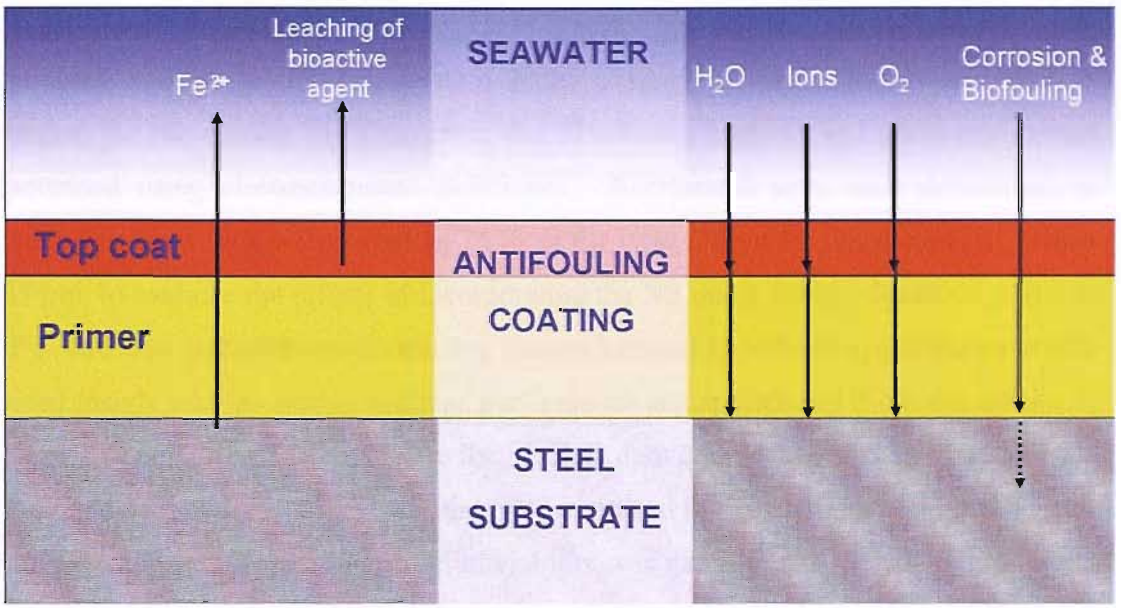

Figure 1.3 Schematic of antifouling system showing the interactive parameters and the coating layers

1.2 Thesis structure

This thesis aims to further the study of natural product based antifoulants by addressing the issue from an applied engineering perspective. To do this a comprehensive literature review (Chapter 2) introduces the technology used in the past, present and especially the development of non-toxic antifouling alternatives for the future. The literature highligthts the need for a multidisciplinary approach to design and build an environmentally acceptable antifouling solution. To address this, the approach used was a biomimetic one. The design was based on the allellochemicals or natural products produced by a marine algae to protect its surfaces from epibionts. In this project, the natural product extracts from the Rhodophycae *Chondrus crispus* were studied. The techniques used to assess the extract of the NP, its efficacy, its chemistry, its incorporation into an AF system, the AF system build, mechanical as well as electrochemical characterisation are outlined in Chapter 3. The task of designing and developing a working coating system was outlined in Chapters 4 and 5. In Chapter 4 an ethanol extract from *C. Crispus* was investigated to compare two differently sourced algal specimens and to test the antifouling efficacy of the extracts in bioassays. Five marine bacteria and five microalgae, as well as two macro algae, were used to assess the antifouling activity of variant extract concentrations (0.1 – 400 $\mu g\ mL^{-1}$). In Chapter 5 the incorporation and application of the NP in a commercially available control depletion polymer (CDP) is described covering details of the substrate

preparation and the surface finish. Once knowledge of the NP in isolation was documented and the antifouling system built, a range of techniques were used to investigate the NP-coating. In Chapter 6, the NP-coating integrity and performance was characterised using electrochemical techniques. Accelerated tests were developed, to heighten sensitivity, and were based on 25 % of the typical dry film thickness (dft), which is 125 μm, to evaluate the effects of incorporating the NP into a control depletion polymer (CDP). The tests included non-destructive electrochemical impedance spectroscopy which provided insight into the wetted coatings performance and specifically the water uptake of the coating system, which is coupled to the biocidal delivery mechanism. In Chapter 7 the antifouling performance of the NP-coating was measured in the laboratory and in the field. The initial colonisation process or biofilm viability was monitored in the laboratory on the coating surface using a nucleic acid staining technique and an episcopic differential interference contrast microscope. Field trials were used to test the effects of varying the NP-coating composition as well as dry film thicknesses. Spectroscopy and both optical and electron microscopy were used to corroborate the coating performance with and without NP additives.

The main philosophy for the process of designing a fully characterised functional system requires many experimental cycles of the key test areas targeted by the flow chart illustrated in Figure 1.4. In Chapter 8 the cross-discipline techniques are critically assessed, the conclusions outlined and a further work plan suggested. The future work section highlights the additional techniques and tests required to further the study of NP-based antifouling systems.

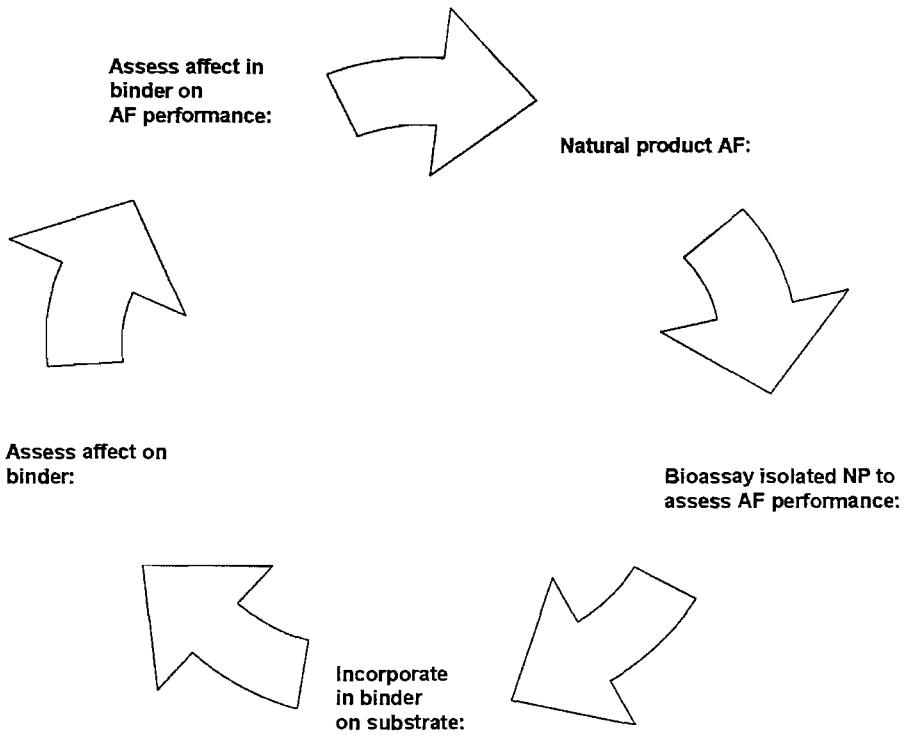

Figure 1.4 Key tests to optimise an NP-based antifouling system

1.3 References

[1.1] C.G. Munger, Corrosion Prevention by Protective Coatings, National Association of Corrosion Engineers, Houston, Tex. 1984.

[1.2] K.V. Thomas, 'Can there be an environmentally 'safe' antifouling paint biocide?' Plenary lecture, 14th International congress on Marine Corrosion and Fouling, July 27-31 2008, Kobe, Japan.

[1.3] International Maritime Organisation, International Convention on the Control of Harmful Anti-fouling Systems on ships AFS/CONF/26 18 October 2001.

Chapter 2 Literature review

The use of antifouling coatings for protection from the marine environment has a long history. By considering the historical and current approaches to antifouling systems, this review presents the use of modern approaches to the design of an environmentally acceptable, broad spectrum antifouling system for application to a large ship's hull.

2.1 Biofouling

The settlement and accumulation of marine organisms on an inanimate substrate can cause large penalties to engineered structures. In heat exchangers, biofouling can clog systems leading to inefficient cooling and performance due to the demand for increased pumping power. On ship hulls it can increase the hydrodynamic drag, lower the manoeuvrability of the vessel and increase the fuel consumption. Biofouling can also affect corrosion rates of immersed surfaces and can therefore directly affect the structural integrity of marine structures. This leads to increased costs within the shipping industry through the increased use of manpower, fuel, material and dry docking time.

The process of biological fouling is often grouped into key growth stages which include an initial accumulation of adsorbed organics, the settlement and growth of pioneering bacteria creating a biofilm matrix and the subsequent succession of micro and macrofoulers (Fig. 2.1). A mature fouling coverage, which would include mortality and emigration of species, is not shown.

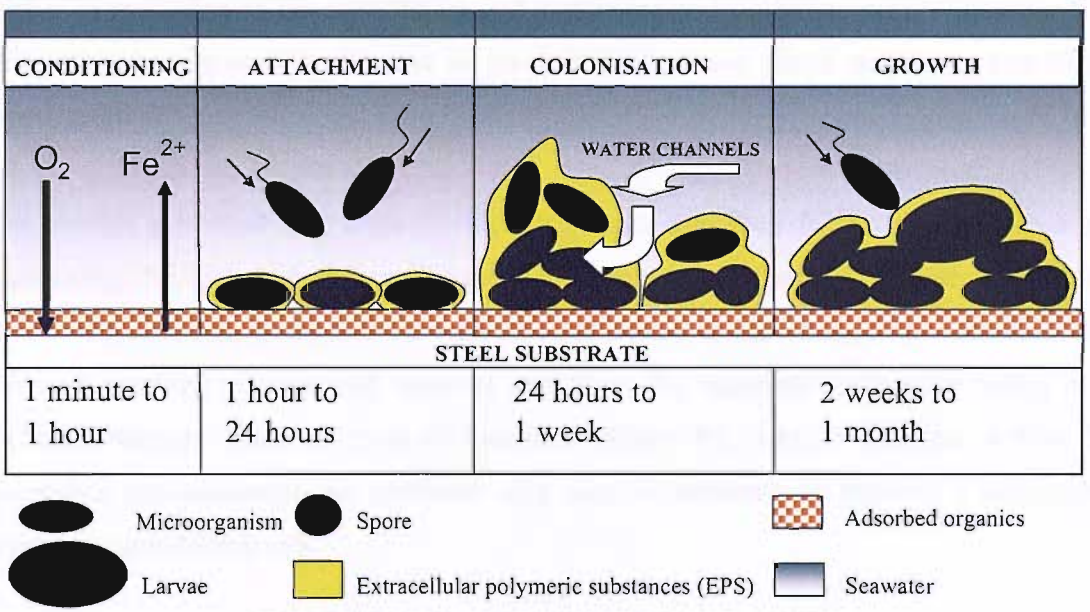

Figure 2.1 Schematic of critical biofouling stages

The sequence of biofouling is not predictable due to the exploitation of substrate niches by higher fouling organisms. Biofilm formation is often a precursor to subsequent fouling by macrofoulers. The succession of biofouling has been experimentally tested by removing initial algal layers resulting in limited further fouling [2.1]. The presence of a biofilm has been recorded to have a positive influence on the settlement of some algal zoospores [2.2], whereas Faimali et al. (2004) [2.3] recorded that an aging biofilm inhibited the settlement of barnacles. In general it is agreed that there is a sequence of events to biofouling and the first stage is usually taken to be the formation of a biofilm [2.4].

When a chemically inert substrate is immersed in seawater an almost immediate accumulation of organic carbon residues adsorb onto the wetted surface, composition of which depends on the ions, glycoproteins, humic and fulvic acids available in the liquid phase. The forces that promote the adsorption and conditioning of the surface include electrostatic interactions and Van der Waal's forces. Pioneering microorganisms can now attach to the surface forming a biofilm. Contact and colonisation between the microorganism and the surface is promoted by the movement of water through Brownian motion, sedimentation and convective transport, although organisms can also actively seek out substrates due to propulsion using flagella. Bacteria and other colonising microorganisms secrete extracellular polymeric substances (EPS) to envelope and anchor them to the substrate thereby altering the local surface chemistry which can stimulate further growth such as the recruitment and settlement of macroorganisms. The effects of other microfoulers such as diatoms on the initial biofilm or slime matrix are also being investigated [2.5].

The biofilm generated is a mass of microorganisms and their EPS which creates a gel matrix (Fig. 2.1) providing enzymatic interaction, exchange of nutrients, protection against environmental stress [2.6] and an increased resistance to biocides [2.7]. Biofilms also interrupt the flow of ions and water to and from the substrate surface by acting as a diffusion barrier. The reduction of localised oxygen by cathodic reactions within the electrolyte can accelerate the corrosion of a metallic substrate by creating a differential aeration concentration cell.

A general review of biocorrosion is given by Videla (1996) [2.6], whilst more recently Beech and Sunner (2004) [2.8] and Barik (2006) [2.9] have looked at biofilm influences on the corrosion of metals. It is important to control microbiological fouling as bacteria can

create a corrosive environment due to their life cycle and their ability to generate decomposition products. This type of corrosion is called microbially induced corrosion (MIC), an example of which is the production of sulphides from sulphate reducing bacteria which can cause the pitting corrosion of steel surfaces [2.10]. The control of MIC is a key outcome for the development of a successful coating which inhibits the attachment of biofouling.

The adhesion techniques employed by fouling organisms are diverse and can often be a two component process with both temporary and permanent adhesion. Barnacle adhesion is a key area of research [2.11] as these hard foulers can dramatically increase the drag on a ship hull. At the critical larval developmental stage of the barnacle, called the cyprid, a temporary adhesive is used while exploring the surface for a place to settle and permanently adhere [2.12]. Barnacles adhere by using a hydrophobic protein which crosslinks using cysteine residues [2.13]. There are many factors which can influence the settlement of barnacles, a key attribute being the presence of other barnacles (conspecific cues) through the remains of old exoskeletons or newly settled cyprids. In a similar manner, the common macroalgae *Ulva* sp., has a temporary and permanent attachment phase to its lifecycle. The motile zoospore stage can temporarily adhere while actively searching for a suitable substratum. When the optimal substrate is detected it transforms into the immotile, settled cell phase which can permanently anchor itself and germinate producing a new plant [2.14]. The hydrated adhesive strength of *Ulva* spore adhesive is 500 mN m^{-1} (indicating a very sticky material) [2.14]. Mussels use byssus threads composed mainly of collagen but have, in contrast to barnacles, a hydrophilic polyphenolic adhesive protein which crosslinks in an oxidation-reduction reaction that occurs in the presence of an enzymatic catalyst [2.14]. Diatoms can attach by producing polysaccharide mucilages which can encapsulate cells forming pads, stalks or tubes [2.15].

The adhesion of species to a substrate is an important aspect of biofouling for if this process could be prevented, fouling could be controlled. Adhesion and settlement is also often a key stage in the life cycle of marine organisms, so the evolutionary pressure to colonise a surface is great. The driving force of adhesion can be considered as being made up of contributions from the interfacial tension between the organism and the substratum, organism and the liquid and between the substratum and the liquid. Methods of experimentally determining these interfacial energies through modelling have been investigated by Ista et al. (2004) [2.16] but they reported that more complex models are

needed as certain estimations of organisms' attachment, such as *Ulva* zoospores, did not model quantitatively. A reason for this was stated that their model does not take surface charge into consideration and that electrostatic interactions may affect the attachment rates. Another contributing factor is that the colonisation of particular substrate features occurs such as rough surface areas to shelter from shear forces and/or flowing systems to maximise nutrient and oxygen concentrations.

2.2 Fouling penalties

Antifouling systems are required wherever unwanted growth of biological organisms occurs. This is often in most saline aqueous phase environments; hence applications include medical, and marine systems. Marine engineered systems have been categorised into seven key types of submerged structures of which ship hulls account for 24 % of the total objects fouled [2.17]. A variety of materials can be used for ship hulls including steel, aluminium and composites such as glass reinforced polymer. The fouling of ship hulls is often prolific as vessels move between a diverse range of environments and remain constantly in the most productive region, the photic zone, of the water column. Although coatings are used for hull protection, they can fail due to the build up of inorganic salts [2.18], exopolymeric secretions, and the calcium carbonate skeletal structures that form the fouling organisms.

Other penalties associated with the unwanted colonisation of a hull surface by marine organisms [2.19], is the negative affects on the vessels hydrodynamics. The drag on a vessel has been recorded to incur a 80 % increase in skin friction and 15 % loss in ship speed with levels as small as 1 mm of algal slime on the ship hull [2.20]. With heavy calcareous fouling, power losses of 86 % at cruising speed have been calculated [2.21]. To better understand the penalties on the hull surface due to biofouling a schematic of the flow regime around a ship is provided (Fig. 2.2).

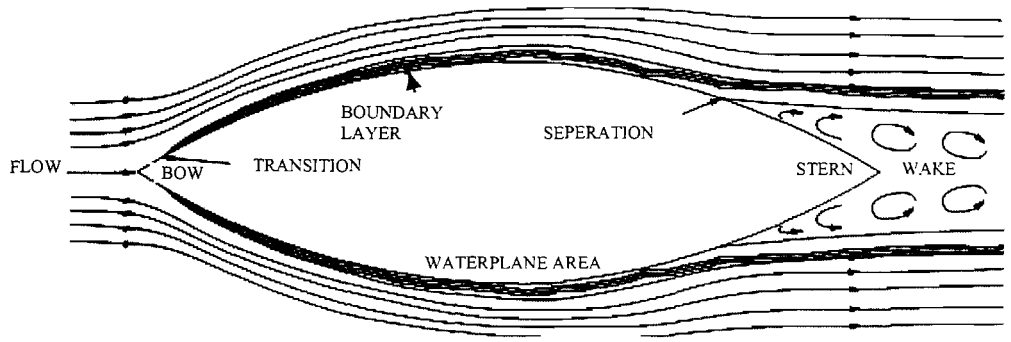

Figure 2.2 Schematic of the boundary layer development along a ship hull [2.22]

The drag on a ship through the water has two components, form drag and skin friction drag. Skin friction drag is most important in relation to the fouling and coating parameters. It is dependant on the shearing forces acting at the interface between the fluid and the hull. Biofouling effects drag by increasing the skin friction of the vessels hull. The surface condition of the hull is important for skin friction and a comparison of clean, new sister ships showed differences in propulsive power of over 20 %, attributed to the painting and hull surface finish [2.23].

The boundary layer is the velocity gradient between the zero 'no-slip' condition at the hull and the freestream velocity. For a ship moving at 10 ms^{-1}, transition to a turbulent flow is established at 0.1 m down stream of the bow [2.22]. Skin friction is related to the roughness height (k-type) or the wall roughness [2.22]. Three different flows exist for k-type roughness and is characterised by a hydrodynamically smooth regime, intermediate regime and a fully rough regime [2.22]. These roughness types are for rigid surface roughness which biofilms and biofouling do not generate. The surface roughness created by biofilms is compliant and due to microorganism exudates forms a biopolymeric coating. Marine biofilm distribution on a substrate is patchy (Fig. 2.3), thus any potential drag reduction due to the damping of turbulent instabilities of this biopolymer compliant layer is lost by the complexity of the biological growth.

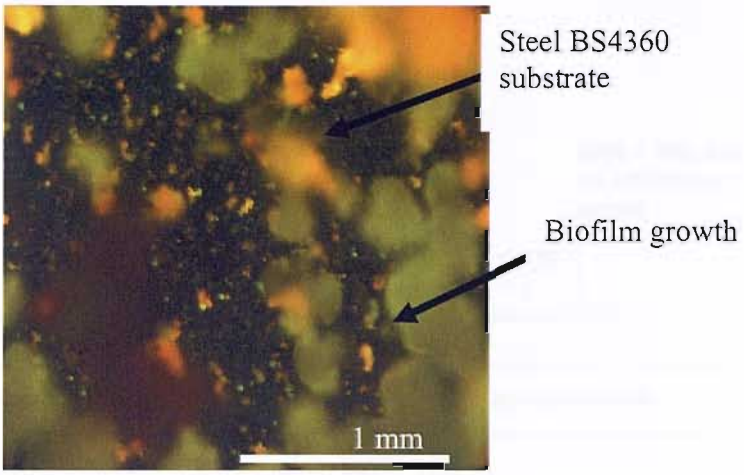

Figure 2.3 Microscope image of biofilm on mild steel

The image in Figure 2.3 clearly illustrates the inhomogeneous and complex distribution of bacteria in the biofilm on the metallic substrate. Two nucleic acid probes were used to illuminate the live marine biological organisms on the steel surface. SYTO® 9 stains penetrate those cells that have intact membranes, indicating a living cell, and allow them to fluoresce green while the propidium iodine penetrates only those cells with broken membranes indicating dead cells. The biofilms thickness and composition are the controlling parameters and can cause an increase in the wall shear stress. Macrofouling aggravates drag further and hard fouling such as barnacles act as rigid surface roughness and affect the hydrodynamically smooth hull surface. An antifouling system requires that the drag on the vessel be kept to a minimum. The negative effects of biofilm roughness on drag were studied by Shultz and Swain (2000) [2.22] and the importance of this initial biological growth on the mean and turbulence profiles of marine vessels were highlighted.

Biofouling exploits ecological niches on a ship's hull, generating varying settlement densities. This can lead to manoeuvrability penalties in specific (e.g., propeller fouling) and non-specific ways (e.g., water line fouling). A vessel's sound signature is also affected, by this degradation of a ship's performance, for both passive and active sonar systems [2.24].

2.3 Historic antifouling methods

The use of toxic antifoulants on ship hulls has been a historic method of controlling fouling but biocides such as lead, arsenic, mercury and their organic derivatives have been banned due to the environmental risks that they posed.

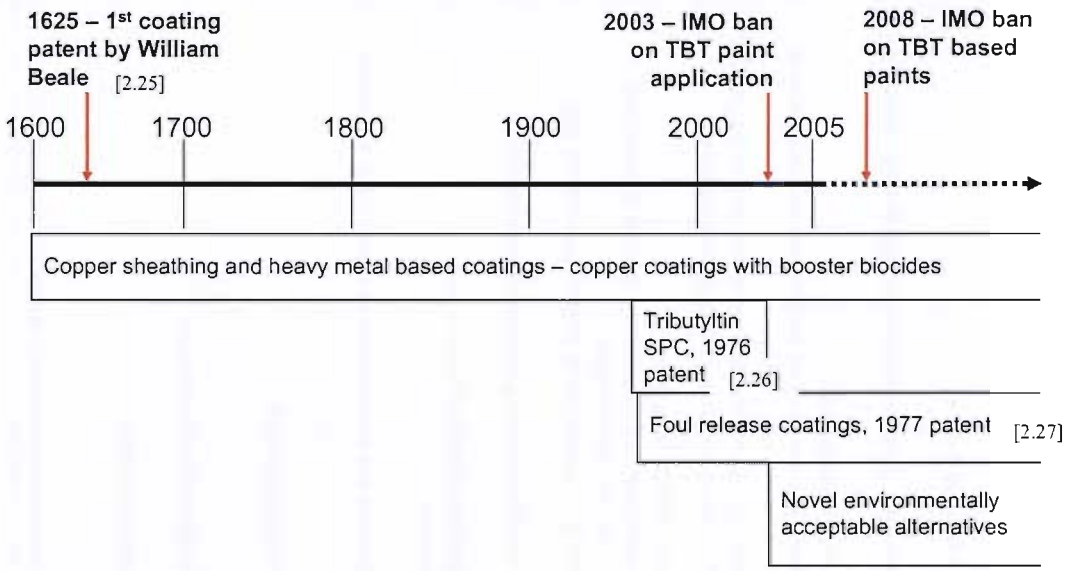

Figure 2.4 Timeline for key antifouling generations

A revolutionary self-polishing copolymer technique employing a similar heavy metal toxic action to deter marine organisms was used with the antifoulant tributyltin (TBT) [2.26]. The use of organotins was eventually banned due to severe shellfish deformities and the bioaccumulation of tin in some ducks, seals and fish [2.28, 2.29], resulting in legislation that culminated in the global ban of tributyltin (Fig. 2.4); as reviewed by Champ, (2000) [2.30] and Terlizzi et al., (2001) [2.31].

Thermoplastic, non-convertible surface organic coatings, which dry due to simple solvent evaporation, are today readily available although volatile organic compound (VOC) controls are limited in antifouling applications. Currently, the UK MOD VOC target levels, as documented in March 2005, are 400 g L^{-1} water free paint [2.32]. The development of antifouling systems has a long history but the last ten years has seen an increase in the focus on environmentally acceptable alternatives (Table 2.1).

Author(s) [ref]	Title	Theme	Year	No. of Refs
Woods Hole Oceanographic Centre [2.25]	Marine fouling and its prevention	Catalogue of fouling organisms and historic antifouling technology.	1952	1091
Fischer, E.C. et al. [2.33]	Technology for control of marine biofouling – A review	Antifouling systems tried and tested	1984	347
Wahl, M. [2.34]	Marine epibiosis. I. Fouling and antifouling: some basic aspects	Review of biological antifouling mechanisms	1989	172
Abarzua, S. & Jakubowski, S. [2.35]	Biotechnological investigation for the prevention of biofouling. I. Biological and biochemical principles for the prevention of biofouling	Biogenic agents to prevent biofouling	1995	128
Clare, A.S. [2.36]	Marine natural product antifoulants: Status and potential	Chemical structures, sources and mechanisms of testing their efficiency	1996	105
Swain, G. [2.37]	Redefining antifouling coatings	Promotion of novel methods	1999	61
Champ, M.A. [2.30]	A review of organotin regulatory strategies, pending actions, related costs and benefits	Focus on organotins and the impending ban in 2003	2000	311
Terlizzi, A. et al. [2.31]	Environmental impact of antifouling technologies: state of the art and perspectives	Influence of TBT on next generation of antifouling technology	2001	69
Lewis, J. [2.38]	Hull fouling as a vector for the translocation of marine organisms: Report 1 and 2	Review of TBT ban and the alternatives as well as focusing on the environmental issue of species translocation	2002	573
Omae, I. [2.39]	General aspects of tin-free antifouling paints	Chemical properties, structures and functions of tin-free alternatives; copper, booster biocides, natural products	2003	165
Yebra, D.M. et al. [2.40]	Antifouling technology-past, present and future steps towards efficient and environmentally friendly antifouling coatings	Antifouling technology is reviewed with particular emphasis on commercial products and the development of an environmentally benign system	2004	201
Railkin, A.I. [2.17]	Marine biofouling colonization processes and defenses	Marine biological approach to the study of fouling, reports on natural as well as artificial methods of antifouling	2004	959
Almeida, E. et al. [2.41]	Marine paints: the particular case of antifouling paints	Historic and environmentally friendly marine antifouling paint systems review	2007	148

Table 2.1 Major reviews on antifouling coatings over the last 50 years

2.4 Modern antifouling alternatives

Many traditional antifouling systems are 'paints', which is a comprehensive term applicable to a variety of materials: enamels, lacquers, varnishes, undercoats, surfacers, primers, sealers, fillers, stoppers and many others [2.42]. Antifoulants are one of many additives usually incorporated within the topcoat paint of a marine protective coating system. The average theoretical spreading rates for commercially available antifouling systems for naval applications is considered to be around 6.2 $m^2 L^{-1}$ at 93 μm dry film thickness, with the majority utilising two coat applications [2.32]. Most antifouling coatings are organic and consist of a primer and a topcoat both of which can include anticorrosive functions. Patenting biocontrol technologies and company property protection has restricted the flow of information regarding comparative values of efficiency. Since the initial phasing out of TBT from the antifouling industry in 2001, alternatives have been available [2.39, 2.43, 2.44,] including biocide-free antifouling coatings [2.45, 2.46].

In Table 2.2, the cost of alternatives can be seen to double with the FR coatings in relation to the TBT based paints, a factor which is increased as alternative technology is not reaching the current service life requirements of 4 to 5 years. To prolong the working life most antifouling coatings use a method of manufacturing the paint matrix composition to control the leaching of the antifoulants.

Antifouling system	Leaching rate	Lifetime	Erosion Rate	Cost/US $ (60 months) [2.38]	Problems
(TBT) self-polishing copolymer paints	Chemical reaction through hydrolysis.	4-5 years [2.31].	Polishing leads to smoothing, reducing fuel consumption.	$680,884 [2.38].	Banned 2008 [2.49].
(Tin-free) self-polishing copolymers	Chemical reaction through hydrolysis of copper, zinc, & silyl acrylate.	5 years.	Polishing leads to smoothing, reducing fuel consumption.	$691,355* [2.38].	Life time shorter then TBT-based paint systems. Increasing the overall cost of ship maintenance.
(Tin-free) conventional Paint	10 $\mu g\ cm^{-2}\ d^{-1}$ [2.47]	12-18 months.	N/A	N/A	Hard non-polishing performance leads to coating build up. Performance only suitable for low fouling environments [2.38].
Control depletion polymers (CDPs) -copper paint	Physical dissolution, works by having a soluble matrix.	3 years.	Matrix erodes due to dissolution of coating binder.	$1,357,786 [2.38].	Biocide release not constant, poor self smoothing, little activity during idle times, higher costs due to necessity of sealer coat on recoats [2.4]. Slow drying time [2.38].
Foul release	Low energy surface, some use leached silicone oils [2.48].	2-5 years.	N/A	N/A	In-water cleaning difficult as brushes may damage silicone, foul release coatings are prone to abrasion damage [2.50].

*Assuming that the TBT-free SPCs are able to provide a 60 month performance and that a one off coating application is required. N/A = Not available [2.38]

Table 2.2 Performance comparisons for the key antifouling systems used

There are two alternative key techniques for controlling the release of antifouling compounds from a coating by using either a soluble or insoluble matrix (Fig 2.5). The self-polishing copolymer (SPC) technique is an example of a soluble matrix which uses both hydrolysis and erosion to control the antifouling activity. Seawater ingress allows for the hydrolysation of the polymer which cleaves the antifouling compound from the polymer backbone and the coatings solubility leaves the surface polished. This controlled dissolution of the surface of the coating allows for a longer lifetime. Yebra et al., 2005 [2.51] have investigated the release rates of commercial rosin binders as effective methods to control this dissolution. Control depletion polymers are examples of an insoluble matrix. The water ingresses and the antifoulants diffuse out leaving behind a leach layer.

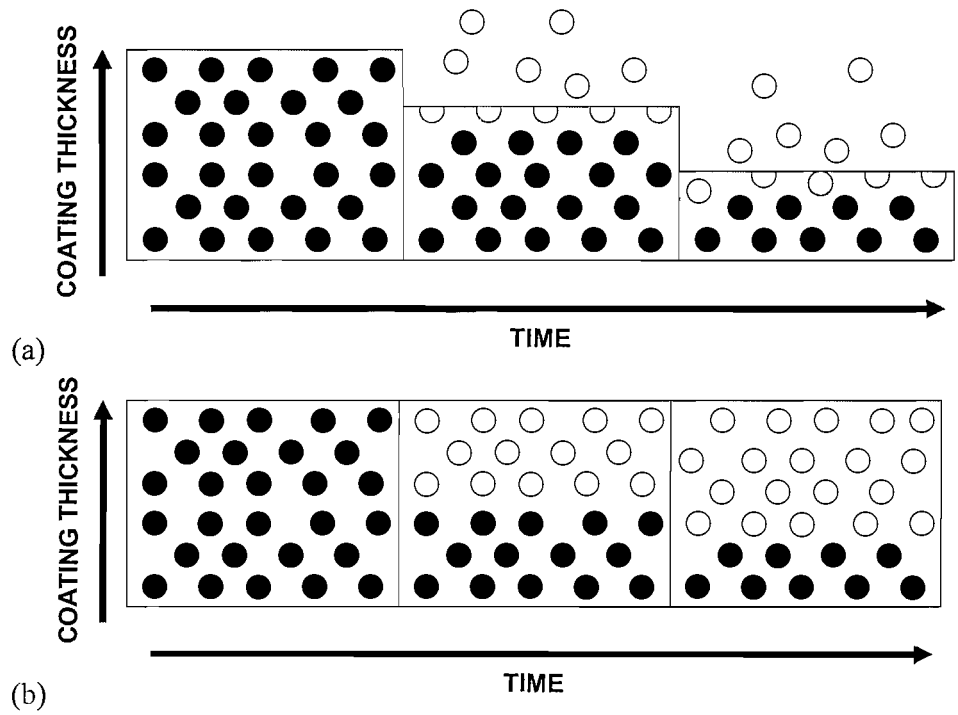

Figure 2.5 Schematic of (a) soluble matrix biocide releasing coating and (b) insoluble biocide releasing coating. ● -loaded antifoulant, ○ - depleted antifoulant

2.4.1 Heavy metals

The ban on TBT in 2003 created a gap in the market and research began into environmentally acceptable replacements (Table 2.1) as reviewed elsewhere [2.31, 2.39, 2.40, 2.44]. In the interim, other metallic species, such as copper and zinc are currently used as substitutes and are delivered in a modified self-polishing copolymer delivery mechanism. Controlled dissolution of antifouling compounds is difficult and copper toxicity is under recent scrutiny [2.19]. Copper is found naturally in the marine

environment at high concentrations and is relatively benign to humans although Environmental Protection Agency (EPA) regulations for drinking water stipulate a limit of 1000 μg L^{-1}. Comparatively, concentrations as low as 5-25 μg L^{-1}can be lethal for marine invertebrates [2.52]. The biomagnification of sequestered copper species through the trophic levels, however, could potentially have an effect on the food industry. Heavy metals are often toxic to marine organisms and humans due to the partitioning of metabolic functions. The reticent use of heavy metals to control fouling in the marine environment due to the TBT ban and increased legislation on toxicity requirements is being replaced in favour of alternative approaches.

2.4.2 Booster biocides approach

As well as increased scepticism over the use of copper, an increased tolerance has been reported for a select group of macrophytes including the key fouling algal species *Enteromorpha* (now *Ulva*) [2.53]. As a result, booster biocides have been incorporated to increase the length and functionality of copper-based antifouling coating systems. Two of the key booster biocides (Irgarol 1051 and Diuron) have been regulated by the UK Health and Safety Executive [2.54, 2.55] with Diuron banned from application and Irgarol restricted to application on vessels not less than 25 m in length. Terrestrial pesticides have also been adapted for marine antifouling systems but have increasingly had issues with their persistence and toxicity [2.56, 2.57]. This approach is often too species specific or conversely too broad, influencing non-target organisms. The effectiveness of the coatings is restricted by their ability to consistently leach the booster biocides. The concentrations of biocide released in free association paints (whether soluble or insoluble) requires better control [2.58]; also their persistence in marine sediments due to such mechanisms as incorporation within degraded paint particles needs continued monitoring [2.59]. The worldwide effects of the key booster biocides in antifouling coatings were reviewed by Konstantinou and Albanis (2004) [2.60]. The use of booster biocides provides an interim solution [2.44] in response to the demands for an effective antifouling strategy to replace TBT.

2.4.3 Foul release approach

Foul release (FR) coatings function due to a low surface energy which degrades an organism's ability to generate a strong interfacial bond with the surface. The smoothness of the coating at the molecular level allows for organisms to be dislodged once the vessel is moving beyond a critical velocity [2.48], i.e. typically 10-20 knots ship speed, depending upon the fouling community [2.40]. These non-stick surfaces remove fouling through shear and tension stresses as well as their own weight by lowering the thermodynamic work of adhesion [2.61]. A combination of the critical surface free energy (22-24 mN m^{-1}) [2.37] and low elastic modulus allows the interface/joint between the organisms adhesive and the coating surface to fracture and fail [2.48]. The adhesion of a marine fouling organism to a wetted substrate creates two surfaces, the surface adhesive interface and the adhesive water interface [2.62]. As described earlier it is these interfacial tensions which control the organisms' ability to adhere.

There are two key types of FR coatings, namely fluoropolymer and silicone based polymer coatings. The application thickness of silicone coatings is typically 150 μm in comparison with 75 μm for fluoropolymers [2.63]. The thickness of the coating allows for the coating modulus to be controlled. A thicker coating as seen with the silicone elastomers is more successful as it requires less energy to fracture the bond between the foulant/coating. Removal of the attached organism occurs through a peeling fracture mechanism as opposed to the shearing associated with the harder, thinner coatings of the fluoropolymer coatings.

Low form biofoulers like diatoms are especially tenacious and are difficult to remove from foul release coatings [2.64]. The implication of this is that the removal of diatomaceous slime from the non-stick coatings when the vessel is in transit is difficult. Using models of low form detachment, FR coatings could be expected to remove 4-6 day old *Ulva* biofilms at operationally relevant ship velocities with greater than 60 % removal of zoospores recorded at 17.7 knots [2.65].

The purely physical deterrent effects of these low energy coatings provide a unique approach to developing an environmentally acceptable alternative to biocide-based antifoulants. It offers a broad spectrum antifoulant without incurring the issues of biodegradation, legislative standards and fees necessary to register an active antifouling compound. This is an effective passive means of approaching the aggressive marine

environment. As this approach does not tackle biofouling while the vessel is berthed dockside where biological communities are allowed to establish. Macrofoulers can then possibly be translocated biogeographically encouraging the environmental issue of alien species transport. The negative effects of alien species on native biological communities include the competition for ecological niches, eradicating indigenous species and generating issues for local biodiversity and aquaculture. There are also issues with the toxicity of the silicone oils in the dockyard and the use by some silicone based paints of the curing agent dibutyltin laureate [2.45]. This organotin catalyst may contain TBT and monobutyltin (MBT) compounds. FR coatings are not a universal antifouling solution for ship hulls and require certain operational profiles to function efficiently. The penalty of increased fuel consumption until the vessel does 'release' the biological foulers has not yet been investigated thoroughly.

Shultz (2004) [2.66] compared the frictional resistance of an FR coating with a SPC coating and determined that the low surface energy coatings had poorer performance and suffered larger increases in frictional resistance coefficient with static exposure time in the marine environment. Candries and Atlar (2005) [2.67] recorded an average increase in friction velocity of between 10-14% for foul release systems and between 13.4-23.5 % for tin-free SPC. Differences in coating application techniques can influence the surface roughness of coatings with an overall increase in the frictional resistance in roller applied FR coatings than spray coated FR coatings reported [2.20].

2.4.4 A biomimetics approach

The term 'biomimetics' deals with the bio-inspired based design rather then direct copying of natural biological functions. The term implies the use of the natural world as a model to base an engineering development or device upon [2.68] or as a 'bottom-up' strategy for hierarchical structures [2.69]. Application of a biomimetics approach for coatings include the control of deposition of inorganics such as silica and silver by biomolecules [2.69]; and an overview of how biomimetics is entering the molecular level with regard to functional coatings has been provided by Tamerler et al. (2003) [2.70].

The diverse mechanisms that marine organisms use to protect their own surfaces from fouling have been investigated [2.34, 2.71, 2.72]. Within the marine ecosystem, evolution has allowed for the development of certain antifouling properties. Marine organisms have both physical and chemical methods to protect themselves from the harmful process of biofouling [2.34, 2.72, 2.73]. Natural chemical defence methods have been of interest over the last two decades. Chemical prospecting for pharmaceuticals has backed this type of research and exploration for new drugs. A molecular approach to antifouling [2.18] has yielded a variety of potential compounds.

The key chemical antifouling mechanism of marine organisms occurs via the production of secondary metabolites (also known as natural products) which deter foulers. Natural products in chemical marine ecology are also termed secondary metabolites which are classified according to their metabolic pathway or biosynthesis.

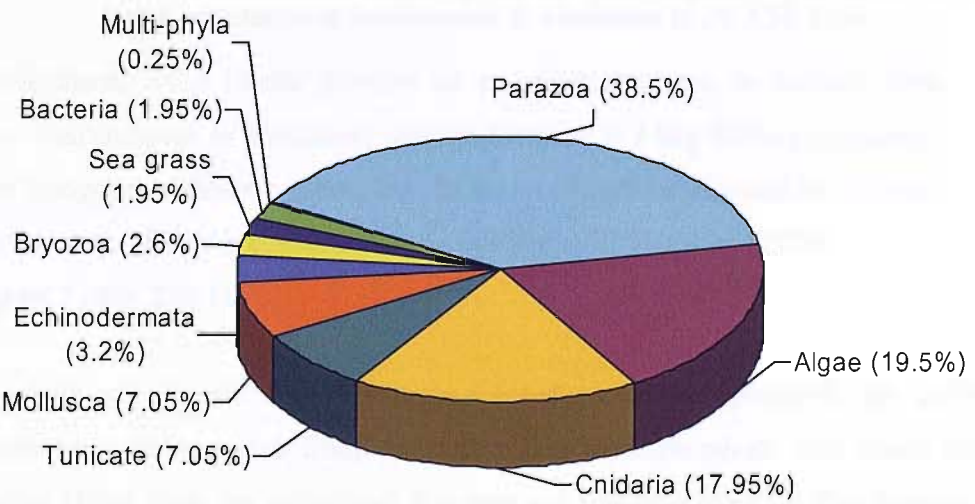

Figure 2.6 Phyletic distribution of 160 reviewed marine species from which potential antifouling natural products have been extracted. Data has been compiled from various sources [2.17, 2.36, 2.39, 2.74, 2.75]

The key phylum investigated as sources of natural antifouling products over the years (Fig. 2.6) include parazoa (e.g. sponges), algae, cnidaria (e.g. corals), echinodermata (e.g. sea-urchins), tunicates (e.g. sea-squirts), bryozoa and bacteria. Of the 160 potential products collated from the literature [2.17, 2.36, 2.39, 2.74, 2.75] 76 % are from sponges, algae and cnidarians. As well as concentrating on individual organisms for inspiration, key trends in surface resistance to fouling have been exploited. Despite research into the use of antifouling natural products over the past 20 years, their incorporation into a functioning system to resist biofouling over a working timescale has yet to occur.

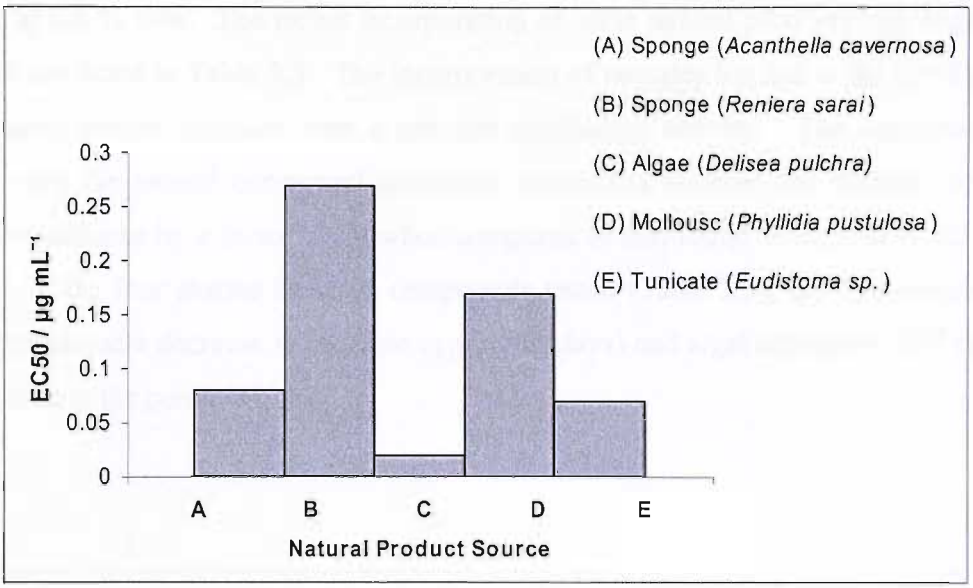

Figure 2.7 The effective concentrations (EC) of various natural products to inhibit 50% of the tested population of the barnacle *B. amphitrite* [2.39, 2.74, 2.76]

The performance of a natural product as an antifoulant can be initially tested by its effective concentration in a bioassay and the barnacle is a key fouling organism used. To date the halogenated furanone from the red seaweed *Delisea pulchra* has proved the most successful, with effective concentration levels for a 50 % effect (EC50) being as low as 0.02 $\mu g\ mL^{-1}$ (Fig. 2.7) [2.76].

When whole-cell marine extracts are processed as natural products the antifeedant chemicals are not separated from the antifouling allelochemicals and could elicit an antifouling effect from the compound that was not naturally used for that purpose. The literature emphasises the 'importance of showing that a compound must be released from, or at, the surface of an organism at an ecologically active concentration before a natural antifouling role can be proposed', see [2.72] as well as [2.36, 2.76-2.78]. De Nys et al., 1998 [2.79] derived a method of determining the natural surface concentrations of marine algal products by solvent extraction. The use of biomimicry in the development of an antifouling system is a unique way to provide the inspiration for aqueous phase, ambient temperature solutions.

The successful immobilisation of natural product compounds is complex due to their inherent high solubility and degradation within the marine environment. A method of controlling the release of natural products was investigated by Price et al., 1992 [2.80] using microencapsulation technology. This approach had some success, through the use of

dry microcylinder powder with entrapped natural product in an epoxy and vinyl based coating at 0.5 % w/w. The recent incorporation of some natural products into engineered coatings are listed in Table 2.3. The incorporation of tannates has led to the development of a cupric tannate pigment with a narcotic antifouling activity. The combination of copper with the natural compound quebracho tannin has lowered the copper content in paint formulations by a factor of 40 when compared to that found in cuprous oxide paints [2.81]. Of the four marine bacterial compounds tested (Table 2.3), the *Pseudomonas* sp. extract exhibited a decrease in barnacle cyprid (12 days) and algal settlement (6-7 days) in comparison to the controls [2.82].

Author, date [ref]	**Natural product source**	**Paint system used**
Armstrong E. et al., (2000) [2.83]	Marine microbial natural products	
Peppiatt C. J. et al., (2000) [2.84]	marine microbial extracts	Resin
Willemsen P R, Ferrari G M (1993) [2.85]	Sponge solvent extracts	Vinyl resin
Burgess J.G. et al., 2003 [2.82]	***Bacteria:*** *Bacillus pumilus* extract *Pseudomonas* sp. extract *Bacillus licheniformis* extract *Bacillus subtilis* extract	Water based paint resin Revacryl 380, Harlaw Chemical Company Ltd.
Sjögren et al., 2004 [2.86]	**Marine Sponge** Bromocyclopeptides: Barettin 8,9-dihydrobarettin	Commercial coatings: SPF SPC Lotréc FabiEco SPC International TF Solid paint/weak SPC Lotréc H2000 Solid paint/weak SPC Lotréc.
Stupak et al., 2003 [2.87]	Sodium benzoate Chestnut tannin Mimosa tannin Quebracho tree tannin	Soluble matrix tannate paint; tannate, calcium carbonate, rosin, phenolic varnish, white spirit. Soluble matrix sodium benzoate paint.
Barrios et al., 2005 [2.88]	Zosteric acid	Polydimethylsiloxane (Sylgard ® 184) an elastomeric silicone kit
Price et al.,1992 [2.80]		epoxy and vinyl based coating

Table 2.3 Some key natural products that have been incorporated into paint systems

The physical defence mechanisms used by marine organisms to defend against biological coverage, range from the spicules of an echinoderm to the mechanical breaching of cetaceans. The behavioural patterns of some species such as crabs have been shown to affect their surface fouling population via burrowing and nocturnal activity [2.89]. On the macro scale, whales and dolphins have recently been studied for their antifouling skin properties [2.90, 2.91]. The design of an antifouling coating with Sharklet AF^{TM} topographies inspired by the placoids of a shark has had the capability of reducing the settlement of the key fouling algae *Ulva* [2.92, 2.93]. Schumacher et al., [2.94] have investigated the use of nanoforce gradients of PDMSe to control *Ulva* settlement. These surfaces are also composed of microtopographies but in this instance it was the accumulative nanoforce gradients of the different sized features ranges from 125 – 374 nN that was attributed to having an antifouling affect. The 374 nN gradient force had the largest reduction in spore settlement at 53 % in comparison to the other nanogradient forces. A study by Carman et al., 2006 [2.93] looked at the effects of polydimethylsiloxane elastomers with tailored architecture on the surfaces wettability and resistance to bioadhesion. There is an increased interest in natural microtopography [2.88, 2.95, 2.97] and synthetic microtextured surfaces [2.16, 2.97-2.99] with antifouling properties. The sensitivity of some organisms' settlement to the size and periodicity of surface topography has also led to the synthetic development of such architectural coatings. Surface properties of shells both physically and chemically are under further investigation [2.96, 2.100]. The effective range of recent micro relief studied and shown to have an antifouling effect can be seen in Table 2.4.

PEGylation is the immobilisation of polyethylene glycol (PEG) on to a surface. The recent development of 'PEGylation' using mussel adhesive proteins has led to the suggestion that they may be used to achieve high densities of protein resistant polymers on surfaces [2.101]. Lewis et al. (2000) [2.102] have examined the development of cell biomembrane biomimicry and the resulting phosphorylcholine (PC) - based polymers have been investigated to establish their potential to resist fouling. The settlement of Ulva zoospores on patterned, fluorinated and PEGlayted monolayer surfaces was tested by Finlay et al., 2008 [2.103]. Navarro-Villoslada et al. (2001) [2.104] also used PC-based polymers to successfully protect luminescent oxygen sensors from biofouling. A 70% decrease in the surface concentration of adhered bacteria under 2.5 mL min^{-1} flow was reported when compared with an uncoated control. The surface free energy [2.105], polar properties and

the tailored micro-architecture [2.98] of materials have also been investigated with the aim of developing novel antifouling surfaces. A recent review of advances in polymers with antifouling performance is made by Krishnan et al. [2.106].

Coating	Organism	Dimensions	Effect	Author, date [Ref]
Polydimethylsiloxane elastomers (PDMSe)	*Ulva* spores	5 μm x 5 μm channels	Preferential attachment	Hoipkemeier-Wilson et al., 2004 [2.99]
PDMSe	*Ulva* spores	Ribs with length 4 - 16 μm, 2 μm wide and 4 μm high, spaced 2 μm apart	Reduced settlement by 86% relative to smooth PDMSe	Carman et al., 2006 [2.93]
Mould of crab (*C. pagurus*) carapace	Barnacle (*Balanus improvisus*)	200 μm circular elevations and 2-2.5 μm long spicules	Repelled for 1st 3 weeks	Bers and Wahl, 2004 [2.95]
-	*Vorticella* sp	-	Repelled in 3rd week	Bers and Wahl, 2004 [2.95]
Mould of mussel (*M. edulis*) shell	Barnacle (*Balanus improvisus*)	1-1.5 μm wide microripples in parallel	Repelled for 1st week, reversed to preferential after 3rd week	Bers and Wahl, 2004 [2.95]
Mould of dogfish (*S. canicula*) eggcase	Cilliate (*Z. commune*)	Longitudinal ridges, 30-50 μm wide, parallel over distances ~ 15-115 μm	Repelled in 2nd week	Bers and Wahl, 2004 [2.95]
-	Barnacle (*Balanus improvisus*)	-	Repelled in 2nd week	Bers and Wahl, 2004 [2.95]
Mould of echinoderm (*O. texturata*)	Cilliate (*Z. commune*)	10 μm diameter knobs spaced about 30 μm apart	Repelled in 3rd week	Bers and Wahl, 2004 [2.95]
Medical grade Poly(methyl methacrylate)	Barnacle (*Balanus improvisus*)	Average roughness (R_a) = 5 - 10 μm Roughness height = 30 - 45 μm	92% inhibition of barnacles after 1 month in field trial	Berntsson et al., 2000 [2.97]
Mussel (*Mytilus galloprovincialis*) shell	Biofouling community	1.5 μm high ridges at distances of 1-2 μm	<10% biofouling after 14 weeks in field trial	Scardino et al, 2003 [2.96]
Pilot whale skin (*Globicephala melas*)		0.1 – 1.2 μm^2 pores enclosed by nanoridges	Proposed antifouling effect	Baum et al., 2002 [2.90]
Lotus leaf		1 - 5 μm relief structures	Self cleaning ability	Barthlott and Neinhus 1997 [2.107]

Table 2.4 Microtexture effects on marine biofouling

2.4.5 Further antifouling coatings

A wealth of alternatives have been initially investigated for various marine applications to replace the use of TBT (Table 1.1). Further alternatives to the approaches of SPC, FR, control depletion polymer, natural products and surface micro-architectures can be seen in Table 2.5.

AF System	Reference or Company	Performance
Glass flake lining technology	Subsea Industries' Ecospeed	Good for ice breakers and other abrasive uses.
Electrochemical control	Matsunaga and Lim 2000 [2.108]	Main application is in closed systems.
Fibre flocking	Phillippi et al., 2001 [2.109]	Long and complex application process.
Enzymes	Pettitt et al., 2004 [2.110] Kristensen et al., 2008 [2.111]	Was not broad spectrum [2.110].
Electrical fields	Leya et al., 1999 [2.112], Perez-Roa 2008[2.113]	Issues with a sound signature for military applications. Expensive to install for large hulls.

Table 2.5 Further antifouling coating alternatives

The process of surface flocking is where electrostatically charged fibres are adhered to a coating perpendicular to the surface and is currently undergoing trials as an antifoulant mechanism. The fibres can be made of polyester, polyamide, nylon or polyacryl [2.45]. Using nylon fibres on a polyvinylchloride plastic sheet a decrease in green algae and barnacles was recorded for a 6 month field trial [2.109]. Other non-toxic coatings have been developed such as the two (base and top) coat system of basecoat polybutadiene or urethane and a topcoat of silicone or hydrocarbon [2.114]. All five two-coat systems were fouled by slime and algae but were resistant to fouling by barnacles and bryozoans in field trials 6–12 months in length. Alternative surfaces that resist bioadhesion such as short chain PEG have been investigated [2.115] as well as alternative surface architecture to resist protein adsorption [2.116].

2.5 System requirements

The navy operates in global waters and so is subject to a broad range of fouling organisms requiring a broad spectrum antifoulant. Vessels need to be capable of rapid deployment and the removal of heavy fouling from sitting dockside is a time consuming process. For this reason antifouling performance should include protection while the ship is stationary. Similar performance to merchant ships is required so the penalties of increased drag, increased emissions and fuel consumption are the same but in addition for naval applications the decrease in manoeuvrability as well as increase in sound signature is a serious problem. There is also a requirement for a long lifetime performance of 5-12 years to reduce docking times and through life costs of ship hull maintenance. At present the copper based systems function with 3 year performance. The antifouling requirements needed for a naval ship hull are outlined in Table 2.6 and additional factors that need to be considered include its life cycle parameters and measurable effectiveness [2.117] which incorporate toughness, erosion and release of the antifouling compound [2.58].

Must be:	**Must not be:**
Anticorrosive	Toxic to the environment
Antifouling	Persistent in the environment
Environmentally acceptable	Expensive
Economically viable	Chemically unstable
Long life	A target for non specific species
Compatible with underlying system	
Resistant to abrasion/ biodegradation/ erosion	
Capable of protecting regardless of operational profile	
Smooth	

Table 2.6 Requirements for a large ship hull antifouling coating

There are three key parameters to consider when optimising an antifouling system. The engineered protective coating, the substrate it is attached to and the environment it is wetted in. These are illustrated in the Venn diagram (Fig. 1.2). All of which have unique properties that will affect the coating integrity and efficacy. The antifouling coating is typically the final top-coat which overlays a primer system to protect the ship hull. It was important to investigate the NP affect on not only the top-coat but as a layer in the full antifouling system.

So far in the development of antifouling systems an incremental approach has been taken. This project aims to combine the individual disciplines of natural product research and coating technology to progress this area of development with a logical stepwise approach.

2.6 Summary and outlook

There are a variety of modern approaches to achieve broad spectrum, environmentally acceptable antifouling performance, particularly for ships hulls. The degree of success of an antifouling coating must be determined with respect to its application. Engineering paints accounted for 29% of the UK coating technology sectors market valued at £1548 million in 2005 [2.118]. Unfortunately, operational profiles vary; hence the application of one universal coating to ship hulls is unlikely and specific coatings designed for the particular needs of certain exposure and operational profiles may need to be targeted individually. This, however, is no different to existing antifouling systems as these also do not cater for all operational profiles. The IMO legislation and the increased legislation of local and regional pesticide control authorities are the largest driving forces for the design and implementation of non-toxic antifouling coatings.

A biomimetic approach provides a method incorporating nature's antifouling solutions to solve its own problems. The limitations of this approach are the practical application of a design solution which successfully mimics an ecologically significant antifouling effect found in the marine natural world. A natural antifouling compound that has both broad spectrum activity and species specific antifouling performance is potentially difficult to isolate from one organism. Also, as biological foulers have a diverse size range and preferential surface attachment criteria one single pattern of tailored microarchitecture may not be effective [2.99]. A synergistic and more realistic biomimetic approach could be found through the combination of an organism's chemical and physical antifouling attributes and may even 'more accurately reflect antifouling strategies adopted by organisms in nature' (Clare et al., (1992) [2.18]). Present modern methods of biofouling control are effective alternatives to the TBT antifouling coatings, but not yet their equal. Therefore, research into varied approaches to the design and implementation of antifouling coating technology must continue.

The literature has concentrated on isolating and synthesising analogues of marine natural products for use in antifouling systems. There is a research gap in the use and delivery of these researched natural products in a paint system. For those natural products that have

been incorporated, no rigorous engineering tests have been made. By incorporating a natural defence solution from nature into a controlled delivery system the objective was to generate a system with the potential for a working life of greater than five years (to replace TBT gap in market). At the same time by using a natural marine solution to inhibit biofouling, the ambition was to avoid adverse environmental impacts and future legislative controls on tin-free non-toxic alternatives.

Due to the research strategies identified in the literature and the state of the art in antifouling coatings, the main aims of this project are to:

(1) Source and extract a natural product
(2) Test the natural product antifouling efficacy in isolation
(3) Develop techniques and procedures to measure NP containing antifouling systems
(4) Test the NP-incorporated coating and determine performance

2.7 References

[2.1] M.J. Dring, The Biology of Marine Plants, Edward Arnold (Publishers) Limited, London, 1982.

[2.2] P. Patel, M.E. Callow, I. Joint, J.A. Callow, *Specificity in the settlement – modifying response of bacterial biofilms towards zoospores of the marine alga Enteromorpha*, Environ. Microbiol. 5 (2003) 338-349.

[2.3] M. Faimali, F. Garaventa, A. Terlizzi, M. Chiantore, R. Cattaneo-Vietti, *The interplay of substrate nature and biofilm formation in regulating Balanus amphitrite Darwin, 1845 larval settlement*, J. Exp. Mar. Biol. Ecol. 306 (2004) 37-50.

[2.4] J.W. Costerton, *Introduction to biofilm*, Int. J. Antimicrobial Agents, 11 (1999) 217-221.

[2.5] P.J. Molino, Wetherbee, R. *The biology of biofouling diatoms and their role in the development of microbial slimes Biofouling*, 24 (5) (2008) 365-379.

[2.6] H.A. Videla, Manual of Biocorrosion, Boca Raton, Florida, US. CRC Press, Inc., 1996.

[2.7] L.H.G. Morton, D.L.A. Greenway, C.C. Gaylarde, S.B. Surman, *Consideration of some implications of the resistance of biofilms to biocides*, Int. Biodeter. Biodegr. 41 (1998) 247-259.

[2.8] I.B. Beech, J. Sunner, *Biocorrosion: towards understanding interactions between biofilms and metals*. Curr. Opin. Biotechnol. 15 (2004) 181-186.

[2.9] R.C. Barik, Environmental factors affecting the marine corrosion performance of nickel aluminuim bronze, Thesis (PhD) University of Southampton, School of Engineering Sciences (2006).

[2.10] R.G.J. Edyvean, The effects of microbiologically generated hydrogen sulphide in marine corrosion, Mar. Technol. Soc. J., 24 (1990) 5-9.

[2.11] N. Aldred, A.S. Clare, *The adhesive strategies of cyprids and development of barnacle-resistant marine coatings*, Biofouling, 24 (5) (2008) 351-363.

[2.12] L. Khandeparker, A.C. Anil, *Underwater adhesion: the barnacle way*, Int. J. Adhes and Adhes, 27 (2007) 165-172.

[2.13] M.J. Naldrett, *The importance of sulphur cross-links and hydrobhobic interactions in the polymerization of barnacle cement*. J. Mar. Biol. Ass. U.K. 73 (1993) 689-702.

[2.14] M.E. Callow, J.A. Callow, *Marine biofouling: a sticky problem*, Biologist, 49 (2002) 1-5.

[2.15] M.E. Callow, *Ship fouling: problems and solutions*, Chem. Ind. (Lond), 5 (1990) 123-127.

[2.16] L.K. Ista, M.E. Callow, J.A. Finlay, S.E. Coleman, A.C. Nolasco, R.H. Simons, J.A. Callow, G.P. Lopez, *Effect of substratum surface chemistry and surface energy on attachment of marine bacteria and algal spores*, Appl. Environ. Microbiol. 70 (2004) 4151-4157.

[2.17] A.I. Railkin, Marine Biofouling Colonization Processes and Defenses, CRC press LLC, 2004.

[2.18] A.S. Clare, D. Rittschof, D.J. Gerhart, J.S. Maki, *Molecular approaches to nontoxic antifouling,* Invert. Rep. Develop. 22 (1992) 67-76.

[2.19] R.L. Townsin, *The ship hull fouling penalty*, Biofouling, 19 (Supplement) (2003) 9.

[2.20] J.C. Lewthwaite, A.F. Molland and K.W. Thomas, *An investigation into the variation of ship skin frictional resistance with fouling.* Trans. RINA, 127 (1985) 269-279.

[2.21] M.P. Schultz, *Effects of coating roughness and biofouling on ship resistance and powering*, Biofouling, Vol. 23, (5) (2007) 331 – 341.

[2.22] M.P. Schultz, G.W. Swain, *The influence of biofilms on skin friction drag*, Biofouling, 15 (2000) 129-140.

[2.23] H. Lackenby, *Resistance of Ships with Special Reference to Skin Friction and Hull Surface Condition*, Proceedings of the Institution of Mechanical Engineers, 176 (1962) 981-1011.

[2.24] E.C. Haderlie, in: J.D. Costlow, R.C. Tipper (eds), Marine Biodeterioration: An Interdisciplinary Study, Naval Institute Press, MD, USA, London E. & F.N. SPON, 1984.

[2.25] Woods Hole Oceanographic Institution, Marine Fouling and its Prevention, US Naval Institute Press, Annapolis, MD, 1952.

[2.26] A. Milne, G. Hails, GB Patent (1976), International Paint, 1,457,590.

[2.27] A. Milne, G. Hails, GB Patent (1977) International Paint, 1,470,465.

[2.28] J. Strand, J.A. Jacobsen, *Accumulation and trophic transfer of organotins in a marine food web from the Danish coastal waters*, Sci. of the Total Environ. 350 (2005) 72-85.

[2.29] S.M. Evans, T. Leksono, P.D. McKinnell, *Tributyltin pollution: a diminishing problem following legislation limiting the use of TBT-based anti-fouling paints*, Mar. Pollut. Bull. 30 (1995) 14-21.

[2.30] M.A. Champ, *A review of organotin regulatory strategies, pending actions, related costs and benefits*, Sci. Total Environ. 258 (2000) 21-71.

[2.31] A. Terlizzi, S. Fraschetti, P. Gianguzza, M. Faimali, F. Boero, *Environmental impact of antifouling technologies: state of the art and perspectives*, Aquatic Conserv: Mar. Freshw. Ecosyst. 11 (2001) 311-317.

[2.32] STMGT Sea Technology Group, Warpaint, Issue 20 (2005).

[2.33] E.C. Fischer, V.J. Castelli, S.D. Rodgers, H.R. Bleile, in: J.D. Costlow, R.C. Tipper (eds), Marine Biodeterioration: An Interdisciplinary Study, Naval Institute Press, MD, USA, London E. & F.N. SPON, 1984.

[2.34] M. Wahl, *Marine epibiosis. I. Fouling and antifouling: some basic aspects.* Mar. Ecol. Prog. Ser. 58 (1989) 175.

[2.35] Abarzua, S.; Jakubowski, S., *Biotechnological investigation for the prevention of biofouling. I. Biological and biochemical principles for the prevention of biofouling.* Mar. Ecol. Prog. Ser. 123 (1995) 301-312.

[2.36] A.S. Clare, *Marine natural product antifoulants: status and potential.* Biofouling, 9 (1996) 211-229.

[2.37] Swain, G. J., *Redefining antifouling coatings*, Prot. Coat. Linings, 16 (1999) 26-35.

[2.38] J. Lewis, Hull fouling as a vector for the translocation of marine organisms: Report 1 & 2, Dept. of Agriculture, Fisheries and Forestry - Australia, Marine Science and Ecology Pty. Ltd. Commonwealth of Australia, 2002.

[2.39] I. Omae, *General aspects of tin-free antifouling paints*, Chem. Rev. 103 (2003) 3431-3448.

[2.40] D.M. Yebra, S. Kiil, K. Dam-Johansen, *Antifouling Technology - past, present and future steps towards efficient and environmentally friendly antifouling coatings* Prog. Org. Coat. 50 (2004) 75-104.

[2.41] E. Almeida, T.C. Diamantino, O. de Sousa, *Marine paints: the particular case of antifouling paints*, Prog Org Coat, 59(1) (2007) 2-20.

[2.42] G.P.A. Turner, Introduction to Paint Chemistry, Science Paperbacks, Chapman and Hall Ltd, London, 1967.

[2.43] B. Watermann, *Alternative antifouling techniques: present and future*, Report, LimnoMar, Hamburg, Germany, May 1999.

[2.44] I. Omae, *Organotin antifouling paints and their alternatives*, Appl. Organometallic Chem.17 (2003) 81-105.

[2.45] B.Watermann, B. Daehne, S. Sievers, R. Dannenberg, J.C. Overbeke, J.W. Klijnstra, O. Heemken, *Bioassays and selected chemical analysis of biocide-free antifouling coatings,* Chemosphere, 60 (2005) 1530-1541.

[2.46] B. Watermann, B. Daehne, M. Wiegemann, M. Lindeskog, S. Sievers, Volume III Performance of biocide-free antifouling paints, LimnoMar, Hamburg/Norderney, 2003.

[2.47] G. Swain, in: Oceans 86 Conference Record, IEEE/MTS: Washington D.C., (1986) 221.

[2.48] R.F. Brady Jr, I.L. Singer, *Mechanical factors favoring release from fouling release coatings*, Biofouling, 15 (2000) 73-82.

[2.49] IMO, International Convention on the Control of Harmful Anti-fouling Systems on ships AFS/CONF/26 18 October 2001.

[2.50] J.A. Lewis, in Proceedings: National Shipping Industry Conference, Sydney, NSW. March 2001. Australian Maritime Safety Authority, Canberra.

[2.51] D.M. Yebra, S. Kiil, K. Dam-Johansen, C. Weinell, *Reaction rate estimation of controlled-release antifouling paint binders: Rosin-based systems*, Prog. Org. Coat. 53 (2005) 256-275.

[2.52] P.V. Hodson, U. Borgmann, H. Shear, in: J.O. Nriagu (Ed.) Copper in the Environment Part II: Health Effects, Wiley-Interscience, New York, 1979 p. 307.

[2.53] N. Voulvoulis, M.D. Scrimshaw, J.N. Lester, *Comparative environmental assessment of biocides used in antifouling paints*, Chemosphere 47 (2002) 789-795.

[2.54] J.C. Chesworth, M.E. Donkin, M.T. Brown, *The interactive effects of the antifouling herbicides Irgaol 1051 and Diuron on the seagrass Zostera marina,* Aquat. Toxicol. 66 (2004) 293-305.

[2.55] S.J. Lambert, K.V. Thomas, A.J. Davy, *Assessment of the risk posed by the antifouling booster biocides Irgarol 1051 and Diuron to freshwater macrophytes*, Chemosphere 63 (2006) 734.

[2.56] K.V. Thomas, T.W. Fileman, J.W. Readman, M.J. Waldock, *Antifouling paint booster biocides in the UK coastal environment and potential risks of biological effects,* Mar. Pollut. Bull. 42 (2001) 677-688.

[2.57] R.A. Devilla, M.T. Brown, M. Donkin, G.A. Tarran, J. Aiken, J.W. Readman, *Impact of antifouling booster biocides on single macroalgal species and on a natural marine phytoplankton community,* Mar. Ecol. Prog. Ser. 286 (2005) 1-12.

[2.58] M. Thouvenin, J-J. Peron, V. Langlois, P. Guerin, J-Y. Langlois, K. Vallee-Rehel, *Formulation and antifouling activity of marine paints: a study by a statistically based experiments plan*, Prog. Org. Coat. 44 (2002) 85-92.

[2.59] K.V. Thomas, M. McHugh, M. Hilton, M. Waldock, *Increased persistence of antifouling paint biocides when associated with paint particles,* Environ. Pollut. 123 (2003) 153-161.

[2.60] I.K. Konstantinou, T.A. Albanis, *Worldwide occurrence and effects of antifouling paint booster biocides in the aquatic environment: a review,* Environ. International, 30 (2004) 235-248.

[2.61] M. Berglin, N. Lönn, P. Gatenholm, *Coating modulus and barnacle bioadhesion*, Biofouling, 19 (Supplement) (2003) 63-69.

[2.62] R.F. Brady Jr., *Properties which influence marine fouling resistance in polymers containing silicon and fluorine*, Prog. Org. Coat. 35 (1999) 31-35.

[2.63] R.F. Brady Jr., *A fracture mechanical analysis of fouling release from nontoxic antifouling coatings*, Prog. Org. Coat. 43 (2001) 188-192.

[2.64] C. Anderson, M. Atlar, M. Callow, M. Candries, A. Milne, R.L. Townsin, *The development of foul-release coatings for seagoing vessels*, J. Marine Design and Operations, B4 (2003) 11-23.

[2.65] M.P. Schultz, J.A. Finlay, M.E. Callow, J.A. Callow, *Three models to relate detachment of low form fouling at laboratory and ship scale*, Biofouling 19 (Supplement) (2003) 17-26.

[2.66] M.P. Schultz, *Frictional resistance of antifouling coating systems*, J. Fluids Eng. 126 (2004) 1039-1047.

[2.67] M. Candries, M. Atlar, *Experimental investigation of the turbulent boundary layer of surfaces coated with marine antifoulings*, J. Fluids Engineering, 127 (2005) 219-232.

[2.68] D. De Rossi, A. Ahluwalia, *Biomimetics: new tools for an old myth*, 1st Annual International IEEE-EMBS Special Topic Conference on Microtechnologies in Medicine and Biology, Lyon, France, IEEE, (2000) 15-17.

[2.69] R.R. Naik, L.L. Brott, F. Rodriguez, G. Agarwal, S.M. Kirkpatrick, M.O. Stone, *Bio-inspired approaches and biologically derived materials for coatings*, Prog. Org. Coat. 47 (2003) 249-255.

[2.70] C. Tamerler, S. Dincer, D. Heidel, M. Hadi Zareie, M. Sarikaya, *Biomimetic multifunctional molecular coatings using engineered proteins*, Prog. Org. Coat. 47 (2003) 267-274.

[2.71] M. Wahl, K. Kröger, M. Lenz, *Non-toxic protection against epibiosis*, Biofouling, 12 (1998) 205-226.

[2.72] A.R. Davis, N.M. Targett, O.J. McConnell, C.M. Young, *Epibiosis of marine algae and benthic invertebrates: natural products chemistry and the mechanisms inhibiting settlement overgrowth.* In: P.J. Scheuer (ed) Bioorganic Marine Chemistry, Vol. 3. Springer-Verlag, Berlin (1989) p. 85.

[2.73] G.J. Bakus, M. Wright, A.K. Khan, B. Ormsby, D.A. Gulko, W. Licuanan, E. Carriazo, A. Ortiz, D.B. Chan, D. Lorenzana, M.P. Huxley, in: M.-F. Thompson, R. Nagabhushanam, R. Sarojini and M. Fingerman (eds) Recent Developments in Biofouling Control. A.A. Balkema, Rotterdam (1994) p. 373.

[2.74] N. Fusetani, *Biofouling and antifouling.* Nat. Prod. Rep. 21 (2004) 94-104.

[2.75] C. Hellio, C. Simon-Colin, A.S. Clare, E. Deslandes, *Isethionic acid and floridoside isolated from the red alga, Grateloupia turuturu, inhibit settlement of Balanus amphitrite cyprid larvae,* Biofouling, 20 (2004) 139-145.

[2.76] R. De Nys, P.D. Steinberg, P. Willemsen, S.A. Dworjanyn, C.L. Gabelish, R.J. King, *Broad spectrum effects of secondary metabolites from the red alga delisea pulchra in antifouling assays.* Biofouling, 8 (1995) 259-271.

[2.77] G.M. Nylund, H. Pavia, *Inhibitory effects of red algal extracts on larval settlement of the barnacle Balanus improvisus,* Mar. Biol. 143 (2003) 875-882.

[2.78] J.R. Pawlik, *Marine invertebrate chemical defenses*, Chem. Rev. 93 (1993) 1911-1922.

[2.79] R. de Nys, S.A. Dworjanyn, P.D. Steinberg, *A new method for determining surface concentrations of marine natural products on seaweeds*, Mar. Ecol. Prog. Ser. 162 (1998) 79-87.

[2.80] R.P. Price, M. Patchan, A. Clare, D. Rittschof, J. Bonaventura, *Performance enhancement of natural antifouling compounds and their analogs through microencapsulation and controlled release.* Biofouling, 6 (1992) 207.

[2.81] M. Pérez, G. Blustein, M. García, B. del Amo, M. Stupak, *Cupric tannate: a low copper content antifouling pigment,* Prog. Org. Coat. 55 (2006) 311-315.

[2.82] J.G. Burgess, K.G. Boyd, E. Armstrong, Z. Jiang, L.Yan, M. Berggren, U. May, T. Pisacane, Å. Granmo, D.R. Adams, *The Development of a Marine Natural Product-based Antifouling Paint.* Biofouling, 19 (Supplement) (2003) 197-205.

[2.83] E. Armstrong, *Marine microbial natural products in antifouling coatings*, Biofouling 16 (2000) 215.

[2.84] C.J. Peppiatt, *Antibacterial activity of resin based coatings containing marine microbial extracts*, Biofouling 16 (2000) 225-234.

[2.85] P.R. Willemsen, G.M. Ferrari, *The use of anti-fouling compounds from sponges in anti-fouling paints*, Surf. Coat. Int. Part A: Coat. J. 76 (1993) 423-427.

[2.86] M. Sjögren, M. Dahlström, U. Göransson, P.R. Jonsson, L. Bohlin, *Recruitment in the field of Balanus improvisus and Mytilus edulis in response to the antifouling cyclopeptides barettin and 8,9-dihydrobarettin from the marine sponge Geodia barrette,* Biofouling, 20 (2004) 291-297.

[2.87] M.E. Stupak, M.T. García, M.C. Pérez, *Non-toxic alternative compounds for marine antifouling paints.* Internat. Biodeterior. Biodegrad. 52 (2003) 49-52.

[2.88] C.A. Barrios, Q. Xu, T.Cutright, B.Z. Newby (2005) *Incorporating zosteric acid into silicone coatings to achieve its slow release while reducing fresh water bacterial attachment*, Colloids and Surfaces B: Biointerfaces, 41 (2005) 83-93.

[2.89] K. Becker, M. Wahl, *Behaviour patterns as natural antifouling mechanisms of tropical marine crabs*, J. Exp. Mar. Bio. Ecol. 203 (1996) 245-258.

[2.90] C. Baum, W. Meyer, R. Stelzer, L.-G. Fleischer, D. Siebers, *Average nanorough skin surface of the pilot whale (Globicephala melas, Delphinidae): considerations on the self-cleaning abilities based on nanoroughness*, Mar. Biol. 140 (2002) 653-657.

[2.91] W. Meyer, U. Seegers, *A preliminary approach to epidermal antimicrobial defense in the Delphinidae*, Mar. Biol. 144 (2004) 841-844.

[2.92] E. Roberts, *Nontoxic antifouling mimics nature's shark-skin solution*, Marine Scientist, 11 (2005) 28-30.

[2.93] M.L. Carman, T.G. Estes, A.W. Feinberg, J.F. Schumacher, W. Wilkerson, L.H. Wilson, M.E. Callow, J.A. Callow, A.B. Brennan, *Engineered antifouling microtopographies – correlating wettability with cell attachment*, Biofouling, 22 (2006) 1-11.

[2.94] J.F. Schumacher, C.J. Long, M.E. Callow, J.A. Finlay, J.A. Callow, A.B. Brennan, *Engineered nanoforce gradients for inhibition of settlement (attachment) of swimming algal spores*, Langmuir 24 (9) (2008) 4931-4937.

[2.95] A.V. Bers, M. Wahl, *The influence of natural surface microtopographies on fouling*, Biofouling, 20 (2004) 43-51.

[2.96] A. Scardino, R. De Nys, O. Ison, W. O'Connor, P. Steinberg, *Microtopography and antifouling properties of the shell surface of the bivalve molluscs Mytilus galloprovincialis and Pinctada imbricata*, Biofouling, 19 (Supplement) (2003) 221-230.

[2.97] K.M. Berntsson, P.R. Jonsson, M. Lejhall, P. Gatenholm, *Analysis of behavioural rejection of micro-textured surfaces and implications for recruitment by the barnacle Balanus improvisus,* J. Exp. Mar. Biol. Ecol. 251 (2000) 59-83.

[2.98] M. Jelvestam, S. Edrud, S. Petronis, P. Gatenholm, *Biomimetic materials with tailored surface micro-architecture for prevention of marine biofouling,* Surf. Interface Anal. 35 (2003) 168-173.

[2.99] L. Hoipkemeier-Wilson, J.F. Schumacher, M.L. Carman, A.L. Gibson, A.W. Feinberg, M.E. Callow, J.A. Finlay, J.A. Callow, A.B. Brennan, *Antifouling potential of lubricious, micro-engineered, PDMS elastomers against zoospores of the green fouling alga Ulva (Enteromorpha),* Biofouling 20(1) (2004) 53-63.

[2.100] A.J. Scardino, R. de Nys, *Fouling deterrence on the bivalve shell Mytilus galloprovincialis*, Biofouling 20 (2004) 249-257.

[2.101] J.L. Dalsin, B-H. Hu, B.P. Lee, P.B. Messersmith, *Mussel adhesive protein mimetic polymers for the preparation of nonfouling surfaces*, J. Am. Chem. Soc. 125 (2003) 4253-4258.

[2.102] A.L. Lewis, *Phosphorylcholine-based polymers and their use in the prevention of biofouling*, Colloids and Surfaces B: Biointerfaces, 18 (2000) 261-275.

[2.103] J.A. Finlay, S. Krishnan, M.E. Callow, J.A. Callow, R. Dong, N. Asgill, K. Wong, E.J. Kramer, C. Ober, *Settlement of Ulva zoospores on patterened fluorinated and PEGlayted monolayer surfaces,* Langmuir 24 (2) (2008) 503-510.

[2.104] F. Navarro-Villoslada, G. Orellana, M.C. Moreno-Bondi, T. Vick, M. Driver, G. Hildebrand, K. Liefeith, *Fiber-optic luminescent sensors with composite oxygen-sensitive layers and anti-biofouling coatings,* Anal. Chem. 73 (2001) 5150-5156.

[2.105] Q. Zhao, Y. Liu, C. Wang, S. Wang, H. Müller-Steinhagen, *Effect of surface free energy on the adhesion of the biofouling and crystalline fouling*, Chem. Eng. Science, 60 (2005) 4858-4865.

[2.106] S. Krishnan, C.J. Weinman, C.K. Ober, *Advances in polymers for anti-biofouling surfaces*, J. Mater. Chem. 18 (2008) 3405-3413.

[2.107] W. Barthlott, C. Neinhuis, *Purity of the sacred lotus, or escape from contamination in biological surfaces*, Planta 202 (1997) 1-8.

[2.108] T. Matsunaga, T.K. Lim, *Electrochemical prevention of biofouling*, Electrochemistry 68 (11) (2000) 847-852.

[2.109] A.L. Phillippi, N.J. O'Connor, A.F. Lewis, Y.K. Kim, *Surface flocking as a possible anti-biofoulant*, Aquaculture, 195 (2001) 225-238.

[2.110] M.E. Pettitt, S.L. Henry, M.E. Callow, J.A. Callow, A.S. Clare, *Activity of commercial enzymes on settlement and adhesion of cypris larvae of the barnacle Balanus amphitrite, spores of the green alga Ulva linza, and the diatom Navicula perminuta,* Biofouling, 20 (2004) 299-311.

[2.111] J.B. Kristensen, R.L. Meyer, B.S. Laursen, S. Shipovskov, F. Besenbacher, C.H. Poulsen, *Antifouling enzymes and the biochemistry of marine settlement*, Biotechnology Advances 26 (5) (2008) 471-481.

[2.112] T. Leya, A. Rother, T. Müller, G. Fuhr, M. Gropius, B. Watermann, *Electromagnetic Antifouling Shield (EMAS) – a promising novel antifouling technique for optical systems*, in: Lewis, J.A. (ed.) 10th International Congress on Marine Corrosion and Fouling, University of Melbourne, 1999: Additional Papers. Report DSTO-GD-0287 (2001) 98-110.

[2.113] R.E. Pérez-Roa, M.A. Anderson, D. Rittschof, B. Orihuela, D. Wendt, G.L Kowalke, D.R. Noguera, *Inhibition of barnacle (Amphibalanus amphitrite) cyprid settlement by means of localized, pulsed electric fields*, Biofouling 24 (3) (2008) 177-184.

[2.114] J.D. Adkins, A.E. Mera, M.A. Roe-Short, G.T. Pawlikowski, R.F. Brady, Jr., *Novel non-toxic coatings designed to resist marine fouling*, Prog. Org. Coat. 29 (1996) 1-5.

[2.115] P. Kingshott, H.J. Griesser, *Surfaces that resist bioadhesion*, Current Opinion in Solid State and Materials Science, 4 (1999) 403-412.

[2.116] G.L. Kenausis, J. Vörös, D.L. Elbert, N. Huang, R. Hofer, L. Ruiz-Taylor, M. Textor, J.A. Hubbell, N.D. Spencer, *Poly(L-lysine)-g-Poly(ethylene glycol) layers on metal oxide surfaces: attachment mechanism and effects of polymer architecture on resistance to protein adsorption,* J. Phys. Chem. B 104 (2000) 3298-3309.

[2.117] H.S. Preiser, A. Ticker, G.S. Bohlander, D.W. Taylor in: J.D. Costlow, R.C. Tipper (eds), Marine Biodeterioration: An Interdisciplinary Study, Naval Institute Press, MD, USA, London E. & F.N. SPON, 1984 p.223.

[2.118] A. Matthews, The Donald Julius Groen Lecture 2005, Institution of Mechanical Engineers Tribology Groups, I Mech E, London, Dec 2005.

Chapter 3 Experimental techniques

3.1 Introduction

For the assessment of an antifouling system, both the antifouling component and the delivery mechanism need to be investigated. In this project a combination of the antifouling compound (a natural product extract) and the delivery system were investigated together. First it was necessary to investigate the natural product extract, then incorporate into a coating and finally assess the antifouling system including the primer layers in the natural marine environment.

The delivery system in this project was a proprietary antifouling paint system. The control of biofouling can occur by a variety of methods but for an open system like a ship hull a protective coating is the most adopted method. The use of a coating reflects the industrial need for an environmentally acceptable solution to follow the 2008 ban on TBT (section 2.4). The incorporation of a natural product extract directly into a coating has not received a great deal of attention in the literature (section 2.4.4, Table 2.3).

This commercial paint matrix was used to assess the characteristics of a natural product in a working system. Electrochemical techniques were used to investigate the effects of natural product incorporation into a coating as well as the blank coating itself. Optical and scanning electron microscopies were also used to assess the physical characteristics of the system. The experimental coatings ability to prevent biofilm growth was assessed using microbiological techniques. The most rigorous test for an antifouling system is a field trial. Field trials were completed in a raft exposure facility, in estuarine dock conditions at the Empress dock, National Oceanography Centre, Southampton, UK.

Coating systems have multiple functions and there are many terminologies to describe them due to their long history and individual manufacturers' goals. To clarify the different interactions Table 3.1 provides the working definitions used through out this thesis.

Term		Definition	Reference
Diffusion	=	Movement of ions/species across a concentration gradient (physical)	Walsh 1993 [3.1]
Solubility	=	The ability of a substance to dissolve in a solvent with regards to its physical properties	BS2015 [3.2]
Depletion	=	Controlled delivery of the additives within a coating by the dissolving of the soluble binder pigments	
Leaching rate	=	Release of antifoulant additive per unit time	
Leached layer	=	The depleted or 'spent' layer of antifoulant in the coating	
Saturation	=	Complete wetting of the coating system	
Water uptake	=	Volume fraction of water absorbed by the coating	
Durability	=	The degree to which the coating system withstands destructive forces of their environment (BS2015)	BS2015 [3.2]

Table 3.1 Terminology for coating characterisation

The range of techniques used in this project (Table 3.2) was required to enable the approach used in this project to design a natural product based antifouling coating as outlined in Chapters 1 and 2. Laboratory based as well as field techniques were used to ensure that an applied perspective was being assessed (i.e. the practicalities of a NP-based coating). Figure 3.1 highlights the collaborative use of the techniques to characterise the NP-coating system.

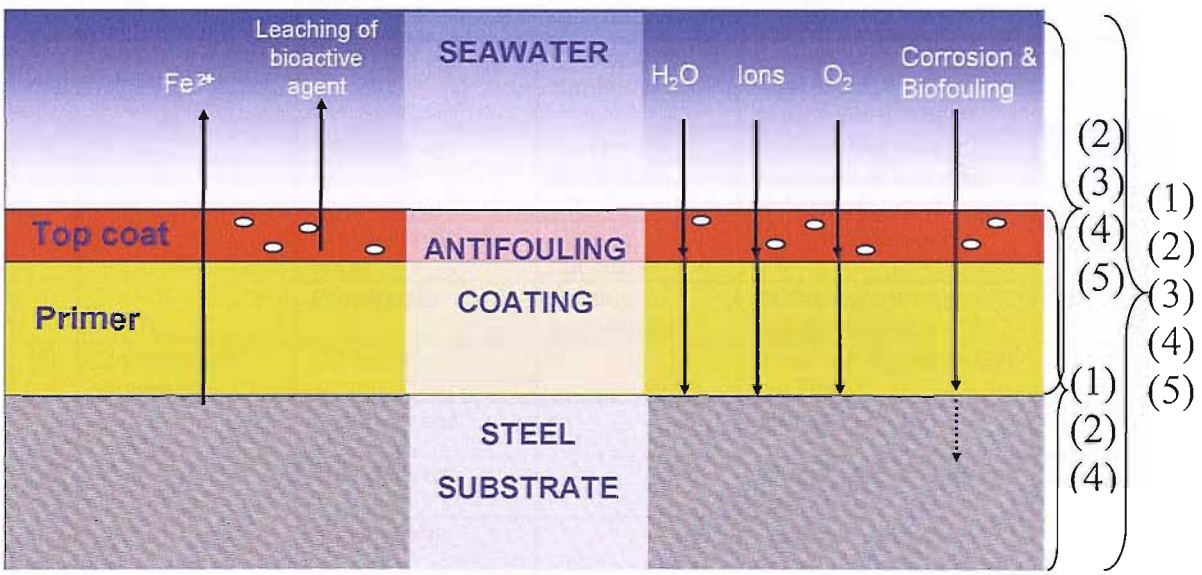

Figure 3.1 Schematic cross-section of an antifouling system showing techniques

#	Technique	Test	Evaluates	Measurement	Chapter
(1)	Electrochemistry	ZRA	Potential	Integrity of coating and corrosion of substrate in Lab	6
		OCP	Potential	Substrate corrosion potential in Lab and Field	6
		EIS	Impedance	Water uptake, matrix depletion in Lab	6
		PR	Resistance	Porosity in Lab	6
(2)	Biofouling	Bioassay	Antifouling efficacy	Minimum inhibitory natural product concentration for range of fouling organisms in Lab	4
		BacLight staining & EDIC	Biofilm growth and viability	Dead/live bacterial community structure & biofilm architecture in Lab and Field	7
		Field trials	Antifouling performance	Performance of NP-coatings in variable environment, dry film thickness and concentration in Field	7
(3)	Spectroscopy	FT-IR	Biofilm growth and NP in matrix	Chemical composition of biofilm from Field, correlation with EDIC analysis and detection of NP in binder	7
		GC-MS	Chemical fractions of natural product	Chemical composition of NP	4
(4)	Microscopy & Surface analysis	Optical	Coating & germination of spores	Corrosion, porosity, cell germination, biofilm	4 5 6 7
		SEM	Coating performance	Cracks, pores & adhesion	5 6 7
		EDX	Chemical composition	Leached layer for depletion & distribution of particles in binder	6 7
		Profilometry	Surface roughness	Average and total roughness of coatings and prepared steel	5
		Coating thickness gauge	Coating thickness	Dry film thickness	5 6 7
		Photographs	Coating performance	Biofouling coverage during field trials	5 6 7
(5)	Environmental parameters	DO probe		Dissolved oxygen in Lab and Field	6 7
		Salinity probe		Salinity in Field	6 7
		Thermometer		Temperature in Lab and Field	6 7
		Conductivity		Conductivity in Lab	7
		Spectrophotometer	light intensity	Concentration of bacteria and microalgae in liquid medium for bioassays	4

Table 3.2 Characterisation techniques used in this project and the parameters they evaluated

In this chapter a brief overview of the key principles associated with each technique are described. Further details of the experimental methodology and equipment are described more fully in the individual chapters in which they were used.

3.2 Electrochemical techniques

A common method of measuring coating integrity and corrosion resistance characteristics is through the use of electrochemical analysis [3.1, 3.3-3.5]. A cross-section of the system under investigation as is shown in Figure 3.1. Electrochemistry can be used to not only assess different materials but also to better understand the mechanisms of corrosion processes.

While biofouling is the unwanted attachment, corrosion is the process of unwanted attack on a metal by its environment. Although microbial corrosion and the presence of a biofilm can also be electrochemically investigated [3.6], in this coating system it is the coating/metal interface that has been considered.

Steel substrates such as hull material and the test sample substrate used in this project corrode in the presence of aqueous environments through electrochemical reactions. The process of ferrous corrosion can be broken down into two main reactions; an anodic reaction and a cathodic reaction. In the anodic reaction; an oxidation (or electron producing) reaction occurs and is shown in equation 3.1.

$$Fe \rightarrow Fe^{2+} + 2e^{-} \qquad (3.1)$$

The half cell reaction shown in equation 3.1 describes how iron atoms go into solution leaving behind two electrons. The cathodic reaction is a reduction (or electron consuming) reaction in aerated water.

$$O_2 + 2H_2O + 4e^{-} \rightarrow 4OH^{-} \qquad (3.2)$$

Both anodic and cathodic reactions are necessary for corrosion to occur. The overall corrosion cell reaction is:

$$2Fe_{(s)} + O_{2\,(g)} + 2H_2O_{(l)} \rightarrow 2Fe^{2+}{}_{(aq)} + 4OH^{-}{}_{(aq)} \qquad (3.3)$$

Electrochemical techniques are a powerful tool for understanding and monitoring corrosion. The main benefits of using electrochemical techniques are as aids to evaluate different materials for the purpose of selection. It allows for the prediction of component lifetime, is relatively rapid and can be employed in the laboratory [3.3]. The main controlling parameters of the corrosion cell shown in equation 3.3 are the potential (V), current (A) and resistance (Ω) [3.4]. All three of these parameters can be measured in a variety of ways. The key reasoning for using a variety of electrochemical techniques is that one of these controlling parameters could lead to the early prediction of the coatings performance in natural exposures [3.5]. Electrochemical techniques are one of the few means of measuring 'real time' corrosion rate information [3.3]. In particular the non-destructive electrochemical techniques allow for continuous measurements over time of parameters such as water uptake and substrate potential.

The coatings under investigation in this thesis act as a protective layer that is not impervious to the diffusion of ions and water. The diffusion barrier generated by the presence of a coating on a ferrous substrate can be analysed using electrochemical techniques to assess the corrosion activity at the coating/metal interface. The evaluation of the polymer paint matrix with and without additives in a short time period, in a non-destructive manner was considered to be an important aspect for evaluating the effect of incorporated NP on the matrix. Three optimal ways of evaluating the coatings is by using the techniques of open circuit potential (OCP), zero resistance ammeter (ZRA) and electrochemical impedance spectroscopy (EIS). The corrosion resistance, galvanic coupling and impedance of the coating system were investigated using these three techniques respectively.

3.2.1 Open-circuit potential (OCP)

OCP and rest potential are equivalent terms. It is the open-circuit potential that will be used in this thesis. The potential of a coated system is a combination of both the anodic and cathodic regions. The more electronegative the potential the more anodic the system is. The samples are exposed to a freely corroding environment and measured using a potentiostat.

3.2.2 Zero resistance ammeter (ZRA)

The ZRA (Zero Resistance Ammeter) measures the current flowing (thereby reaction rates / charge transfer rates) between two electrodes with effectively zero resistance between them. The instrument measures the current flowing in the circuit without introducing a voltage drop as normally found in a standard ammeter [3.7]. An operational amplifier is used to supply any necessary current at its output terminal to maintain a zero potential difference between two input terminals. In this manner zero potential is maintained between the two inputs and is particularly useful for investigating coupled samples. It can be used to measure low levels of current, such as coated samples, with high precision.

3.2.3 Electrochemical impedance spectroscopy (EIS)

Organic coatings such as paint have been extensively studied using impedance measurements [3.5, 3.8-3.15]. It is a non-destructive technique that can measure the electrochemistry occurring at the metal/coating and coating/electrolyte interfaces. EIS is used to evaluate the performance of organic coatings on a metal substrate particularly within corrosive environments.

The principle of this technique is to apply a small sine wave (where ω is the frequency) to the working electrode so the voltage is $E(\omega)$ and measure the response through the resulting current ($I(\omega)$). This allows the frequency dependant impedance to be calculated ($Z(\omega) = E(\omega) / I(\omega)$). Equivalent circuits have been developed that describe electrochemical systems such as solid/liquid interfaces. The Randles or equivalent circuit, models the electrochemical processes occurring on the surface of the electrode and can be used to predict corrosion events [3.10].

The key steps in electrochemical impedance spectroscopy are to, apply an electrical perturbation, acquire an electrical response, and determine an equivalent circuit to relate components of the equivalent circuit to key physical and chemical characteristics of the test system

Experimental impedance spectra can provide information on the kinetics of the corrosion processes that are occurring on the sample surface [3.12], in this project it is a mild steel substrate. The values obtained experimentally from the impedance of the system are then used to compare with the theoretical impedance of the electrical model [3.13]. An

equivalent circuit model depicting an organic coating on a metal substrate can be seen in Figure 3.2.

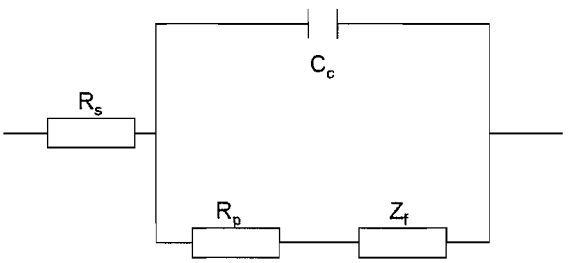

(a)

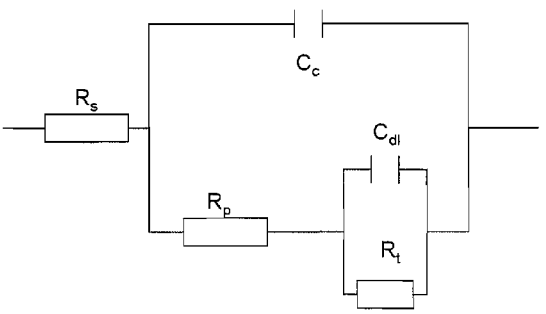

(b)

Figure 3.2 Equivalent circuit of (a) an organic coating on a metal substrate and (b) a coated metal with a defect [3.13]

C_{dl} = double layer capacitance
R_t = charge transfer resistance at coating/metal interface
Z_f = electrochemical processes at the coating metal interface
R_s = electrolyte resistance
C_c = capacitor, the protective coating covering most of the metal surface
R_p = pore resistance (transport of electrolyte through the coating thickness)

Ideally, a coating that is impermeable to the electrolyte acts as a capacitor with $C_{dl} = 0$, R_t = infinite this results in a intact coating slope of -1 (Figure 3.3). With an increase in exposure time the system departs from the typical capacitor characteristics as the water, oxygen and ions permeate the coating and reach the metallic substrate beneath. As expected, an increasing rate of corrosion occurs with the degradation of the coating. With increased corrosion, the R_p decreases, the C_{dl} increases and the slope of the magnitude versus frequency plot decreases substantially moving towards 0 (Figure 3.3). The pore resistance R_p is dependent on the thickness of the coating. When plotted the theoretical lines representing circuit in Figure 3.2 (a) and (b) look as shown in Figure 3.3.

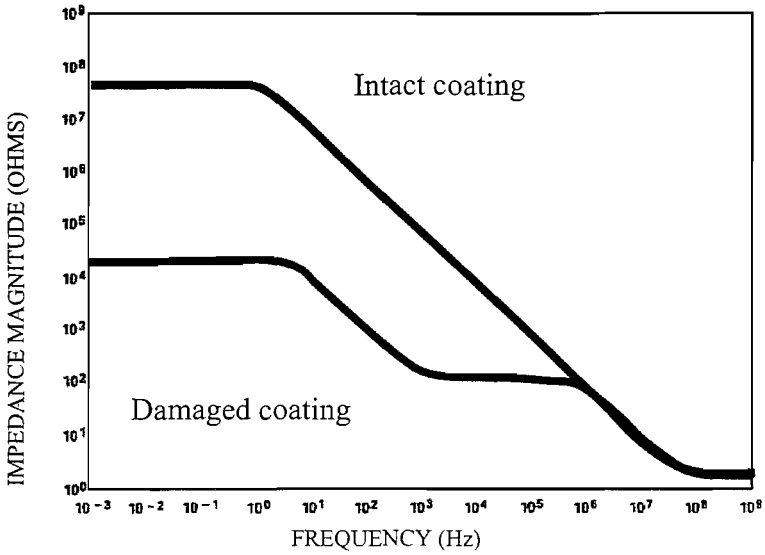

Figure 3.3 Theoretical magnitude plots based on the intact and damaged coating equivalent circuits [3.13]

EIS can provide information on water uptake, since this incorporation of polar molecules leads to an increase in the dielectric constant of the coating' Grundmeier et al., 2000 [3.14]. The dielectric properties of the coating system can also be calculated and the difference in the capacitance of a dry coating to a saturated coating can be used to calculate the water uptake, see Amirudin et al., 1995 [3.15].

One research paper has suggested this method as a means to evaluate the hydrophobicity and the water uptake of TBT-acrylate copolymer (antifouling) systems [3.8] but no experimental data was provided. The authors stated that the 'water sensitivity of an organic coating is an essential parameter in relation to its performance'. The main model used to estimate water uptake is the Brasher & Kingsbury model [3.9] as shown in equation 3.4 derived from the relationship $C_t / C_0 = 80^x$.

$$Xv = \frac{\log(C_t / C_0)}{\log 80} \tag{3.4}$$

80 = dielectric constant of water at room temperature

C_t = capacitance at time 't'

C_0 = capacitance at time '0'

Xv = Volume fraction of water in coating

Electrochemical techniques are a well established means of measuring non-antifouling coating performance and its ability to degrade in variable environments. The use of EIS to

investigate the organic coating/metallic substrate interface in a non-destructive manner is of interest for evaluating marine paint systems [3.12, 3.13, 3.16]. Electrochemical analysis has been seldom applied in the study of antifouling coatings [3.9, 3.17, 3.18]. The novelty of using these techniques to assess the experimental coatings permeation to the electrolyte adds an interesting aspect to this project.

3.3 Biofouling analysis techniques

A method used to evaluate the antifouling performance of a prospective deterrent is often through settlement and growth bioassays. Microfoulers such as biofilm formation and bacteria counts can be quantified using luminescent bacteria test [3.19] and nucleic acid stains [3.20]. Direct comparisons of the performance data of antifouling coatings are complicated as a result of inconsistencies with the materials and methods used to measure new compounds and surface coating properties

3.3.1 Biofilm analysis

The assessment of biofilm growth on the experimental coatings was determined to be an important assay. Although, the simplified biofouling sequence (as shown in section 2.1) does not always require a biofilm for further growth, initial bacterial coverage is often indicative of a surface that will foul further. The techniques available to analyse biofilm and in particular their interactions with metals was summarised recently by Beech [3.21]. Here a nucleic acid and differential interference microscopy was used to visualise the marine biofilm on coated substrates. The use of double nucleic staining technique was chosen over the more conventional plate counting method as it can often underestimate bacterial viability [3.20]. There are other stains that could be used including DAPI (4', 6-diamidino-2-phenylindole), however, these yield a count of the present number of bacteria and does not allow for the viability of the bacterial community to be assessed. These coatings are intended for application to ship hulls, and so the number of bacteria present is perhaps not as important as if a biofilm has developed and a measure of its relative health. The best method for this purpose is to use bacterial viability stain such as the bacterial viability stain LIVE/DEAD® *Bac*Light™ used in this study.

The dead and live cells were visualised as red and green fluorescence respectively using Episcopic Differential Interference Contrast (EDIC) microscope (described in detail in section 4.3.2) with fluorescence. The reason for using these stains was two fold. The use

of the direct staining method allowed for a rapid and *in situ* investigation of the biofilm generated on the experimental coatings.

Double staining nucleic acid stains, such as *Bac*Light™, have not frequently been used to measure marine biofilms on antifouling coating surfaces but it has been used to assess alternative antifouling technology. Matsunaga and Lim 2000 [3.20] successfully used double nucleic acid staining to measure the bacterial viability of their electrochemical antifouling prevention mechanism (Table 2.5).

3.3.2 Field exposure trials

Exposure trials are an important technique to use for the assessment of protective coatings. The transition of coating performance from laboratory scale to the field is important to evaluate. The procedures of a direct incorporation NP antifoulant and trial in the marine environment for natural products is not well documented. The next logical step is to see how these compounds can function in the marine environment, so this project deployed samples in marine sea trials. A raft site in the Southampton dock area was chosen to best simulate the dockyard environmental regime for the ship hull relevant of naval applications. The Southampton dock is a temperate climate location with an estuarine condition.

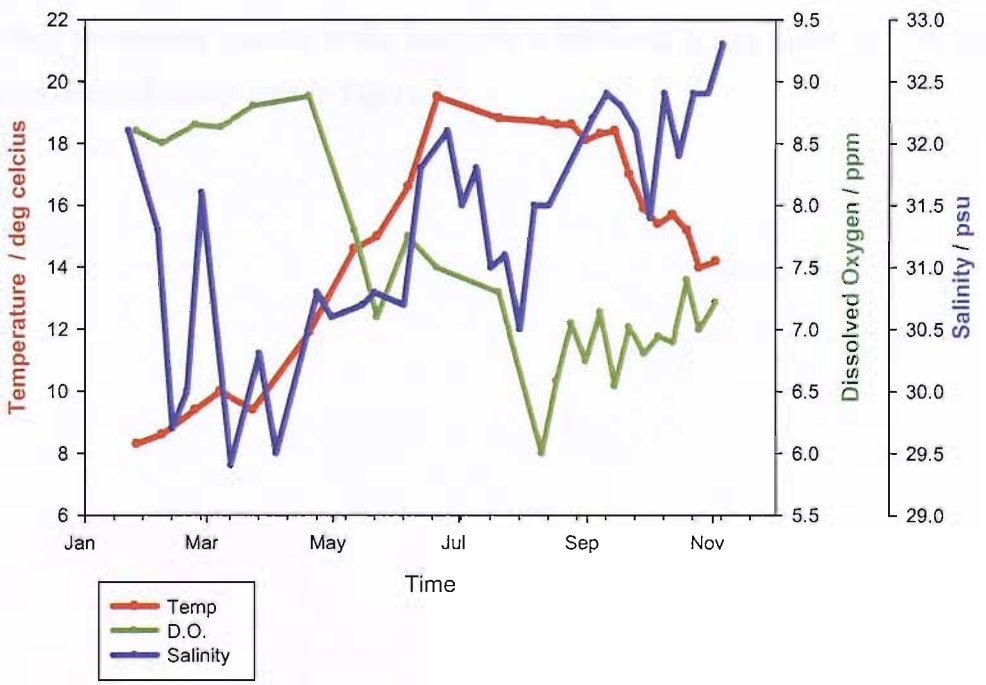

Figure 3.4 Solent water environmental parameters at 1 m depth 2007

The fluctuating salinity measurements in Fig. 3.4 especially in Feb to April are due to the fact that salinity was sampled at 9 to 9.30 each morning and so is affected by low and high tides. As the dock area is estuarine water the low tide has low salinity due to the river flowing out and high salinity with the returning sea water.

Seawater is a complex mix of salts and minerals as outlined in Table 3.3.

Constituent	**g/kg in Seawater***	**Percentage by Weight**
Chloride	19.35	55.03
Sodium	10.78	30.65
Sulfate	2.71	7.72
Magnesium	1.28	3.65
Calcium	0.410	1.17
Potassium	0.390	1.13
Bicarbonate	0.140	0.36
Bromide	0.067	0.19
Boron	0.026	0.07
Strontium	0.007	0.02
Total		99.99

*** Salinity = 35 psu**

Table 3.3 Composition of seawater, after S. Libes [3.22]

The fouling community specific to the local area is tabulated in Appendix III. The field trials were sampled as outlined in Figure 3.5.

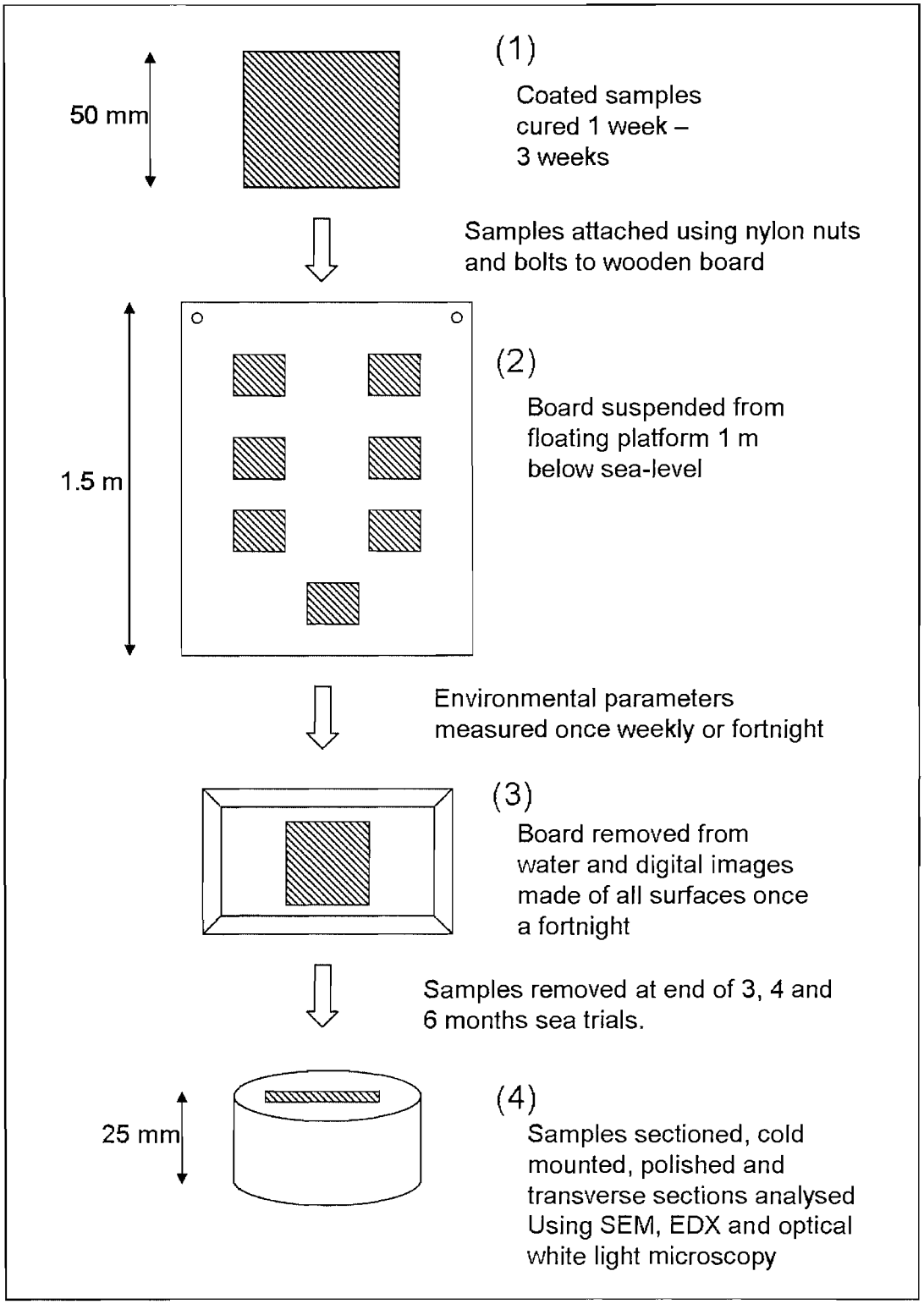

Figure 3.5 Field trial testing protocol

3.3.3 Environmental parameters

The coated samples were exposed to three different environments, fully aerated 3.5 wt % NaCl solution in distilled water, seawater from Southampton Solent brought up to the lab and the open water of Southampton Solent. Oceanic parameters such as salinity and temperature were recorded by the National Oceanography Centre at the pontoon using a

Microprocessor Conductivity meter (Tetracon LF323). The dissolved oxygen content both at the raft exposure site and laboratory was measured using a hand held Hanna instruments H19145 DO probe (± 1.5 % of the full scale) with a salinity compensation of 32 for all measurements. The instrument requires passage of water past the probe sensor at a minimum speed of 0.3 ms^{-1} so as to replenish the oxygen depleted at the membrane surface. pH measurements in the laboratory were made using the Combo by a Hanna waterproof probe (HI 99129). Conductivity measurements were made using ATI Orion model 162. Temperature measured in the lab using a thermometer in °C.

3.4 Microscopy & Spectroscopy

An array of microscope and imaging techniques were required to handle the multidisciplinary aspects of this project. The chemical measurements included Gas chromatography mass spectrometry (GC-MS), biological measurements included episcopic differential interference contrast (EDIC), and fourier transform infra-red (FTIR) microscopy, while the surface engineering techniques used included scanning electron microscopy (SEM), and energy dispersive x-rays (EDX) and both approaches required optical microscopy.

3.4.1 Fourier transform infra-red (FTIR) microspectroscopy

Fourier transform Infra-red (FTIR) microspectroscopy is a technique that allows for molecular interactions to be assessed. It has been used to measure potential antifouling coatings performance regarding protein adhesion [3.23]. The instrument excites vibrations in the bonds between molecules and provides characteristic IR spectra which can be used to identify key molecules and more specifically in this study the presence of a microbial community. The main advantage of this technique over others is that spectra can be obtained for proteins and in a broad range of environments and on various substrate materials including polymers.

3.4.2 Episcopic differential interference contrast (EDIC) microscopy

A modified confocal microscope was used to investigate biofilm growth. The Episcopic Differential Interference Contrast (EDIC) microscope is a facility at the Environmental Healthcare Unit, School of Biological Sciences at the University of Southampton. The first EDIC prototype was invented by Prof. Bill Keevil [3.24], and it incorporated the reconfiguration of a Nikon Labophot-2 microscope which combined an epifluorescent

attachment with differential interference contrast (DIC) illumination above the light stage. A diagram of the EDIC's optical light path is shown in Figure 3.6.

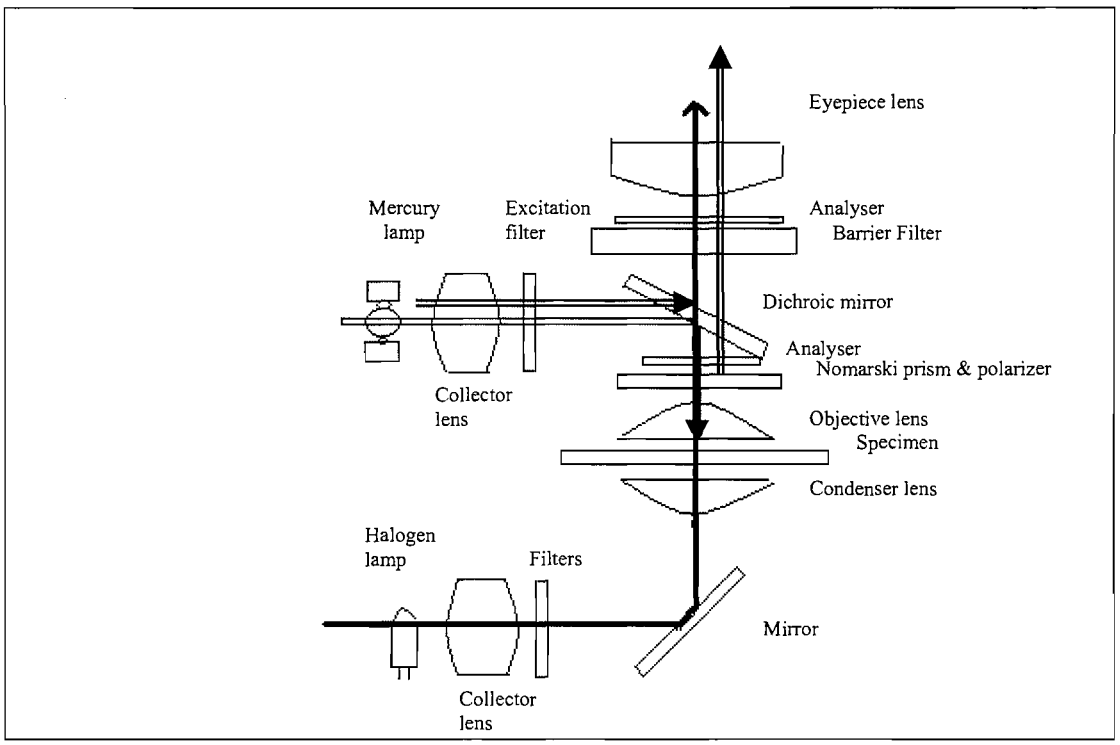

Figure 3.6 Diagram of the optical light path in an EDIC microscope, after [3.24]

The non-contact objectives of the EDIC as well as the long focal length result in the ability to observe biofilm structure accurately and without the need for additional artefacts. Due to the design of the microscopes, the samples do not need cover slips and can be viewed submerged in water, eliminating mechanical damage to the biofilm surface. The use of EDIC with epifluorescence (EF) is particularly useful for studying fouling on opaque surfaces such as metal or plastic [3.24].

3.4.3 Scanning electron microscope (SEM) and EDX

The scanning electron microscope is a powerful tool to measure the 3-D surface of the sample. A scanning electron microscopy allows for high resolution imagery. It scans a small electron beam across the sample surface and measures the density of the material. It allows for the direct sampling of elements and their percentage. The energy dispersive X-ray (EDX) technique is one way of assessing the elemental composition of the substrate. The sampling area of the beam is tear-drop shaped (Fig. 3.7). The bombardment of the

material with the electron gun gives rise to the emission of a signature x-ray for each element.

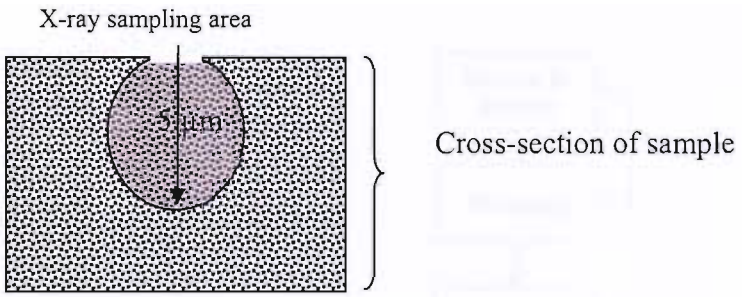

Figure 3.7 Scanning electron microscope electron gun spot size sampling area

Most electron microscopy techniques require the sample to be under vacuum however environmental SEM in the wet mode can be used as a useful tool to assess antifouling additives and coating integrity [3.25].

3.4.4 Optical microscopy

A white light microscope optical microscope fitted with a digital camera was used to image the samples. The three microscopes included a Prosilica Model GE1350C digital colour camera mounted on an Olympus Microscope BH-2, as well as a moticam 1000 digital colour camera 1.3 M pixel mounted on Olympus BH. The macroscope used was a Moticam 2000 digital colour camera 2.0 M pixel on the Wild Macroscope.

The experimental test summary is outlined in Figure 3.8 which highlights the different substrate materials, two characterisation themes, electrochemical and biofouling and the post test analysis. Each section is also shown with the corresponding chapter that addresses those aspects on the right hand side.

3.4.5 Gas chromatography – mass spectroscopy (GC-MS)

Gas chromatography mass spectrometry (GC-MS) is an analytical technique by which complex mixtures of chemicals can be separated, quantified and identified. This is key for environmental samples as many low molecular weight compounds can be identified. The ionisation technique used in this project was the electron ionisation (EI) on a Single quadrupole GC-MS Micromass platform. The chemical sample to be analysed is injected into the GC inlet in solution where it is vaporised and carried through the machine by a carrier gas. The mixture of compounds are separated in the GC column by virtue of their

affinity with the coating of the column (stationary phase) and the carrier gas (mobile phase). The compounds are then ionised and analysed by a quadrupole mass analyser.

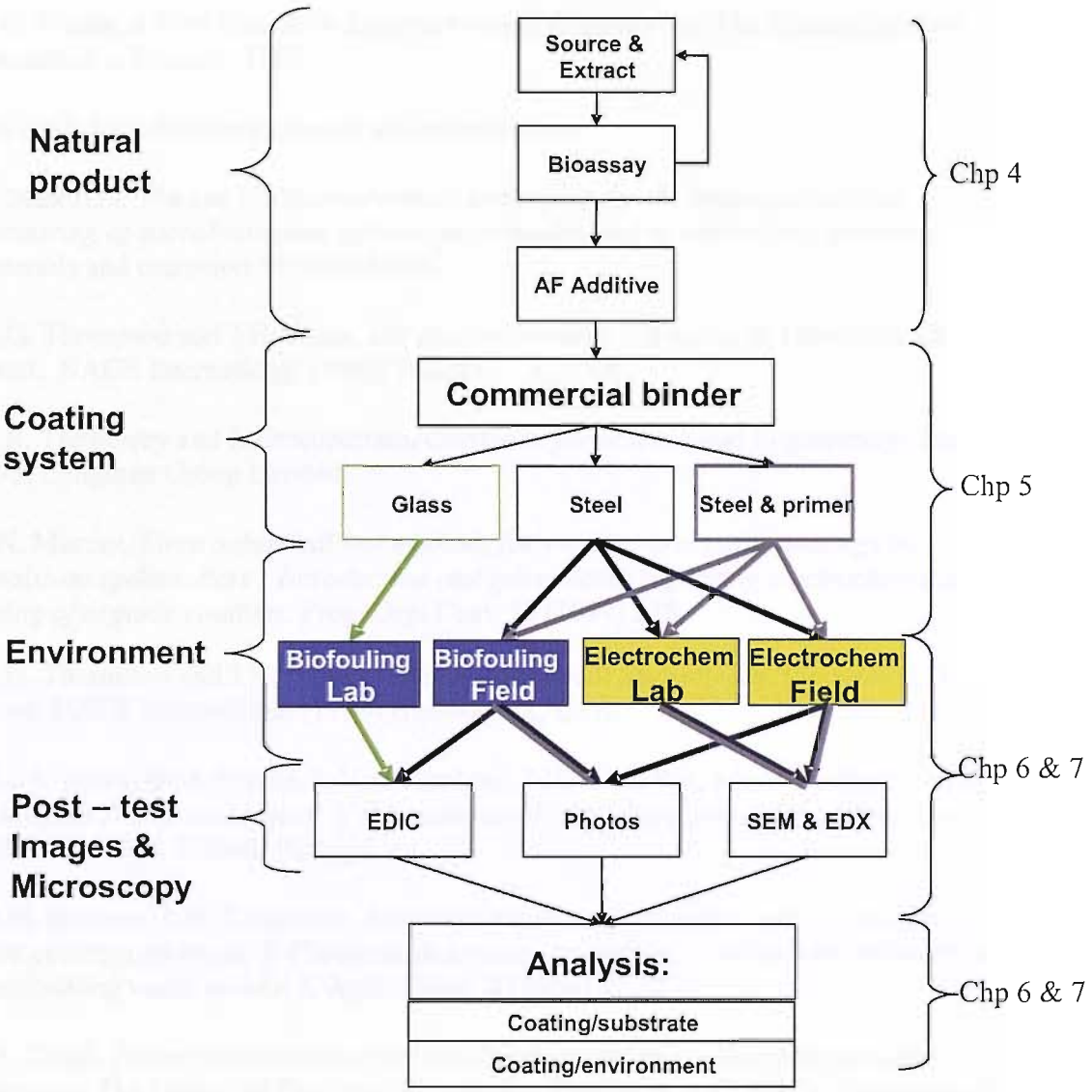

Figure 3.8 Experimental testing programme and designated chapters

3.5 References:

[3.1] F.C. Walsh, *A First Course in Electrochemical Engineering*, The Electrochemical Consultancy, Romsey, 1993.

[3.2] BS 2015:1992 Glossary of paint and related terms

[3.3] F. Mansfeld, *The use of electrochemical techniques for the investigation and monitoring of microbiological influenced corrosion and its inhibition - a review.* Materials and corrosion 54 (2003) 489.

[3.4] N.G. Thompson and J.H. Payer, *DC electrochemical test methods*, (Series ed.) B.C. Syrett, NACE International (1998) Houston TX, USA.

[3.5] K.R. Trethewey and J. Chamberlain, *Corrosion for Science and Engineering.* 2nd ed. 1995: Longman Group Limited.

[3.6] J.N. Murray, *Electrochemical test methods for evaluating organic coatings on metals: an update. Part 1 Introduction and generalities regarding electrochemical testing of organic coatings*, Prog. Org. Coat. 30 (1997) 225.

[3.7] N.G. Thompson and J.H. Payer, *DC electrochemical test methods*, (Series ed.) B.C. Syrett, NACE International (1998) Houston TX, USA.

[3.8] H.J.A. Bruer, G.M. Ferrari, J. Van Turnhout, J.H.W. de Wit, *Modern experimental techniques for the assessment of the water sensitivity of organic coatings,* Euromat, 22-24 July 1998, Lisbon, Portugal.

[3.9] D.M. Brasher, A.H. Kingsbury, *Electrical measurements in the study of immersed paint coatings on metal. I. Comparison between capacitance and gravimetric methods of estimating water uptake*, J. Appl. Chem. 4 (1954) 62-72.

[3.10] Y. Puget, *Failure mechanism of polyurethane coated steel subjected to erosion-corrosion*, The Degree of Doctor of Philosophy, Engineering Materials, University of Southampton, 1999.

[3.11] O. Ferraz, E.Cavalcanti and A.R. Di Sarli, *The characterisation of protective properties for some naval steel/polymeric coating/3% NaCl solution systems by EIS and visual assessment.* Corrosion Science, 37 (1995) 1267.

[3.12] J.C. Rowlands and D.J. Cutter, *A.C. Impedance measurements on marine paint systems*, Corrosion science, 23 (1983) 331-340

[3.13] H.P. Hack and J.R. Scully, *Defect area determination of organic coated steels in seawater using the breakpoint frequency method*, J. Electrochem. Soc., 138 (1991) 33.

[3.14] G. Grundmeier W. Schmidt, M. Stratmann *Corrosion protection by organic coatings: electrochemical mechanism and novel methods of investigation* , Electrochemica Acta 45 (2000) 2515-2533.

[3.15] Amirudin, A. and D. Thierry, *Application of electrochemical impedance spectroscopy to study the degradation of polymer-coated metals. Progress in Organic Coatings* 26 (1995) 1-28.

[3.16] J-T. Zhang, J-M. Hu, J-Q. Zhang, C.N. Cao, *Studies of water transport behaviour and impedance models of epoxy-coated metals in NaCl by EIS*, Progress in Organic Coatings, 51 (2004) 145.

[3.17] S.A Kumar, T.Balakrishnan, M.Alagar, Z. Denchev, *Development and characterization of silicone/phosphorous modified epoxy materials and their application as anticorrosion and antifouling coatings*, Progress in Organic Coatings 55 (2006) 207.

[3.18] Bressy C, Hugues C, Margaillan A (2008), *Characterization of chemically-active antifouling paints using Electrochemical Impedance Spectrometry and erosion tests*, Prog Org Coat, in press. DOI: 10.1016/j.progcoat.2008.07.014.

[3.19] B.Watermann, B. Daehne, S. Sievers, R. Dannenberg, J.C. Overbeke, J.W. Klijnstra, O. Heemken, *Bioassays and selected chemical analysis of biocide-free antifouling coatings,* Chemosphere, 60 (2005) 1530-1541.

[3.20] T. Matsunaga, T.K. Lim, *Electrochemical prevention of biofouling*, Electrochemistry 68 (11) (2000) 847-852.

[3.21] I.B. Beech, *Corrosion of technical materials in the presence of biofilms-current understanding and state-of-the art methods of study*, Int. Biodeter. Biodegrad. 53 (2004) 177-183.

[3.22] S.M. Libes, An Introduction to Marine Biogeochemistry, John Wiley and Sons, Inc. Canada (1992).

[3.23] M. Müller, T. Rieser, K. Lunkwitz, J. Meier-Haack, *Polyelectrolyte complex layers: a promising concept for antifouling coatings verified by In-situ-ATR-FTIR Spectroscopy*, Macromol. Rapid Commun. 20 (1999) 607-611.

[3.24] C.W. Keevil, *Rapid detection of biofilms and adherent pathogens using scanning confocal laser microscopy and episcopic differential interference contrast microscopy.* Water Science and Technology 47(2003): 105-116.

[3.25] F. Fay, I. Linossier, V. Langlois, D.Haras, K.Vallee-Rehel, *SEM and EDX analysis: Two powerful techniques for the study of antifouling paints*, Progress in Organic Coatings 54 (2005): 216-223.

Chapter 4 Natural product antifoulant

This Chapter covers the areas highlighted in red on Figure 1.4 below which include the sourcing and choice of natural product as well as its extraction. It also demonstrates the isolated extracts antifouling efficacy through bioassays against micro and macro marine biofouling organisms.

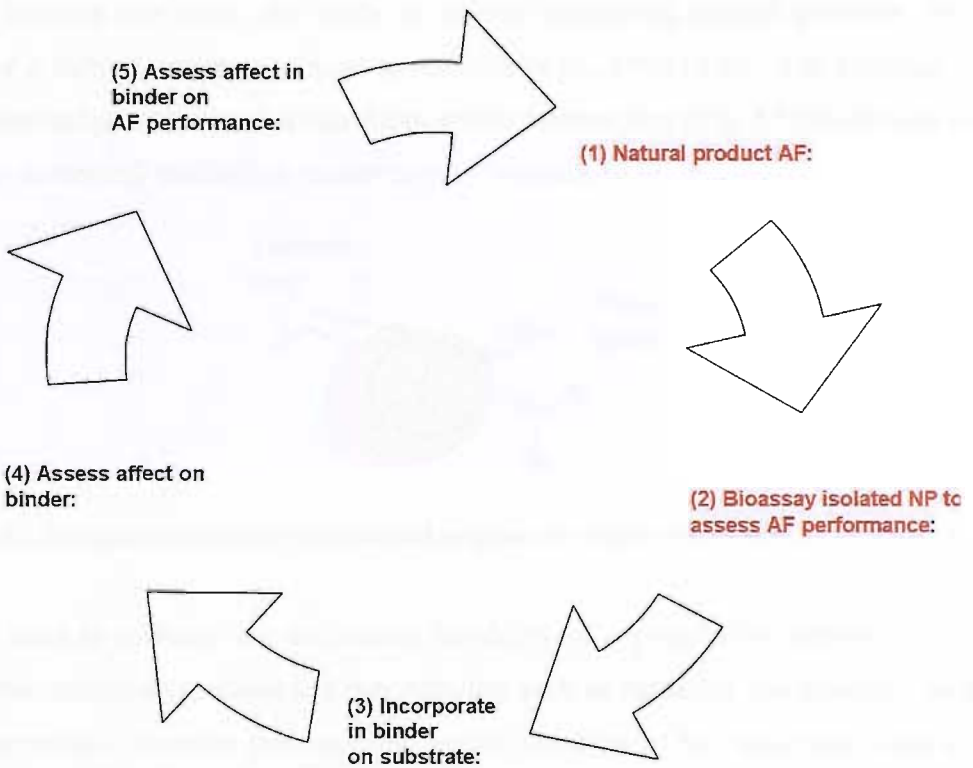

Figure 1.4 Key tests to optimise an NP-based antifouling system

This chapter aims to:

(1) Identify the natural product antifoulant sources

(2) Extract the natural product

(3) Outline procedures for the bioassay of the natural product and present results

4.1 Natural products introduction

Natural products can function as antifoulants through different methods including the dissolution of the organisms' adhesives, interference with metabolism, inhibition of settlement, inhibition metamorphosis or growth (allelopathy) or the promotion of negative chemotaxis [4.1] and surface energy modifiers [4.2-4.4]. They can also act as repellents and biocides. Antifouling marine natural products have been classified by their biosynthetic pathways into five main compounds, terpenoids (isoprenoids), steroids and saponins, fatty acid-related, bromotyrosine derivatives and heterocyclic compounds. Chemical features that unify the study of marine antifouling natural products are the presence of a lactone moiety as found by de Nys et al., 1995 [4.5]. The presence of a specific chemical structure such as the furan and/or lactone ring (Fig. 4.1) is claimed to be a feature in successful antifouling marine natural products [4.6].

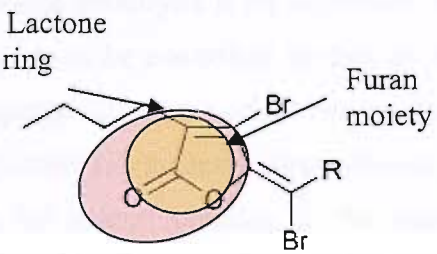

Figure 4.1 Chemical structure of the natural product furanone where R = Br or R=H [4.7]

A method used to evaluate the antifouling capability of a prospective deterrent is often through settlement assays, where key macrofoulers such as barnacles and algae are used to test for percentage coverage and removal, mussel attachment has also been used as an indication of success [4.8].

Antifouling systems, coatings or products with biochemical repellents are deemed non-agricultural pesticides by the Advisory Committee on Pesticides (ACP) [4.9] for the United Kingdom. This makes the approval of new compounds expensive and time consuming. One way of designing new tin-free non-toxic alternatives is through the use of biomimetics. Natural defence mechanisms fall into two key biological groups, autogenic and xenogenic. Autogenic are those produced by the individual to protect its own body surface and xenogenic is where the individual is protected by the characteristics of neighbouring individuals.

4.2 Issues with natural products

Presently, the working life of TBT-based paints is 5 years and this has proven to be difficult to match. The reasons for this include the fact that as described in section 2.4.2 an increased tolerance to copper has been reported for a select group of algae [4.10] and the effectiveness and environmental acceptability of booster biocides is under scrutiny. Natural products are also classified as a biocide and as such come under extensive legislation such as the biocide product directive (98/8/EC) in the EU, and the environmental protection agency in the US.

One of the key issues investigated in this thesis is the possible loss of coating system functionality caused by encapsulation/embedding of natural product extracts. The natural solubility and degradation through photolysis is an important consideration in the use of natural products. Delivery needs to be controlled so that the antifoulant is not leached from the binder matrix too rapidly. If release of the natural product from an antifouling system can be controlled, its potential as an antifouling technology increases dramatically. Tested delivery mechanisms for natural products in the marine environment include microencapsulation techniques as this allows a controlled release, permitting the work-life of the protective coating to be increased. However, before adapting the delivery mechanism we must first characterise the affect that a natural product antifoulant may or may not have on the binders and other compounds within the paint system. In this manner a step wise approach can be used to alter or advance the coating technology. The use of an already existing top-coat system allows for compliance with application procedures and underlying coatings. This is a conservative approach that clearly facilitates the development of an economical coating system. This was why a control depletion polymer was used to incorporate the NP. Before getting to this stage, first the NP needed to be sourced, extracted and tested using a bioassay for antifouling efficacy.

4.3 Natural product source

In section 2.4.4 the distribution of animals from which potential antifouling natural products have been extracted are shown. The wide range of animals with defence mechanisms requires a choice to be made. A key driver for the use of algal extracts in this project is that algae are cultivable, relatively easy to harvest and the extract yield is high. Algal extracts therefore represent cost effective alternative AF compounds and are an

attractive source for a commercially viable product. Algae are often sedentary and therefore act as a biomimetic solution for static ship operational profiles. Some algae can tolerate exposure out of the marine environment and a ships hull would mimic this exposure/immersion at the waterline or splash zone.

Annual global seaweed aquaculture production is approximately 6.9 Mt fresh weight, 4.3 % of which is produced by Europe [4.11]. Due to the high volume of production this is an attractive antifoulant source (cheap/high volume). Hydrocolloids are a significant product of this industry. Carageenans from red seaweeds such as *Chondrus crispus* are a processed hydrocolloid source.

4.4 Natural product antifoulant

"The challenge is to characterize a natural product with low toxicity, stable in a paint formulation, biodegrable when released, with broad-spectrum activity and which can be obtained in commercially relevant quantities either by chemical synthesis, recombinant technologies and culture" [4.12]. The choice of seaweed *Chondrus crispus* (Class Rhodophyceae) as the source phylum was based on the literature survey (Fig. 2.6), and the specific species on its availability and previous bioassays [4.13]. Furthermore, extracts of *C. crispus* have shown promising inhibitory activities on the germinating spores of fouling macroalgae [4.14]. These extracts have also been found to inhibit diatoms, especially from the genus *Amphora* [4.15]. The ethanolic extract of *C. crispus* has been reported to be non-toxic to sea urchin larvae [4.16] and showed no toxic effects on lysosomal and mitogenic activities against mouse fibroblasts even up to concentrations of 1000 $\mu g\ mL^{-1}$ [4.17]. Hexose oxidase has been patented by Poulsen from the food company Danisco [4.18] for use with a precursor enzyme in an antifouling system to break down glucose and form the antifoulant hydrogen peroxide. This enzyme can be isolated from a variety of marine algae but *C. crispus* is one of the most readily available.

The isolation and synthesis of chemical compounds from a new source is a restricting factor in a three year project and limits the speed at which a coating can be developed and submerged in an exposure trial (minimum of 18 months). As cited by authors in the field of natural products 'educational goals are not served well through routine programs for isolating and screening natural products' [4.19]. In this study the crude ethanol extract is used in its entirety which provides a mixture or 'cocktail' approach to harnessing any antifoulant properties. This was done to achieve a broad spectrum activity as opposed to

using specific constituents that have activity to resist specific fouling species. The literature proves that there are specific antifouling activities of *C. crispus* extracts; our goal with this compound was to see how the crude natural product extract from a potential source for antifouling systems could function by direct incorporation into a paint matrix as part of a full antifouling system. The first step was to extract samples from the algae and compare the extracts from two different sources through bioassay performance. For the purpose of the work reported in this thesis the search for a less exotic 'commercial off the shelf' antifouling solutions was a requirement. To test the economic viability the *C. crispus* product was sampled from an industrial source as well as from a local shore as highlighted in section 4.6.1.

4.5 Natural product antifoulant characterisation

The most effective means of testing or screening antifouling compounds is through the use of bioassays. These incorporate natural population dynamics of fouling species to assess the efficiency of the bioactive compound through either settlement, behavioural rejection of surfaces or toxicity tests.

There is a wide range of antifouling bioassaying techniques which are reviewed by Dahms and Hellio [4.20]. Settlement assays are a common method used to evaluate the antifouling capability of a prospective deterrent, where key macrofoulers such as barnacles and algae are used to test for percentage coverage and removal. Mussel attachment has also been used as an indication of success [4.8]. Microfoulers such as biofilm formation and bacteria counts can be quantified using luminescent bacteria tests [4.21] and nucleic acid stains [4.22]. However, direct comparisons of the performance data of antifouling coatings are complicated as a result of inconsistencies with the materials and methods used to measure new compounds and surface coating properties.

Testing of potential natural products for marine antifouling is usually through a series of bioassays and toxicity tests [4.13, 4.18, 4.23]. The choice of species to assay can greatly affect the comparative success of an experimental coating. The seasonal and bio-geographical variance of shipping paths means that an antifouling compound that is effective in temperate water may be ineffective in tropical waters due to the variety of species present. Therefore, it is important to test the antifouling efficacy against a broad spectrum of organisms and marine environments. Settlement as well as growth bioassays are needed.

Initially it was necessary to measure the antifouling activity of the natural product (NP) extracted from the red seaweed *Chondrus crispus*. This was done by completing a bioassay of isolated crude ethanolic extract concentrations against a range of organisms. The extraction procedures are detailed in the following section. Extracts were also immobilised on to glass slides and incorporated into coating systems on steel which were trialled in the open ocean, discussed later in Chapter 7. First the efficacy of the natural product extract had to be verified against key fouling species.

4.5.1 Extraction

Dried seaweed was purchased from Carraig Fhada Seaweed which is harvested from the north Atlantic off the coast of Ireland, washed in clean water and dried in the sun (extract A). Samples harvested in spring 2007 from Calshot UK (Latitude: 50.809298 Longitude: -1.306901) were also investigated (extract B). Whole algae samples excluding the holdfast were used and prepared by washing with distilled water and ethanol and then dried 24 h. The extraction methodology was based on that used by Hellio et al. [4.23]. 200 g dried seaweed was dispersed in 300 mL ethanol 95 % using a general purpose disintegrating head for 5 minutes at 3000 rpm then 4000 rpm was used for a further 15 minutes. The temperature of the algae-ethanol solution ranged from 20-35 °C. Filtration was carried out under vacuum, passing the solution through a Whatman glass microfibre filter with 12 μm size pores. The ethanol was evaporated using a rotary evaporation under vacuum, in light, where the water bath temperature was maintained below 32 °C. Ethanol was used as the extraction solvent as this was found to have a better yearly antifouling activity then the dichloromethane and aqueous extracts [4.13].

4.5.2 Bioassay

The ethanol algal extract from a dried source (A) and a locally harvested source (B) were prepared in 96-well plates made of clear polystyrene from Fisher Scientific. Plates with extract were prepared using a gradient in a range of concentrations of 0.1, 1, 10, 25 and 50 $\mu g\ mL^{-1}$. Each extract concentration and control was replicated 6 times i.e. 6 wells were filled with each concentration. The extract was prepared in concentrations of 70 % ethanol, pipetted into the plate as shown in (Fig. 4.2) and dried under vacuum in a sterilised UV environment.

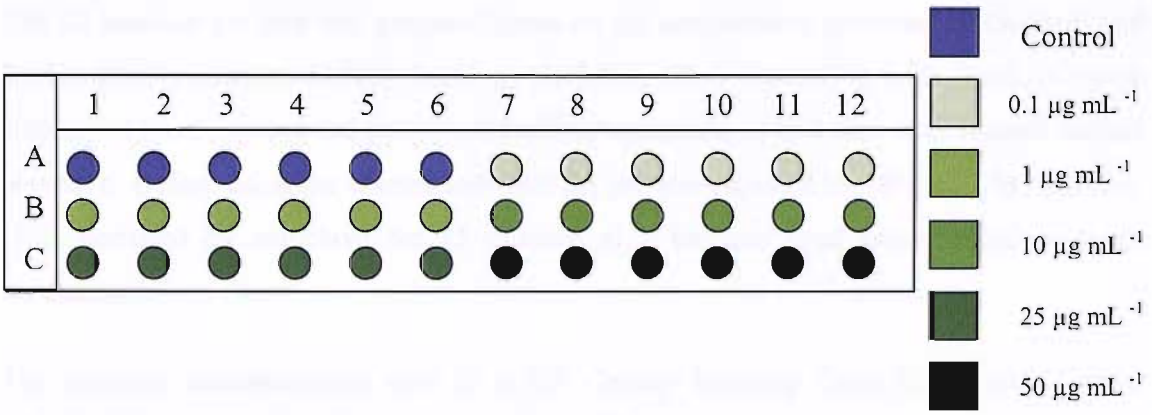

Figure 4.2 Schematic of a 96-well plate and concentration regime used for bioassays

4.5.2.1 Microfouler bioassay

Five marine bacterial strains *Pseudoalteromonas elyakovii, Vibrio estuarius, Polaribacter irgensii, Halomonas marina, Shewanella putrefaciens* and five phytoplankton strains *Chlorarachnion reptans, Cylindrotheca cloisterium, Exanthemachrysis gayraliae, Navicula jeffreyi, Chlorarachnion globosum* were provided from the culture collection of the University of Portsmouth. All the microorganisms used were representative of fouling species in both estuarine and marine environments. Marine bacteria were cultivated in marine broth (5% Tryptone in filtered seawater) and assayed based on Marechal et al., 2004 [4.24]. The bacterial strains were incubated for 5 days at 30 °C and all of the microalgae species were cultured in f/2 medium for 5 days prior to use.

(1) Trace elements (chelated) per litre stock solution	**concentration / g**
Na_2 EDTA	4.160
$FeCl_3.6H_2O$	3.150
$CuSO_4.5H_2O$	0.010
$ZnSO_4.7H_2O$	0.022
$CoCl_2.6H_2O$	0.010
$MnCl_2.4H_2O$	0.180
$Na_2MoO_4.2H_2O$	0.006
(2) Vitamin mix stock solution	
Cyanocobalamin (Vitamin B12)	0.0005
Thiamine HCl (Vitamin B1)	0.100
Biotin	0.0005

Table 4.1 Compounds in f/2 medium used to culture bacteria and micro-organisms

The f/2 medium per litre was prepared based on the composition proposed by Guillard and Ryther [4.25], namely; $NaNO_3$ 0.075 g, $NaH_2PO_4.2H_2O$ 0.00565 g with 1 mL of stock solution (1) and (2) as listed in Table 4.1. This was made up to 1 litre with filtered natural seawater. Before using the filtered seawater the pH was adjusted to 8.0 with 1 M NaOH or HCl, sterilised by autoclave for 15 minutes at 1 bar and used once cooled to room temperature.

The bacterial concentrations used (2 x 10^8 Colony Forming Units (CFU) mL^{-1}) were calculated by measuring the optical density (O.D.) using a spectrophotometer at 630 nm wavelength which can measure light intensity. This can then be converted using the Amsterdam 1996 [4.26] equation as outlined in Table 4.2. Once the corrected dilutions of the bacteria were made, 50 µL were added to the prepared 96-well plates under aseptic conditions and incubated for 48 h at 30 °C.

Optical density at 630 nm	Volume of the bacterial solution / µL to add to 10 mL of culture medium
0.20	50
0.25	40
0.30	33
0.35	29
0.40	25
0.45	22
0.50	20
0.55	18
0.60	16
0.65	15

Table 4.2 Conversion of optical density measurements to µL to gain known concentration of bacteria

The microalgae bioassay used here was based on Plougerne et al. [4.27]. A known volume of microalgae in a culture medium was passed through a 0.2 µm glass filter paper. This filter paper was then added to a known volume of acetone and macerated to liberate the pigment. A 1-cm cell cuvette was filled with the pigment – acetone solution and placed in a spectrophometer to measure the optical density. The concentration of microalgae was assessed using the Lorenzen equation, seen in eq 4.1 [4.28], by calculating the *chlorophyll a* content.

$$Chl\ a\ [\text{mg m}^{-3}] = (11.6\ D_{665} - 1.31\ D_{645} - 0.14\ D_{630})\ v\ l^{-1}\ V^{-1} \quad (4.1)$$

Where v is the volume of acetone (ml), l is the cuvette cell length (cm), V is the volume of filtered microalgae solution in (L) and D_{665}, D_{645} and D_{630} are the optical density measurements at the varying wavelength (nm) denoted as a subscript. The three wavelength measurement technique is known as a tri-chromatic method and from these parameters the *chlorophyll a* content *Chl a* can be calculated. Dilutions were then made to achieve 1 mg L^{-1} *chlorophyll a*. Additions of 50 µL solution were made to the prepared extract treated 96-well plates and the inoculated plates were placed in a light/dark (18/6 h) growth room for 3 days. After the incubation period both the bacteria and microalgae plates were visually assessed for antifouling activity and the minimum inhibitory concentration (MIC) recorded. An inhibitory activity was designated when 3 or more of the 6 replicate wells showed no signs of growth. Growth was observed in all 6 wells of the control.

4.5.2.2 Macroalgae bioassay

Two macroalgae were used to test the efficacy of the extracts. *Undaria* sp. (Phaeophyta) seaweed alien species to the south of England [4.29] and *Ulva* sp. (Chlorophyta) which is a synonym with *Enteromorpha* sp. [4.30]. It is a native U.K. fouling alga and is a common antifouling test species [4.31, 4.32]. The macrofouling bioassay procedure was based on Fletcher 1989 [4.31] (Fig 4.3). Both algal plants were collected from the intertidal region of Southsea Portsmouth in May/June 2007. Fragments of the seaweed frond were placed into a repli-dish with Von Stosch solution where cell viability and concentration were then determined (Fig 4.3). Von Stosch solution was made from 5 L of twice pasteurised seawater (73 °C) and 5 ml of Na_2EDTA, NA_2HPO4, $FeSO_4$, $NaNO_3$, $MgCl_24H_2O$ and vitamins. The viability of the spores was assessed by their movement away from light under the microscope. A Haemocytometer was used to measure the concentration of algal zoospores in the Von Stosch solution. 10 counts were made showing 2.5 spores per 20 nL for *Ulva* sp. and 4.2 spores per 20 nL for *Undaria* sp. which is 10500 per 50 µL.

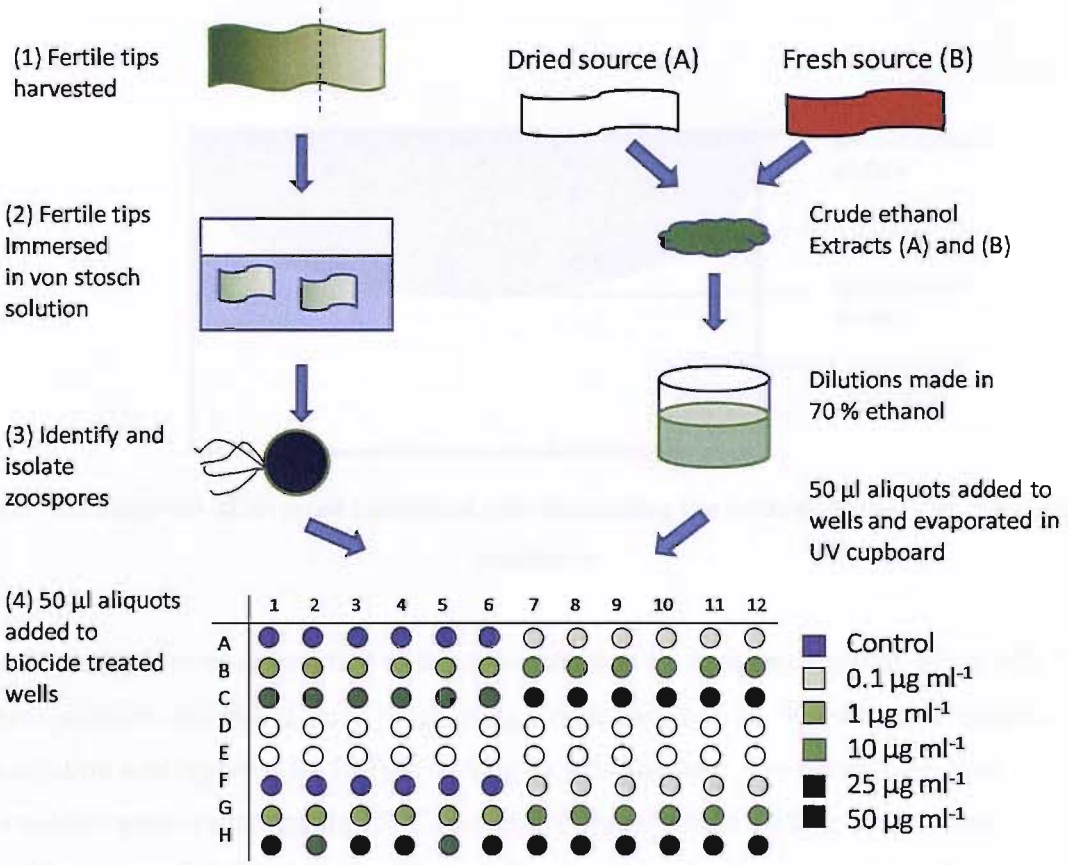

Figure 4.3 Flow chart for the process of 96-well plate treatment with extracts and bioassay, adapted from Fletcher [4.31]

A range of concentrations tested using Extract A was 4, 40, 400, 1000, 5000 µg mL^{-1} while extract B was tested using 0.1, 1, 10, 25 and 50 µg mL^{-1}. A wider range of concentrations were used to test the algae extract A to better understand its range of performance. The prepared 96-wells were inoculated with 50 µL of spore solution and covered in darkness for 3 hours. Wells were inverted after 1 hour to increase the robustness of the experiment i.e. causing the spores to preferentially swim towards the settlement surface not just fall to the bottom of the well (Fig 4.4) (Fletcher 2007, personal communication). When inverted the spore solution formed a droplet and remained covering the base of the well through surface tension.

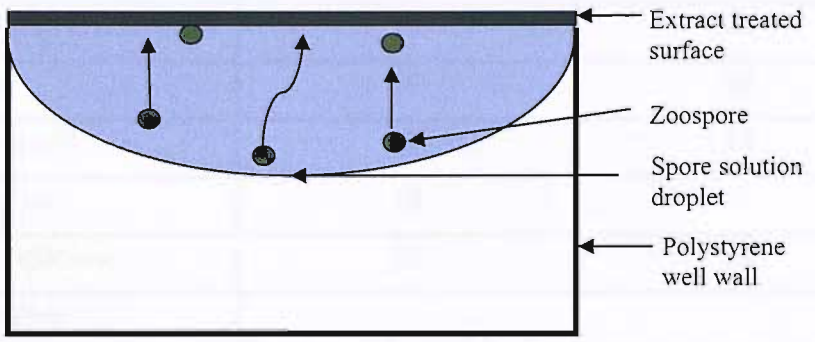

Figure 4.4 Diagram of inverted individual well illustrating the settlement assay of macroalgae zoospores

The 96-well plates were emptied of the spore solution by a vigorous shake, filled with Von Stosch solution and rinsed three times using a pipetting motion, this was then emptied and the solution was replaced by 100 µL of Von Stosch solution. The plates were then laid out in a control room (temperature 15 °C) under UV lights with a 14/8 hr on/off timer. After 4 days (*Undaria sp*) and 5 days for *Ulva sp*, 50 µL of Von Stosch solution was removed and replaced with 10 % formalin to stop further germination. The samples were viewed using an optical microscope 20 x magnification. Counts were made in 10 different fields of view in three different wells of the same extract concentration (n = 30). *Undaria* spores were considered to be germinating if a minimum of two cells were visible. *Ulva* spores were considered to be germinating when the germ tube was twice as long as the spore diameter of 5 µm [4.31].

4.5.3 Results

The micro-fouler bioassay results are shown in Table 4.3. Extract A had lower minimum inhibitory concentrations then extract B with activity against 6 out of the 10 organisms at 10 µg mL^{-1}. The results show that the minimum inhibitory concentrations for the five bacterial strains were as low as 1 µg mL^{-1} and no greater then 25 µg mL^{-1} for extract A. Only one species of bacteria *H. marina* was completely resistant to extract B.

Bacteria species	Extract A MIC / μg mL^{-1}	Extract B MIC /μg mL^{-1}
Pseudoalteromonas elyakovii	10	25
Vibrio estuarius	25	50
Polaribacter irgensii	10	25
Halomonas marina	10	-
Shewanella putrefaciens	25	25
Microalgae species		
Chlorarachnion reptans	10	25
Cylindrotheca cloisterium	1	10
Exanthemachrysis gayraliae	10	10
Navicula jeffreyi	25	25
Chlorarachnion globosum	25	10

Table 4.3 Minimum inhibitory concentrations for *C. crispus* ethanol extracts from (A) dried source and (B) fresh source against key microfoulers

The effect of varying concentrations of extract A and extract B against the percentage germination of spores for both *Undaria* and *Ulva* are shown in Fig 4.5 and 4.6 respectively.

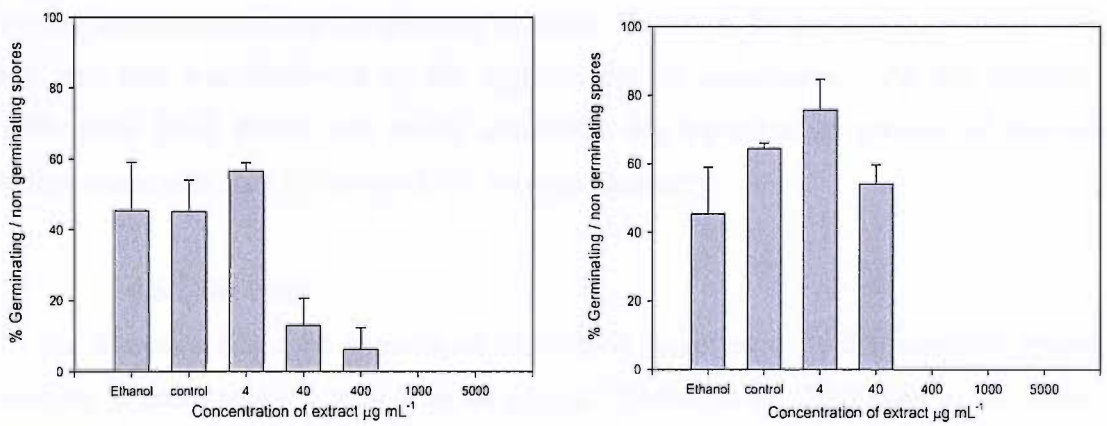

(a) (b)

Figure 4.5 Extract (A) germination resistance against (a) *Undaria* and (b) *Ulva* spores. Means of n=30 plotted with standard deviation error bars

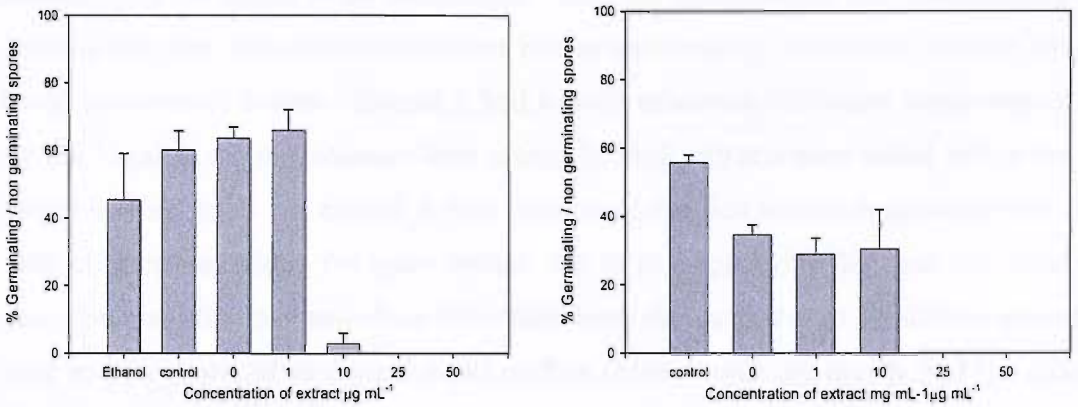

(a) (b)

Figure 4.6 Extract B germination resistance vs. (a) *Undaria* and (b) *Ulva* spores. Means of n=30 plotted with standard deviation error bars

Due to the range of tested extract A concentrations being higher then B their relative performance against two key macrofoulers can not be directly compared. However, for *Undaria* spores there was a low germination percentage (~ 15 %) at concentrations of 40 µg mL^{-1} for extract A and no germination at concentrations of 25-50 µg mL^{-1} for extract B, indicating an antifouling effect at similar concentrations.

4.6 Discussion

4.6.1 Extraction

As noted by Savary et al., 2001 the air-dried fronds of the fresh harvested seaweed tended to clog the screens during the grinding process. However, the packaged air dried samples did not; this was attributed to the higher level of desiccation. As the crushing of sufficiently dried fronds was easily achievable the lypholisation process of the fronds before extraction used by Savary 2001 was not necessary.

4.6.2 Bioassay

In the literature ethanolic extracts of *C. crispus* inhibited 6 of the sensitive strains of bacteria at concentrations as low as 24 µg mL^{-1} (Hellio et al., 2001) and in this study no greater then 25 µg mL^{-1} for extract A inhibited growth against all five bacterial strains. To put this into an industrial context the minimum inhibitory concentrations against a range of bacterial strains for TBTO and $CuSO_4$ have been calculated to be 6 µg mL^{-1} (Hellio et al., 2001). The algal extracts inhibited germination of the macroalgae at concentrations of 40 µg mL^{-1} (extract A) and 10-25 µg mL^{-1} (extract B). Both extracts showed a lower inhibiting concentration against the *Undaria* spores than *Ulva* suggesting an increased

sensitivity of the spores to the antifoulants. Both the microfouling and macrofouling assay indicate that the crude ethanolic extract has an encouraging antifouling activity against a broad spectrum of foulers. Extract A had a lower minimum inhibitory concentration at 25 $\mu g\ mL^{-1}$ against the microfoulers than extract B. Both extracts were tested within the paint matrix in field trials but extract A was considered the best option to proceed with and to fully characterise within the paint system due to its good antifouling activity against the microfoulers. Microbial and slime films have been shown to lead to significant increases in drag and powering of mid-sized naval surface ships at cruising speeds [4.34]. Although the end goal is to prevent all types of foulers, by being a broad spectrum antifoulant to the microfouling assemblage as initially exhibited by the extract A, there exists a greater chance of potentially resisting higher foulers.

The philosophy behind investigating a crude extract is that it may have an ecological role as the chemical defence mechanisms by organisms may function as mixtures of natural products as seen with terpenes [4.35]. The crude extract has potential as it contains multiple components which may mimic a natural world solution closer then an isolated fraction. Evolutionary reasons for employing a multicomponent defence mechanism include broad spectrum activity and/or a reduction in the evolutionary possibility of species adapting or gaining a resistance [4.35]. The affects of a crude natural product are hypothesised here as being synergistic. The synergy implies that the mixture of compounds has a greater broad spectrum affect then the isolated extracts. Although there are a wealth of compounds in the crude extract, antifouling activity can be attributed by the bioassay results to the whole cell extract. Good antifouling activity was obtained by the crude NP extract so this was the starting antifoulant composition used to investigate the NP-coating system. Shortage of time precluded further studies into the functionality of each fraction of the extract. Now that the NP antifoulant has shown an antifouling efficacy the next question to answer was could it be incorporated into a coating, if so what affects did it have to the binder and what antifouling performance if any could be detected. These aspects are investigated in Chapter 6.

The GCMS spectra for the dried Algal NP extract 'A' is shown in Figure 4.7. This chemical characterisation of the antifoulant agent shows a wide range of peaks. This is most probably due to the wide range of metabolites in extract A, as a result the GC-MS spectrum was possibly masking specific peaks beneath wider signal bandwidths.

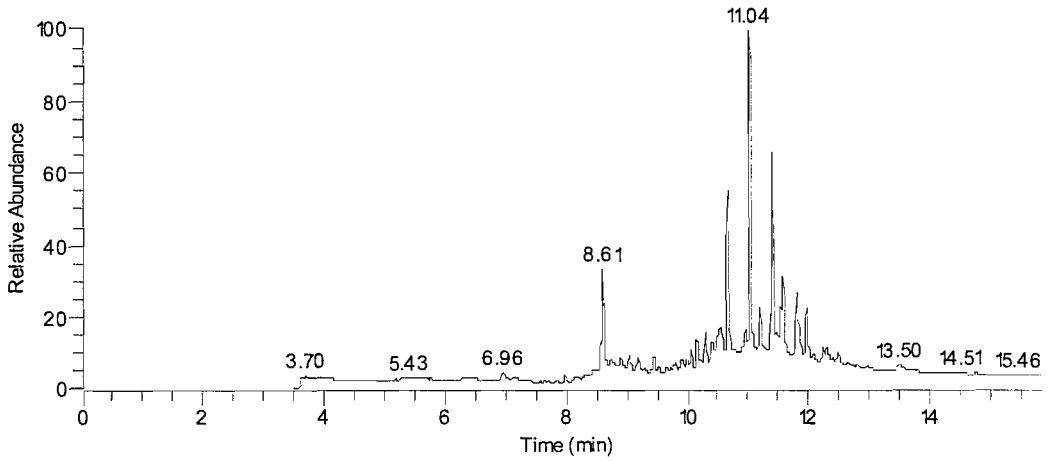

Figure 4.7 GC-EIMS - Electron Ionisation mass spectrometry of algal NP

A wide range of compounds were retrieved from the GC-MS library for the spectra and Table 4.4 lists the key compounds and their confidence level as a percentage (out of 100%). Important to note that terpenes are key defence metabolite and are present in the extract.

Compound	Percentage	CAS #	Additional information
Withaferin A	63.70%		Found in the Solanaceae family of plants, potent angiogenesis
Dodecanoic acid			Aliphatic acid - fatty acid occurring as glycerides
Gibberellic acid	72.50%	510-50-9	Homorone found in plants
Thunbergol	73.60%	25269-17-4	Terpenoid
Retinoic acid	69.70%	339-16-2	Vitamin A

Table 4.4 Compounds from GC-Electron Ionisation mass spectrometry of algal NP extract

4.7 Conclusions

- The ethanol extract of the red algae *Chondrus crispus* was selected as the natural product source which coupled antifouling potential with economic viability as it is an industrially aquacultured. Algal extract A (dried source) had a greater antifouling efficacy then extract B against microfoulers at 25 $\mu g\ mL^{-1}$.

- The dried source has the better antifouling efficacy from the microfouler bioassay tests which suggests that the product had a longer shelf and therefore could be more economical.
- Macroalgae tests indicate that the natural product has an anti-germination activity
- The combination of bacteria, microalgae and macroalgae as bioassay organisms provided a broad range of fouling specific species which the natural product was shown to have antifouling activity against.
- Crude ethanol extracts had a good antifouling activity so the natural product investigated in this thesis is a whole cell extract. It is hypothesised here that this approach will harness the combination effect seen in natural systems and therefore its broad spectrum activity. This is further confirmed with GC-MS spectra showing a mixture, including a hormone and a terpene.

4.8 References

[4.1] M.J. Cowling, U.T. Hodgkiess, A.C.S. Parra, M.J. Smith, S.J. Marrs, *An alternative approach to antifouling based on analogues of natural processes* Sci. Total Environ. 258 (2000) 129-137.

[4.2] A.S. Clare, *Marine natural product antifoulants: status and potential.* Biofouling, 9 (1996) 211-229.

[4.3] A.R. Davis, N.M. Targett, O.J. McConnell, C.M. Young, *Epibiosis of marine algae and benthic invertebrates: natural products chemistry and the mechanisms inhibiting settlement overgrowth.* In: P.J. Scheuer (ed) Bioorganic Marine Chemistry, Vol. 3. Springer-Verlag, Berlin (1989) p. 85.

[4.4] D. Rittschof, *Natural product antifoulants: one perspective on the challenges related to coatings development.* Biofouling, 15 (2000) 119-127.

[4.5] R. De Nys, P.D. Steinberg, P. Willemsen, S.A. Dworjanyn, C.L. Gabelish, R.J. King, *Broad spectrum effects of secondary metabolites from the red alga delisea pulchra in antifouling assays.* Biofouling, 8 (1995) 259-271.

[4.6] A.S. Clare, *Towards nontoxic antifouling.* J. Mar.Biotechnology, 6 (1998) 3.

[4.7] N. Fusetani, *Biofouling and antifouling.* Nat. Prod. Rep. 21 (2004) 94-104.

[4.8] A. Nishida, K. Ohkawa, I. Ueda, H. Yamamoto, *Green mussel Perna viridis L.: attachment behaviour and preparation of antifouling surfaces*, Biomolecular Engineering, 20 (2003) 381.

[4.9] Advisory Committee on Pesticides, *A guide to pesticide regulation in the UK and the role of the advisory committee on pesticides*, D.E.F.R.A. Affairs, Editor. 2003, Health and Safety Executive.

[4.10] N. Voulvoulis, M.D. Scrimshaw, J.N. Lester, *Comparative environmental assessment of biocides used in antifouling paints*, Chemosphere 47 (2002) 789.

[4.11] Michael D. Guiry (2006) National University of Ireland Galway, Source: http://www.seaweed.ie/aquaculture/WorldProduction.lasso. Accessed [07-09-06].

[4.12] Maréchal in Advances in Marine Antifouling Coatings and Technologies, Ed. C. Hellio and D. Yebra, In Press.

[4.13] C. Hellio, C. Simon-Colin, A.S. Clare, E. Deslandes, *Isethionic acid and floridoside isolated from the red alga, Grateloupia turuturu, inhibit settlement of Balanus amphitrite cyprid larvae,* Biofouling, 20 (2004) 139-145.

[4.14] C. Hellio, J. Pascal Berge, C. Beaupoil, Y. Le Gal, Y. and N. Bourgougnon, *Screening of marine algal extracts for anti-settlement activities against microalgae and macroalgae.* Biofouling 18 (2002) 205-215.

[4.15] S. Jackson, *Microalgae: their status as fouling organisms.* Oebalia 17 (1991) 295–303.

[4.16] C. Hellio, G. Bremer, A. Pons, Y. Le Gal, N. Bourgougnon *Inhibition of the development of microorganisms (bacteria and fungi) by extracts of marine algae from Brittany (France),* J. Appl. Microbio. and Biotech., 54 (2000) 543-549.

[4.17] C. Hellio, J-P Marechal, B. Véron, G. Bremer, A.S. Clare, Y. Le Gal, *Seasonal variation of antifouling activities of marine algae from the Brittany coast (France),* Mar. Biotechnol. 6 (2004) 67-82.

[4.18] C.H. Poulsen, K.M. Kragh, Danisco, Antifouling composition, Patent EP1282669, 2003.

[4.19] R.L. Townsin, *The ship hull fouling penalty,* Biofouling, 19 (Supplement) (2003) 9.

[4.20] Dahms and Hellio in Advances in Marine Antifouling Coatings and Technologies, Ed. C. Hellio and D. Yebra, In Press. (2009)

[4.21] B.Watermann, B. Daehne, S. Sievers, R. Dannenberg, J.C. Overbeke, J.W. Klijnstra, O. Heemken, *Bioassays and selected chemical analysis of biocide-free antifouling coatings,* Chemosphere, 60 (2005) 1530-1541.

[4.22] T. Matsunaga, T.K. Lim, Electrochemistry 68 (11) (2000) 847.

[4.23] Hellio, C., De La Broise, D., Dufossé, L., Le Gal, Y. & Bourgougnon, N. *Inhibition of marine bacteria by extract of macroalgae: potential use for environmentally friendly paints*, Mar. Environ. Res. 52 (2001) 231-247.

[4.24] J-P. Maréchal, G. Culioli, C.Hellio, H.Thomas-Guyonc, M. E. Callow, A.S. Clare, A. Ortalo-Magne, *Seasonal variation in antifouling activity of crude extracts of the brown alga Bifurcaria bifurcata (Cystoseiraceae) against cyprids of Balanus amphitrite and the marine bacteria Cobetia marina and Pseudoalteromonas haloplanktis*, J. Exp. Mar. Bio. 313 (2004) 47-62.

[4.25] Guillard R.R.L. and J.H. Ryther, *Studies of marine planktonic diatoms. I. Cyclotella nana Hustedt and Detonula confervaceae (Cleve),* Gran. Can. J. Microbiol. 8 (1962) 229-239.

[4.26] Amsterdam D., 1996. Susceptibility testing of antimicrobials in liquid media p52-111. In Lorian V., (ed.) Antibiotics in laboratory medicine 4th ed. Williams and Wilkins, Baltimore, MD.

[4.27] E. Plouguerné, C. Hellio, B. Véron, V. Stiger, E. Deslandes, *Anti-microfouling activities of extracts of two invasive algae: Grateloupia turuturu and Sargassum muticum.* Bot Mar (2008) in press.

[4.28] C.J. Lorenzen, *Determination of chlorophyll and phaeophytin spectrophotometric equation.* Limnol. Oceanogr. 12 (1967) 343-346.

[4.29] Fletcher R.L. and C. Manfredi, The occurrence of *Undaria pinnatifida* (Phaeophyceae, Laminariales) on the south coast of England, Botanica Marina, 38, 355-358 (1995)

[4.30] Hayden H.S., J. Blomster, C.A. Maggs, P.C. Silva, M.J. Stanhope, J.R. Waaland, *Linnaeus was right all along: Ulva and Enteromorpha are not distinct genera*, European J. of Phycology, 38, 277-294 (2003)

[4.31] Fletcher, R.L. *A bioassay technique using the marine fouling green alga Enteromorpha*, International Biodeterioration 25 (1989) 407-422.

[4.32] T. Hattori and Y. Shizuri, *A screening method for antifouling substances using spores of the fouling macroalga Ulva conglobata Kjelleman*, Fisheries Science, 62 (1996) 955-958.

[4.33] B.J. Savary, K.B. Hicks, J.V. O'Connor, *Hexose oxidase from Chondrus crispus: improved purification using perfusion chromatography*, Enzyme and microbial technol. 29 (2001) 42-51.

[4.34] Schultz M.P. *Effects of coating roughness and biofouling on ship resistance and powering*, Biofouling 23 (2007) 331-341.

[4.35] Gershenzon & Dudareva, *The function of terpene natural products in the natural world*, Nature Chemical Biology 3, (2007) 408 – 414.

Chapter 5 Building the antifouling system

This Chapter covers the areas highlighted in red on Figure 1.4 below which include the incorporation of the antifoulant additive natural product into a coating system and the application of this system to a substrate.

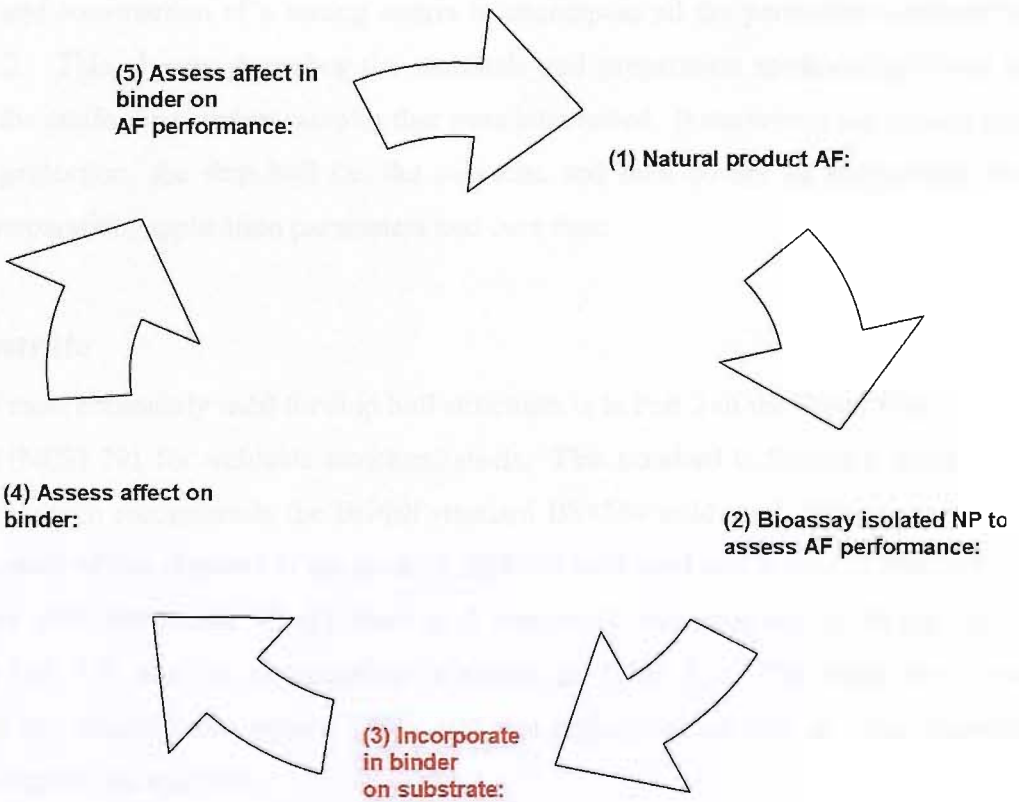

Figure 1.4 Key tests to optimise an NP-based antifouling system

One of the main thrusts of this project is the development of a marine antifouling system for the application to large ship hulls and platforms. Natural products must first be practical as antifoulants to be developed further into a functional system by their incorporation into surfaces or coatings. To demonstrate this, the natural product under investigation was homogenised into a blank proprietary antifouling paint system binder, applied to primed and un-primed ship grade steel and immersed in marine environments. Although simplistic in design, the complexity of the antifouling system is apparent in the building and construction of a testing matrix to encompass all the parameters outlined in Figure 1.2. This chapter describes the materials and preparation methodology used in building the antifouling system samples that were later tested. It starts with the surface that requires protection, the ship hull i.e. the substrate and then covers its preparation, the coating preparation, application parameters and cure time.

5.1 Substrate

The steel most commonly used for ship hull structures is to Part 2 of the Naval Engineering Standard (NES) 791 for weldable structural steels. This standard is for notch tough mild steel plate which recommends the British standard BS4360 mild steel. The most widely available steel of this standard is the grade A BS4360 mild steel and is used in this project. Mild steel (BS4360 Grade 43 A) sheet at 2 mm thick was supplied by Wyatt Metal Services Ltd, UK and the composition is shown in Table 5.1. The steel sheet was sectioned into 50 x 50 mm square, 150 x 100 mm rectangular as well as 1 cm diameter circular coupons for analysis.

Chemical Specification of BS4360 grade 43 (A)	
Carbon	0.24 %
Lead	0.04 %
Sulphur	0.045 %
Nitrogen	0.009 %

Table 5.1 Chemical composition of carbon steel substrate

The surface preparation has a direct influence on the integrity of the coating applied. Debris on a substrate surface can lead to defects at the coating/substrate interface and in the coating. Due to the hot-rolled preparation of the samples the as-received steel had a mill scale. The mill scale was removed from the test samples by grinding. Substrates were

prepared using SiC wet/dry polishing cloths, 600 grit for electrochemical experiments, abrasive ground (3M 577f) to R_t of 10 μm in accordance with SA 2 ½ for sea trials and polished with 6 μm diamond paste for SEM. The edges were smoothed to remove any fins and the surface was free of loose scale in accordance with BS 7079-A3:2002. Edge grinding was used to eliminate any sharp edge effects on the coating. All surfaces were washed and degreased using acetone and stored in desiccators.

5.2 Coating

For antifouling protection of ships a system of coatings is required to protect the hull substrate. Antifouling paints are made up of a vehicle termed the binder and pigments which include additives, colour, and extenders. The antifouling additives are included in the top-coat or final coating layer of the multi-coat marine antifouling system. For each type of coating several coats can be used to build up film thicknesses to minimize defects. There are three main environmental zones that have been identified by coating companies that have variable requirements, the 'atmospheric zone' the 'waterline zone' and the 'submerged zone' [5.1]. Surfaces such as ballast and freshwater tanks would also be susceptible to biofouling and corrosion issues. The antifouling coatings investigated in this thesis are concerned with the protection of the exterior waterline and submerged surfaces of the ship.

5.2.1 Primer

The primer used in this investigation is a barrier coating called 'Primocon' from International Paint Ltd UK. This is a tar-free conventional primer for all substrates underwater such as steel, wood, glass-reinforced polymer and aluminium. Samples were pre-primed with Primocon and 10-15 % thinner, before 2 further coats of Primocon were used to achieve the recommended dry film thickness at 40 μm dft.

Pre priming or a primer build-coat would occur on a ship hull with a further anticorrosive layer. However, in that instance the electrochemical characteristics would be much more difficult to detect. Hence, pre-priming / buildcoat was not applied in the current study. However, the positive control provided by the dockyard does have a buildcoat.

5.2.2 Top-coat

The paint kindly provided by International Marine Coatings Ltd. is a tin-free, controlled depletion polymer (CDP) antifouling system without any antifoulants. The paint provided had a low pigment volume concentration (PVC) of 23 % to allow for the addition of biocides directly into the paint. Additions were made on a weight basis for screening purposes. The CDP top-coat has a typical dry film thickness (dft) of 125 μm. It is designed for below the waterline application over a primed hull. The coating functions through an exponential decay of biocide release over the service life of 36 months International paints [5.2]. Its main constituent is rosin with zinc oxide as the soluble pigment. The rosin binder system functions by allowing the seawater to permeate the paint film through the hydrolysis of the rosin and release the biocides held within the matrix. The chemical reactions at the solid surface between the coating and the seawater is based on the assumption that as seawater is drawn up into the coating system, it reacts with the soluble portion of the polymer and dissolves out into the bulk solution. The rosin hydrolyses with water as illustrated in equation 5.1 [5.3] where R = polymer.

$$RCOOH + OH^- \rightarrow RCOO^- + H_2O \qquad (5.1)$$

Rosins often have abietic acid as a key constituent allowing the coating to dissolve in seawater over time [5.2]. This effectively allows for a diffusion process. The 'exponential' decay in leaching rate causes an excessive release in the initial days of immersion which dissipates rapidly. This coating system is a soluble matrix coating as described in Fig. 2.5 (a). Other CDP commercial antifouling systems are sold under a variety of pseudonyms including 'ablative', 'polishing', 'hydrolysable activated' and 'eroding'. With CDP coatings a leach layer develops as the insoluble film forming binder (e.g. resins and plasticisers) is left as a skeleton coating (Figure 2.5). Assumed dissolution mechanism of a rosin based control depletion polymer is that the carboxyl groups react with sodium and potassium ions present in the sea water leaving resinates of high solubility [5.3, 5.4].

Diffusion controlled leaching of a biocide creates a concentration gradient developing from the outer surface of the coating [5.5, 5.6] making the degradation of the polymer the controlling function in the antifouling efficiency. As the leach layer becomes thick, the release of the antifouling compound becomes more constrained as both the water ingress is slowed and the pathway for the biocide release becomes more tortuous. It is important to

understand the function of this topcoat to appreciate the physical and chemical phenomena, but the key reason for studying this topcoat layer was to allow for a comparative test vehicle for new experimental natural products. The natural origin of rosin has been suggested to involve a better compatibility with future naturally occurring antifoulants such as those investigated in this thesis [5.4].

5.2.3 Positive control coatings

The control antifouling system is Interspeed Ultra ® from International Paint Ltd., UK which contains copper(I)oxide, dichlofluanid and rosin and the recommended dry film thickness is 43 μm dft. This is a high strength and hard, scrubbable antifouling system used on commercial shipping and is sold as ideal for fast powerboats. The application to large ship hulls with operational profiles that include lengthy stationary periods would not be suitable. As well, the use of booster biocides such as dichlofluanid are coming under increasing legislative pressures. Additionally, a naval ship sample was kindly provided by the MOD as a positive control. On to the steel panel was applied, Epigrip ® an epoxy zinc phosphate buildcoat (2-pack) at 250 μm dft, a Resistex ® m535 pitch free a single pack, vinyl copolymer resin based underwater coating at 50 μm dft intermediate layer and an antifouling 2 Envoy TF500 ® with a dft of 75 μm. This topcoat advertised mechanism of action is ablative (i.e similar to the control depletion polymer). The intermediate coating is used in situations where coal tar pitch products are excluded on health and safety grounds or where bleed through of pitch into topcoats is not acceptable.

5.3 Antifouling additives

Two additives were incorporated into the blank paint top-coat using a L4RT high shear mixer from Silverson; a natural product (NP) extract from the red seaweed *Chondrus crispus* and as a control, the booster biocide Chlorothalonil. Bioassays were used to quantitatively analyse the antifouling activity of the NP. Effective testing against a broad spectrum of organisms is required to regulate the antifouling coatings success. Two differently sourced natural product extracts (A and B) were tested in isolation against five microfoulers, five bacteria foulers and two key macroalgae foulers. All bioassyed organisms are relevant UK water foulers.

5.3.1 Natural product extract

The source for the natural product as outlined in Chapter 4.4 in this thesis was the red seaweed *Chondrus crispus* (Stackhouse). As the bioassays (Section 4.5.2) indicated good

antifouling performance the industrially dried algal extract (A) was incorporated into a proprietary blank antifouling system as specified in this section.

The algal crude extract was incorporated into the coating system at 1 % wet w / w in the form of a gel. Antifoulants were incorporated into coatings at a wet weight so when the coating cured the final concentration would be increased. From the literature the main constituents of *C. crispus* are the polysaccharide carrageenan and other plant metabolites. The antifoulant characteristics from the FTIR and GCMS suggest that the whole cell extract is a combination of fatty acids, hormones and terpenes.

5.3.2 Control biocide

Chlorothalonil (2,4,5,6-tetrachloroisophthalonitrile) Pestanal®, purchased from Sigma-Aldrich was used as the control biocide. It has a low solubility in seawater of 0.0009 g L^{-1} at 20 °C. It is one of the most widespread alternative antifoulants [5.7]. As compared to other booster biocides such as *N*_-(3,4-dichlorophenyl)-*N*,*N* dimethylurea, called 'Diuron', which is relatively soluble in water (0.035 g L^{-1}at 20 °C) whereas the *N*-(dichlorofluoromethylthio)-*N*_,*N*_- dimethyl-*N*-*p*-tolylsulphamide, called Tolylfluanid, is of a similar solubility(0.0009 g L^{-1}).

Chlorothalonil is used commercially as a fungicide, bactericide, and nematocide. It was adapted recently for use as an antifouling paint booster biocide [5.8, 5.9]. The current maximum level in existing antifouling products is 3.0 % w/w [5.10]. Chlorothalonil is toxic to aquatic organisms and is known to act as an inhibitor of electron transport in the mitochondria of the cells of terrestrial animals [5.11]. The primary fate of this biocide is through photodegradation or hydrolysis with a half-life of 0.18 to 8.8 days in both aerobic and anaerobic conditions [5.12]. This biocide was incorporated into the coatings as a white crystalline powder at 1 % w/w.

5.4 Application

The experimental coatings were applied using a Sheen instruments drawbar (doctor blade BS 2015:1992) and air dried at 18 ± 2 °C in a fume cupboard. Dry film thicknesses (dft) were measured using a 456 Standard Ferrous Coating Thickness Gauge from Elcometer accurate to within ± 2 % or 0.5 μm thickness which ever is the greater of the stated measured values. Variable coating thicknesses were investigated ranging from 12 μm to 80 μm. The coating depletion rate on ships in 1984 was on average 0.3 μm day^{-1}, which is

300 μm every 2.5 years, a normal docking period [5.5]. With this consideration, for the field trials, a lower minimum thickness of 30-40 μm dft was used for the top-coat suggesting a working life of 4 months. This was an approximation, as dynamic rotation tests of the antifouling coating (Interspeed® 340) at around 125 μm dft in seawater showed a leached layer of 55 μm after 90 days [5.2].

5.5 Material characterisation

The average roughness (R_a) and total (peak to valley) roughness (R_t) on the steel substrate after treatment can be seen in Figure 5.1 as measured using a stylus Taylor Hobson Talysurf 120L profilometer.

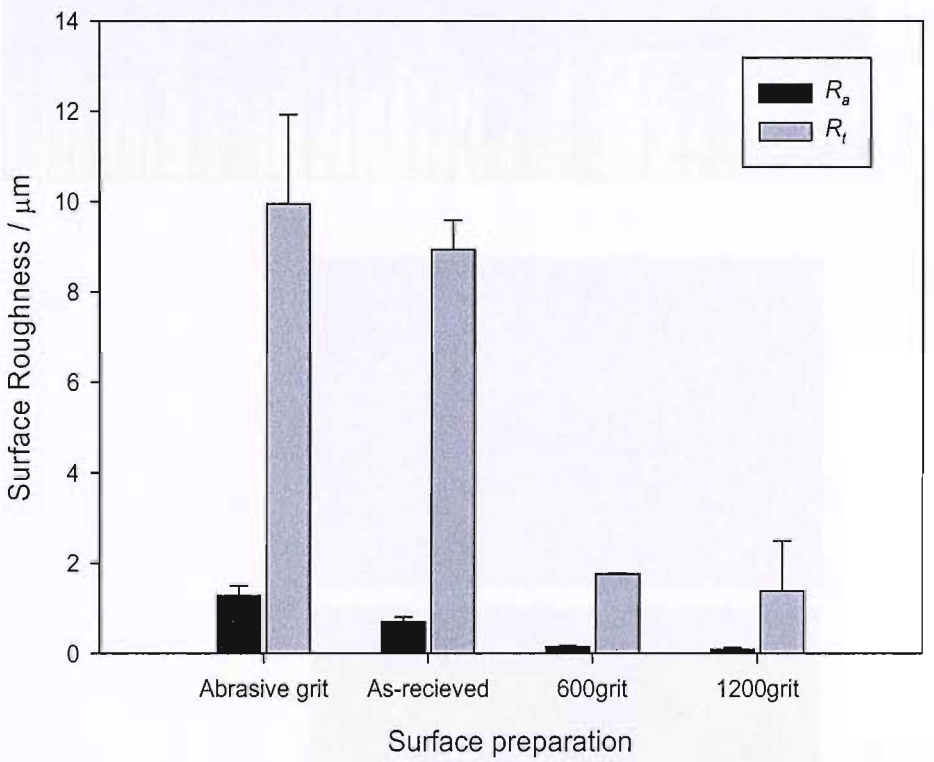

Figure 5.1 Average roughness (R_a) and total roughness (R_t) measurements for different steel substrate preparations (n = 3)

The thickness tolerance of the steel coupons after grinding was 1.78 ± 0.02 mm. The coating/steel interface is critical as the keying of the coating to the substrate is a main failure mechanism [5.13]. For the electrochemical characterisation the substrate was smooth grit polished to 600 grit (SiC wet/dry) for all topcoat applications. For the sea field trials the surface preparation conformed to a closer representation of in-service ship hull requirements by using an abrasive grit polish. Figure 5.2 highlights the keying of the primer to the two different surface preparations through optical, white light microscopy (a and b) and scanning electron micrographs (c and d).

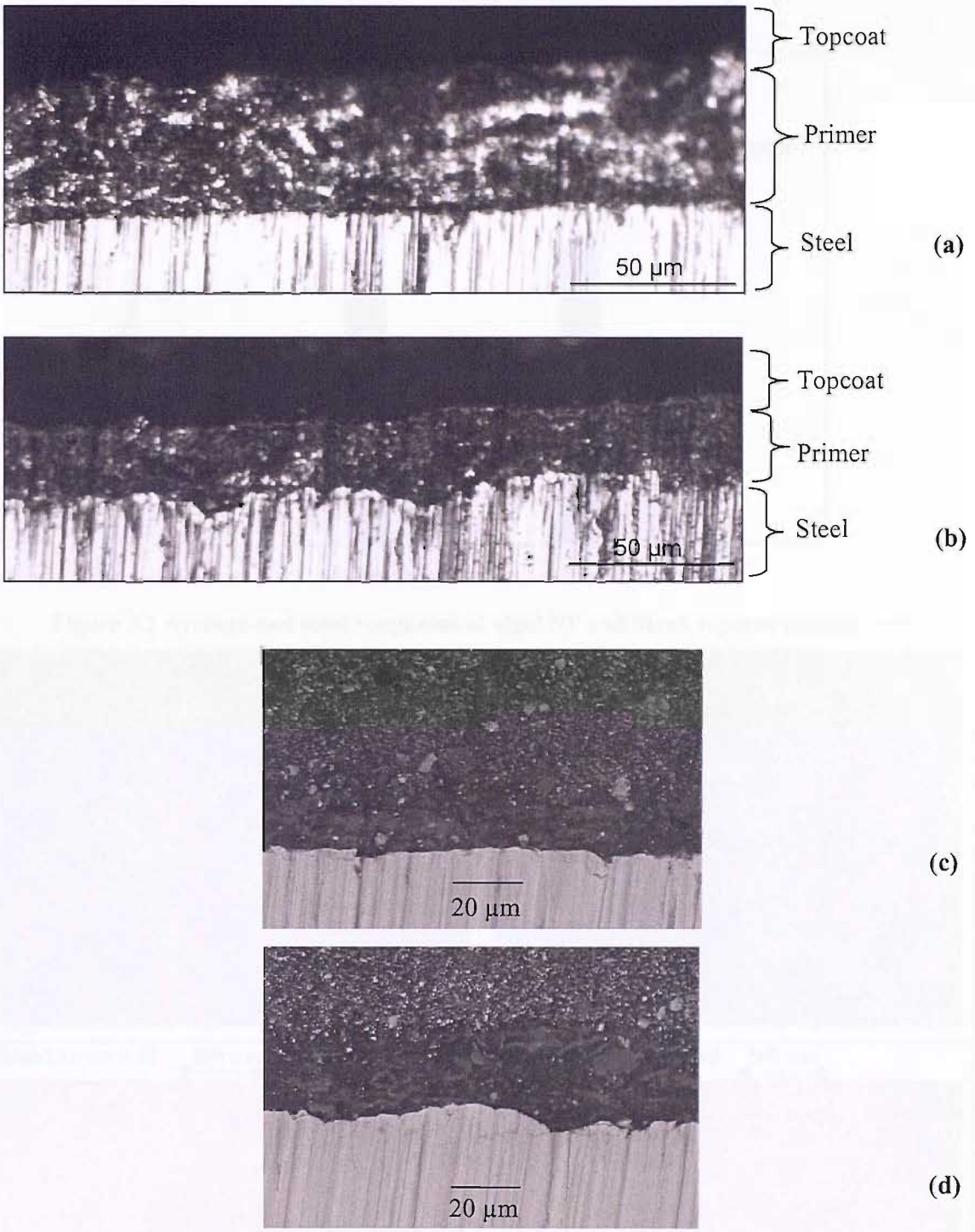

Figure 5.2 Optical micrographs of the transverse section of blank AF coating system on (a) 600 grit steel surface (b) abrasive grit steel surface and SEM micrographs of (c) 600 grit steel surface (d) abrasive grit steel surface

The micrographs of the transverse section of coating system on the two surface preparations used through out this study showed good adhesion of the primer to the steel substrate (Fig. 5.2). The applied coating surfaces were examined for uniformity (Fig. 5.3).

There is no statistically significant (t-test, $p<0.01$) difference in the surface roughness of the coatings with or without algal extract incorporation.

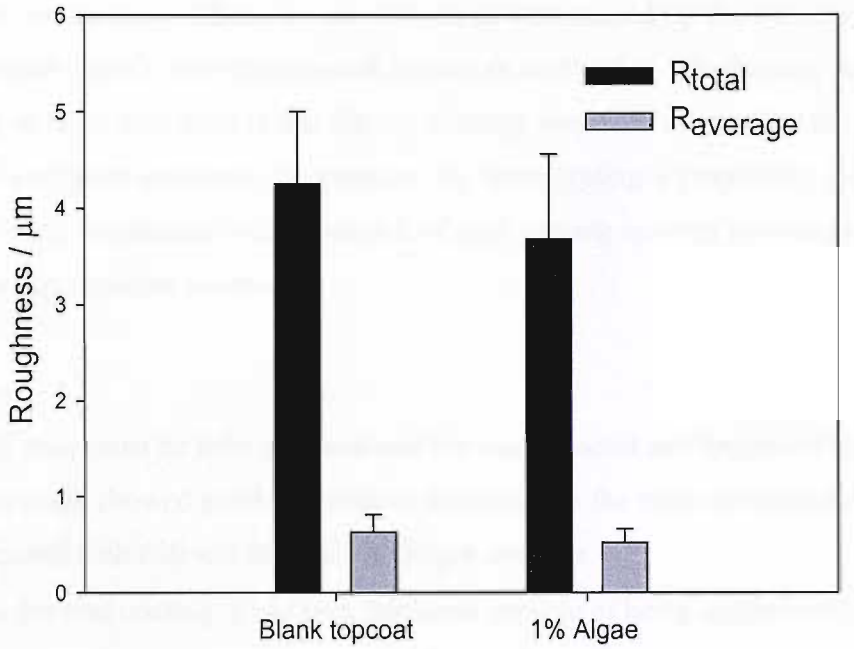

Figure 5.3 Average and total roughness of algal NP and blank topcoat surface (n=3)

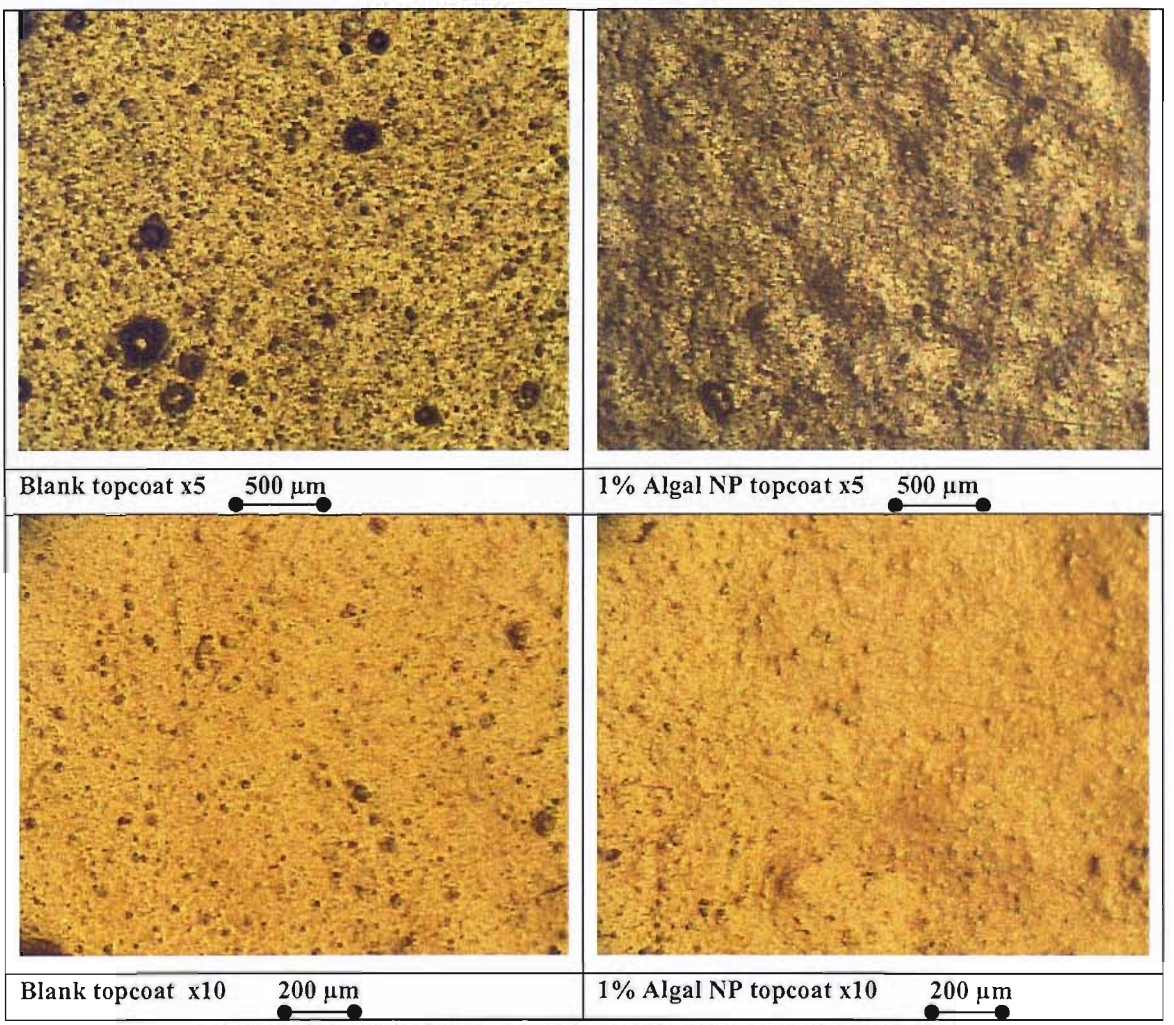

Figure 5.4 Optical micrographs of un-wetted coatings on steel

In Figure 5.4 the optical micrographs of the un-wetted surfaces of the blank topcoat and NP-topcoat can be seen. There are no obvious defects caused by the incorporation of the natural product directly into the top-coat system as outlined in this chapter. An issue with the coating of large ship hulls is that the dry docking time is limited so the fewer coats and frequency is of great economic importance. By investigating a proprietary system in this thesis, one issue to examine is the potential of such coating systems as vehicles for natural products as experimental platforms.

Conclusions:

- Mill scale must be fully removed and the steel cleaned and degreased before use. This study showed good adhesion of the primer to the steel substrate surface prepared with 600 wet/dry SiC and larger abrasive.
- The thinnest coating of uniform thickness capable of being applied using the drawbar system was approximately 12 μm dft.
- There is no statistically significant (t-test, $p<0.01$) difference in the surface roughness of the coatings with or without algal extract incorporation.
- No obvious defects were caused by the incorporation of the natural product directly into the top-coat system using the high shear mixer as outlined in this chapter.

5.6 References

[5.1] R. Lambourne, T.A. Strivens, Paint and surface coatings Theory and practice 2nd Ed, Woodhead publishing Ltd. 2004.

[5.2] C. D. Anderson, TBT Free Antifoulings and Foul Release Systems, http://www.internationalmarine.com/antifoulings/TBT_FreeAF_TechPaper.pdf Accessed [9/10/08].

[5.3] Woods Hole Oceanographic Institution, Marine Fouling and its Prevention, US Naval Institute Press, Annapolis, MD, 1952.

[5.4] D.M. Yebra, S. Kiil, K. Dam-Johansen, *Antifouling Technology - past, present and future steps towards efficient and environmentally friendly antifouling coatings* Prog. Org. Coat. 50 (2004) 75-104.

[5.5] F. H. de la Court, *Erosion and hydrodynamics of biofouling coatings*, Marine Biodeterioration an interdisciplinary study, eds J.D.Costlow and R.C. Tipper (1984) 230.

[5.6] Yebra, D.M., S. Kiil, K. Dam-Johansen, C. Weinell, *Reaction rate estimation of controlled-release antifouling paint binders: Rosin-based systems*. Progress in Organic Coatings 53 (2005) 256-275.

[5.7] F. Cima, M. Bragadin, L.o Ballarin *Toxic effects of new antifouling compounds on tunicate haemocytes I. Sea-Nine 211^{TM} and chlorothalonil*, Aquatic Toxicology 86 (2008) 299–312.

[5.8] N. Voulvoulis, M.D. Scrimshaw, J.N. Lester, *Comparative environmental assessment of biocides used in antifouling paints*, Chemosphere 47 (2002) 789-795.

[5.9] I.K. Konstantinou, T.A. Albanis, *Worldwide occurrence and effects of antifouling paint booster biocides in the aquatic environment: a review,* Environ. International. 30 (2004) 235-248.

[5.10] Adivsory Committee on Pesticides, *Evaluation on: Chlorothalonil: use as a booster biocide in antifouling products*, Health and Safety Executive, Merseyside, UK. (2002).

[5.11] A.R Fernàndez-Alba, M.D. Hervando, L. Piedra, Y. Chisti, *Toxicity evolution of single and mixed antifouling biocides measured with acute toxicity bioassays*, Anal. Chim. Acta 456 (2002) 303–312.

[5.12] Caux, P-Y., R.A Kent, G.T. Fan, G.L. Stephenson, *Environmental fate and effects of chlorothalonil: a Canadian perspective.* Crit. Rev. Environ, Sci. Technol. 26 (1996) 45-93.

[5.13] J.O. Bello, Evaluation and characterisation of the tribological properties of polymeric coatings for downhole application. Thesis (PhD) University of Southampton, School of Engineering Sciences (2003) 228p

Chapter 6 Electrochemical characterisation

The affect of the NP on the binder is further investigated with regards to its performance (Fig 1.4) in this chapter and is assessed using electrochemical techniques.

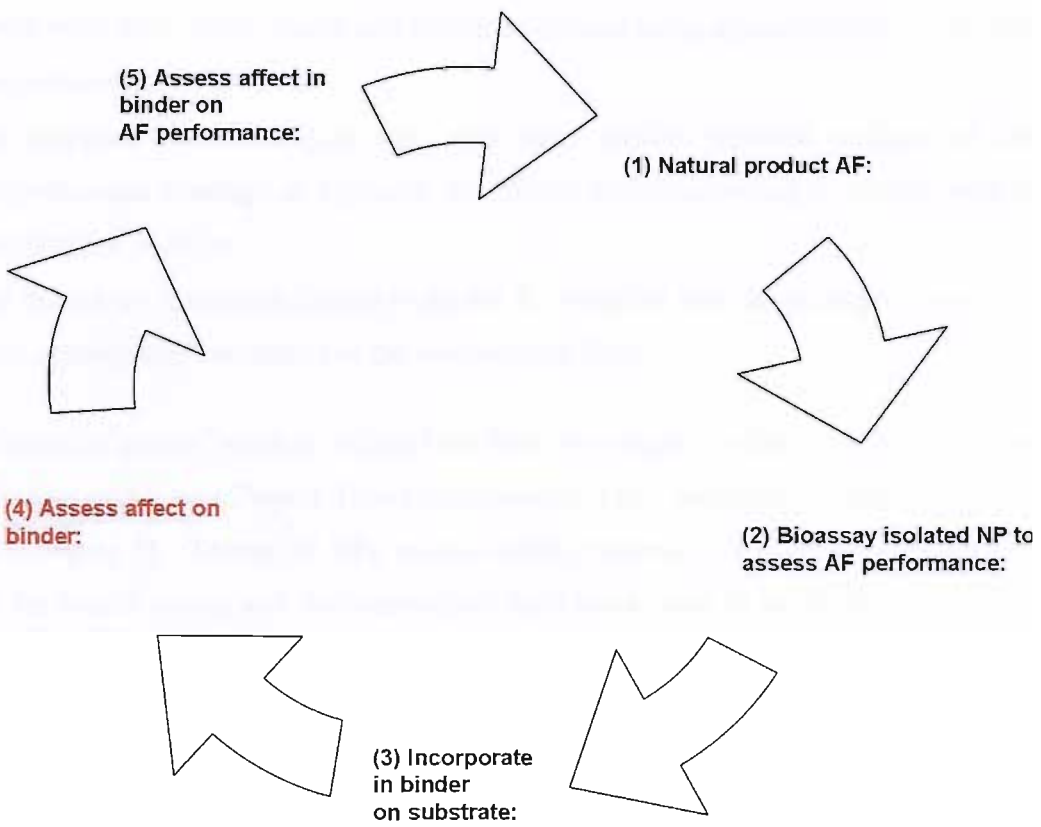

Figure 1.4 Key tests to optimise an NP-based antifouling system

The aims of this chapter are:

- to investigate electrochemical techniques to better understand antifouling coating ability over time with and without antifouling natural product additives in marine environments in a non-destructive manner,
- to characterise the topcoat physicochemical interactions with and without additives with regards to water uptake and barrier resistance using open-circuit potential and impedance measurements,
- to compare electrochemical data with other parallel physical analysis of the experimental coatings to highlight the effects of incorporating a natural product antifoulant additive
- to design an equivalent circuit to model the physical and chemical phenomena at the coating/steel substrate and the coating/bulk fluid.

Extracts from the algae *Chondrus crispus* have been investigated in this study as sources of NP antifoulant additives (Chapter 4) and incorporated into a proprietary control depletion polymer (Chapter 5). Testing of NPs within coating systems is a relatively new area of research for which *in-situ* and non-destructive techniques need to be further developed. One such way is by using electrochemical techniques (Section 3.2).

The effects of incorporating NPs into the coating were characterised using two non-destructive electrochemical techniques, open-circuit potential (OCP) which is a DC electrochemical technique and electrochemical impedance spectroscopy (EIS) which is an AC technique. Seawater and 3.5 % NaCl w/v solutions were used as electrolytes. The corrosion potential of the steel substrate under the coating was measured with OCP and the impedance of the coating was measured using EIS; both parameters were monitored over time periods of 5 and 14 days. The *in-situ* antifouling performance of 40 μm dry film thick (dft) coatings on primed carbon steel were measured visually and using OCP in a 105 day trial in the lab and a 90 day marine exposure trial in Southampton, UK.

Various electrochemical techniques have been used to evaluate polymer coatings. Electrochemical Impedance Spectroscopy (EIS) in particular has been used to study ion diffusion in organic coatings [6.1], water transport of 3.5% NaCl in organic coatings [6.2], and on marine anticorrosive paint systems in seawater [6.3-6.5]. Also, specific to this thesis test series is the study by Amirudin et al., 1995 [6.6] which investigated anti-corrosive pigments using EIS in seawater. The project study follows a similar principle

but investigated antifouling additives. Although EIS is a powerful tool for studying of coated metals it is not a stand-alone solution [6.7] so other dc techniques were used to assess the experimental coatings.

6.1 Electrochemical characterisation

The antifouling system from the substrate to the topcoat was characterised using DC and AC electrochemical methods to investigate the effects of substrate preparation, coating thickness and incorporated NP and biocide on the coating system functionality. It also assessed the feasibility of the techniques to measure such a complex system. Three coatings and 1 positive control coating as well as bare steel were investigated. The three experimental coatings were a blank topcoat (section 5.2.2), a 1% w/w algal NP topcoat and a 1% w/w biocide topcoat (section 5.3). A range of dry film thicknesses (12 – 80 dft) were examined.

A steel substrate (section 5.2) provided the working electrode in all of the electrochemical measurements. All potentials quoted in this thesis were measured against the standard silver/silver chloride (Ag/AgCl) reference electrode. The electrolytes in this study were representative of the marine environment ie. similar salinity (32), conductivity (50-54 mS), pH (approx 8), DO (approx 7 ppm). Measureable currents from these tests are assumed to be a product of the steel oxidizing beneath any applied coatings and subsequent ion diffusion/ reactants within pores (e.g. O_2, Fe^{2+}). The four electrochemical techniques used as discussed previously in section 3.2 were OCP, zero resistance ammeter (ZRA), electrochemical impedance spectroscopy (EIS) and linear polarisation resistance (LPR). A list of the samples, their dft and assessment is tabulated in Appendix IV.

6.1.1 Open-circuit potential (OCP)

A Gamry Instruments potentiostat was used to measure the open-circuit potential (OCP) in 3.5 % NaCl solution and an ACM instruments Galvogill^{TM} was used to measure OCP in fresh seawater. The OCP was measured by connecting a silver / silver chloride (Ag/AgCl) reference electrode and working electrode (steel coated sample) to a voltmeter. The electrolyte was either, 3.5 % NaCl, or aerated fresh seawater sampled from Southampton dock (32 salinity). Measurements were taken daily and constant temperature and aeration were maintained through each experiment. The electrolyte was topped up with distilled water to compensate for evaporation loss. For the field trial samples were electrically wired, araldite sealed, suspended 1 m below the waterline and measured weekly for 105

days as outlined in section 3.2.2. Samples were pulled to the surface once every two weeks to document the coatings using photography. The OCP values were plotted against time over seconds, minutes, days and weeks to measure the time variability in the measurement of the potential of the substrate to corrode.

6.1.2 Zero resistance ammetry (ZRA)

Coupled potential and galvanic currents were measured using an ACM instruments Galvogill™ zero resistance ammeter (ZRA) with a measurement resolution of 1 μV± over a current range of 100 pA to 7 mA. The ZRA measures the current flowing between 2 electrodes with effectively zero resistance between them as described in section 3.2.2.

Mill scale mild steel (BS4360) was mechanically ground to remove the mill scale and 600 SiC polished to create an average surface roughness of R_a = 0.4 ± 0.05 μm (section 4.5). A final dry film thickness of ~ 12 μm was used without primer. Electrochemical tape was used to tape off coupon edges making the exposed area 6.25 cm^2. Araldite epoxy resin was used to waterproof the electrical connection to the bare metal of the working electrodes WE1 and WE2. Each couple was immersed in an aerated beaker of solution with a 40 mm PTFE spacer to control the distance between the samples (Fig. 6.1). A sample surface area ratio of 1:1 was used. The samples were immersed in fresh seawater with a dissolved oxygen concentration of approximately 7.2 ± 4 ppm, pH = 8.4 and a room temperature of 15.5 ± 0.5 °C for 5 days.

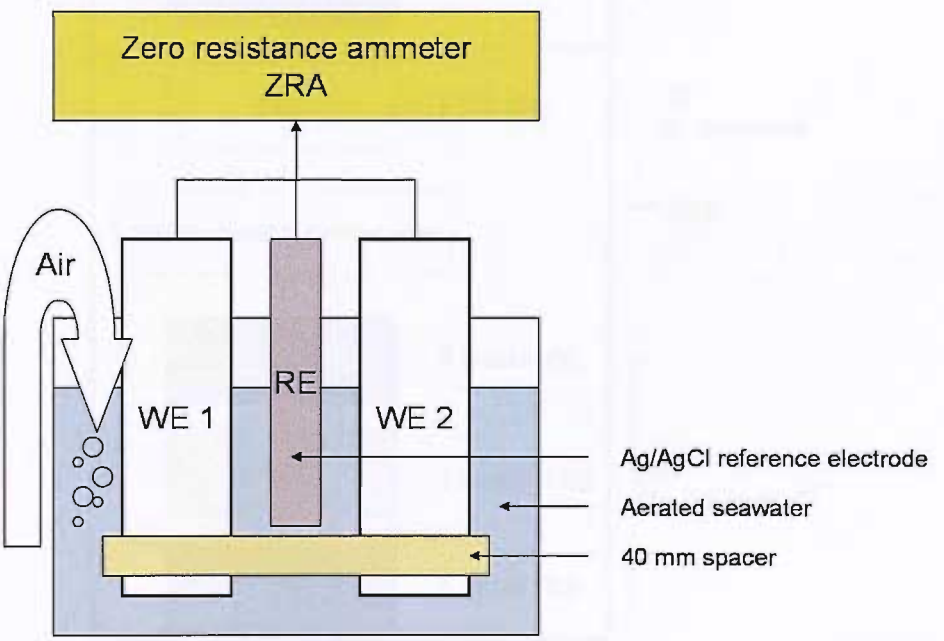

Figure 6.1 Galvanic couple arrangement for ZRA experiments

Six couples were tested as detailed in Table 6.1. Decoupling of the samples for a duration of 30 minutes every day allowed the decoupled open-circuit potentials to be measured using an Iso-Tech (Model IDM91E) digital multimeter (± 1 mV) and an Ag/AgCl reference.

	Working Electrode 1 (WE1)	*Vs.*	Working Electrode 2 (WE2)
Couple 1	Base rosin		Raw steel
Couple 2	Base rosin & biocide		Raw steel
Couple 3	Base rosin & algae extract		Raw steel
Couple 4	Base rosin		Base rosin
Couple 5	Base rosin & biocide		Base rosin & biocide
Couple 6	Base rosin & algae extract		Base rosin & algae extract

Table 6.1 Galvanic couple connections for ZRA experiment

The procedure for the ZRA test included EIS and OCP measurements before and after the 5 day trial. The key stages of the testing are highlighted in a procedures flow chart in Figure 6.2. As well as the ZRA test, the before and after EIS tests were all repeated in the same manner.

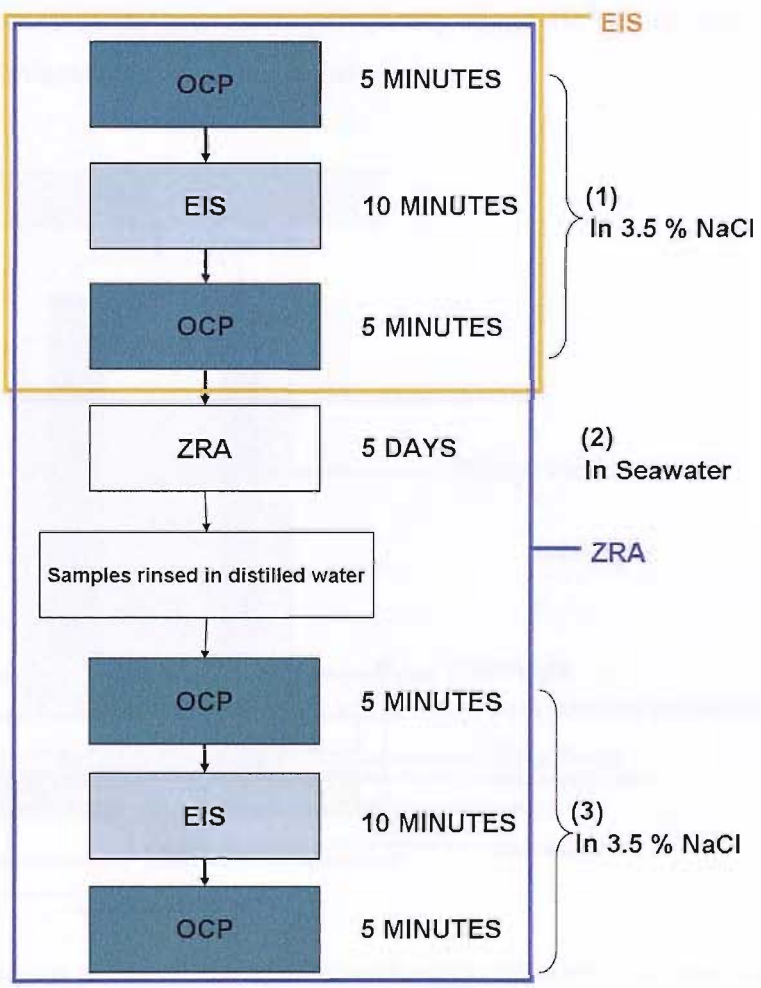

Figure 6.2 Flow chart of the procedure of each experiment for EIS boxed in orange and ZRA boxed in blue

6.1.3 Electrochemical impedance spectroscopy (EIS)

Electrochemical Impedance Spectroscopy (EIS) is used to evaluate the integrity and performance of organic coatings on a metal substrate particularly within corrosive environments. There are no reaction product build up because there is no net current flow making this a non-intrusive technique. Impedance relates to porosity level, coating thickness, water uptake [6.3], time-stability of wetted coating, ion diffusion [6.1] within coating degradation and substrate degradation through corrosion [6.6].

Experimental analysis of the coatings was made using a three-electrode system connected to a Gamry potentiostat as shown in Figure 6.3. A counter electrode (CE) of graphite, a reference electrode (RE) of Ag/AgCl, and a working electrode (WE) of the sample, in this case mild steel, were used in the electrochemical cell (Fig. 6.3). The experimental coating area exposed within the flange cell was 7 cm^2 and was sealed with a nitrile O-ring. The electrolyte used was aerated 3.5 % NaCl solution. All measurements were conducted at room temperature 20 ± 3 ° C in an earthed Faraday cage. Samples were subjected to a sine wave perturbation ± 10 mV across the frequency range 10^{-1} to 10^5 Hz. The use of a Faraday cage eliminated electrical noise disturbance.

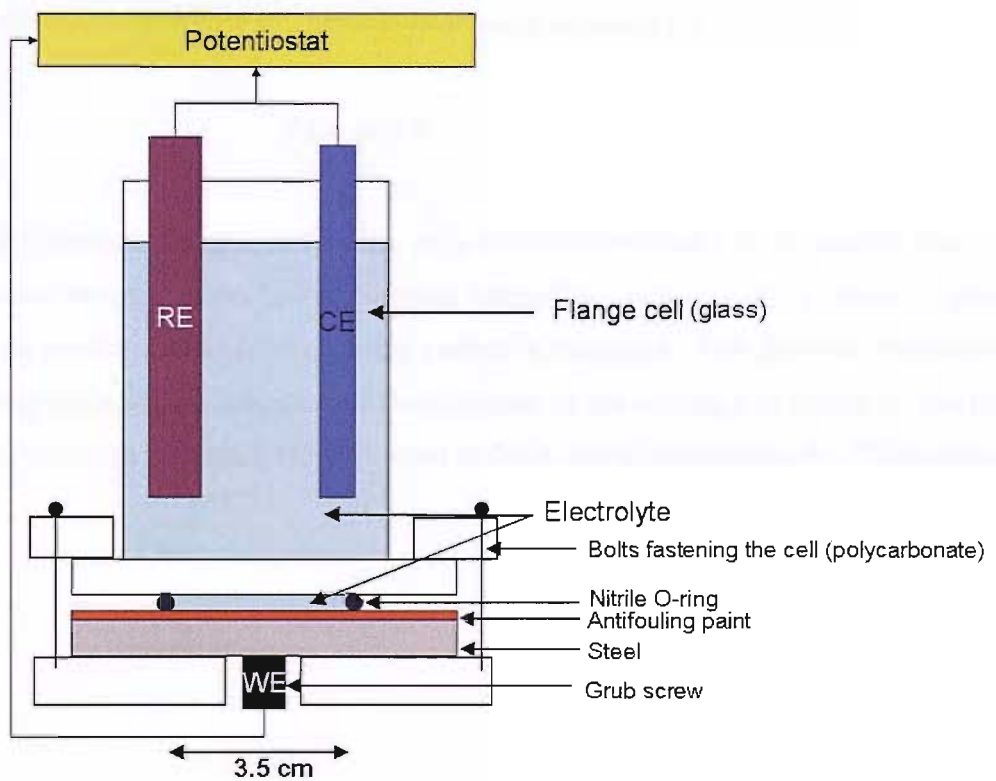

Figure 6.3 Apparatus of three electrode electrochemical cell with 7 cm^2 working area for EIS and OCP laboratory experiments

In order to measure and compare the three experimental coatings (blank, algal extract and biocide) a rapid failure technique was required. To sensitise the coating to any affects that the incorporation of the algal extract may have caused, thin coatings were applied (30 ± 5 μm). As noted by Amirudin et al., 1995 [6.7] who also studied artificially thin dry film thicknesses of 30 ± 5 μm, results can be obtained in a reasonable time due to the decreased length in the diffusion path. As well, if too thick coatings were used the measurements would be largely capacitive potentially masking the response of incorporated compounds. A Gamry instruments potentiostat was used. Blank, biocide and algal NP 1 % w/w coatings (30 μm dft) were immersed in 3.5 % NaCl electrolyte. Open-circuit potentials were measured before and after (Fig 6.2) using both Gamry Instruments for 200 seconds and an Iso-Tech (Model IDM91E) digital multimeter (± 1 mV) with an Ag/AgCl reference electrode. The shift in the OCP due to the EIS was ± 11 mV *vs.* Ag/AgCl reference.

6.1.4 Linear polarisation

The porosity of coatings and their corrosion resistance can be measured electrochemically [6.8]. Blank topcoats of 25, 30, 65 and 75 μm dft were measured using the linear polarisation technique. The linear polarization resistance is calculated from the slope of the overpotential versus the current plot and can be used to calculate the coating resistance R from which the resistivity can be calculated using equation 6.1.

$$RA = \rho e \times x \qquad 6.1$$

Where R is the resistance, A is the area, ρe is the resistivity and x is the coating thickness. The electrochemical system has its potential stepped at a rate of 1 mV s^{-1} from a cathodic state to an anodic state and the resulting current is measured. The electrical resistance of the coating can act as an indication of the efficiency of the coating as a barrier to ions [6.6]. Linear polarisation resistance (LPR) is used in this study to corroborate the EIS impedance data.

6.2 Results

6.2.1 Substrate preparation effects

The initial surface preparation for coating adhesion was investigated at room temperature using open circuit potential (Fig 6.4). The keying of the coating to the substrate affects the timing and degree with which corrosion can occur over the steel surface. Such electrochemical interactions at the interface need to be suppressed or eliminated if high performance organic coatings are to be developed. It is also extremely important that the bare steel is fully characterised if coated samples are to be analysed using electrochemical techniques. A test of the bare steel (600 SiC grit prepared) was made over 0.5, 3 and 24 h durations. Over the short time scale of 0.5 h the surface of as-received (mill scale) steel was compared with 600 and 1200 wet SiC ground steel (Figure 6.4).

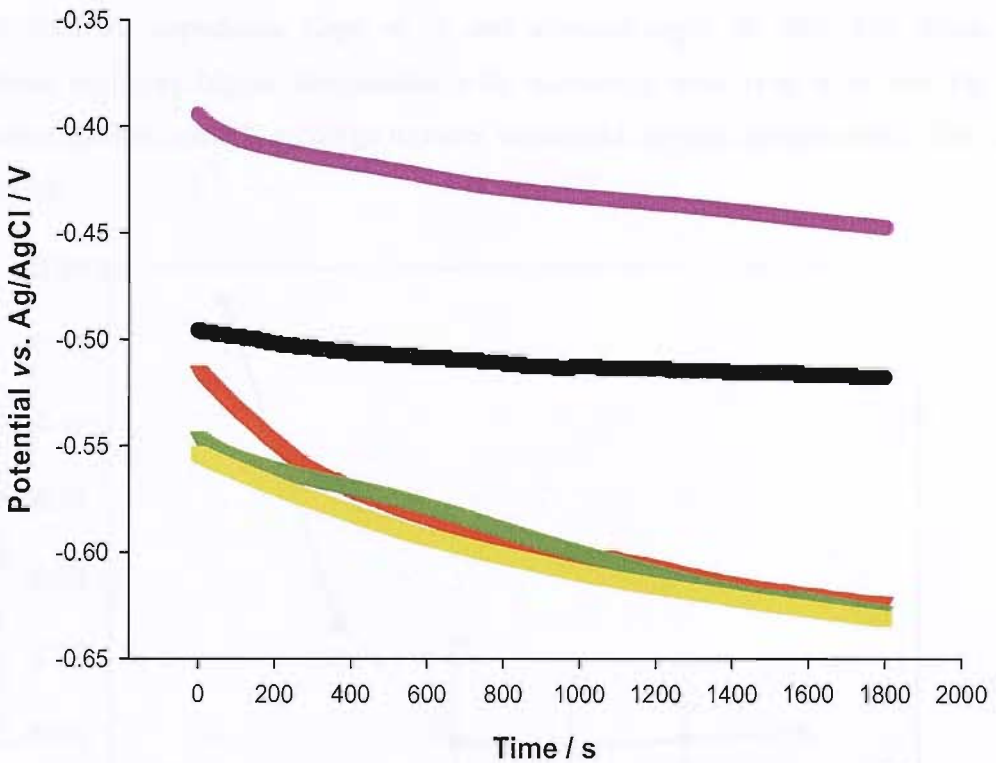

Figure 6.4 OCP of varying steel surface preparation methods of mill scale ● ● as well as 600 ● ● and 1200 ● SiC wet/dry polish

In Figure 6.4 the OCP takes up to 500s to stabilise. The mill scale is an iron oxidised layer from the hot-rolling process of the steel sheet production. The mill scale acts as a protective coating making the corrosion potential 100 to 200 mV *vs.* Ag/AgCl less negative. The preparation of the steel substrate using 600 grit SiC wet/dry was reproducible and the OCP varied only by ± 5 mV (Fig 6.4) when the surface roughness was made smoother using 1200 grit. The 600 SiC polish finish was used as the surface preparation technique for all electrochemical measurements in the laboratory (section 5.1).

The 600 SiC grit was chosen as it provided a larger surface average roughness, than 1200 SIC grit, to facilitate mechanical interlocking (section 5.5, Figure 5.1) yet had a uniform surface for electrochemical measurements to be made. The adhesion of the coating to this surface preparation was visually assessed (Fig. 5.2) and deemed suitable.

To investigate the time dependence of corrosion phenomena, bare steel (600 grit prepared) was measured in 3.5 % NaCl over 3 (Figure 6.5) and 24 h (Figure 6.6). The OCP is shown as well as the bode plot which includes an impedance plot against frequency and a phase angle against frequency plot. Over the period of 3 hours (Fig 6.5) the OCP of the steel reached a steady state at - 610 mV vs Ag/AgCl. Both graphs show a corroding system, with the impedance vs frequency plots illustrating that with increasing time the impedance increases indicating a build up of products on the steel surface. A pure capacitive system would yield an impedance slope of -1 and a phase angle of -90°. The phase angle maximum shifts to higher frequencies with increasing time (Fig 6.5b and Fig 6.6b) indicating a move towards a charge transfer dominated physical phenomena at the surface of the steel.

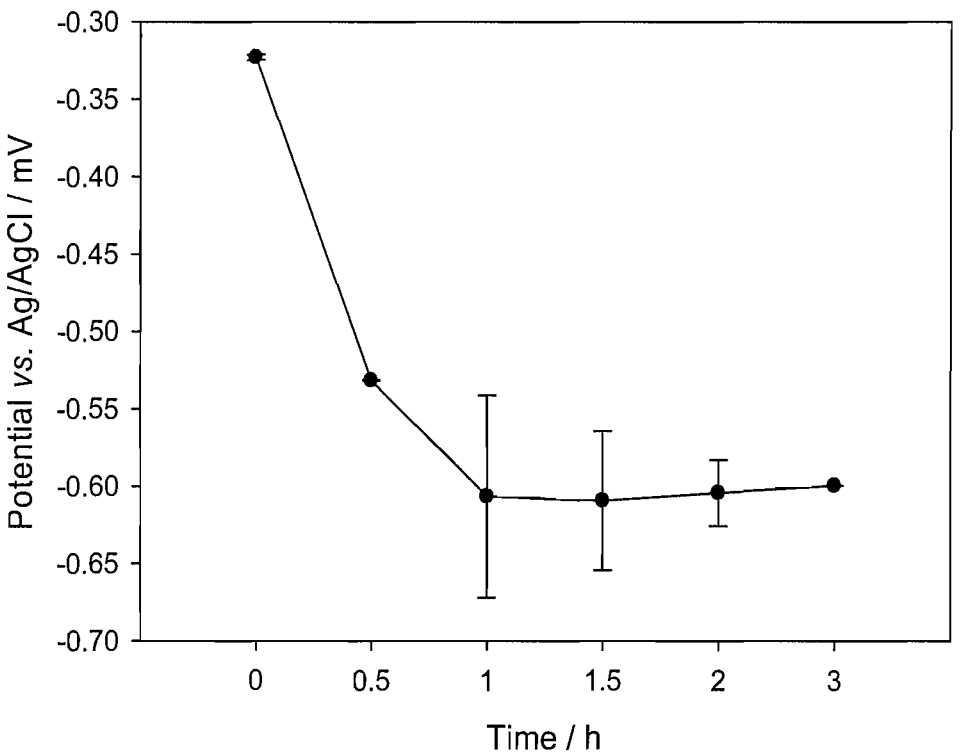

(a)

(b)

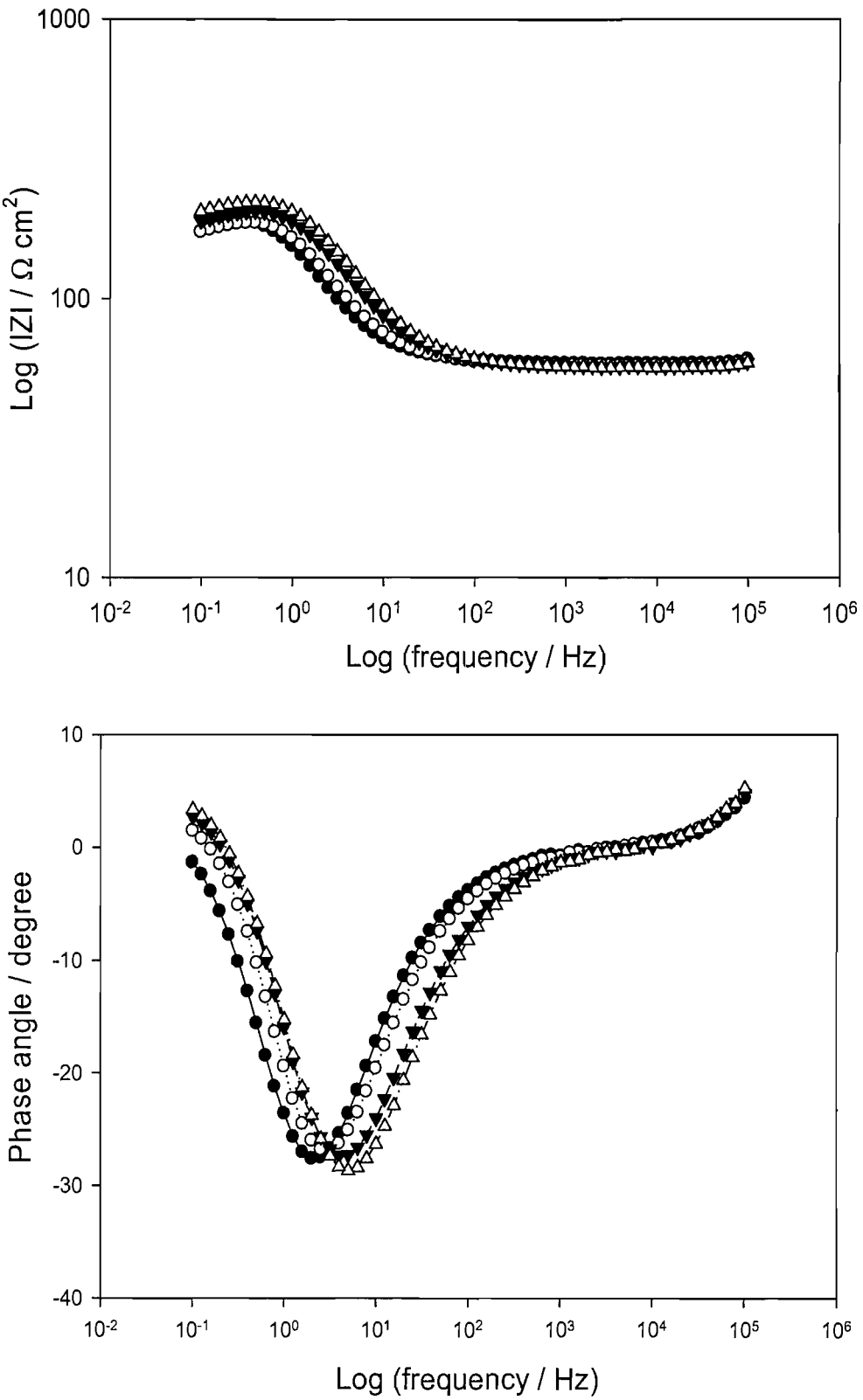

Figure 6.5 Characterisation of steel in 3.5 % NaCl solution at 0.5● 1○1.5 ▼and 2 △ h using (a) open-circuit potential and (b) electrochemical impedance spectroscopy as a Bode plot

(a)

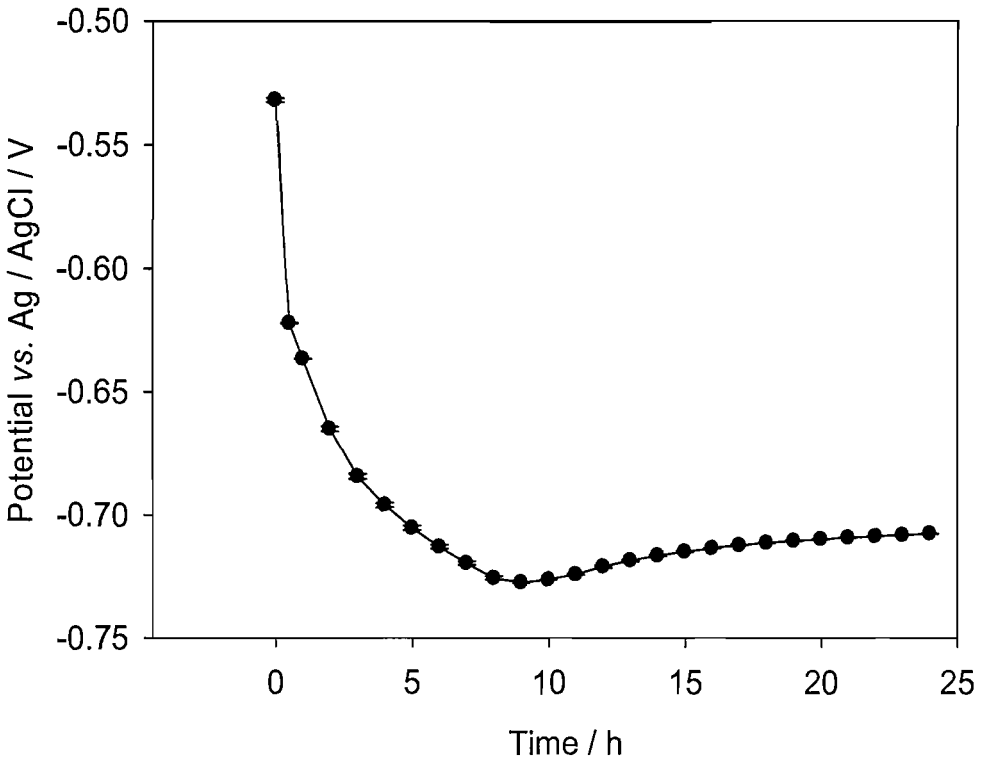
-0.50
-0.55
-0.60
-0.65
-0.70
-0.75
Potential vs. Ag / AgCl / V
0
5
10
15
20
25
Time / h

(b)

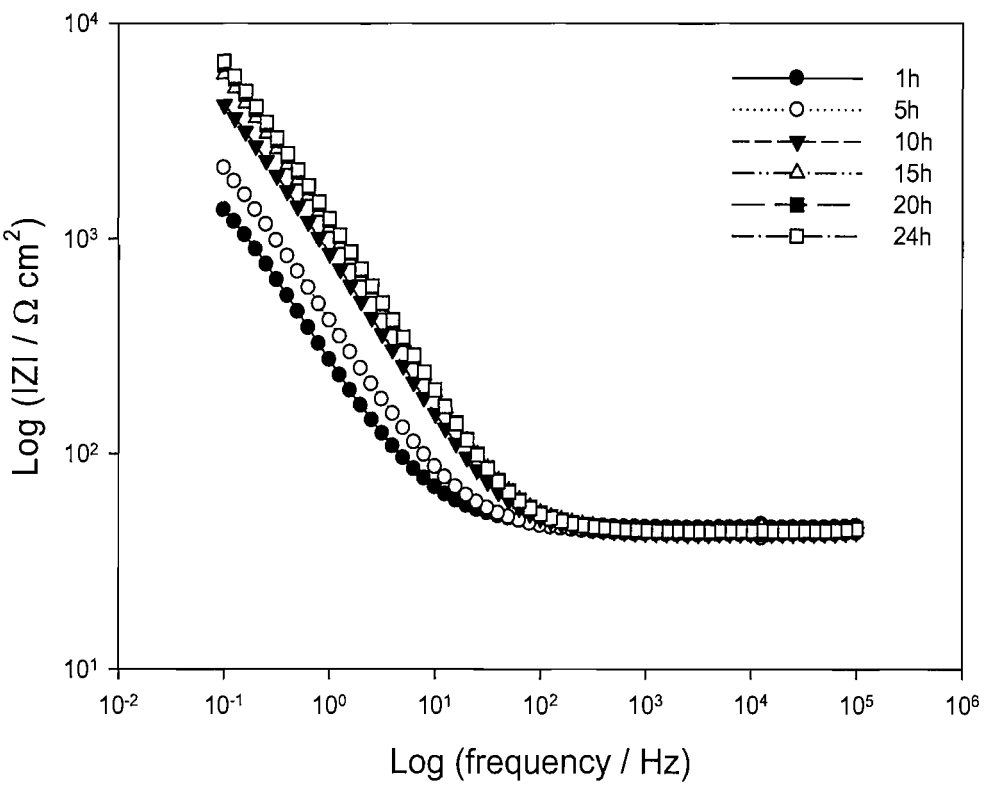
10^4
10^3
10^2
10^1
Log (|Z| / Ω cm^2)
10^{-2}
10^{-1}
10^0
10^1
10^2
10^3
10^4
10^5
10^6
Log (frequency / Hz)
1h
5h
10h
15h
20h
24h

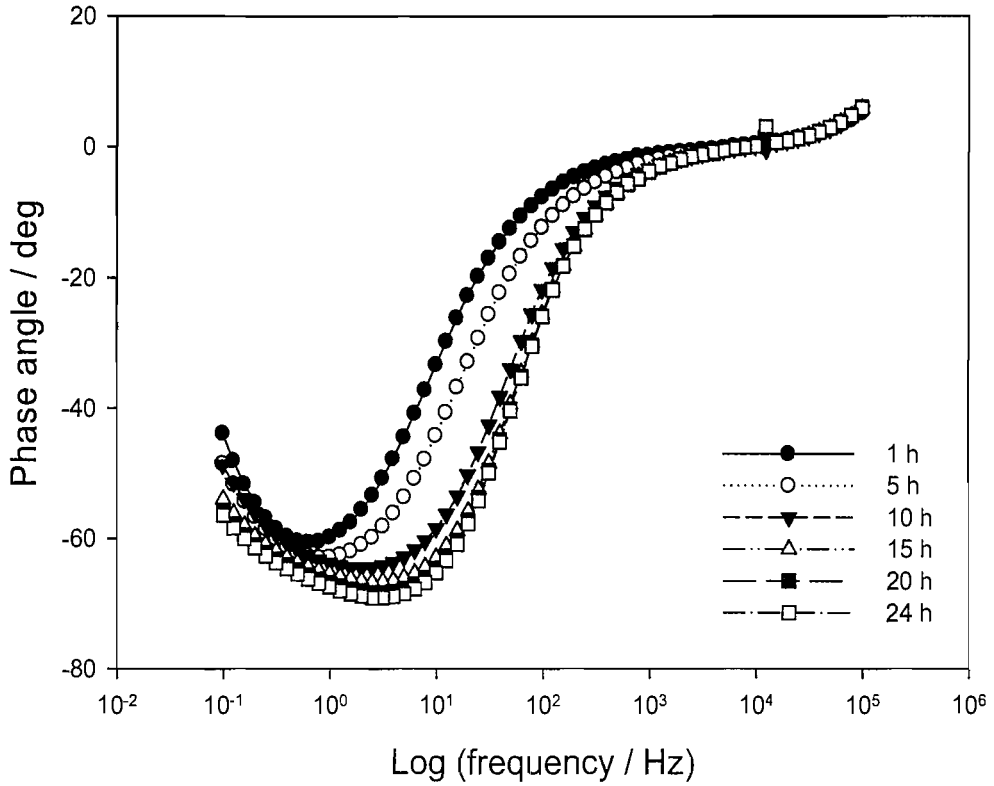

Figure 6.6 A twenty-four hour characterisation of steel in 3.5 % NaCl solution using (a) open-circuit potential and (b) electrochemical impedance spectroscopy as a Bode plot

The OCP of steel in aerated 3.5 % NaCl for 3 h (Figure 6.5(a)) shows a plateau after 1 h at approximately -610 mV *vs.* Ag/AgCl and the weight difference in the steel sample, after immersion of 3 h, measured gravimetrically was 5.3 mg. After 9 h (Figure 6.6(a)) the OCP drops off to -730 mV *vs.* Ag/AgCl before recovering to a more positive potential +20 mV and stabilising at -710 mV *vs.* Ag/AgCl. This dip and subsequent recovery does not feature in the Bode plot 6.6(b). The Bode plot illustrates that the electrochemical system is resistance dominated, due to the flat slope of the plot at higher frequencies ($\geq 10^1$ Hz), from 30 minutes (Fig 6.5 (b)) up to 24 hours ($\geq 10^2$ Hz) in Figure 6.6 (b).

6.2.2 Coating thickness effects

Once the surface corrosion of the bare steel substrate was characterised using EIS the basics of the coated system were investigated. A range of varying coating dfts (25 – 115 μm) were examined. Coating thickness effects on the blank rosin topcoat were investigated using OCP of the coatings as shown in Figure 6.7, LPR as shown in Table 6.2 and EIS as shown by the impedance measurements plotted in Figure 6.8. For the blank topcoat in a 3.5 % NaCl w/v solution there was a decrease in the OCP as the coating thickness increases after the first 10 minutes (Fig 6.7).

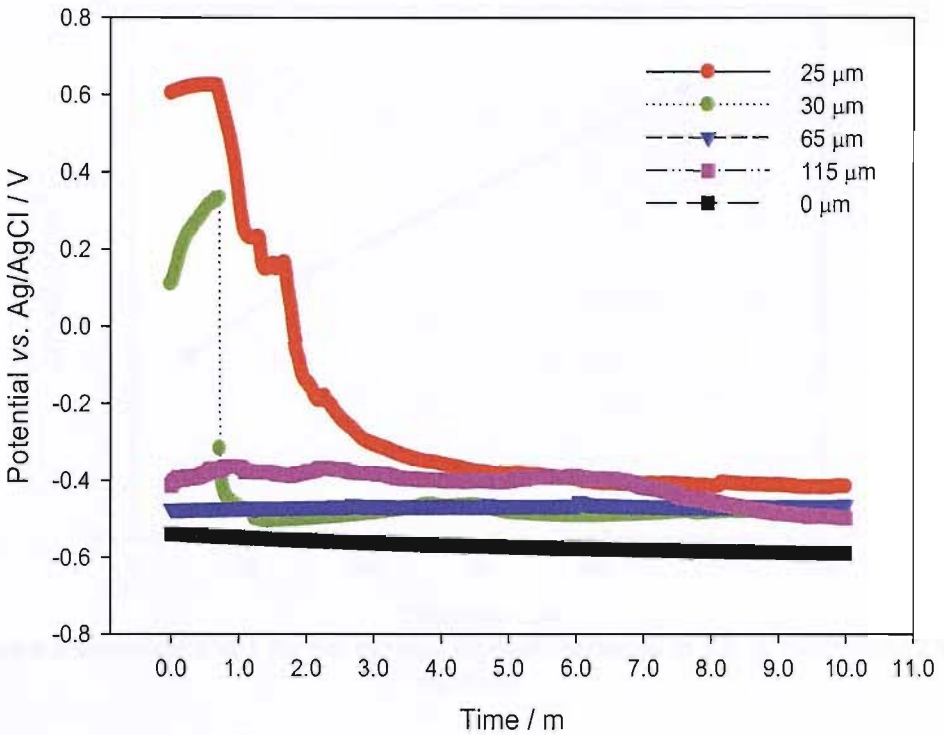

Figure 6.7 OCP for blank topcoat with increase in thickness after 10 minute immersions in 3.5 % NaCl

However, after the steady state was reached at 5 minutes the 115 µm thick coating has the highest potential. Measurements to calculate the blank coating resistivity using LPR were made on 25, 30, 65 and 75 µm dft. Higher thicknesses were beyond the instrument detection level. Impedance measurements were made just before the polarisation of the coating to help to correlate the AC and DC techniques. The resistivity results from the linear polarisation technique are tabulated in Table 6.2 and the resistance results from the EIS are shown in Figure 6.8.

Time immersion / h	x / µm	R / Ω	A / m^2	ρe / Ω cm
2	25	1.00E+09	0.07	2.80E+12
2	65	2.00E+10	0.07	5.60E+13
2	75	2.00E+11	0.07	5.60E+14

Table 6.2 Effect of increasing coating thickness on resistivity of the blank topcoat in 3.5 % NaCl *vs.* Ag/AgCl

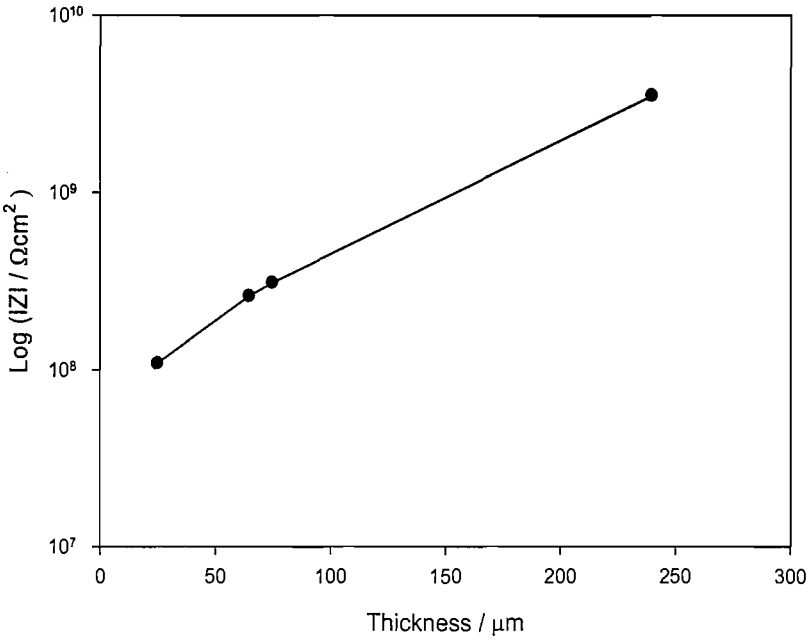

Figure 6.8 Impedance at 1 Hz for varying topcoat thickness in 3.5 % NaCl after 2 h *vs.* Ag/AgCl

Although these are one off measurements there is a trend. There is an increase in the resistivity of the coatings with increased coating dry film thickness which correlates well with the impedance measurements at low frequencies where the sample is resistance dominated.

6.2.3 The effect of antifoulant additions to coatings on steel

Since both the underlying steel and the blank coating thickness effects had been shown, the next aspect was to better understand the effects of the incorporated antifoulants. Thin coatings were galvanically coupled together (Table 6.1) to allow for the measurement of coupled and decoupled open circuit potentials as well as the current density. In Figure 6.9 and 6.10 the coupled mixed potentials measured using ZRA are plotted as a function of time. In both graphs (Fig. 6.9 and 6.10) the coating thickness varies between 10 to 15 µm dft.

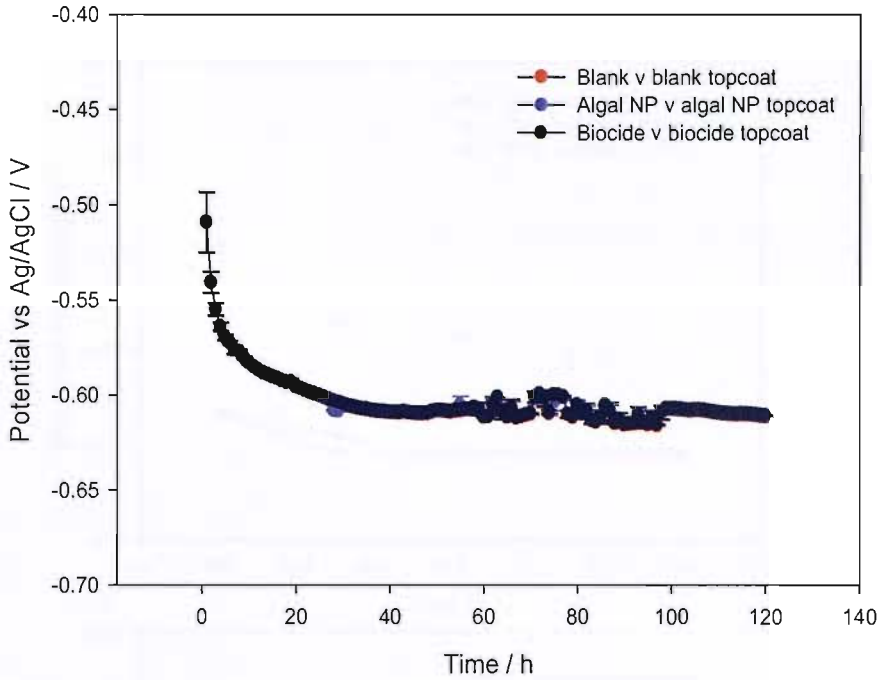

Figure 6.9 OCP of coupled 12 ± 2 µm coatings in seawater (all in same beaker)

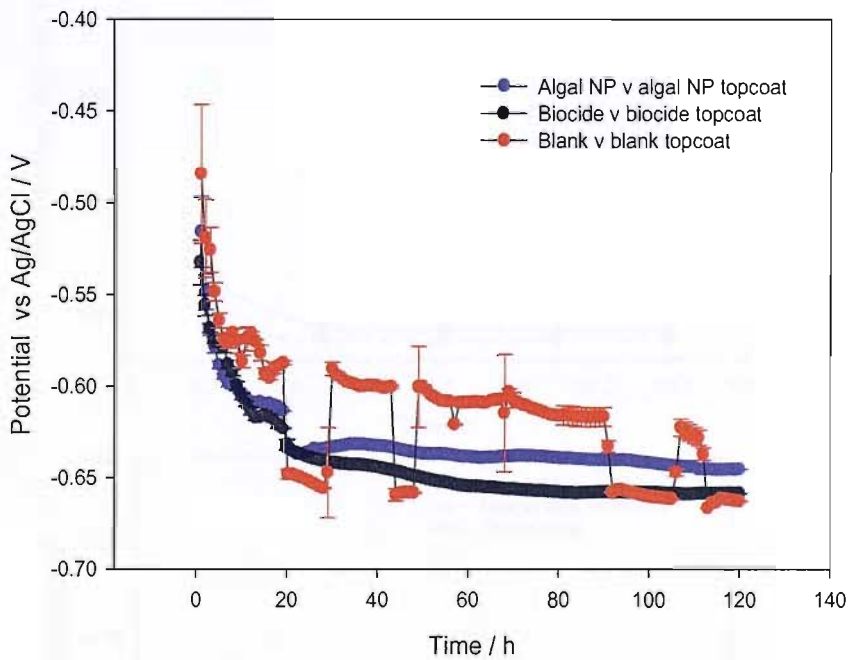

Figure 6.10 OCP of coupled 15 µm dft coatings in seawater (all in separate beakers)

In both Figure 6.9 and 6.10 the OCP reading stabilises after 24 hours, at -600 mV to -620 mV *vs.* Ag/AgCl in Figure 6.9 and in Figure 6.10 at approximately -650 mV *vs.* Ag/AgCl. The blank basecoat in Figure 6.10 fluctuated but these corresponded with the decoupled measurements taken each day at 17, 42, 66, 90 and 114 hours. When the couples are reconnected the more cathodic sample is dominating the electrochemical OCP response over varying periods of time before recovering to the more anodic mixed potential.

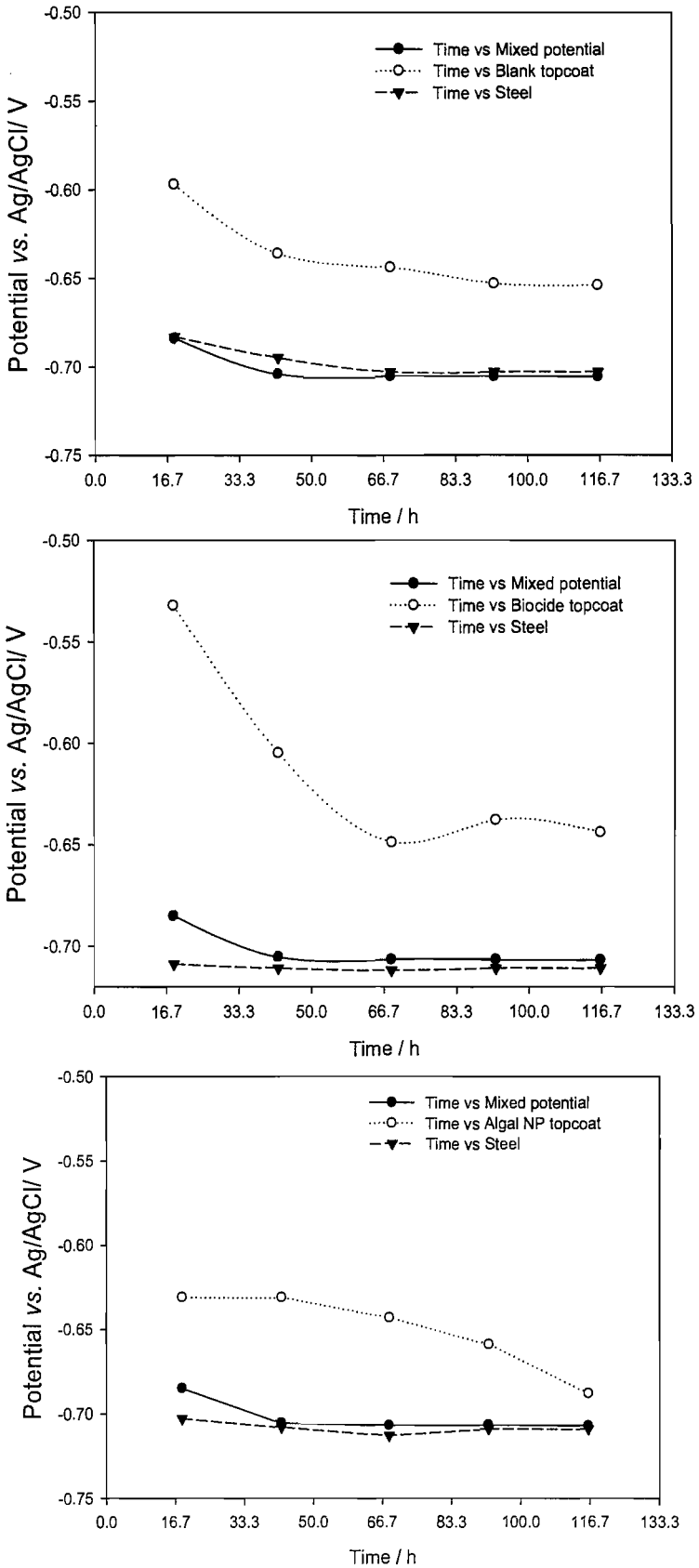

Figure 6.11 ZRA mixed potentials and decoupled potentials of (a) Blank topcoat (12 ± 2 dft) (b) Biocide (15 ± 2 dft) and (c) Algal NP extract (13 ± 2 dft) topcoats coupled to uncoated steel

Figure 6.11 plots the mixed and 30 minute decoupled potentials of the three thin (10-15 μm) coatings coupled to bare steel over a period of five days. After day three (72 h) the potentials of both the blank topcoat (Fig. 6.11 (a)) and biocide based (Fig. 6.11(b)) coating systems stabilise, however, the algal NP coating (Fig. 6.11 (c)) continues to drop to a more negative potential. After the fifth day, all the coatings showed blistering and corrosion on the exposed surface.

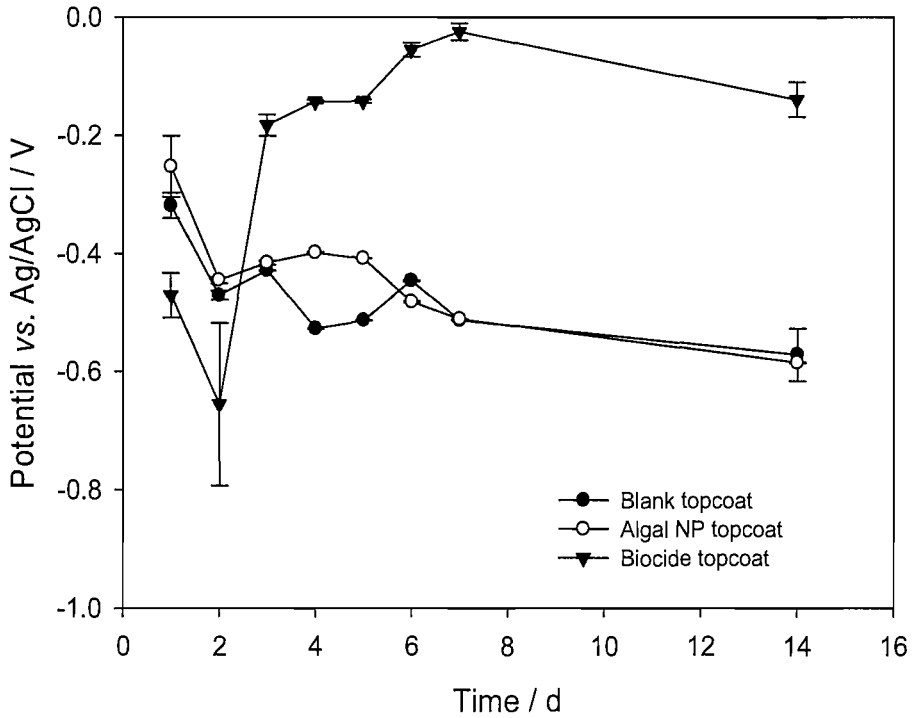

Figure 6.12 Top-coat (30 μm) of blank, biocide and algal NP OCPs in 3.5 % NaCl over two weeks (day mean with standard deviation error bars)

The measurements taken every 5 s were averaged over 24 h as shown in Figure 6.12. In Figure 6.12 on day three (72 h) the biocide incorporated coating jumped to a much higher (+ 200mV) and remained at this higher potential for the duration of the study. The physical meaning of this could be that after an initial potential drop, due to the electrolyte reaching the steel on day two, the coating stopped further ingress. A suggestion for this stopping could be that a defect such as a pinhole corroded and that the corrosion product is blocking water ingress causing a less negative potential. However, when taking OCP readings before making an EIS measurement the changing time-dependant mechanisms associated with this coating were made obvious (Fig. 6.13). A second drop to a bare steel corrosion level was recorded when the OCP was measured before the EIS. On removal of the sample to the EIS equipment the corrosion product at that defect may have been dislodged giving the lower -800 mV *vs.* Ag/AgCl reading day 3 as again a recovery to the

much higher potential of approximately -200 mV *vs.* Ag/AgCl was noted for day four (Fig. 6.13).

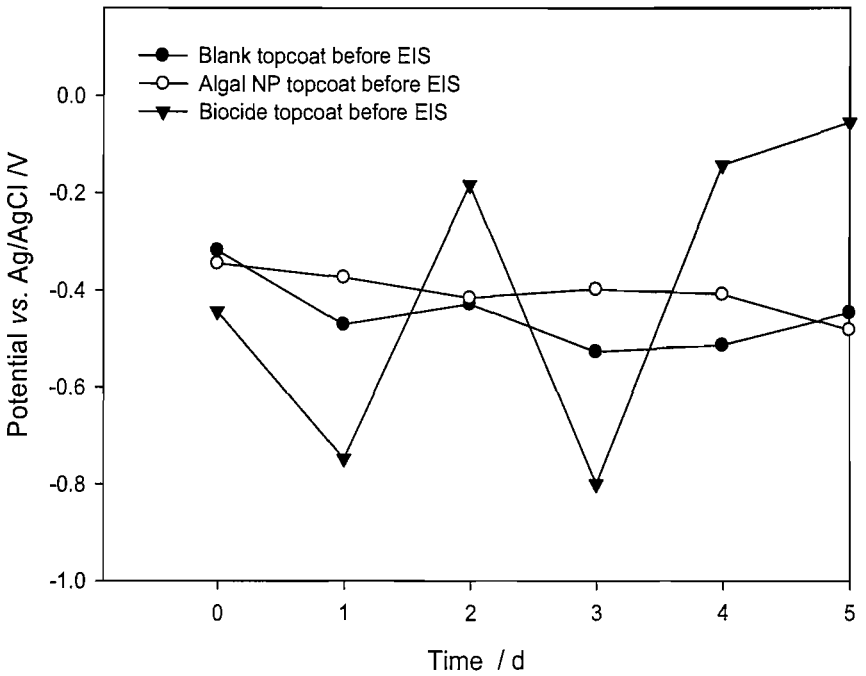

Figure 6.13 Blank topcoat, Algal NP topcoat, Biocide topcoat (30 μm dft) OCPs in 3.5 % NaCl over five days

The EIS data spectrum for a series of blank, 1 % algal NP and 1 % biocide topcoats, in 3.5 % NaCl over 2 weeks, are shown in Figure 6.14, 6.15 and 6.16 respectively.

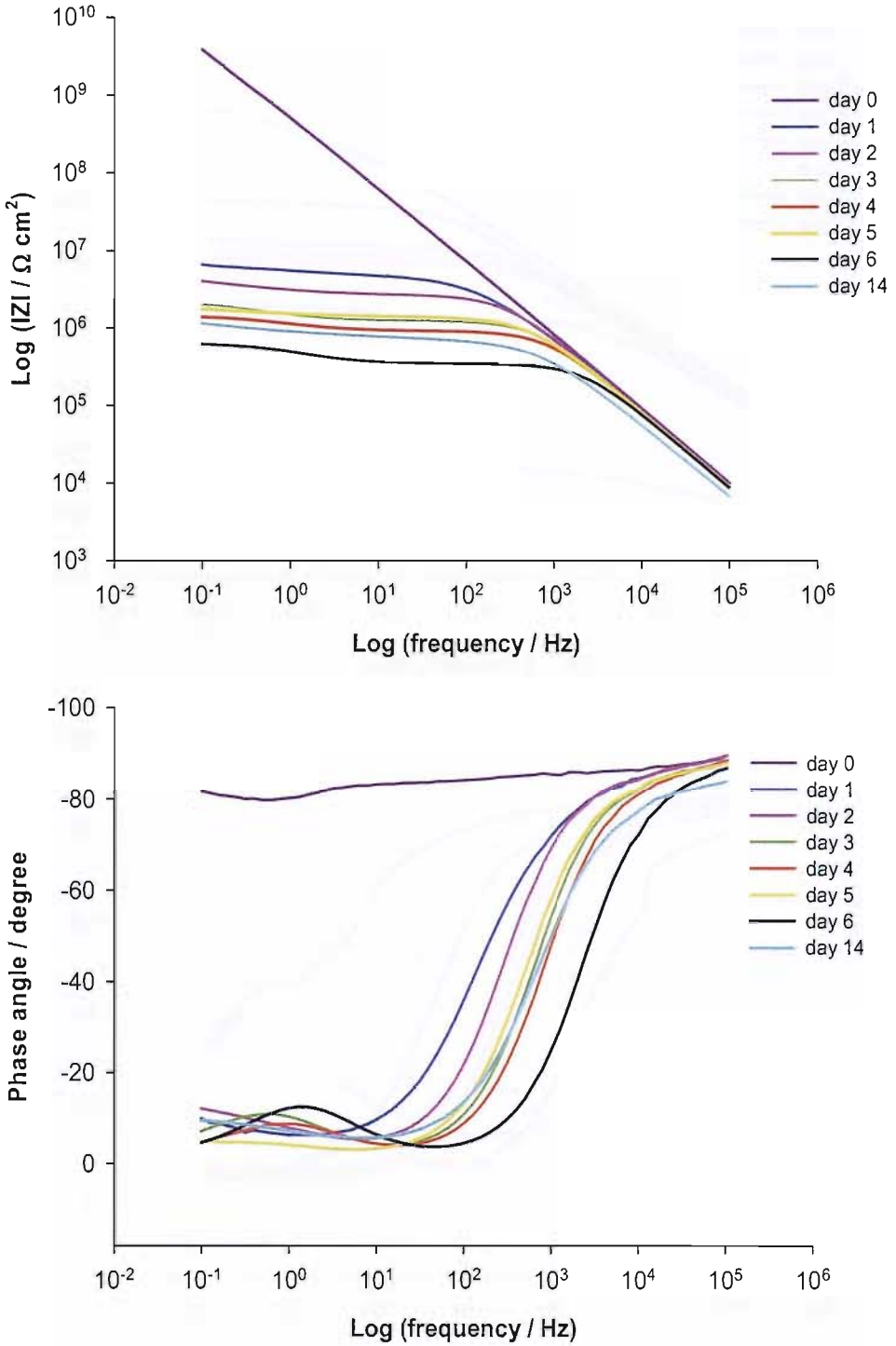

Figure 6.14 EIS Bode plot for 30 µm blank topcoat in 3.5 % NaCl for two weeks

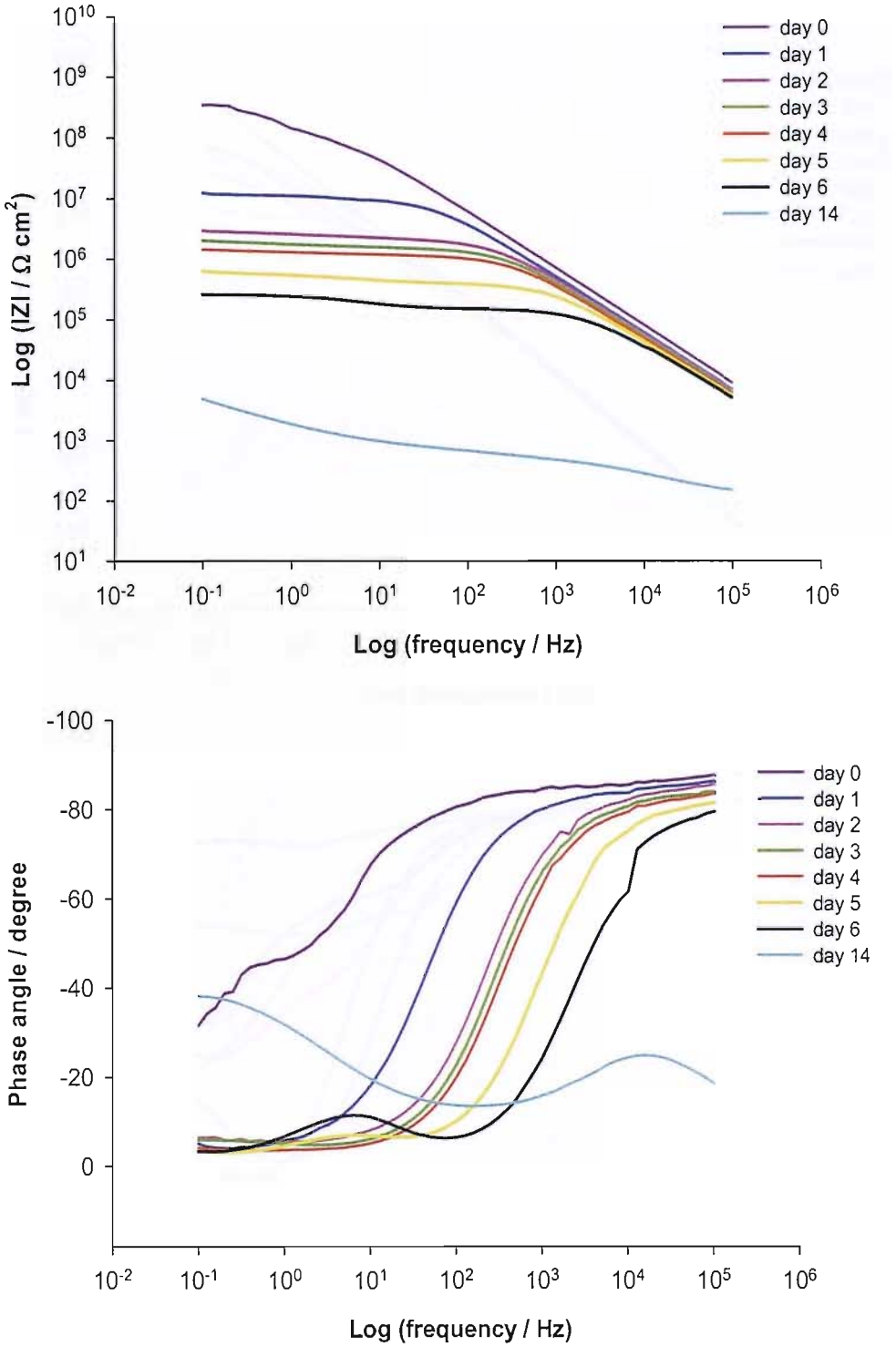

Figure 6.15 EIS Bode plot for 30 μm algal NP topcoat in 3.5 % NaCl for two weeks

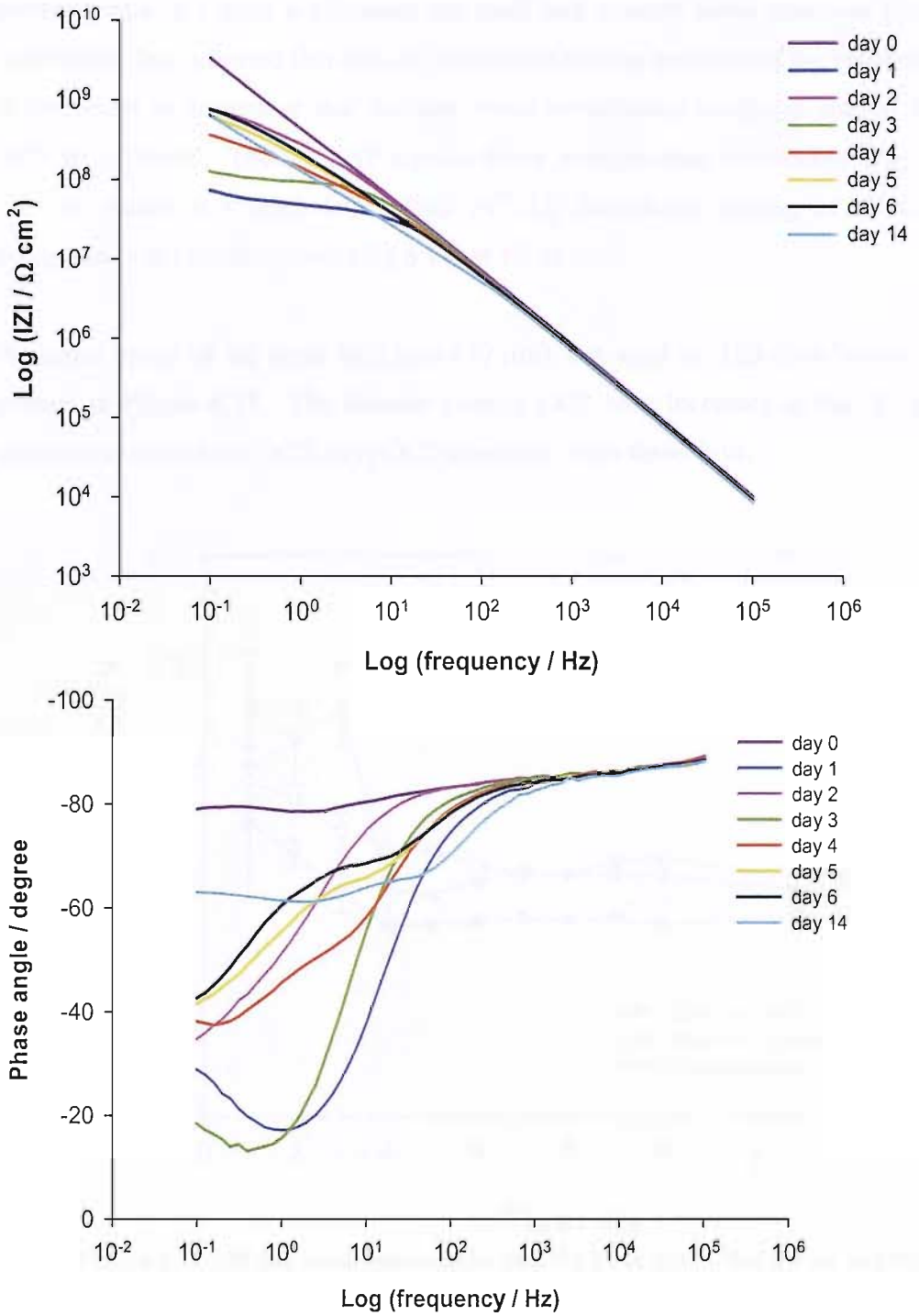

Figure 6.16 EIS Bode plot for 30 μm biocide topcoat in 3.5 % NaCl for two weeks

A transition can be detected from a region of slope = -1 as seen on day 1 to a more resistive slope nearing zero on day 14 for both the blank and the algal NP topcoat. This same feature was not visible on the biocide topcoat data set. A drop in the OCP (Fig 6.13) is reflected in

bode and the phase angle plots for day 1 and 3 of the biocide coating (Fig 6.16). The impedance is lowered by an order of magnitude. Figure 6.16 correlates with the OCP features seen in Figure 6.13, when the steel had a more noble potential (i.e. +ve) the impedance data reflected this with an increase in the log modulus of the resistance area. It is important to remember that the sine wave perturbation oscillates around the starting OCP by ± 10 mV. The algal NP topcoat drops in impedance irreversibly (Fig. 6.15) over the two weeks to a much lower final 14th day impedance reading of 10^4 Ω cm^2 then compared to the blank topcoat (Fig 6.14) at 10^6 Ω cm^2.

A further study of the same thickness (30 μm), but aged by 100 days before wetting, is plotted in Figure 6.17. The biocide coating OCP only increases at day 3. For all the coatings a steady state (± 20 mV) OCP is reached after three days.

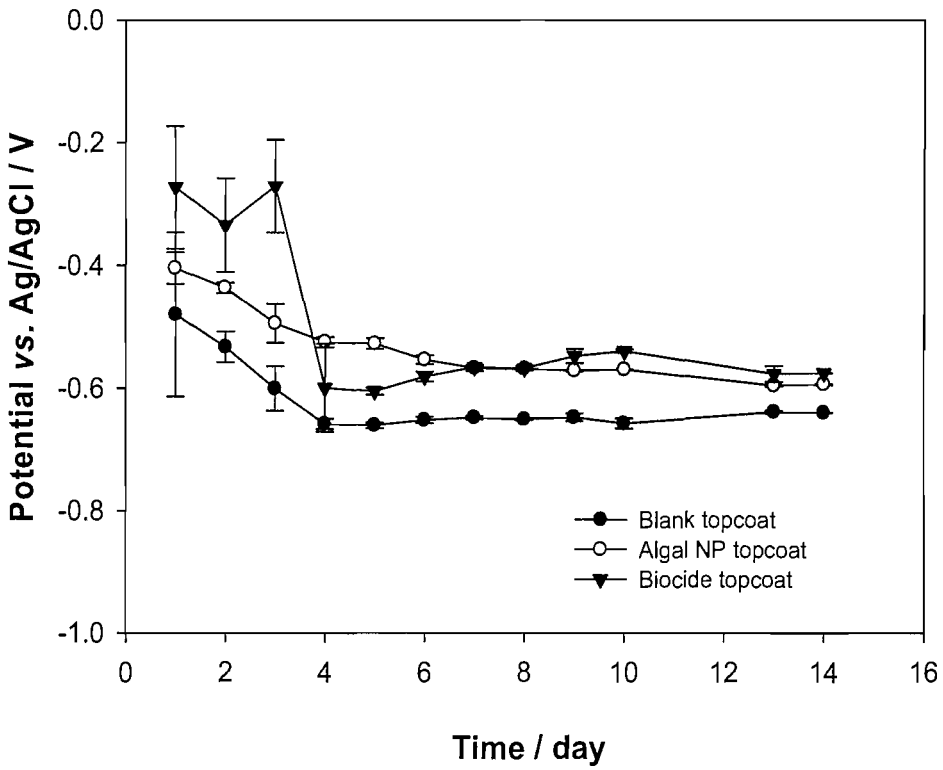

Figure 6.17 100 day aged top-coat (30 μm) OCPs in 3.5 % NaCl over two weeks

Natural seawater sampled from the Solent in May 2006 and aerated in the laboratory was used as an electrolyte to assess the open-circuit potential of the fully coated samples with primer (Fig 6.18). As the seawater was only aerated, the system was nutrient limiting but initially contained organics and organisms. The fluctuation of the coatings is relatively small (± 50 mV) but a trend of the algal coating having a higher potential is visible (Fig 6.18).

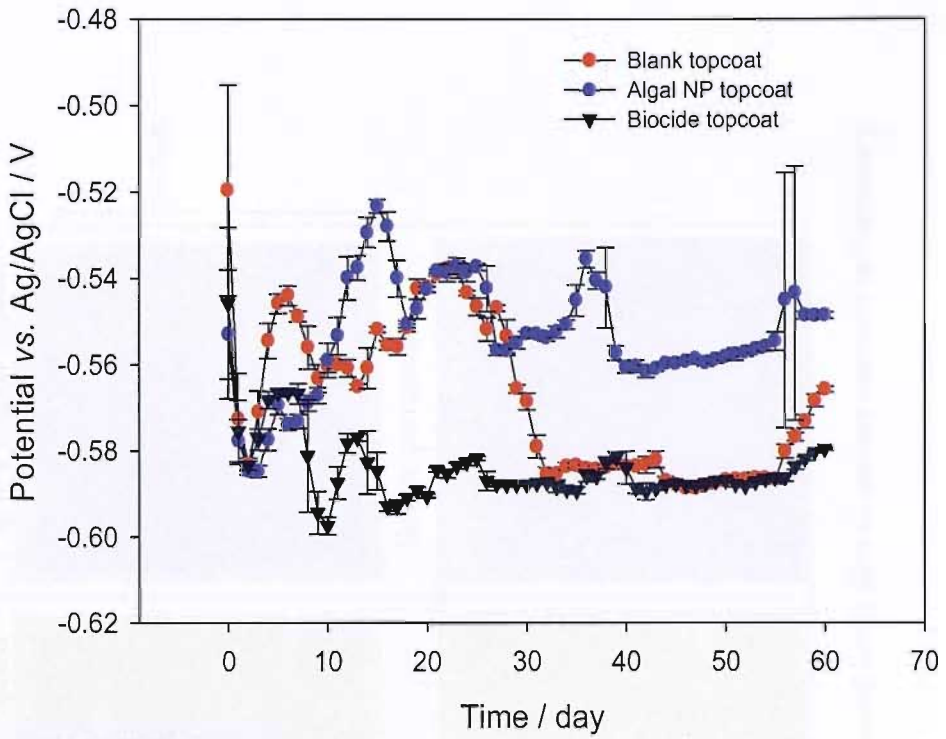

Figure 6.18 OCP of 80 µm thick coatings with primer in seawater at laboratory (nutrient limiting)

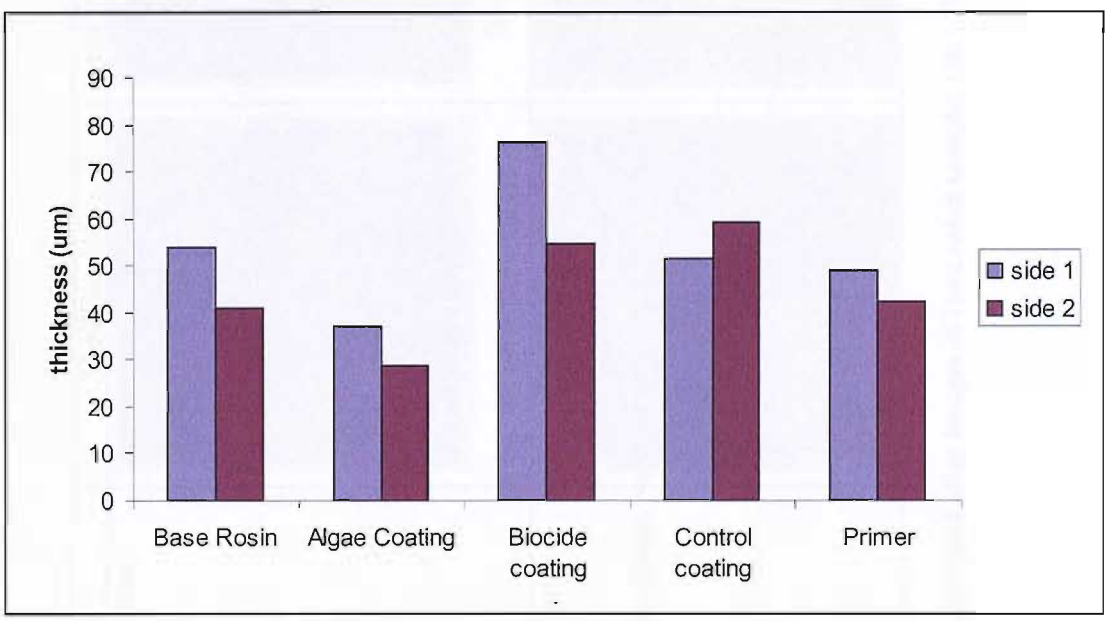

Figure 6.19 Dry film thickness increase of the 80 µm coating system after immersion in aerated seawater in laboratory for 60 days on side 1 (front) and side 2 (back) of the coated sample

The dry film thickness measurements are shown in Figure 6.19 and images of the coated samples after the immersion are shown in plate 6.1. All samples showed signs of corrosion, particularly at the edges, at the end of the 60 day trial in aerated seawater (Figure 6.20).

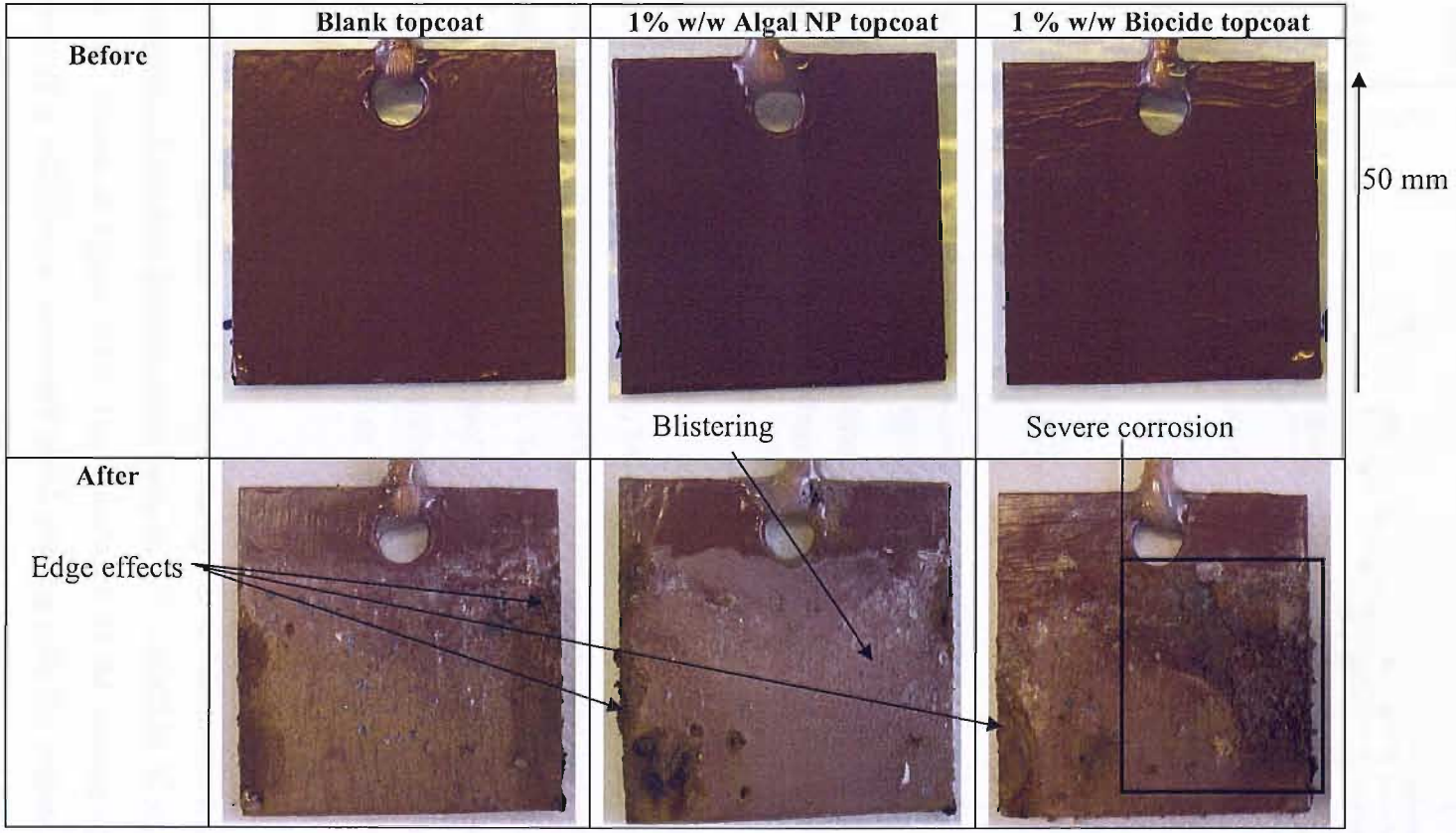

Figure 6.20 Before and after images of the coated samples (50 x 50 mm) immersed for 60 days in aerated seawater in laboratory

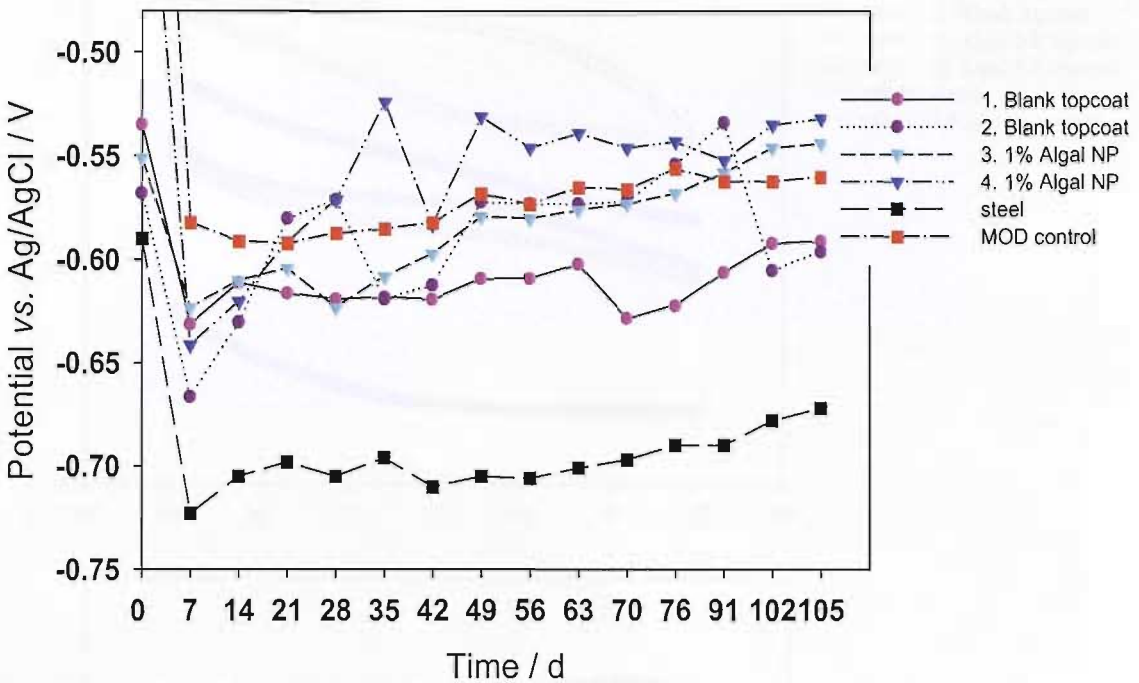

Figure 6.21 OCP of 100 µm thick coatings with primer in Solent seawater summer field trial (nutrient rich)

To further investigate the experimental coatings OCP performance against an organism and a nutrient rich environment *in-situ*, field trials were made. Coated samples with primer at a total thickness of between 125 – 145 µm were investigated and were incorporated on to board 3 of the field trails (Chapter 7, Table 7.4). Figure 6.21 plots the OCP over the 105 day duration as well as a positive control in the form of the MOD supplied system (section 5.2.3) and a negative control of a grit abraded (section 5.5) bare steel surface. Following the initial reading at time zero, all of the OCP measurements drift to more positive potentials over the 3 month period.

After 105 days immersion and 5 days storage in a laboratory fridge at 5 °C, EIS measurements of the final coatings were made in 3.5 % NaCl 18 °C ±2 and the Bode plot results are shown in Figure 6.22. The impedance of the coating systems versus the frequency (Fig 6.22) has a downward trend, starting with the highest impedance as the MOD control > blank topcoat > algal NP topcoat > steel. This was the order of the best to worst coating area resistance performance. This was not obvious from the OCP plot against time (Fig 6.21).

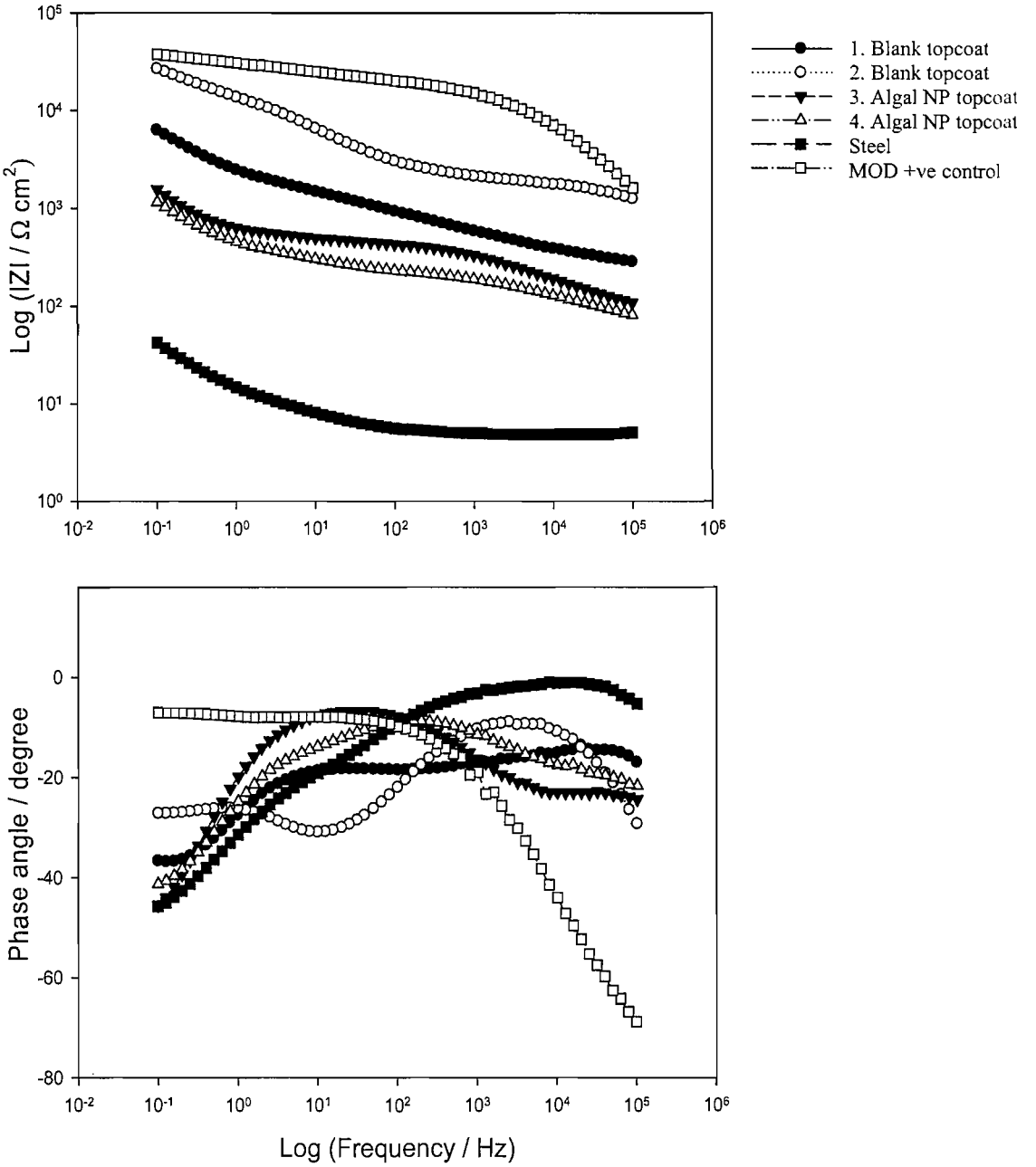

Figure 6.22 Bode plots of the field trial samples in 3.5 % NaCl, 18 °C ± 2 after 105 days

The phase diagram shows a capacitive system for the MOD positive control coating in the high frequency range as it tends towards -90°. This is what would be expected for an intact coating. The steel phase plot is the reverse of this and the experimental coatings are in-between. The number 2 blank topcoat has both the most dynamic OCP over the 105 day experiment and also has a phase angle plot which suggests it has two time constants, indicative of a failed coating. This is not easily visible from the surface images.

The surfaces of the coatings are shown at 42 days and at the end of the field trial (105) days after being rinsed with distilled water.

# and OCP logged sample	42 days immersion	105 day immersion
1. Blank topcoat (50 x50 mm)		
2. Blank topcoat (50 x50 mm)		
3. 1 % Algal NP topcoat (50 x50 mm)		
4. 1 % Algal NP topcoat (50 x50 mm)		

Steel (50 x50 mm)		
+ve control (Envoy TF500 ®) (150 x 100 mm)		

Figure 6.23 Images of the field trial samples of the online OCP data set at 42 days and on removal at 105 days (Nov 2007)

Number 4 (algal NP topcoat) has the highest open circuit potential (Figure 6.21), lowest impedance (Figure 6.22) and from the images (Figure 6.23) has a large area of corrosion in the bottom right hand corner. The fouling is minimal on all coated samples as noted for the entire field trial 3 (Chapter 7).

To further characterise the coated system an equivalent circuit as described in section 3.1.3 needs to be defined. Using the equivalent circuit models described in Figure 3.2 as a starting point and the raw EIS data the proposed circuit, noted in the literature for paints is shown in Figure 6.24. It is assumed that the pores are straight through pores and the walls of the pore are not electrochemically active.

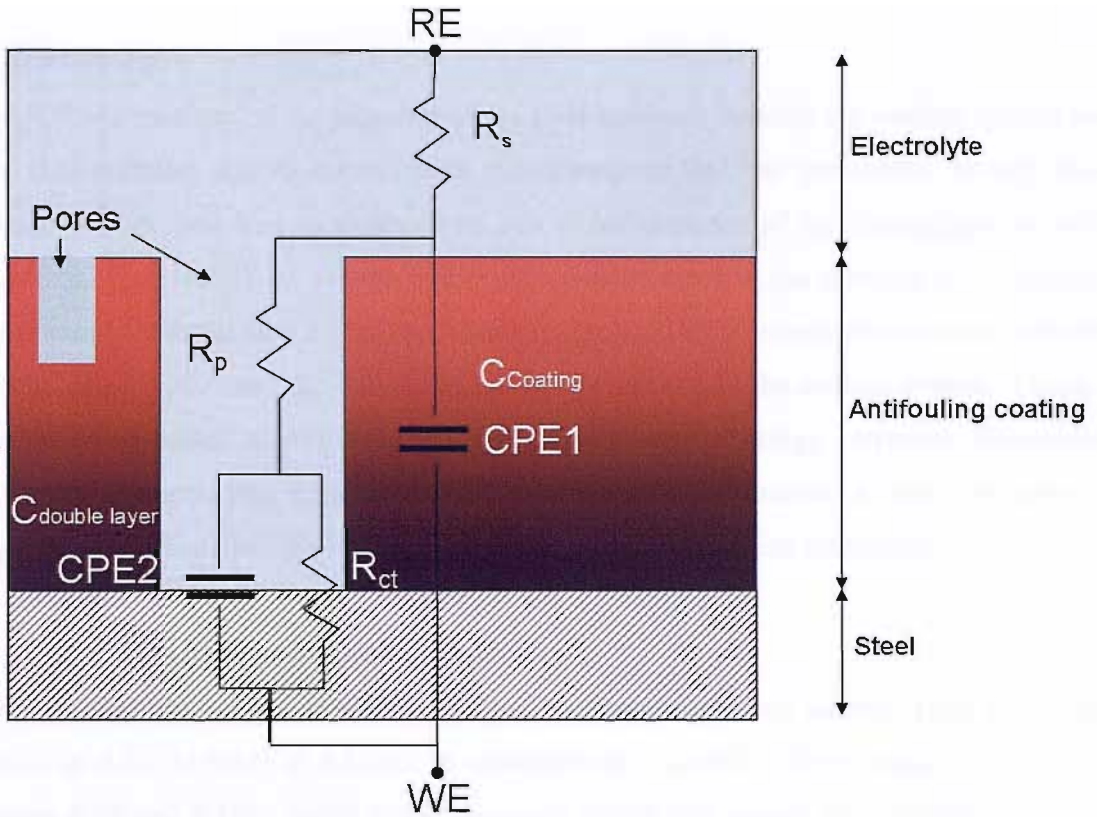

Figure 6.24 Proposed equivalent circuit for an antifouling coating on steel

Rs – bulk solution resistance
Rp – polarisation resistance; transport of electrolyte through the coating thickness dominated by pores
Rct – charge transfer process at the coating/metal interface
CPE 1 – coating is control depletion polymer i.e. does not act as a true capacitor
CPE 2 – Base of the pore/metal interface is corrosion dominated i.e. does not act as a capacitance double layer

This is a very similar model to the Randles circuit but because the capacitors in the system do not behave ideally a constant phase element (CPE) is used. The constant phase element is mathematically modelled by equation 6.2. Where Y_0 is the admittance and w is the angular frequency and n is a factor.

$$CPE = \frac{1}{Y_0 (jw)^n} \qquad \text{Eq 6.2}$$

A CPE represents a variety of elements such as a non-ideal dielectric behaviour ($-1 \leq n \geq 1$) and it has a constant phase angle making it independent from the frequency. The coating capacitance, in this study, is influenced by ion diffusion both in and out of the coating. Water ions going in, and soluble matrix as well as antifoulant moving out into the bulk solution which causes a varying thickness and composition of the coating. This can be modelled as CPE behaviour. This model fits the data with a Chi squared (X^2) test of $\leq 10^{-4}$.

6.3 Discussion

The OCP is a measure of the potential of the steel substrate beneath the coating system to react (i.e. corrode) due to contact with the electrolyte that has permeated through the coating. It was used here to measure the barrier performance of the coating system and provide an overview of the relative performance differences in the coatings with/without incorporated antifoulants at a 1 % w/w addition. Isolated OCP measurements were limited in their use as it informs little on the mechanistic protection of the coating system. Linear polarisation provided a verification of the experimental coatings corrosion resistance performance. Supporting evidence using EIS was needed to construct a clearer picture of the physical and chemical phenomena occurring in the electrochemical system.

6.3.1 Substrate preparation affects

The bare steel was investigated in 3.5 % NaCl solution over half an hour (Fig. 6.4) two hours (Fig. 6.5), 24 hrs (Fig. 6.6) and in seawater over a period of days, weeks and months (Figures 6.18 and 6.19). Initial characterisation of the mill scaled steel surface with the varying grit surface preparation helped to check what affect it had on the OCP and that the polishing of the surface was repeatable.

The dip at 9 hours of the steel OCP and subsequent recovery (Figure 6.6 (a)) does not feature in the Bode plot 6.6 (b). This illustrates how the combination of AC and DC electrochemical techniques allows for a more thorough understanding of the complex coating dynamics. By using an AC technique such as EIS this surface interaction with the electrolyte could be further analysed. The EIS data of the bare steel in Figures 6.5 and 6.6 can be interpreted by considering both the phase angle and the impedance *vs.* frequency plots. The Bode plot (Fig. 6.5 (b)) illustrates that the electrochemical system is resistance dominated. With increasing time, the phase angle maximum shifts to the right to higher frequencies. This indicates that an electron transfer is occurring. Normally this would cause a decrease in the impedance but due to the physical build up of corrosion products on the surface the impedance increases with time (Fig. 6.5 and 6.6 (b)).

6.3.2 Coating thickness affects

The electrochemistry of the ZRA measurements illustrated that the coatings were quickly dominated by their defects due to the very thin dry film thickness used at approx 15 μm

dft. In Figure 6.25 the blisters and white deposits which are salt precipitates are easily visible.

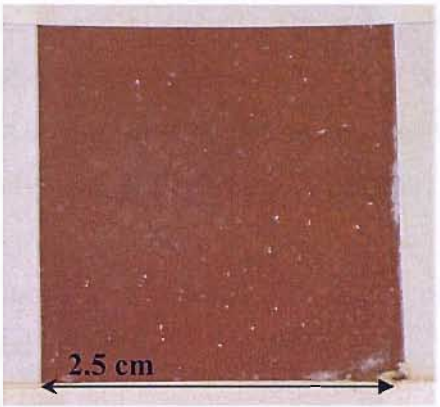

Figure 6.25 Exposed surface of blank topcoat in a blank to blank topcoat couple measured using ZRA in laboratory aerated seawater for 5 days

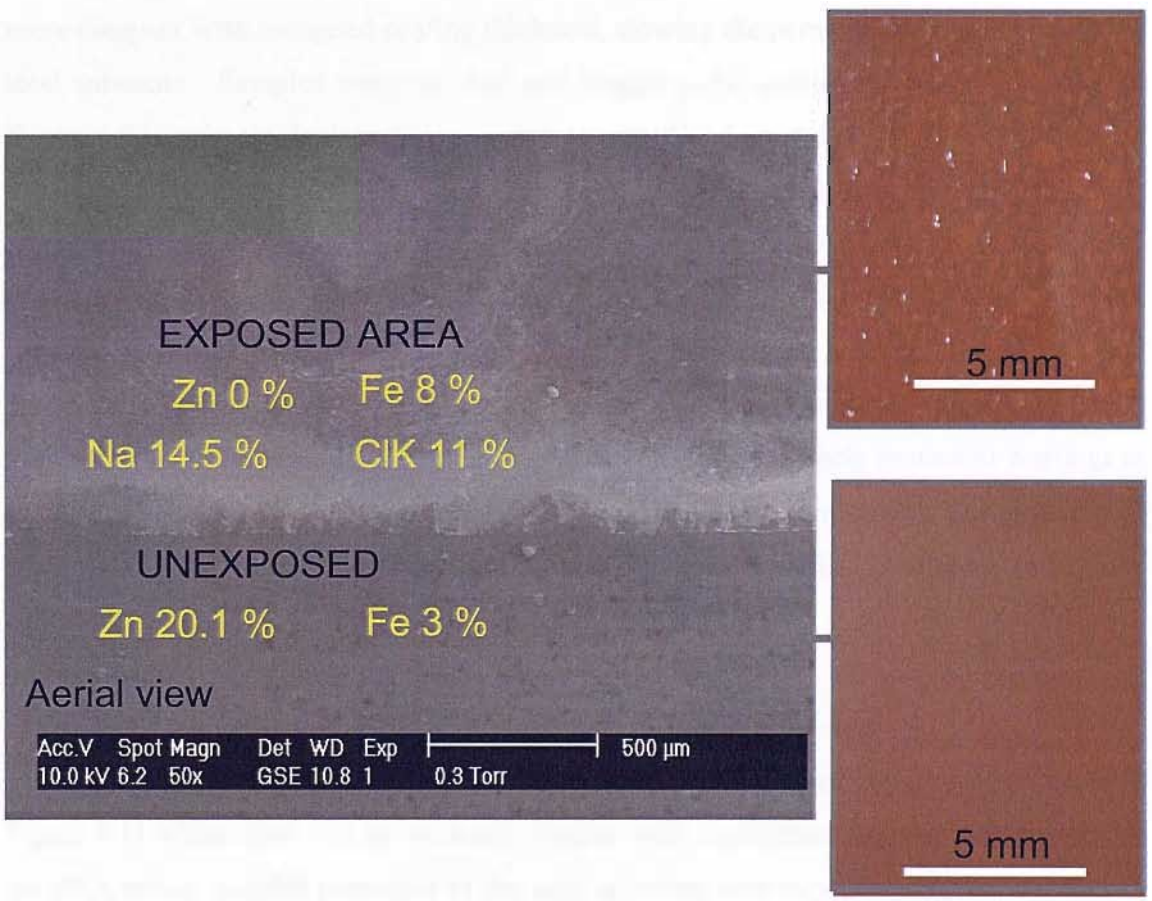

Figure 6.26 SEM micrograph of blank topcoat after 5 day ZRA experiment, with optical microscope images of the exposed (top) and unexposed (bottom) and element percentages from EDX spot analysis in yellow

Figure 6.26 highlights that the zinc, which is the key soluble element (pigment) controlling the depletion of the polymer (section 5.2.2) is exhausted from the surface of the exposed

coating and illustrates how the taped off section was not. A coated specimen is often cathodic when compared to an uncoated metal sample when it is exposed to the electrolyte [5.2]. This was proven to be the case in this experiment when the thin coated samples were decoupled from the bare steel (Fig. 6.11 (a,b,c)). The steel potential is consistent with that reported in fresh seawater typically at -700 mV. The three coatings (blank, algal NP and biocide topcoats) coupled OCP dropped to -650 mV *vs.* Ag/AgCl within 16 hrs which is nearing the OCP of the underlying steel at -700 to -750 mV *vs.* Ag/AgCl (Figure 6.9).

OCP, EIS and LPR were used to investigate the affect of coating thickness on the electrochemical response and to compare the techniques. In Figure 6.7 there was a stabilisation period with the two thin coatings 25 and 30 μm fluctuating the most in the first 5 minutes. After this stabilisation period the thickest coating (115 μm) had the highest potential. This was to be expected as the porous pathways would become increasingly more complex with increased coating thickness, slowing the permeation of the water to the steel substrate. Samples were too thin and fragile to be sectioned. Note that although Figure 6.8 is only single data measurements, a clear trend can be seen that with increasing thickness there is an increase in the impedance measured as one would expect i.e. the larger and more dense the barrier the higher the impedance. A coating having an area resistance of 10^6 Ωcm^2 is considered to be a good organic coating; this value is only valid for steel substrates [6.9] as in this project. Both the EIS and the LP data sets confirm that increased coating thickness increases the area resistance and that over the first 24 h of immersion in 3.5 % NaCl that 30 μm dft is above10^6 Ωcm^2. Poorly protective coatings at $\approx$ 30 μm dft decrease during immersion falling rapidly to 10^4 Ωcm^2 [6.10], this is similar to what we see for the coatings coated at 30 μm dft for both with and without antifoulant additives.

6.3.3 The affect of antifoulant additions to coatings on steel

The data tabulated in Table 6.3 is from the coupled and decoupled measurements made in Figure 6.11 where steel was galvanically coupled with experimental coated coupons. From the ZRA mixed coupled potentials of the steel substrate with experimental coating, and an assumed steel Tafel slope (an electrochemical corrosion parameter) of 145 mV [6.11], the porosity of the coatings after 24 h can be calculated using the mixed potential equation as shown in Eq. 6.3 [6.12].

$$\log\left(\frac{Sc}{Sa}\right) = 10^{E_m = E^A_{corr} + b_A} \qquad \text{Eq. 6.3}$$

Where E_m is the mixed potential of the coupled coated and uncoated metals, E^A_{corr} is the corrosion at the anodic metal surface, b_A the anodic Tafel slope of that anodic metal and $\frac{Sc}{Sa}$ is the ratio of the cathodic and anodic surfaces.

	Steel	Steel & blank rosin	Steel & 1% NP	Steel & 1% Biocide
E^{steel}_{corr} (mV *vs.*Ag/AgCl)		-683	-703	-709
b_A (mV dec^{-1})	145			
E_m (mV *vs.* Ag/AgCl)		-683	-684	-685
Porosity rate % $(S_C/S_A)^{-1}$		100	74	68

Table 6.3 Porosity rate after 24hrs in 3.5 % NaCl 22 ±1°C aerated solution ≈ 13 µm dft

This data demonstrates that the natural product and the biocide are performing in a similar manner as indicated by the ZRA coating *vs.* coating couples OCP in Figures 6.9 and 6.10. However, the 100 % porosity measurement for the blank coating suggests that there is a defect such as a pinhole which is dominating the electrochemistry of the sample. The high porosity measurements illustrate what is easily visible on the coating surface at the end of the trial that the coatings are too thin at ~15 µm dft, allowing pinholes and blisters to dominate the electrochemistry (Figure 6.24). These coatings were too thin.

The dry film thickness can be used as an indication of any disturbance by either corrosion build up or swelling of the coating (Fig. 6.19). The OCP (Fig. 6.18) correlates with the dft measurements (Fig. 6.19) where the biocidal topcoat had the lowest OCP and showed the largest increase in dry film thickness. This is also indicated by the high OCP, lower dft for the blank topcoat and the even higher OCP and lower dft for the 1 % w/w algal NP topcoat. Dry film thickness measurements (Fig. 6.19) of the uncoated samples suffer one major difficulty in cross comparison. The tenacity of the coated sample with under-corrosion prevents the corrosion products from being washed away when rinsed with distilled water as easily as the bare substrate.

As with a coated steel sample, on the bare corroding steel an increase in impedance of the corroding steel means that there is a barrier, most likely corrosion product as is verified by the phase angle plot which will indicate if electron transfer is occurring. In the coated systems a recovery to higher impedance over increasing time can suggest a corrosion product build up at a pore interface [6.13]. This is what is indicated in the blank rosin coating (Figure 6.14) where at day 5 there is a return of the impedance plot to higher impedance. It could also be that the ion diffusion from the film to the bulk solution could not be sustained and the conductivities of the pore and bulk solution stabilise registering a recovery in the film resistance as reported for PVC in NaCl solutions [6.14]. The 'pore-blocking' effect is suggested here to be the reason for the OCP drop to a bare steel OCP of -750 mV for the biocide coating in Figure 6.12. Where corrosion product from specific pores has become dislodged during transit between equipment and the steel corrodes and re-blocks the isolated pore.

OCP does vary with incorporated additive. The NP coating tends to have a higher OCP as seen after 5 days and after 30 days in Fig 6.18. Results show for both 30 μm dft coating trials (Figures 6.12 and 6.17) that the algal NP coating functions as a barrier system in a similar manner to the blank coating with marginally more positive OCPs. This indicates that the coating protection of the steel substrate has not been disturbed by the incorporation of the algal NP. OCP steady state was achieved for all coatings in 3 d (Fig. 6.11) and 4 d (Fig. 6.17) showing a time dependence on electrolyte ingress. With regards to the EIS data set, the impedance performance of the algal NP coating compares well with the blank control coating for the first 5 days. After this period there is a larger decrease in the total impedance of the algal NP coating at low frequencies, as the diffusion of reactants to the interface increases. This discrepancy can be seen more clearly in the water uptake measurements of the coating. Using the Brasher and Kingsbury model outlined in section 5.4, calculated water uptake measurements were plotted (Fig. 6.27) where increases in coating capacitance indicate water uptake [6.15].

(a)

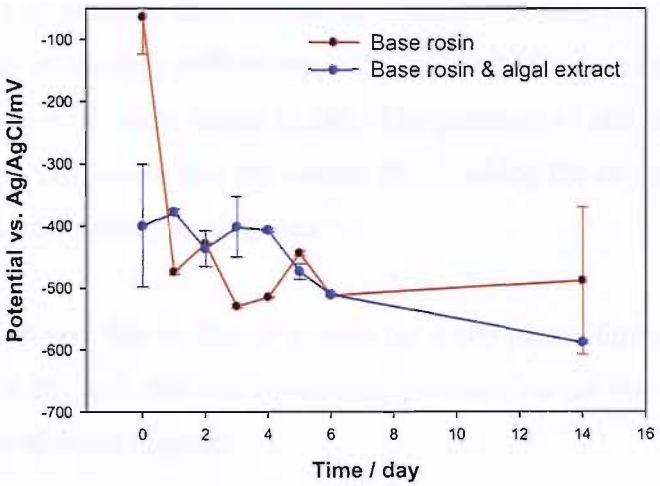

(b)

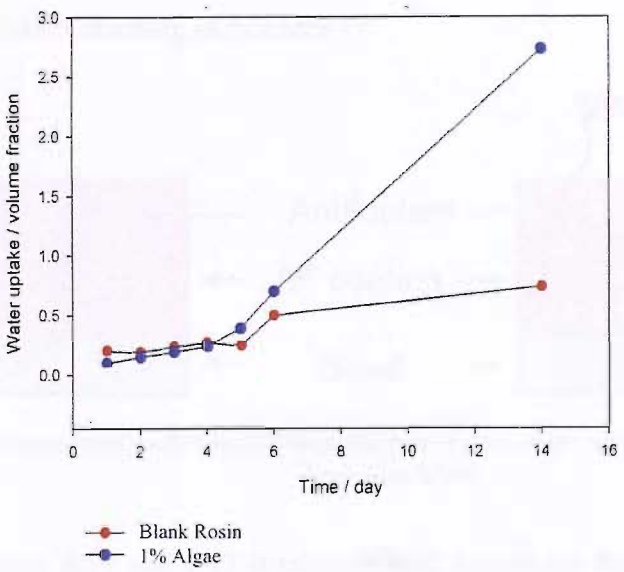

Figure 6.27 (a) OCP data and (b) water uptake measurements for 30 µm dft blank and algal coating on steel in 3.5 % NaCl solution at 18±2 °C

Figure 6.27 describes for the rosin a saturation point at day 4 with a volume fraction of 0.25 which plateaus and then on day 6 moves to a different level. By calculating the water uptake measurements it is the water permeability that is being characterised and so can only be interpreted as indirect information on the coating deterioration and the risk of underlying corrosion. Water uptake by the coating film leads to an increase in the film dielectric constant and thus results in a capacitance rise [6.15]. This explains how as the coating degrades the capacitance increases. Water and oxygen transported more rapidly then Na^+ and Cl^- [6.14] and so although the dielectric constant of water of 80 is used to calculate the water uptake, this may change over the course of longer timescales. Due to

the fact that the controlled depletion polymer is designed to create a porous top-layer (leach layer) all porosity does not detract from the coating performance and in actuality is necessary for antifouling performance. Oxygen and H_2O take one day, Na takes between 1 and 10 days and Cl^- takes longer [6.16]. The presence of salt ions in the electrolyte slows down the water diffusion into the coating [6.1] making the estuarine field trials (Chapter 7) an important low salinity testing area.

It is suggested here that in this AF system the water passes through the coating in two main ways (Fig. 6.28) and that the controlling pathway varies between these two with time. Mechanisms of water ingress:

(1) Pores and voids

(2) Binder depletion/leaching of biocides

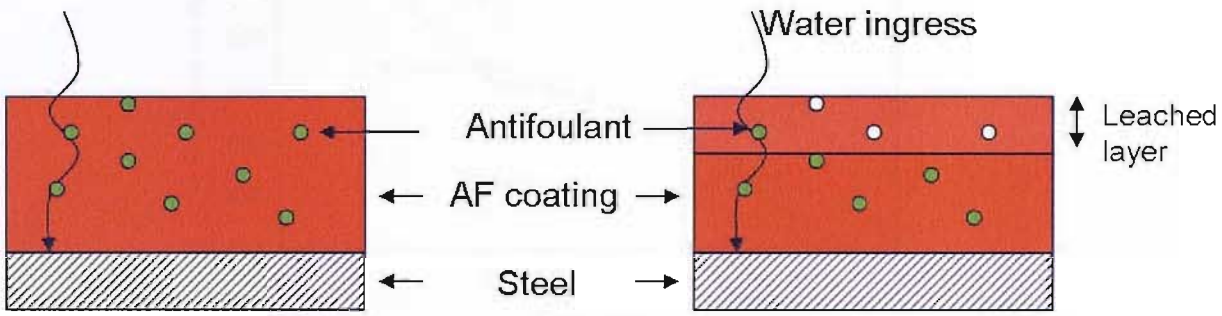

Figure 6.28 Schematic of pathway (1) through pores and voids and (2) through the controlled depletion layer

As seen in Figure 6.11 and 6.17 it takes around 3 days for the OCP to stabilise. In the impedance data set of 6.14, 6.15 and 6.16 there is a large drop in impedance from day one to day 3 for all three coatings. Both of these electrochemical techniques are considered to indicate the dominance of water permittivity caused by pathway 1 (dominance of pores and voids).

With regards to pathway 2, theoretically depletion of the coating matrix occurs in an even manner from the surface parallel to the water front. As outlined in section 5.2.2 the whole coating becomes hydrated followed by degradation of the coating occurring in the entire film thickness. The rate of hydration is linked to the erosion mode [6.15]. The release of a biocide from an antifouling coating is 'greatly dependant on the macromolecular matrix and the erosion mode' [6.15].

The natural product antifoulant works to a certain extent by this dissolution process i.e. the water must come in so that the degradable antifoulant components can leach out. This starts to explain why the water-uptake measurements increase so quickly after day 4 (Figure 6.28 (b)). The lower water uptake at day 1 by the algal NP topcoat suggests that it is not pore dominated but hydration has occurred quicker than the blank topcoat and the increase after day 4 indicates that the water uptake may be due to an increased rate of depletion of the algal incorporated coating (i.e. pathway 2).

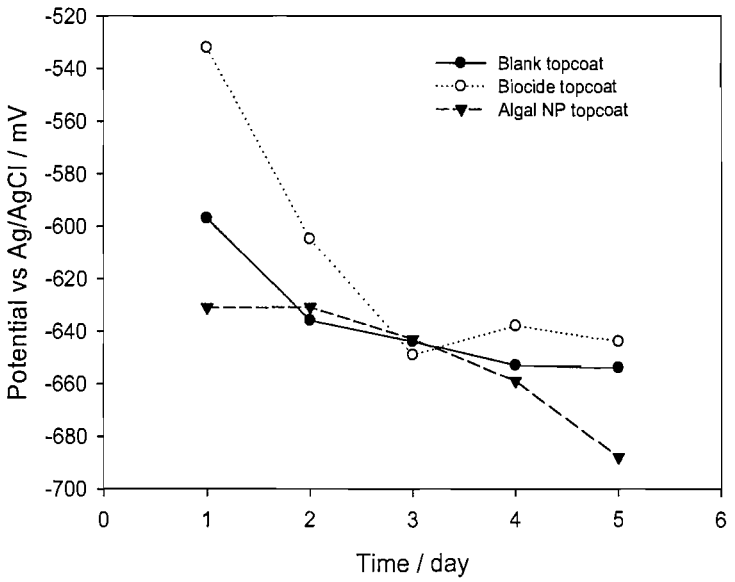

Figure 6.29 Decoupled OCP measurements of 12 µm dft in aerated seawater

The OCP readings from the decoupled thin coatings from the ZRA experiment (Fig. 6.29) agree with the hypothesis of an accelerated depletion of the coating with incorporated algal NP. While both the biocide and the blank topcoat stabilise after 3 days the algal NP topcoat continues to drop to a lower OCP (-40 mV *vs.* Ag/AgCl). It has been reported in the literature for two antifoulant booster biocides Diuron and Tolyflunaid that the releases rate is changed due to the solubility of the compounds [6.15].

6.4 Conclusions

Electrochemical testing complimented the systems approach used through out this project by allowing the physical and chemical phenomena to be measured on both the steel/coating and coating/environment interfaces. The coupling of DC and AC techniques was an important feature in this test series. The aim was to investigate the potential of electrochemical techniques to assess the functionality of the antifouling coatings and the key findings are outlined below.

- By using thin coatings (15 and 30 μm) an increased sensitivity to coating degradation was observed. The coating dft was too thin at 15 and so compromised the coatings integrity. Coating dft of 30 μm had a coating resistance area of over 10^6 Ωcm^2 after 24 hrs for all three experimental coatings (blank, 1% algal NP and 1 % biocide). This verified that good organic coatings were being produced at 30 μm dft and that their performance was not initially degraded by the incorporation of the algal NP or biocide antifoulant additives. From the LP data the 30 μm dft performs as a good coating over the first 24 hrs in 3.5 % NaCl. Timescales of less than 5 days should be investigated to encompass the hydration and initial depletion of the antifouling coating system.
- ZRA was a useful tool which provided an understanding of the interactions between the coatings and the steel substrate, and helped to identify what sample preparation and coating techniques were adequate. However, the focus of this research was not on corrosion protection and so other techniques were adopted to further investigate the marine environment, topcoat interactions.
- Using EIS, the algal NP topcoat showed a higher water uptake, but showed no increase in open-circuit potential. This is hypothesised here to be due to the different pathways of the electrolyte into the coating due to NP additive. Increased water uptake may be due to an increased rate of depletion of the algal incorporated coating.
- The number of tests conducted on the EIS of the variable additive coatings is not enough to conclusively suggest that the addition of NP affects the water uptake but from the data as a set suggests that this is a possible factor. As such the controlled delivery of NPs needs to be optimised.
- The coupling of OCP and EIS as non-destructive techniques to assess the functionality of the coatings has been shown here to be an interesting and original way to look at antifouling top coats and the direct incorporation of the antifoulant

natural products. The OCP measurements can assess the stability of the system but the EIS can measure the more subtle responses of the electrochemical cell. It can identify processes that may remain masked to other techniques. The OCP and EIS in particular probed the interface between the Antifouling coating and its environment effectively and in turn could help to inform future antifouling system development.

- The binder system provided a useful test vehicle in the laboratory and the electrochemical field trial. Further development of the controlled leaching of the natural products from the system would be enabled by better designing the release mechanism or tethering for soluble compounds. Aspects of this will be highlighted and discussed in the further work section of Chapter 8.

6.5 References

[6.1] F. Deflorian, S. Rossi, *An EIS study of ion diffusion through organic coatings*, Electrochemica Acta 51 (2006) 1736-1744.

[6.2] J-T Zhang, J-M. Hu, J-Q Zhang, C-N. Cao. *Studies of water transport behaviour and impedance models of epoxy-coated metals in NaCl solution by EIS*. Progress in Organic coatings 51 (2004) 145-151.

[6.3] D.M. Brasher, and A.H. Kingsbury, *Electrical measurements in the study of immersed paint coatings on metal. I. Comparison between capacitance and gravimetric methods of estimating water-uptake*. Journal of Applied Chemistry, 4 (1954) 62-72.

[6.4] J.C. Rowlands and D.J. Chuter, *A.C. Impedance measurements on marine paint systems*. Corrosion science, 23 (1983) 331-340.

[6.5] P.L. Bonora, F. Deflorian, L. Fedrizzi, S. Rossi, *Electrochemical evaluation of coatings for marine corrosion control*, Proceedings of the 9th International Congress on Marine Corrosion and Fouling, held at the University of Portsmouth , In Developments in Marine Corrosion. Ed. S.A. Campbell, N. Campbell and F.C. Walsh. Royal society of Chemistry,(1998) pp 163-180.

[6.6] A. Amirudin, C. Barreau, R. Hellouin, D. Thierry, *Evaluation of anti-corrosive pigments by pigment extract studies, atmospheric exposure and electrochemical impedance spectroscopy*. Progress in Organic Coatings 25 (1995) 339-355.

[6.7] A. Amirudin, and D. Thierry, *Application of electrochemical impedance spectroscopy to study the degradation of polymer-coated metals. Progress in Organic Coatings* 26 (1995) 1-28.

[6.8] F.C. Walsh, Ponce de León, C., Kerr, C, Court, S. and Barker, B.D. Electrochemical characterisation of porosity and corrosion resistance in electrodeposited metal coatings. *Surface and Coating Technology*, 202, (21), (2008) 5092-5102.

[6.9] J.R Scully and S.T. Hensley, Corrosion/93 National Association of Corrosion engineers, New Orleans, LA, USA Paper No. 359.

[6.10] C-T. Chen, B.S. Skerry, *Assessing the corrosion resistance of painted steel by AC impedance and electrochemical noise techniques*, Corrosion/91 National Association of Corrosion engineers, Science, 47 (1991) 598-611.

[6.11] J. Creus, H. Mazille, H. Idrissi, *Porosity evaluation of protective coatings onto steel, through electrochemical techniques*, Surface and Coatings Technology 130 (2000) 224-232.

[6.12] J.N. Murray, *Electrochemical test methods for evaluating organic coatings on metals: an update. Part I. Introduction and generalities regarding electrochemical testing of organic coatings*, Progress in Organic Coatings 30 (1997) 225-233.

[6.13] Y. Puget, Failure mechanism of polyurethane coated steel subjected to erosion-corrosion. Thesis (PhD) University of Southampton, Dept. of Engineering (1999).

[6.14] R.G. Duarte, A.S. Castela and M.G.S. Ferreira, *Influence of the solution cation mobility on the water uptake estimation of PVC Plastisol freestanding films by EIS.* Progress in Organic Coatings 57 (2006) 208-415.

[6.15] J. R. Scully, *Electrochemical impedance of organic-coated steel: correlation of impedance parameters with long-term coating deterioration*, J. Electrochem. Soc., 136 (4) (1989) 979-989.

[6.16] F. Fay, I. Linossier, V. Langlois, K. Vallée –Rehel, *Biodegradable poly(ester-anhydride) for new antifouling coating*, Biomacromolecules 8 (2007) 1751-1758.

Chapter 7 Biofouling characterisation

A key investigation for the development of a NP-based antifouling system was to measure what antifouling affect the compound had within a coating system (Figure 1.4) as well as what affect if any did the NP have in the natural marine environment.

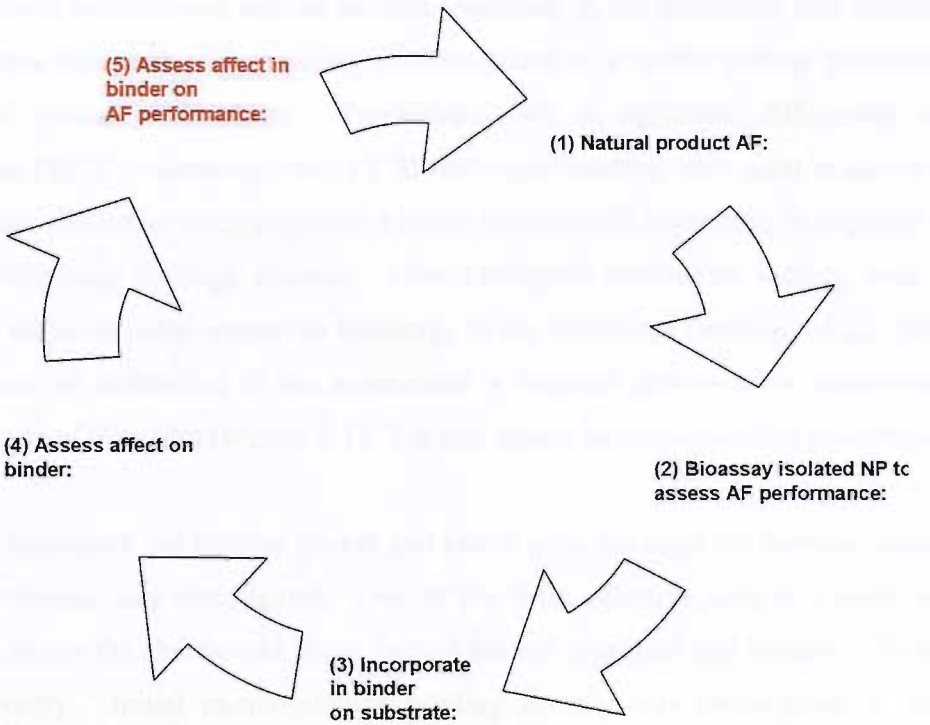

Figure 1.4 Key tests to optimise an NP-based antifouling system

The aims of this chapter were to:

- assess the antifouling efficacy of the experimental antifouling coatings through bacterial viability and percentage coverage measurements. In the laboratory, 1, 5 and 10 % w/w of the algal NP (industrially dried source) topcoat was compared to the blank topcoat.
- assess the antifouling efficacy of the NP extract immobilized using silane-gluteraldehyde on a glass slide against biofilm formation in a field trial
- investigate the fouling community and structure of Southampton Solent waters in response to NP antifoulant using biological (EDIC) and surface engineering (FTIR) techniques.
- assess the antifouling efficacy of the algal NP topcoat against biofouling in field trials at variable dry film thicknesses (50, 100, 150 μm) and NP concentrations (1, 5 and 10 % w/w) against the blank topcoat.

The biofouling experiments were to assess the antifouling efficacy of the developed NP topcoat as a system. The algal extract functioned as an antifoulant in isolation (Chapter 4), was incorporated (Chapter 5) and further characterised in the paint vehicle (Chapter 6). In this chapter the algal NP (from the industrially dried source, extract 'A' in Chapter 4) antifouling performance against biofilm formation in the laboratory and biofouling in the field was analysed. The topcoat was examined as a useful testing platform for novel natural product antifoulants. Techniques such as episcopic differential interference contrast (EDIC) microscopy and FT-IR microspectroscopy were used to assess the marine biofilms. Effective testing against a broad spectrum of organisms is required to regulate the antifouling coatings success. Microbiological antifouling activity was previously tested on the isolated extract in bioassays in the laboratory (section 4.5.2). Although the sequence of biofouling is not regimented a frequent precursor to macrofouling is the formation of a biofilm (section 2.1). For this reason bacterial viability was investigated.

In the laboratory the biofilm growth and viability on the algal NP topcoat compared to the blank topcoat was investigated. One of the most effective tests is a field trial (section 3.2.2) where the abiotic and biotic factors are not regulated and there is a diverse fouling community. Initial microbiological fouling activity was investigated in this way on isolated extracts immobilised on to glass slides. Macrobiological fouling activity was monitored on the full coating system with extracts incorporated into the topcoat as outlined in Chapter 5.

7.1 Marine biofilm analysis

Nucleic acid staining and EDIC microscopy as a measuring tool for biofilm growth on an antifouling coating was assessed as an assay for antifouling efficacy. The difference in the viability and percentage coverage of the bacteria were measured in both the laboratory and the field. Natural marine biofilms were used as the water was collected from the sea (section 3.3.2) and brought to the laboratory. The first experiment investigated the biofilm viability in the laboratory on 1 % algal NP and blank topcoat over a period of four weeks. A second experiment in the laboratory compared bacterial viability on 1 %, 5 % and 10 % algal NP, blank topcoat and glass slide controls for three weeks. The marine biofilm from samples in a field trial was also examined and is outlined in the field trial section 7.2. The sample preparation and staining technique used through out this investigation are described in section 7.1.1 and 7.1.2 respectively.

7.1.1 Biofilm analysis methods

Bare steel and glass microscope slides (76 x 25 mm) were washed and degreased with acetone. Glass slides were coated using a knife edge (≈ 10 µm dft) for a uniform surface and air dried for 1 week. Samples were immersed in beakers of seawater collected earlier that day. The first laboratory trial was in waters sampled on the 28th April 2006 which is an early fouling season and the second trial was from the 9th July 2007, which is in the later fouling season. Seawater was retrieved from the surface waters (≈ 1 m) of the Southampton National Oceanography Centre at Empress Dock (section 3.3.2). The seasonality of the water was chosen to capture the highest fouling pressure environment. The seawater was continually aerated with oxygen and environmental parameters (section 3.2.3) were measured daily.

Samples of 1% algal NP topcoat, blank topcoat and uncoated glass slides were immersed in beakers as described in Figures 7.1 and 7.2. In Figure 7.1 the experimental coatings remained in the same beaker (volume of seawater 500 mL) and were placed flat on the base of the beaker in approximately 70 mm of seawater. In the second experiment (Figure 7.2) the samples were immersed in separate 250 mL beakers (volume seawater 150 mL) and placed at an angle to the base of the beaker (Figure 7.3) these beakers were then placed in a temperature controlled water bath. This modification in laboratory trial 2 (Fig. 7.3 b) was done to avoid a saturation build up of antifoulant in the solution, and the sample positioning changed to eliminate the gravitational colonisation of the surface.

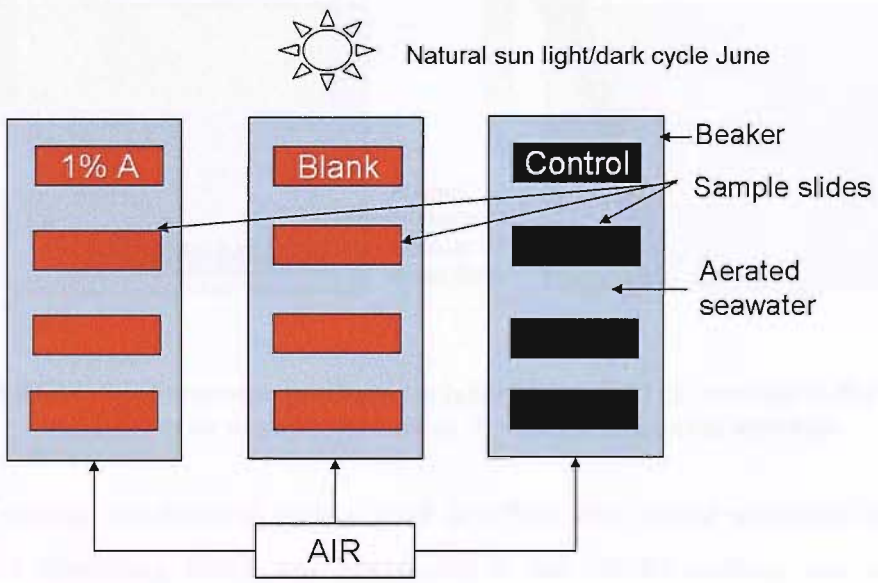

Figure 7.1 Plan view of experimental immersion set up (trial 1) of the biofilm viability experiment on 1% algal NP topcoat, blank topcoat and uncoated glass slides

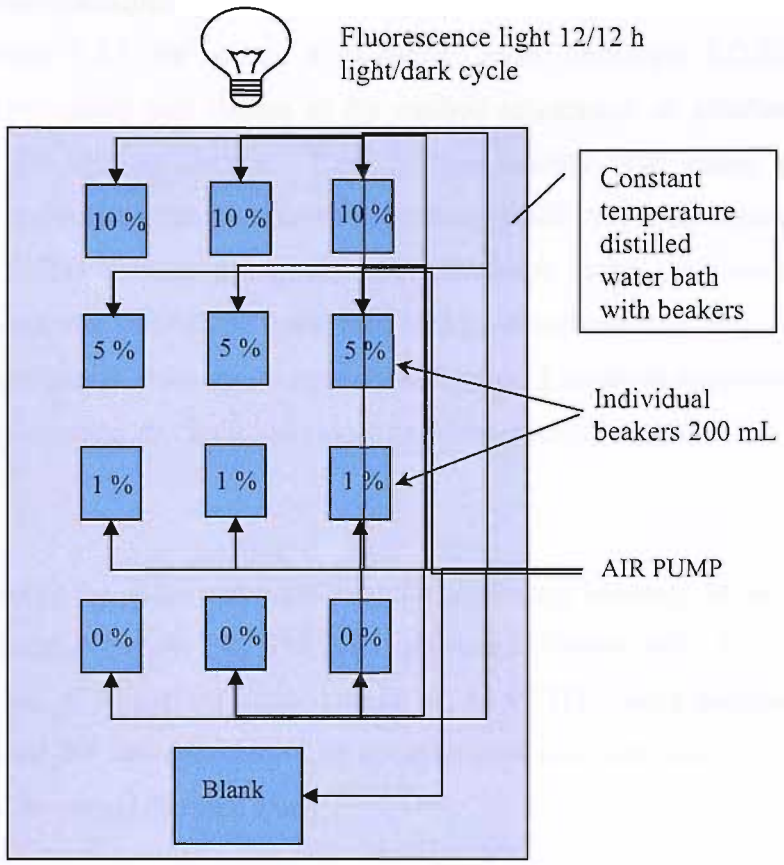

Figure 7.2 Plan view of experimental immersion set up (trial 2) of the biofilm viability experiment on 1, 5 and 10 % algal NP and blank topcoat

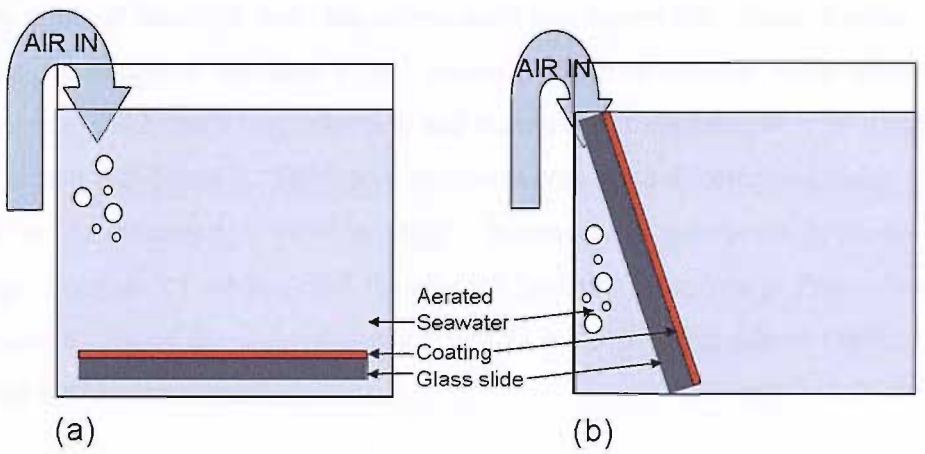

Figure 7.3 Glass slide immersion positions for laboratory trial 1 (a) parallel to the base, and trial 2 (b) at an angle to the base of the beaker in aerated seawater

A sample coating was removed once a week to a Petri dish, rinsed with distilled water to remove any interfering media and transported to the lab for staining and microscope imaging.

7.1.2. Staining technique

As outlined in section 3.2.1 the use of a molecular probe technique LIVE/DEAD® BacLight™ (from Invitrogen) was chosen as the method to measure an attached mixed species biofilm on the coating surface. Two different nucleic acid stains, a green-fluorescent SYTO 9 stain and a red-fluorescent propidium iodide stain were used to assess biofilm viability. SYTO 9 stain penetrates cells that have intact membranes while propidium iodine penetrates only those cells with broken membranes i.e. dead or dying cells. As outlined in Chapter 3 the use of staining and adapted confocal microscope is an effective means of measuring the bacterial coverage without interfering with the surfaces under examination.

The protocol for staining the slides and measuring the percentage coverage of the live and dead bacteria is outlined in Figure 7.4. The BacLight was defrosted and a 50:50 ratio of stain was used. 10 μL of propidium iodide and 10 μL of SYTO 9 were combined for a total of 20 μL to adjust for wastage. 18 μL of the combined stain was added to 6 mL of filtered (0.2 μm pore diameter) distilled water.

A 0.5 mL droplet of the double nucliec acid stain solution was added to each surface of the experimental coatings. Samples were then covered in tinfoil and left for 30 minutes in the dark. On removal from the dark, the excess stain was tipped off. Using a white light, red and green fluorescence adjusted EDIC microscope, three images were taken at x 10 (imaged area = 2.42 mm^2) magnification and three images captured at x 50 magnification (imaged area = 0.096 mm^2). Thickness measurements were documented using the z-scan function on the microscope viewing stage. Images were processed by measuring the percentage coverage of the bacterial fluorescent intensity using Image Pro software. The chosen wavelength of the light was important as well as the exposure capture time for comparing fluorescent intensities.

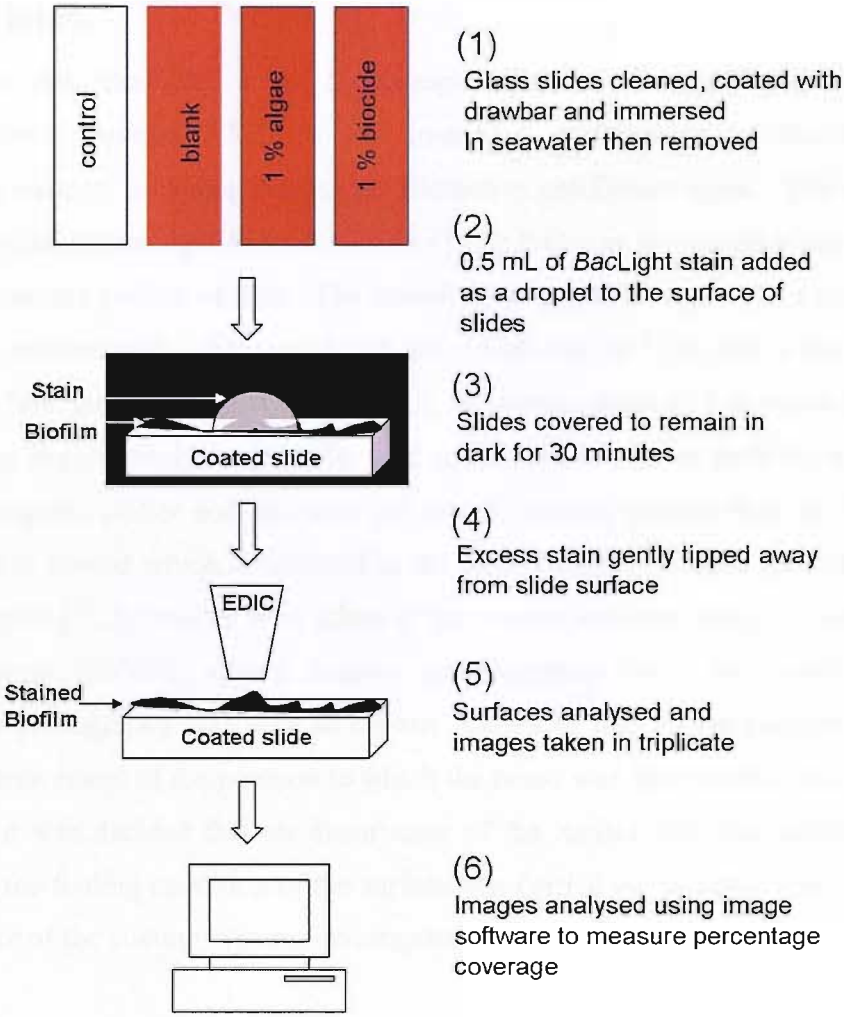

Figure 7.4 Live/dead bacteria staining protocol

7.1.3. FT-IR

The use of FT-IR (Fourier transform – Infra red) to determine the structure and presence of biological macromolecules has increased in the last few years. The facility used for this study was at Daresburys' synchrotron radiation source UK with an aperture of 8 x 8 μm. The reason for using a radiation source was the high spatial resolution. The equipment was a Nicolet nexus FTIR spectrometer which was coupled to a Nicolet continuum IR microscope with a movable stage and 32 magnification objective lens. Two modes were used transmission and reflectance mode. Sample particles were used in a compression diamond cell. Experimental coatings using a drawbar as well as the pure extracts were applied on Low-e FTIR slides (Kevley Technologies, Ohio, USA) and stored in desiccators. Band positions at 'characteristic' frequency ranges identified the type of molecules present in the sample area. Protein and polysaccaharides are two key characteristic marker bands for a bacterial biofilm [7.1]. All graphed spectra were baseline-corrected.

7.2 Field trials

Field trails were conducted at the Southampton National Oceanography Centre in the Empress Dock (section 3.3.2) to test in-service performance of the experimental antifouling coatings including NPs as an alternative antifoulant agent. The environment specifically under investigation in this thesis (Table 2.6) was for vessels when alongside at dock for extended periods of time. The central dock area of an estuary is a prime example of such an environment. Empress Dock has a high tide of 12 m and a low tide of 8 m [7.2]. The tidal range in this area is 4 m with an average depth of 5 m below chart datum. The seafloor is composed of a fine silty mud and the water column itself has high levels of nutrients, organic matter and silt with the salinity usually greater then 30 [7.3]. Light penetration is limited which is reflected in the small quantity of algae growth confined to shallow depths [7.3]. Images were taken of the coating surfaces using a Canon EOS 20D SLR or Sony DSC-P51 digital camera approximately every two weeks. Initially underwater photography was used to capture images of the coating surfaces. However, due to the movement of the pontoon to which the board was fastened the camera could not focus and it was decided that air disturbance of the surface was unavoidable. A basic ranking of the fouling condition of the surface was carried out to better assess the relative performance of the coating systems investigated.

7.2.1 Immobilised natural product field trial

The two aims of this experiment were to test the antifouling performance of immobilised algal natural product extract in a heterotrophic marine sea-trial and to validate the EDIC microscope data with respect to FT-IR analysis. The isolated natural product extract in ethanol at 25, 50 and 1100 $\mu g\ mL^{-1}$ concentrations were immobilised on to a silanized glass microscope slide using glutaraldehyde as a crosslinking agent. The glass microscope slides (Kevley technologies) were silanized following the procedure of Costa et al., 2001 [7.4], by immersing them in 4 % (v/v) γ-aminopropyltriethoxy silane (Sigma) in acetone solution at 45 °C for 24 h. The slides were then rinsed in distilled water and immersed in 2 % v/v aqueous glutaraldehyde solution for 2 h at room temperature. Slides were rinsed with distilled water and dried for 1 h at 60 °C. Varying concentrations (25, 50 and 1100 $\mu g\ mL^{-1}$) of the crude algal extract in ethanol were added to the treated surfaces and allowed to evaporate at room temperature (24 h). Slides were then split in half, pinched between two perspex sheets with gaskets (see Figure 7.5) and exposed at 1 m below the waterline in the sea through a 3.5 cm diameter window for 1 week (14^{th} to 21^{st} Sep 2007). After one week samples were removed and one half was subjected to the live/dead

BacLight™ staining (section 7.1.1) and the other half was studied within 24 h using FT-IR at the Daresbury synchatron radiation centre (section 7.1.3).

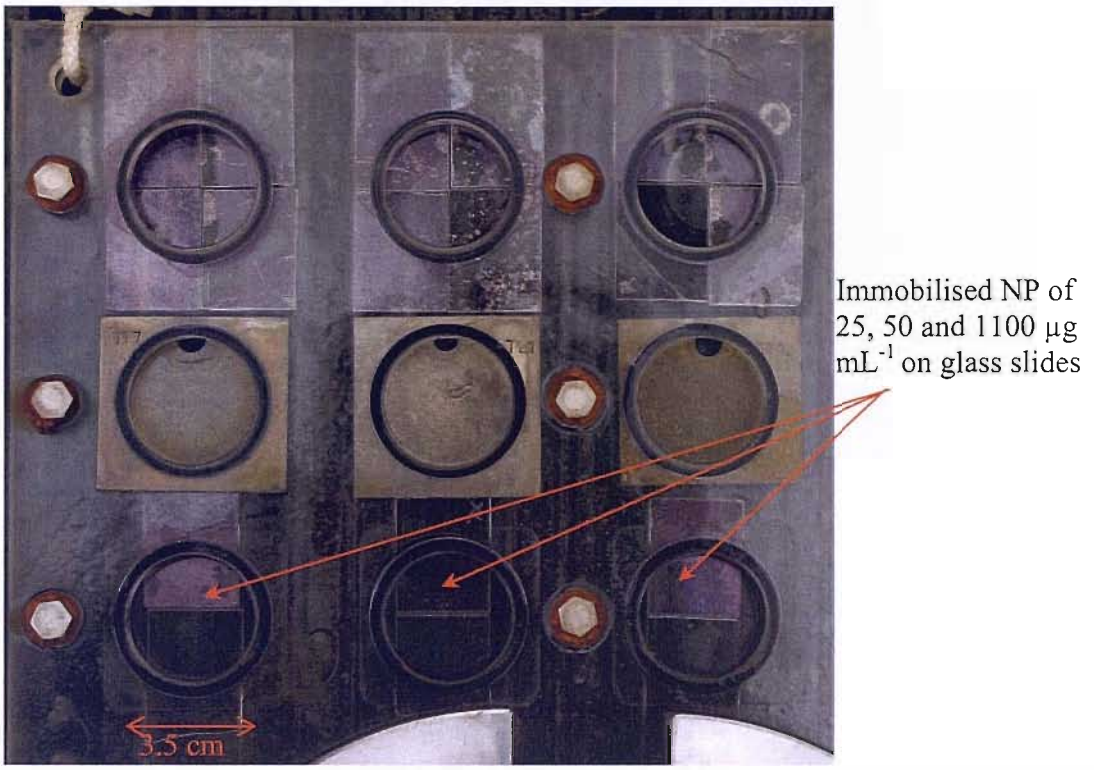

Figure 7.5 Immersion board for the immobilised natural product field trial

7.2.2 Experimental antifouling coatings field trials

Three field trails (1, 2 and 3) were made on coated steel samples as outlined in section 5.2. Samples were attached to varnished wooden boards with nylon nuts ands bolts and suspended 1 meter below the water line with rope off of a floating pontoon in Southampton dock. The matrix tested is outlined in both Tables 7.1 and 7.5. Immersion boards were lifted and monitored every two weeks using visualisation and photographs (Figure 3.5). The total air time was no longer than 30 minutes maximum.

Field trial No.	Time / months	Sample dimensions / mm	Primer
1	4 (May-Aug 2006)	50 x 50	With/without
2	6 (April – Sept 2007)	100 x 150	With
3	3 (Aug – Nov 2007)	50 x 50	With

Table 7.1 Field trials 1, 2 and 3 and the tested systems duration, dimensions and undercoats

In Tables 7.2, 7.3 and 7.4 the coating parameters are outlined for field trial 1, 2 and 3 respectively. The dfts are for the exposed front surfaces of the panels.

Sample no.	Date	Mean coating thickness (μm) (n=10)	Standard deviation (μm) (n=10)	Coating type	Primer	Environment April 21 - August 16
1	21/04/2006	39	4	Blank topcoat		Field trial
2	21/04/2006	83	22	Blank topcoat	X	Field trial
3	21/04/2006	37	3	1% Algal NP topcoat		Field trial
4	21/04/2006	86	13	1% Algal NP topcoat	X	Field trial
5	21/04/2006	40	5	Biocide topcoat		Field trial
6	21/04/2006	84	16	Biocide topcoat	X	Field trial
7	21/04/2006	67	12	Interspeed Ultra	X	Field trial
8	21/04/2006	54	10	Primer	X	Field trial
9	21/04/2006	0	0	Bare steel		Field trial

Table 7.2 Field trial 1 board of coating systems and dry film thickness

Sample no.	Date	Mean coating thickness (µm) (n=10)	Standard deviation (µm) (n=10)	Coating type	Primer	Environment March 23 - September ?
1	19/03/07	150	35	Base rosin	X	Field trial
2	19/03/07	204	35	Base rosin	X	Field trial
3	19/03/07	300	20	Base rosin	X	Field trial
4	19/03/07	120	18	1% Algae	X	Field trial
5	19/03/07	151	24	1% Algae	X	Field trial
6	19/03/07	210	30	1% Algae	X	Field trial
7	19/03/07	536	-	Envoy TF500	X	Field trial
8	19/03/07	510	-	Envoy TF500	X	Field trial
9	19/03/07	520	-	Envoy TF500	X	Field trial
10	19/03/07	100	35	Interspeed Ultra	X	Field trial
11	19/03/07	210	24	Interspeed Ultra	X	Field trial
12	19/03/07	270	36	Interspeed Ultra	X	Field trial

Table 7.3 Field trial 2 board of coating systems and dry film thickness

Sample no.	Date	Mean coating thickness (µm) (n=10)	Standard deviation (µm) (n=10)	Coating type	Primer	Experimental technique	Environment August 10 - November 2
	10/08/07			Rosin	X		Field trial
3	10/08/07	171	15.8	1% Algae (compound A)	X		Field trial
4	10/08/07	151	12.3	1% Algae (compound A)	X		Field trial
5	10/08/07	123	16.9	5% Algae (compound A)	X		Field trial
6	10/08/07	148	13.1	5% Algae (compound A)	X		Field trial
7	10/08/07	123	9.3	10% Algae (compound A)	X		Field trial
8	10/08/07	211	14.9	10% Algae (compound A)	X		Field trial
10	10/08/07	110	9.76	1% Algae (compound B)	X		Field trial
11	10/08/07	127	18.9	1% Algae (compound B)	X		Field trial
12	10/08/07	148	25	5% Algae (compound B)	X		Field trial
13	10/08/07	116	20.3	5% Algae (compound B)	X		Field trial
14	10/08/07	111	18	10% Algae (compound B)	X		Field trial
9	10/08/07	195	20.5	10% Algae (compound B)	X		Field trial
	10/08/07	500	-	Envoy TF500	X	OCP	Field trial
	10/08/07	0	0	Steel		OCP	Field trial
1	10/08/07	148	15.2	Blank topcoat	X	OCP	Field trial
2	10/08/07	121	6.33	Blank topcoat	X	OCP	Field trial
3	10/08/07	134	6.24	1% Algae (compound A)	X	OCP	Field trial
4	10/08/07	134	11.7	1% Algae (compound A)	X	OCP	Field trial

Table 7.4 Field trial 3 board of coating systems and dry film thickness

Modifications to immersion boards used in the field trials were made in response to observations of the fouling community. The crevice created by the proximity of the coupons to the backing board offered a colonising niche for some marine organisms as it can act as a shelter from the turbulent water flow. The coupons were offset by a larger degree in trials 2 and 3 due to the fact that board fouling was encroaching on the samples limiting the accuracy of fouling coverage measurements captured on camera. A cage was also used in trial 3 to prevent fish scarring as is illustrated and described in the discussion section.

DFT / µm	MOD Control (Naval AF topcoat)	Positive control (Off-the-shelf AF topcoat)	Negative Control (Blank topcoat)	1 % Biocide	1 % NP 'A'	5 % NP 'A'	10 % NP 'A'	1 % NP 'B'	5 % NP 'B'	10 % NP 'B'
30		1,2	1,2,3	1	1,2,3	3	3	3	3	3
100		2	2		2					
150		2	2		2					
500	2,3									

Table 7.5 Distribution of experimental coatings across field trials 1, 2 and 3

A stage classification was given to the fouled surfaces of the immersed coupons at every lifting of the board for imaging, and at the time of the final retrieval. A ranking was used of numbers 1 – 10 based on the stage classifications outlined in Swain (1982) [7.5].

Stage	**Predominant organisms**
Primary (1,2 and 3)	Microscopic unicellular slimes Bacteria, diatoms, protista, etc.
Secondary (4,5 and 6)	Microscopic organisms Multicellular sessile organisms; i.e. bryozoans, barnacles, tubeworms, brown and green algae
Tertiary (7,8 and 9)	Evidence of secondary attachment of sessile species and some subsequent over-growth of the previous stage's forms; i.e tunicates, mussels, sponges, larger algal growths etc.
Quaternery (10 = climax)	Complex community Depending upon the ecology of the region the community is generally dominated by one or two organisms; i.e. tunicates, mussels, sponges, bryozoans.

Table 7.6 Stage classification of biotic progression involved in marine fouling, after [7.5]

This is a basic ranking of the fouling condition of the surface to better assess the relative performance of the coating systems investigated, the stage assignments are shown in Table 7.6 and the ranking is plotted against time.

7.3 Results

7.3.1 Microbiological biofilm

Initial tests on steel samples were analysed to better understand the fouling microbial community on its surface.

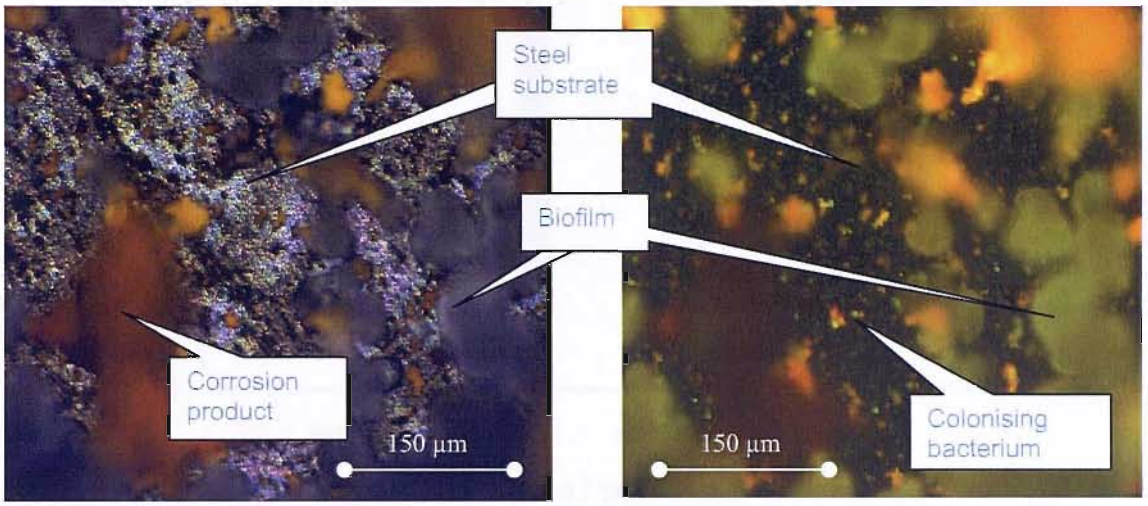

Figure 7.6 Biofilm staining of steel after 1 week immersion in aerated seawater in the laboratory at room temperature (≈ 18 °C)

As is clearly illustrated in Figure 7.6 the biofilm formation was heterogeneous with discreet pioneering bacteria easily visible on the steel samples submerged in aerated seawater after 1 week in the laboratory. The biofilm was not uniform or flat but globular and discreet clumping is visible. The complexity of a marine biofilm community on a glass slide is apparent after 3 weeks in aerated seawater in the laboratory in Figure 7.7. Along with bacteria there are diatoms, and other microorganisms present on a glass slide.

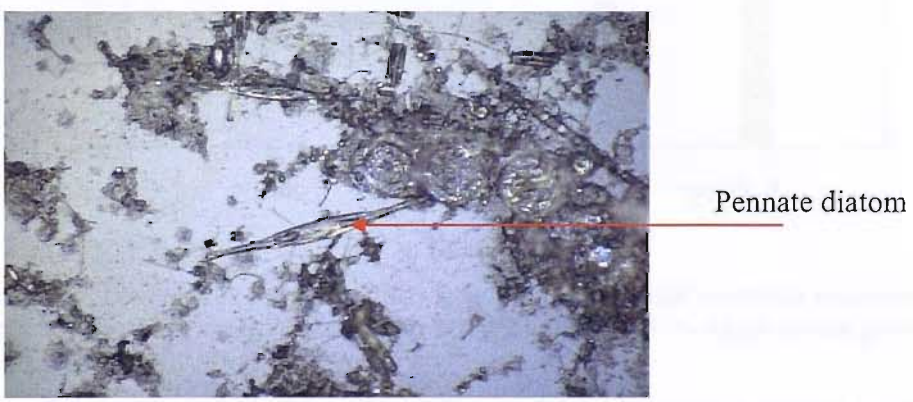

Figure 7.7 Marine biofilm after 3 weeks of glass slide in laboratory trial 2

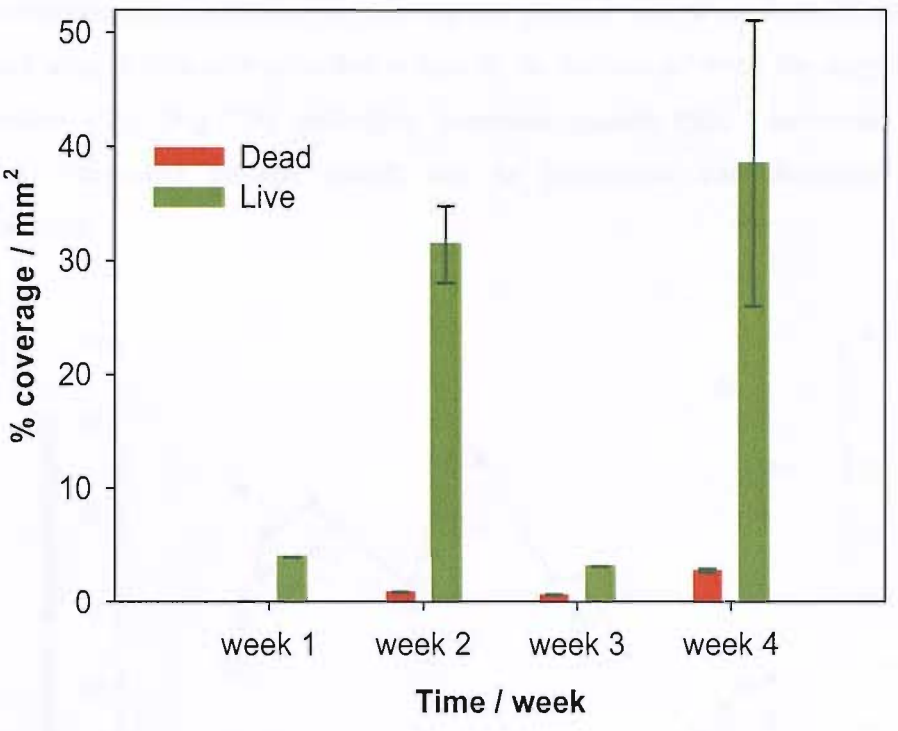

(a)

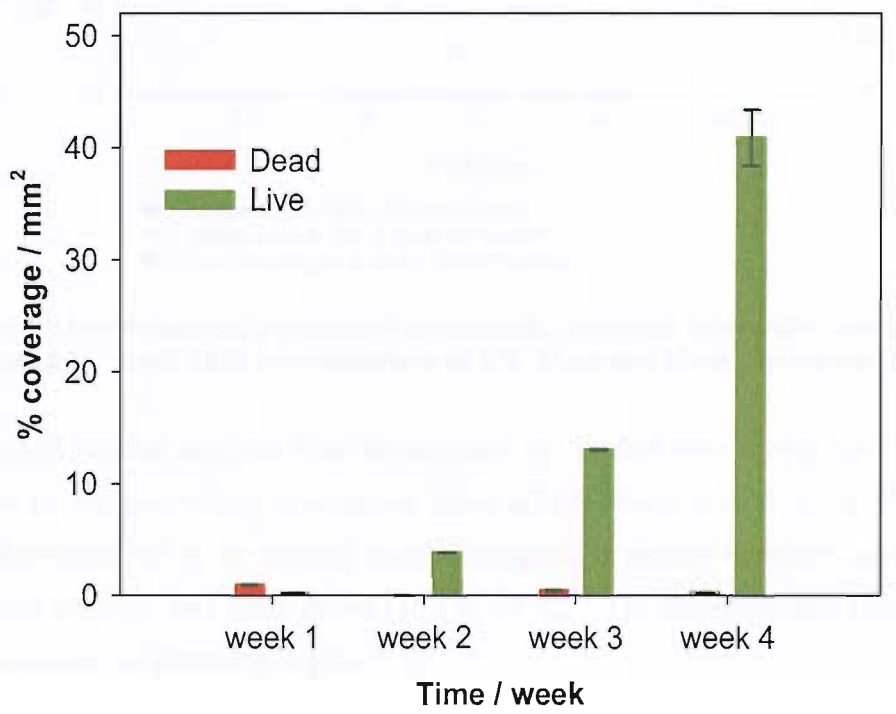

(b)

Figure 7.8 Live/dead bacterial viability in laboratory aerated seawater (nutrient limited environment) for comparison of Blank topcoat (a) and 1 % Algae (b) on glass slides

In Figure 7.8 the percentage coverage of live and dead bacteria is plotted against 4 weeks and compares 1 % extract A and base rosin coatings. Although the end bacterial coverage for the algal NP topcoat is similar to the blank topcoat control there is a notable difference in the measurements for week 2 (Figure 7.8). Standard deviation error bars indicates samples in triplicate.

The environmental parameters for this test are plotted over 4 weeks in Figure 7.9. The dissolved oxygen was only recorded in tank 2. In the second week the oxygen is low and temperature high (Fig 7.9) indicating increased growth rate. Increased temperature stimulates increased growth, which due to respiration can decrease the oxygen concentration.

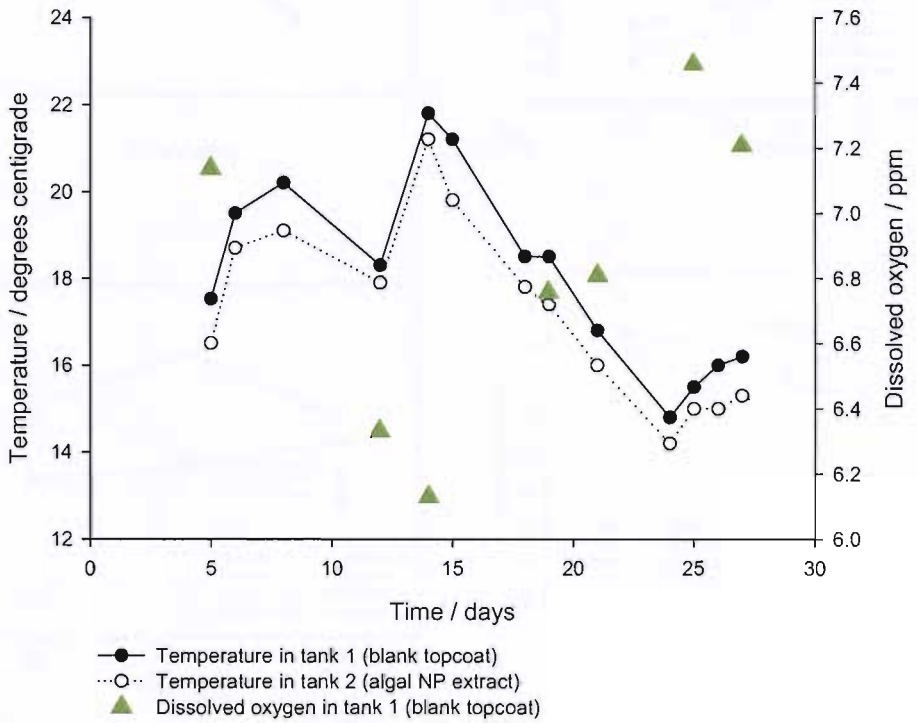

Figure 7.9 Environmental parameters of immersion tanks for laboratory aerated seawater sampled 26th April 2006 for comparison of 1 % Algae and Blank topcoat on glass slides

The second biofilm analysis trial investigated the growth on varying concentrations of additive in the antifouling coating on glass slides coated thin. 1 %, 5 % and 10 % antifoulant algal NP in the coating were investigated in aerated seawater conditions under controlled UV light and temperature (16.5 ± 1.5 °C). The environmental parameters over the experiment are plotted in Figure 7.10.

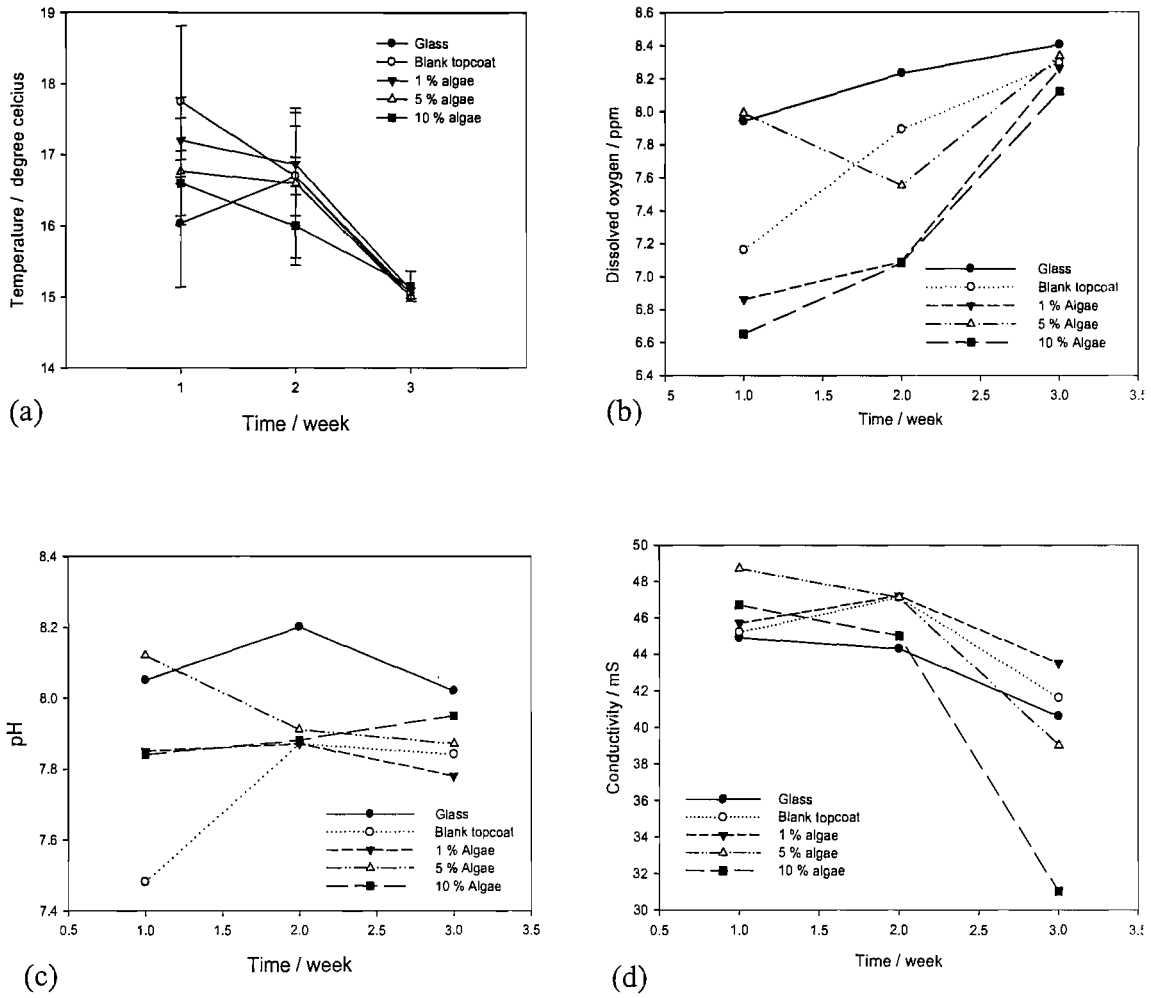

Figure 7.10 Individual (a) temperature (b) dissolved oxygen (c) pH and (d) conductivity data for 1 %, 5 %, 10%, blank and control seawater in beakers

The trend for the environmental parameters is that with time the temperature decreases, conductivity decreases and oxygen increases. The pH is variable but stabilises by week 2 at around 7.9 pH. With regards to the variation between the 1, 5 and 10% concentration at the end of 3 weeks the pH, 10 % > 5 % > 1 % and for the conductivity, 1 % > 5 % > 10 %. The BacLight^{TM} for the differing variations of live biofilm on the experimental 1, 5, and 10 % w/w additions of algal NP to the topcoat are shown in Figure 7.11.

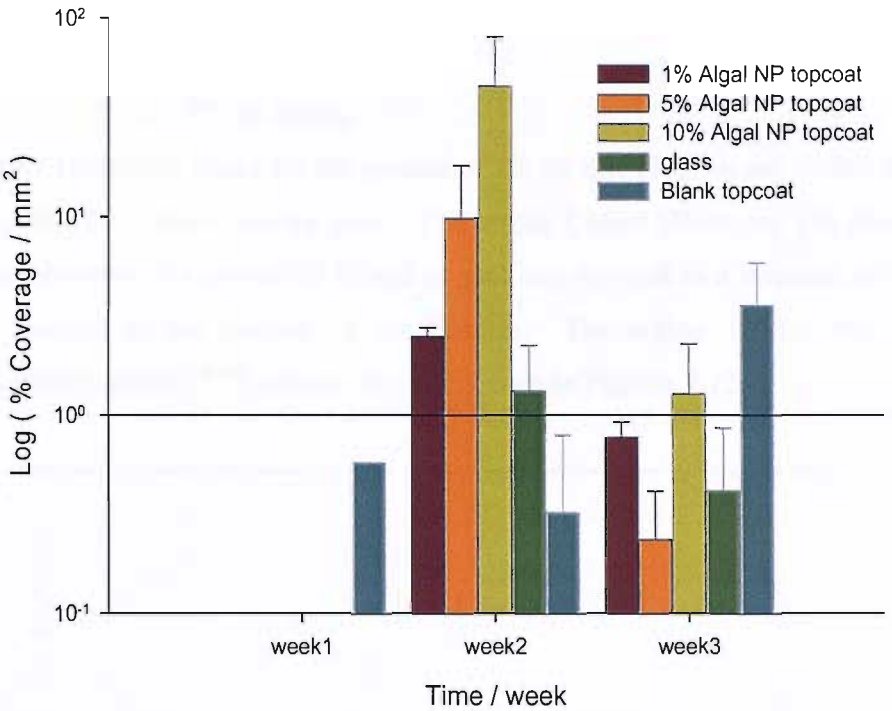

Figure 7.11 Live bacterial percentage coverage on 1, 5 and 10 % algal NP topcoat, glass slide and blank topcoat

The coverage is very low for this experiment and so a log scale has been used to visualise the differences. As shown in Figure 7.11, the 10 % algal coating has the highest percentage coverage in week 2 even higher then the negative controls. This could be due to the increased algal content acting as a nutrient supply and encouraging growth. This data set undergoes a similar profile of low live biofilm in the first week, spike in second week and return to low coverage in third week as seen for the blank topcoats bacterial viability in laboratory trial 1 (Figure 7.7a). This suggests that there is natural life and death curve being sampled for the marine bacterial community in a nutrient limited environment and that it is of three weeks.

7.3.2 Field trial immobilised extract

7.3.2.1 FT-IR results

In Figure 7.12 the key peaks for the spectra of 25, 50 and 1100 μg mL^{-1} after immersion in the field trial for 1 week can be seen. . The amide I band (1650 cm^{-1}) is due to the back bone peptide units of a protein [7.6] and as such can be used as a measure of the adsorbed protein amount on the surface i.e the biofilm. The region 1200 – 900 cm^{-1} is the polysaccharide region [7.7] and can be clearly seen in Figures 7.12.

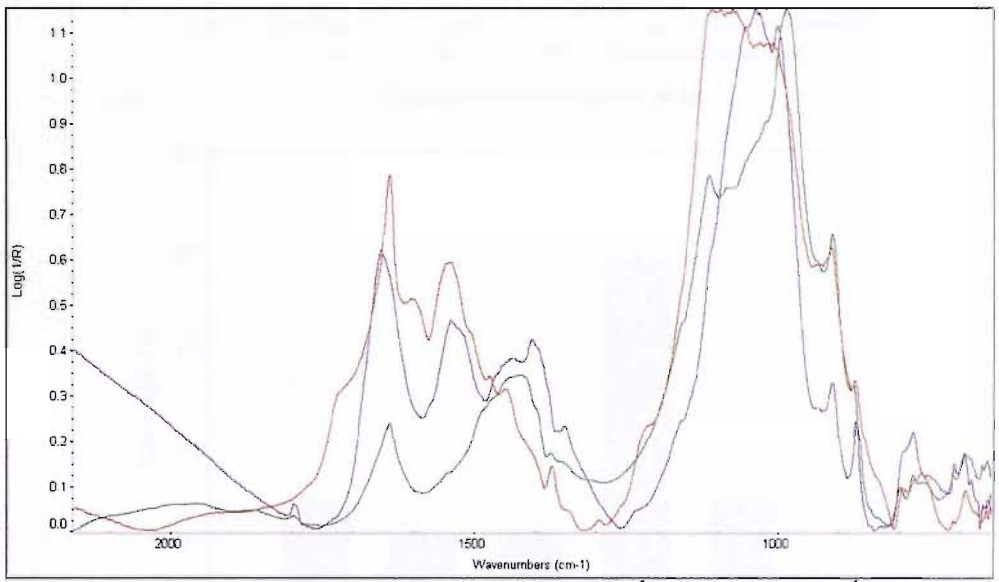

Figure 7.12 FTIR baseline corrected spectra of 25 μg mL^{-1} (red), 50 μg mL^{-1}(green), 1100 μg mL^{-1} (purple) algal NP chemically immobilised on glass slides and immersed in seawater for 1 week

Figure 7.12 showed the spectra of the biofilm present on the slides of immobilised algal extract of varying concentration. All of the spectra have very similar peak distribution. The amide I absorption band at 1650 is clearly visible for all three overlayed spectra confirming the presence of a biofilm. In the 300 and 1450 wavelength region the 1100 μg mL^{-1} concentration is higher then the other two. At the 1650 wavelength, which is the amide I region the lowest concentration has the highest peak. The lowest algal NP concentration has the highest peak, indicating it was the least effective against biofilm growth.

7.3.2.2 EDIC results

The results analysed and plotted in Figure 7.13 are the duplicate half of the slide used in the FT-IR experiment. Samples were stained and analysed within 2 h of removal from the field trial and 24 h before being transported to Daresbury for FT-IR.

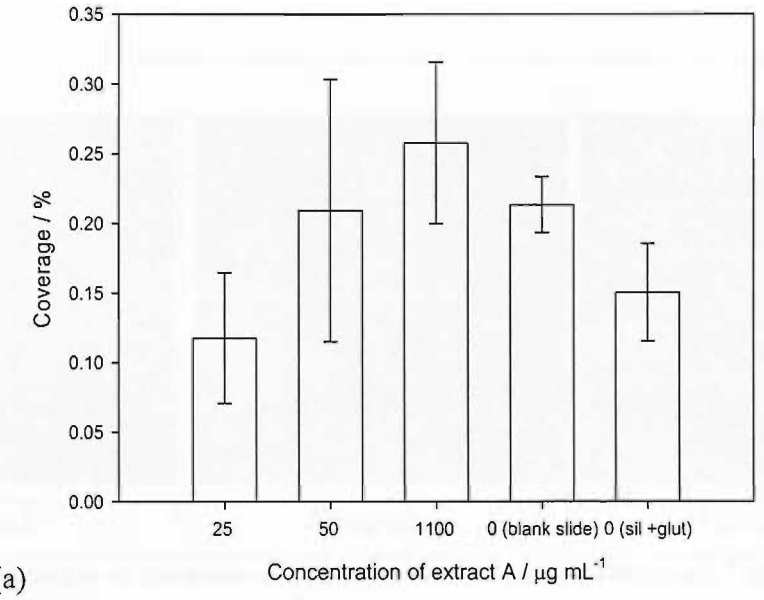

(a)

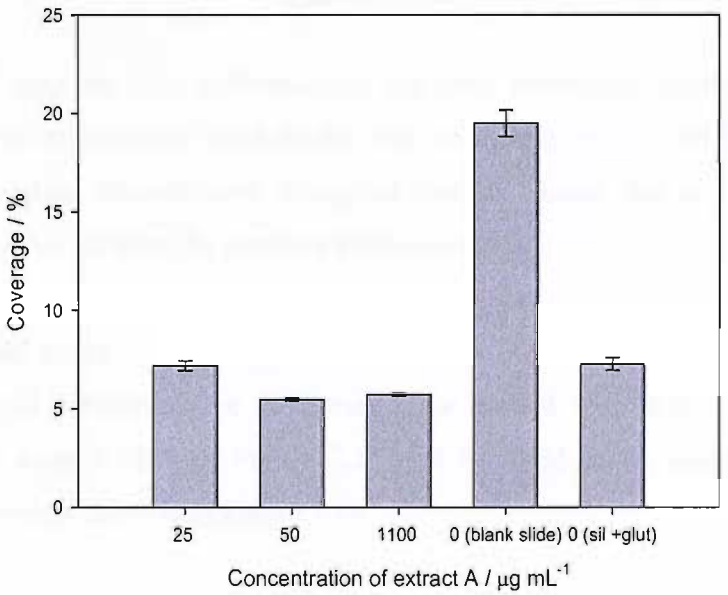

(b)

Figure 7.13 Live (a) and dead (b) viability of seawater biofilm on 25, 50 and 1100 µg mL^{-1} algal NP immobilised onto glass slides, error bars are standard deviation

Both the 50 and 1100 µg mL^{-1} concentrations are higher in the live measurements than the controls and lower in the dead measurements than the controls. The low percentage coverage in the first week of the field trial (Figure 7.13) is consistent with the percentage coverage measured in the laboratory trials of coated samples. The samples immersed in field trials, such as Figure 7.13, have been exposed to a flow regime. The percentage coverage is below 10 % and is comparable to the static flow laboratory experiments such as the two other EDIC experimental results (Figures 7.8 and 7.11). There is a small increase in the live percentage coverage (0.1 %) with increasing extract concentration. The control samples also have quite low fouling coverage.

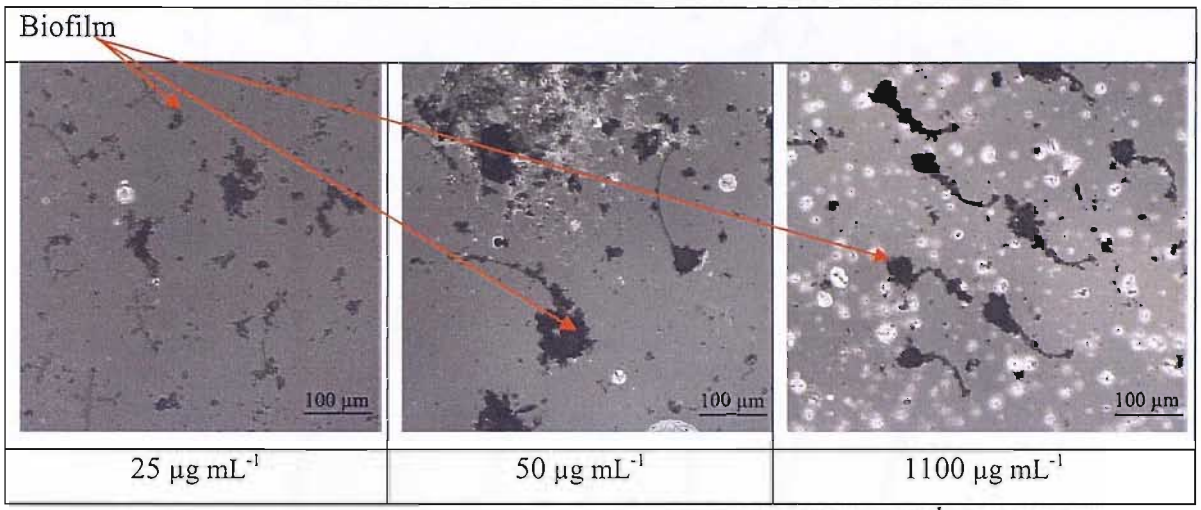

Figure 7.14 Images of the marine biofouling on 25, 50 and 1100 µg mL^{-1} algal extract concentrations

Although there may be little difference in the total colonising numbers, Figure 7.14 illustrates how the environment such as the flow conditions in the field trial can alter the biofilm by generating characteristic elongated biofilm clumps that all fall in the same direction when removed from the aqueous environment.

7.3.3 Field trials

The environmental parameters for field trial 1 are plotted with time over the 4 month period April to August 2006 in Figure 7.15 and for field trial 2 and 3 the period of February to November 2007 is in Figure 7.16.

The starting temperature of 6 °C (Figure 7.15) is indicative of winter sea temperatures and the drop off in the last week suggests that the key fouling season was captured during this field trial in 2006. Rainfall is the key reasoning behind the salinity drops in the data set (weeks 3 and 6). The reading of dissolved oxygen in week 10 of 9.3 ppm is relatively high and was due to a thick bloom of phytoplankton being present at this time in the dock waters. This bloom increased the dissolved oxygen content due to the photosynthenthetic production of oxygen. In 2007 (Figure 7.16) even at an earlier time of February the sea temperature is 2 °C higher at 8 °C and so allowed for the earlier start to field trial 2. 2007 sea temperature was not as warm as 2006. Both years had similar salinity profiles with lower measurements of 29.5 psu captured during the rainy spring season of 2007.

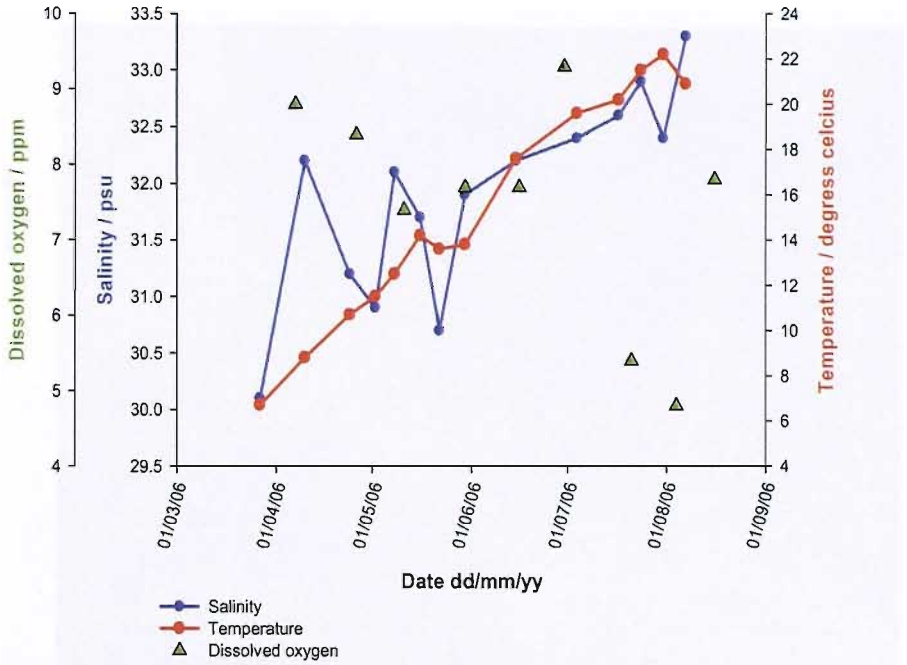

Figure 7.15 Field trial 1 environmental parameters April – Aug 2006, Empress Dock, Southampton

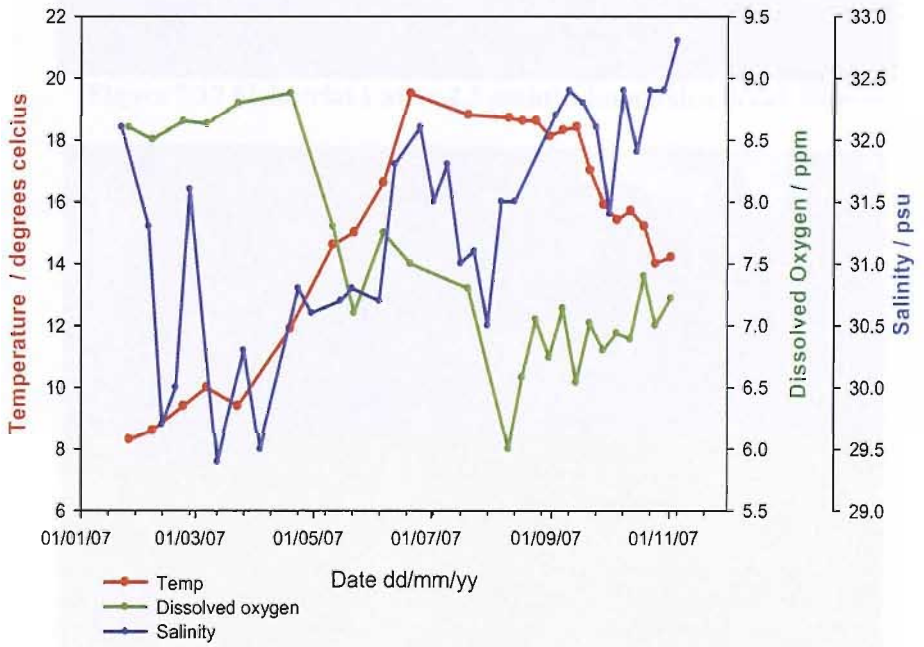

Figure 7.16 Field trial 2 and 3, environmental parameters Feb – Nov 2007, Empress Dock, Southampton

Field trial 1, 2 and 3 middle and end images are in Figures 7.17, 7.18, 7.19, 7.20, 7.21 and 7.22 respectively.

Figure 7.17 Field trial 1 after 2.5 months immersion (June 2006)

Figure 7.18 End of field trial 1 after 4 months immersion (August 2006)

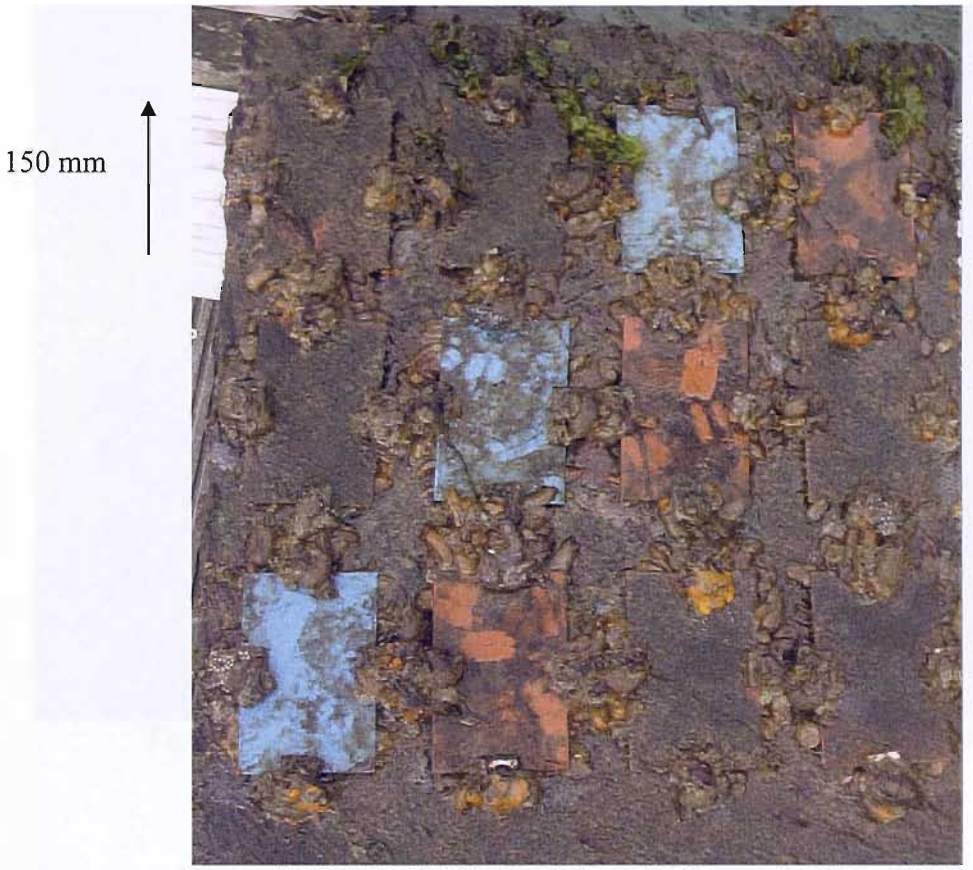

Figure 7.19 Field trial 2 after 2.5 months immersion (June 2007)

Figure 7.20 End of field trial 2 after 6 months immersion (September 2007)

Figure 7.21 Field trial 3 after 1.5 months immersion (September 2007)

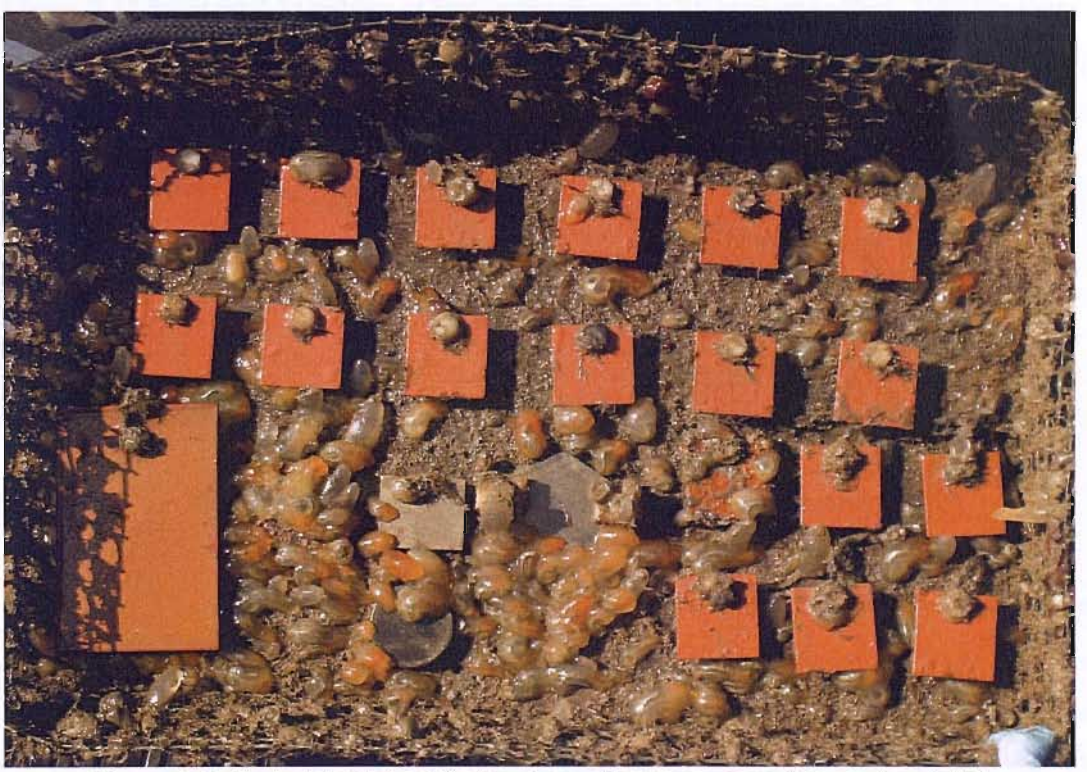

Figure 7.22 End of field trial 3 after 3 months immersion (November 2007)

For field trail 1 (Figures 7.17 and 7.18), the fouling succession is ranked and compiled in Figure 7.23.

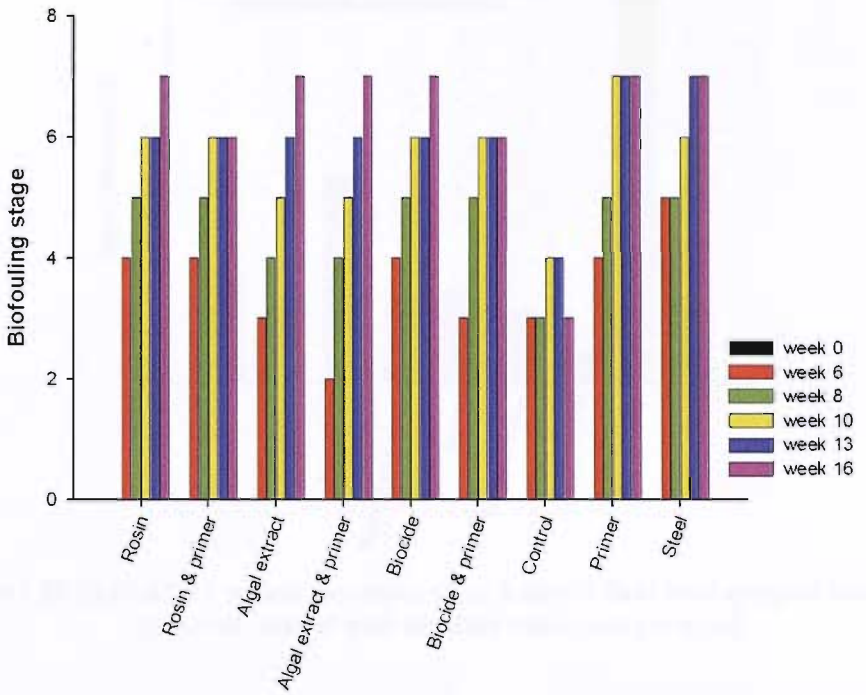

Figure 7.23 Field trial 1 ranking of biofouling growth with respect to time, 2007 Empress Dock, Southampton

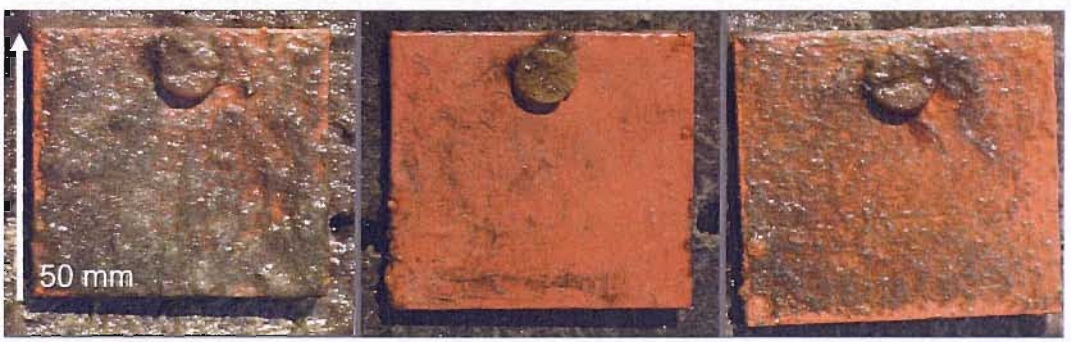

Figure 7.24 Biofouling field trial 1 after 6 weeks immersion

From Figure 7.24 it is easy to distinguish a delay in the biofouling of the algal natural product coating when compared to the other coatings. The ranking of the fouled surfaces in Figure 7.23 indicates that the algal natural product antifouling coating outperforms all other experimental coatings, showing limited fouling in the first 10 weeks. In the 13th week, however, the surfaces of all the coatings are much the same with a ranking of no. 6. This peak in the biofouling correlates with a peak in temperature and a decrease in the dissolved oxygen of the seawater. The main species found at the end of the trial on the experimental coating surfaces included the Phylums Bryozoa (*Bugula* sp., *Scrupocellaria*

sp., and encrusting bryozoans), Crustacea (*Balanus modestus*), Subphylum Tunicata (Ascidians), Polychaeta (*Pomatoceros triqueter*), and filamentous green algae (*Ulva* sp.).

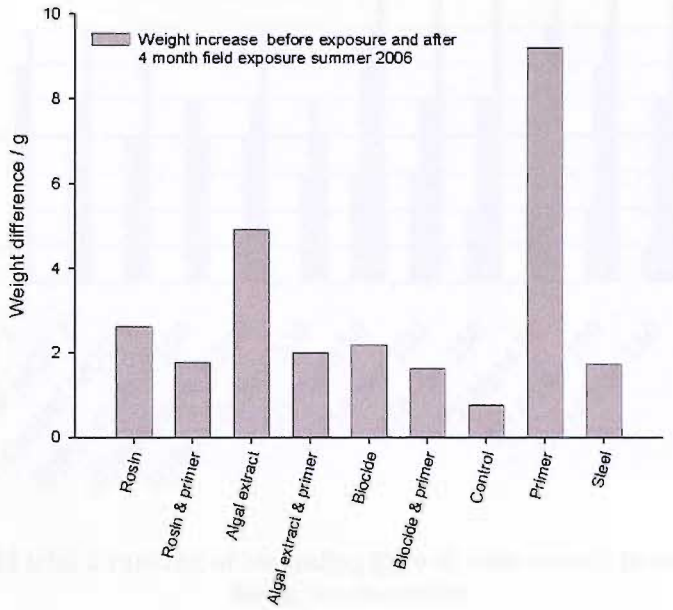

Figure 7.25 Field trial 1 weight increases after 4 month field trial samples have been removed, rinsed with distilled water and air dried

The weight increases shown in Figure 7.25 for the samples of trial 1 qualitatively relate the coatings effectiveness as an antifouling system. The weight increases are assumed to include only corrosion products and biological mass on the coupons surface as the surface has been rinsed of debris and air dried for 3 h. From Figure 7.25 the sample with the least amount of weight, i.e. corrosion/biofouling, is the positive control then the biocide topcoat, then the blank and finally the algal NP topcoat.

Field trial 2 (Figures 7.19 and 7.20) was undertaken to see if there was repeatability in the performance of the algal NP coating and to see if a prolonged antifoulants affect could be generated by increasing the coating thickness. The ranking of key fouling stages for field trial 2 are plotted in Figure 7.26 and are only ranked over the time when comparative surfaces were able. No ranking could be used once the marks from the fish were made. Scarring of the surface of the coatings occurred by the local fish community, mainly composed of mullet. The mouths of the fish leave distinctive tracks which in this case are of a mullet as imaged in Figure 7.27. Although the samples biofouling community was damaged there does not seem to be an increased antifouling performance with a corresponding increase in coating dry film thickness.

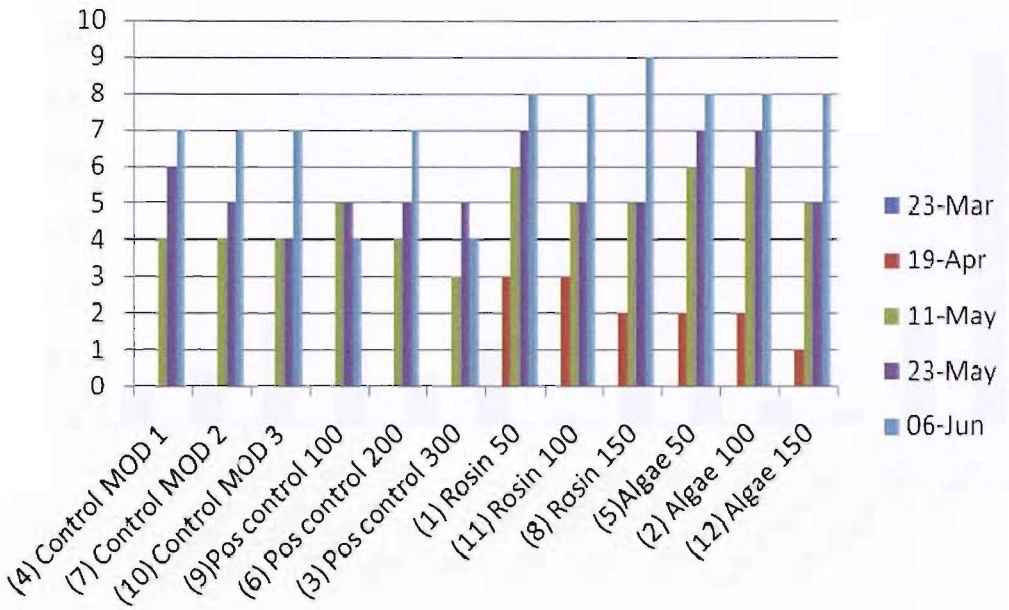

Figure 7.26 Field trial 2 ranking of biofouling growth with respect to time, 2007 Empress Dock, Southampton

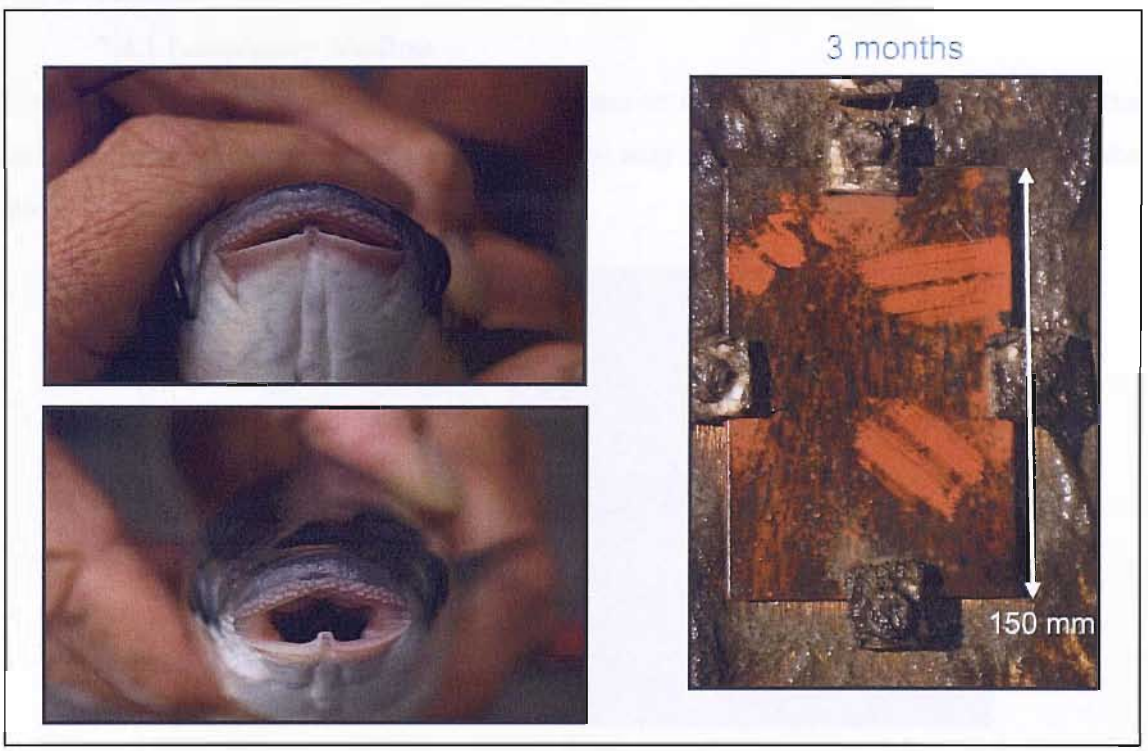

Figure 7.27 Fish scarring on field trial 2 coated ssample and the fish mouth responsible

As can be seen in Figures 7.20 and 7.21, the variation in the concentration of extract tested in field trial 3 did not show any large fouling organisms or algal growth on the surface of the experimental coatings making it impossible to rank the visual biofouling.

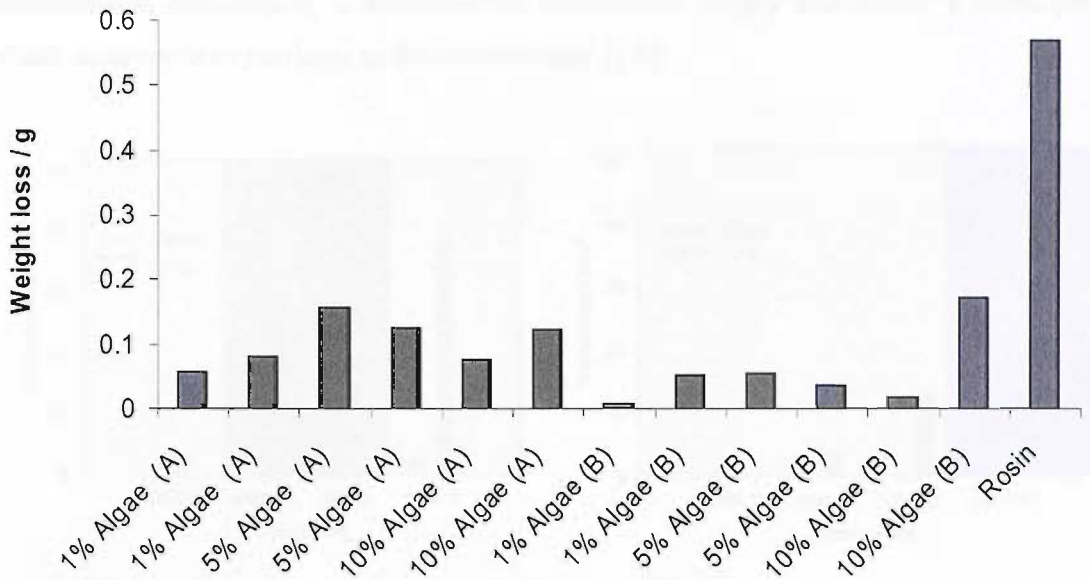

Figure 7.28 Field trial 3 weight loss of samples before and after immersion

7.4 Discussion

7.4.1 Laboratory biofilms

Corrosion products are also detected by the stain in the EDIC microscope images of the biofilm growth on the surface of the steel. This may make it difficult in use to detect the bacteria associated with these structures.

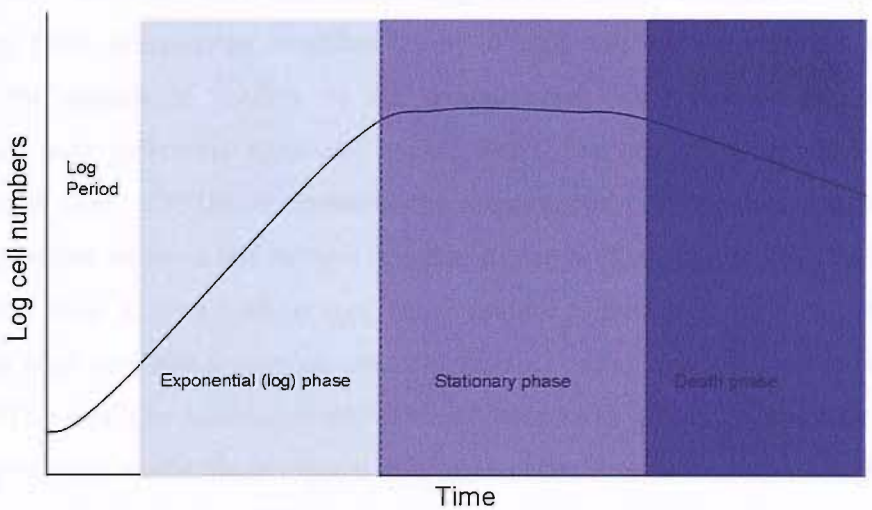

Figure 7.29 Bacterial growth diagram for a nutrient limited environment

It is suggested here that the lower coverage may be an indication of antifouling activity suppressing the first onset of bacterial growth. A typical growth curve for bacterial growth in a nutrient limited environment is illustrated in Figure 7.29 showing initial growth and

accumulation followed by a saturation of the nutrient supply and finally a death phase which re-introduces nutrients to the environment [7.8].

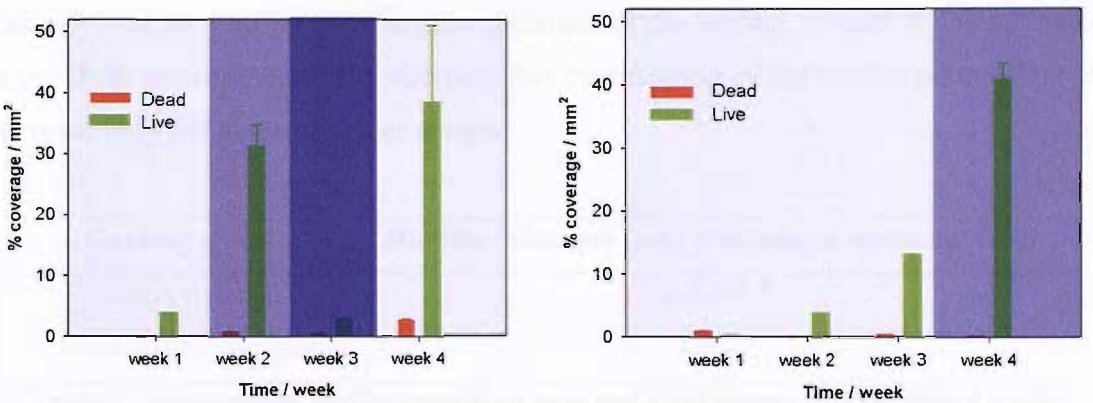

Figure 7.30 Hypothesised growth phases overlaid on bacterial viability data from surface of (a) a blank topcoat and (b) a 1 % algal NP coating

In Figure 7.30 a suggested growth pattern (Figure 7.29) is overlaid on-top of the data set. This highlights the nutrient deficiency in the system that can only be alleviated by the death and thereby re-introduction of nutrients.

The immersion environmental parameters (Fig 7.9) for the 1st Baclight bacterial viability trials using EDIC microscopy correlate the hypothesis that the algal extract coating may suppress the growth of biofilm in the second week when the oxygen is low and temperature high indicating increased growth rate. The growth of live bacteria on the blank topcoat (Fig. 7.30 (a)) is sporadic, the reading in the 2nd week corresponds with a steep temperature increase and oxygen decrease as can be seen on day 14 (Fig. 7.9). A key reason for a drop in dissolved oxygen concentration is due to aerobic respiration. The reason this peak does not feature on the algal extract coating measurement in the 2nd week (Fig. 7.30 (b)) could be because it inhibited the increase of growth at that time. The drop in the live bacteria on the blank topcoat in week 3 is characteristic of the death phase in the growth curve of bacteria (Fig. 7.29), possibly caused by nutrient limitations generated from the peak in the 2nd week. The onset of species re-growth in the 4th week on the blank topcoat (Fig. 7.30) is possibly stimulated by the return of nutrient availability from dead cells.

Growth on the algal NP topcoat increases exponentially with time. This could either reflect the release of antifouling component from the coating or the removal of other

coatings from the tank. Either way when compared with the rosin based coating it indicates that a time lag in the biofouling of the natural product based coating occurred. The z-scan function of the EDIC light microscope was employed to measure the thickness (Table 7.7) of the biofilm growth. The thickness of the biofilm at week four was thicker on the blank control topcoat but also note that the thickness of the biofilm on the algal NP topcoat is only just above the error margin.

Coating system	Biofilm thickness (μm) ± standard deviation (n=3)
Blank topcoat	9.4 ± 4.3
1 % algal NP topcoat	4 ± 1.1

Table 7.7 Thickness of biofilm growth on base and algal extract coating after 4 weeks immersion in aerated seawater

Further analysis would indicate if there was a change in the morphology of the biofilm established on antifouling coatings with natural products. Table 7.7 was useful to assess the marine biofilm thickness capable of being cultured in the laboratory. To put this in context Table 7.8 highlights the variable seawater biofilms measured on antifouling coating systems for a range of 6 months, 38 days and 1 month time intervals.

Coating	Environment	Time	Biofilm thickness / μm	Reference
TBT-SPC	Seawater immersion field	6 months	11	Jackson and Jones, 1988 [7.9]
TBT-SPC	ASTM class 2 seawater laboratory	38 days	22-38	Mihm and Loeb, 1988 [7.10]
Cu-based paint	Seawater immersion field	1 month	2-30	Bishop et al., 1974 [7.11]

Table 7.8 Thicknesses for various seawater biofilms from the literature

Initially, analysis from the EDIC was qualitative which aided as a crucial learning tool to better understand the water channels and morphology of biofilm growth on the surface of the coatings.

7.4.2 Field trial biofouling

Immobilised natural product extract on glass slides was used to investigate the antifouling properties in a marine field trial. FT-IR was used here to show the limited difference in characteristic peaks between surface fouling on various concentrations of extract

immobilised in a silanization process at 25, 50 and 1100 μg mL^{-1}. It also was used to cross correlate the EDIC microscopy data by verifying the presence of a surface marine biofilm. FT-IR has shown that the characteristic amide I and II bands are on all the samples which are indicative of a biofilm which has been further verified by the nucleic acid staining and EDIC microscope. As can be seen in Figure 7.12 the 25 μg mL^{-1} spectra has a higher peak in the 1500 – 1700 wavenumber range. The amide I absorption band at 1650 is clearly visible for all three overlayed spectra. This indicates that there is more biofilm present on the 25 μg mL^{-1} immobilised natural product extract then on the higher concentration coated glass slides. The EDIC results also indicate (Figure 7.13) that there is a 2 % higher percentage coverage of biofilm on the 25 μg mL^{-1} coated slide and the background silane gluteraldehyde then on the higher concentrations. With this initial data set the techniques have been shown to cross correlate each other as well as suggest that the higher immobilised concentrations resisted biofilm growth better than the lowest concentration of 25 μg mL^{-1} and both the controls. There are no indications that the 50 and 1100 μg mL^{-1}differed in their antifouling activity. The bioassay completed, in Section 4.5.3, of the pure extract compounds correlates with these results by also reporting an antifouling efficacy at concentrations equal to or greater than 25 μg mL^{-1}.

Field trial 1 showed the greatest promise with regards to the NP performance as an antifoulant in a coating system. Once a biofilm is established, further growth is often encouraged [7.12]. As shown in section 7.1 this biofilm growth in the laboratory is easily measureable within a week reaching thicknesses of 5 – 10 μm in four weeks. Single diatoms (e.g. *Amphora sp., Amphiprora sp.* and Navi*cula sp.*) and algal spores can colonise the surface. They settle as single cells that form into dense sheets on the surface leading to a visible brown slime [7.13]. Bishop, 1974 [7.11] found diatom slimes on copper-based paints with no added algaecide after a month's immersion. It is interesting to note that the booster biocide experimental coating in this project also did not protect against this diatomaceous slime in the 6^{th} week (Fig. 7.31). This may indicate the leaching of the biocide in this experimental system are possibly compromised as also indicated by the limited change in capacitance in the coated in Figure 6.16 and the dynamic OCP in Figure 6.13.

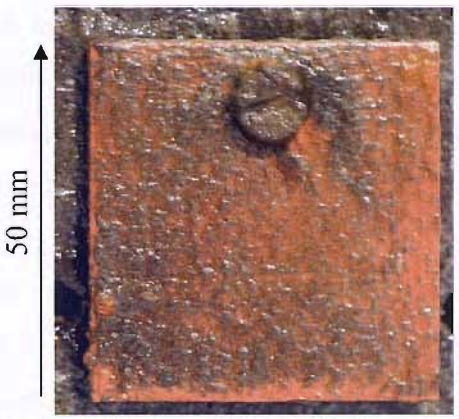

Figure 7.31 Diatomaceous slime on surface of biocide topcoat after 6 weeks seawater exposure

The immersion trial was conducted over the peak fouling season (April to August 2006 see Figure 7.15). After 10 weeks the natural product antifouling coating was seen to outperform all other coatings, showing limited fouling. However, after 13 weeks the antifouling extracts were ineffective and heavy biofouling had covered the working surface of the algal extract coating. This suggests that the antifoulant leached too quickly, or that the release may have been hindered through the paint film. However, over the 4 months the biocide loaded paint system was comparable, thus showing great promise.

Field trial 2 examined the variation in thickness of the 1% Algal, blank and both positive and negative control antifouling coating systems. The outcome clearly illustrated that there were no increased or decreased antifouling performance in the experimental coating system due to thickness. The main difference between trial 2 and trial 1 was that the rosin binder system of the topcoat was a year older and so may have affected the performance as well as the change in the fouling environment.

At six weeks there was visible fish scarring of the surfaces of some antifouling coating surfaces. Fish scarring is a common occurrence on boat hulls as the fish feed by scrapping the biofilm from the hull for food. The scarring seems to be selective as can be seen in the end of trial images (Figures 7.19 and 7.20). At each board retrieval, it was recorded that the fish selectively scraped the same surfaces, of the positive control antifouling systems. Lack of fish scarring of the surface of the antifoulant coatings has been suggested to be evidence of antifeedant properties of the coating surface. However, it is the authors' belief that in this instance it is the surface foul release properties of the Interspeed Ultra ® positive control coating and the decreased roughness of the airless sprayed prepared Envoy TF500 ® positive control samples. These surface interfacial properties could provide an

easier surface from which to feed, as the force required by the fish to scrape clean the biofouling would be less then the other experimental coating surfaces. Another controlling parameter may be the central positioning of these samples on the board providing a more stable surface from which to feed.

The lack of fouling on the surfaces in field trial 3 prevented any surface ranking (Figures 7.21 and 7.22). Reasons for the reduced fouling could include the immersion at a late fouling season and a decrease in the fouling community due to the change in the microhabitat by the introduction of the cage structure to the immersion board. The cage lid was cleaned on each removal for images to reduce biofouling growth on it and to increase the light reaching the immersion board surface.

From field trial 3, cross sections of the paint chips of 1, 5 and 10 % included Algal NP were made and SEM micrographs recorded. These images demonstrate the coating integrity (Fig. 7.32). It is obvious from these micrographs that the 10 % inclusion coating has a crack running through it.

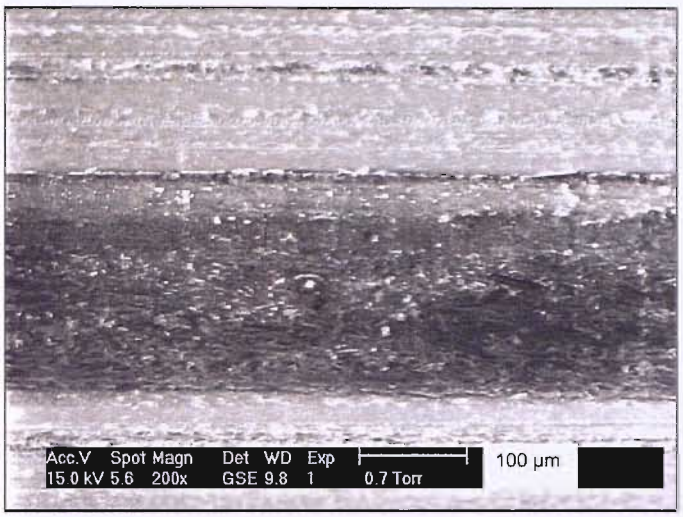

1% Algal inclusion

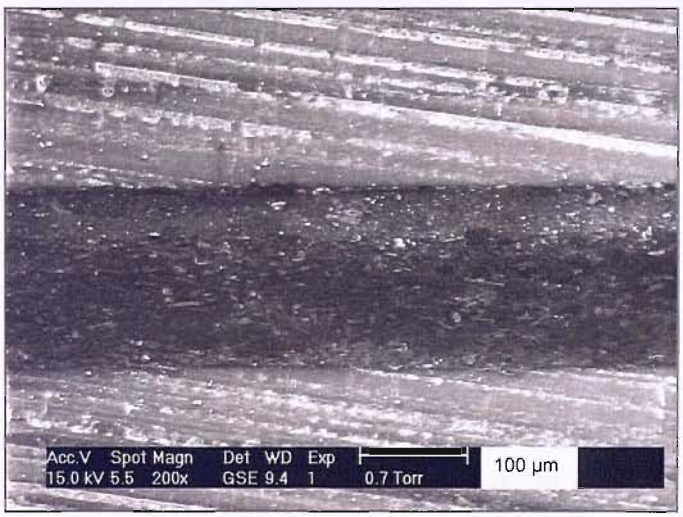

5% Algal inclusion

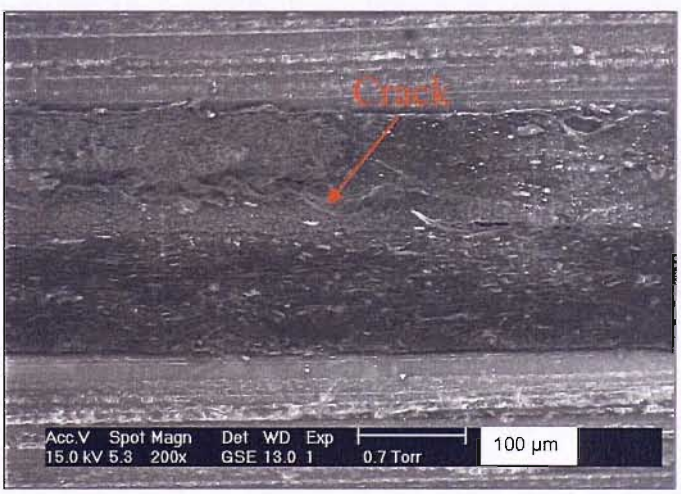

10% Algal inclusion

Figure 7.32 SEM micrographs of the cross sections of the 1, 5 and 10 % Algal coating

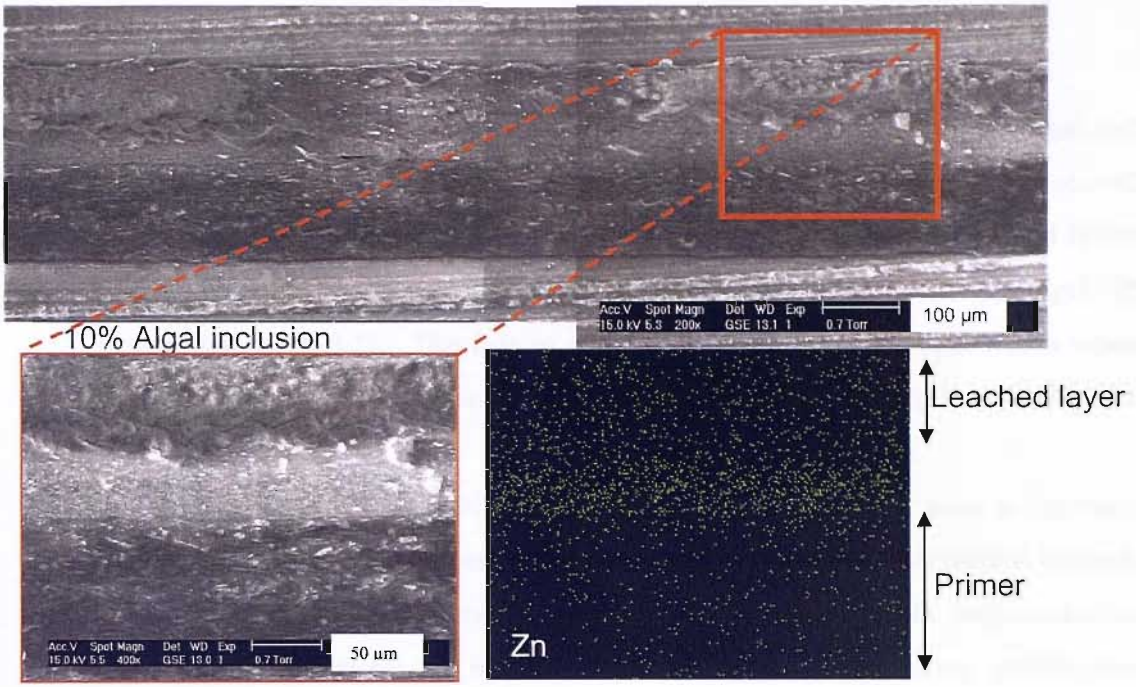

Figure 7.33 10 % algal NP topcoat with a close up of a section and the corresponding SEM-EDX map

Figure 7.33 illustrates how the cracking in the 10 % algal NP coating system is propagating along the interface between the leached layer and the un-reacted matrix below. The EDX map of the element zinc (Zn) clearly highlights this cohesive mechanism. One would expect a loading of 10 % antifoulant additive to be too much for the coating matrix as percentages for antifouling additives in coatings range from 1-5 %.

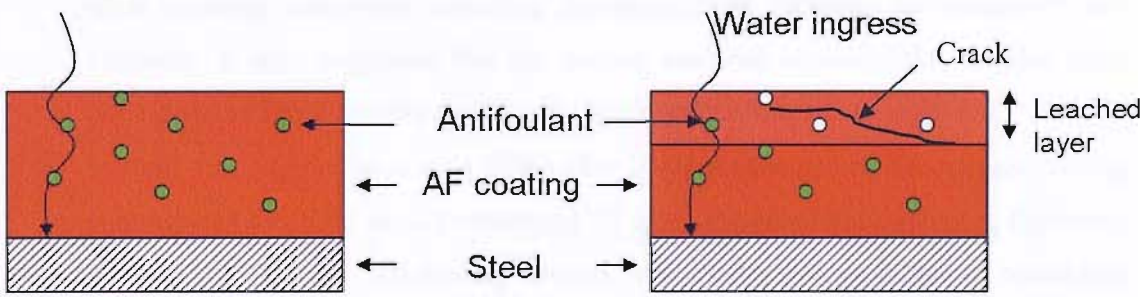

Figure 7.34 Schematic of pathway (1) through pores and voids and (2) through the controlled depletion layer and its erosion

The leach layer is parallel to the water front as assumed in the electrochemical analysis (Figure 6.27). Here the water would ingress due to the crack propagation along the reacted/un-reacted coating interface (Figure 7.34). It is plausible that a crack would occur here, as the structural integrity of the leached layer is much lower due to the loss of soluble pigment (i.e. zinc). The post analysis SEM and EDX start to explain how the loading of NP antifoulants may affect the leaching rate.

7.5 Conclusions

- In the laboratory trial, bacterial growth occurred within 1 week on both algal and base rosin coatings. The growth patterns on the two coatings varied in the second week with the environmental data indicating an increase in growth reflected in the percentage coverage values of 31 % on the blank topcoat but not on the algal NP extract topcoat at 3 %. The loss in activity looks to be exponential which when coupled with a bacteria phase diagram indicates that the coating is releasing the active ingredients.
- A field trial of immobilised NP algal extract A was successfully used to correlate FT-IR with EDIC measurements, proving that a biofilm was established through the presence of the characteristic amide I band (~ 1650) and the polysaccharide band (1200-900) on all the immersed samples. EDIC microscopy verified the biofilm presence and provided bacterial viability data that supported the FT-IR findings.
- Although the EDIC microscopy did not verify any antifouling performance of the NP it was extremely useful as a rapid means to estimate *in-situ* biofilm coverage and bacterial viability. Both the algal coating and base rosin had final live bacterial coverages of 40 % mm^{-2}, however the final biofilm thickness after 4 weeks of immersion was half the height on the algal coating (~ 4 μm) than the blank rosin coating (~9.5 μm). This technique overcame the issues of the more conventional plate counting techniques requiring microbiological facilities for incubation and culturing. It also suggested that the marine bacterial communities sampled from Southampton Dock survive for 2 weeks in a nutrient limited environment.
- In field trial 1 (April to August 2006) after 10 weeks the natural product antifouling coating was recorded as outperforming all other experimental coatings. However, by week 13 the NP antifouling system was ineffective with heavy biofouling covering the surface. It is hypothesised here that the antifoulant leached too quickly due to an increased water uptake as calculated in the laboratory (section 6.3.3).
- The 10% algal NP w/w inclusion was too high resulting in visible cracking, 1 and 5% did not show the same cracking features. The crack is propagating at the interface between the leached and un-reacted matrix of the coating, verified by EDX mapping of the zinc. This illustrates a cohesive failure.

7.6 References

[7.1] J.P. Arp, *Characterization of corrosion products and microbes on various types of metal coupons using beamline 1.4.3*, Advanced light source compendium of users abstracts (1999).

[7.2] Southampton port website
http://www.plimsoll.org/Southampton/TheDocks/EasternDocks/FactFile.asp
Accessed [26/08/08]

[7.3] K.J. Collins and J.J. Mallinson, Marine flora and fauna of Southampton docks, Report to the Nature Conservancy Council February p. 26 (1987).

[7.4] S.A. Costa T. Tzanov, A. Paar, M. Gudelj, G.M. Gübitz, A. Cavaco-Paulo. *Immobilisation of catalases from Bacillus SF on alumina for the treatment of textile bleaching effluents*, Enzyme and Microbial Technology 28 (2001) 815-819.

[7.5] G.W.J. Swain, The prevention of marine fouling by the controlled dissolution of copper and its alloys, PhD Thesis, University of Southampton, (1982).

[7.6] M. Müller, T. Rieser, K. Lunkwitz, J. Meier-Haack, *Polyelectrolyte complex layers: a promising concept for antifouling coatings verified by in-situ ATR-FTIR spectroscopy*, Macromol. Rapid Commun. 20 (1999)607-611.

[7.7] A. Karadeņizli, F. Kolayli, K. Ergen, *A novel application of Fourier-transformed infrared spectroscopy: classification of slime from staphylococci*, Biofouling 23 (2007) 63-71.

[7.8] D.R. Roszak, R.R. Colwell, *Survival strategies of bacteria in the natural environment*, Microbiological reviews 51 (1987) 365-379.

[7.9] S.M. Jackson and E.B.G. Jones, *Fouling film development on antifouling paints with special reference to film thickness*, Int. Biodeterior. 24 (1988) 277-287.

[7.10] J.W. Mihm and G.I. Loeb, *The effect of microbial biofilms on organotin release by an antifouling paint*, Biodeterioration. 7 (1988) 309-314.

[7.11] J.H. Bishop, S.R. Silva, V.M. Silva, *A study of microfouling on antifouling coatings using electron microscopy*. J. Oil Colour Chem. Assoc. 57 (1974) 30-35

[7.12] J.W. Costerton, *Introduction to biofilm*, Int. J. Antimicrobial Agents, 11 (1999) 217-221.

[7.13] D.M. Yebra, S. Kiil, C.E. Weinell and K. Dam-Johansen, *Presence and effects of marine microbial biofilms on biocide-based antifouling paints*. Biofouling, 22 (2006) 33.

Chapter 8 Conclusions and Further Work

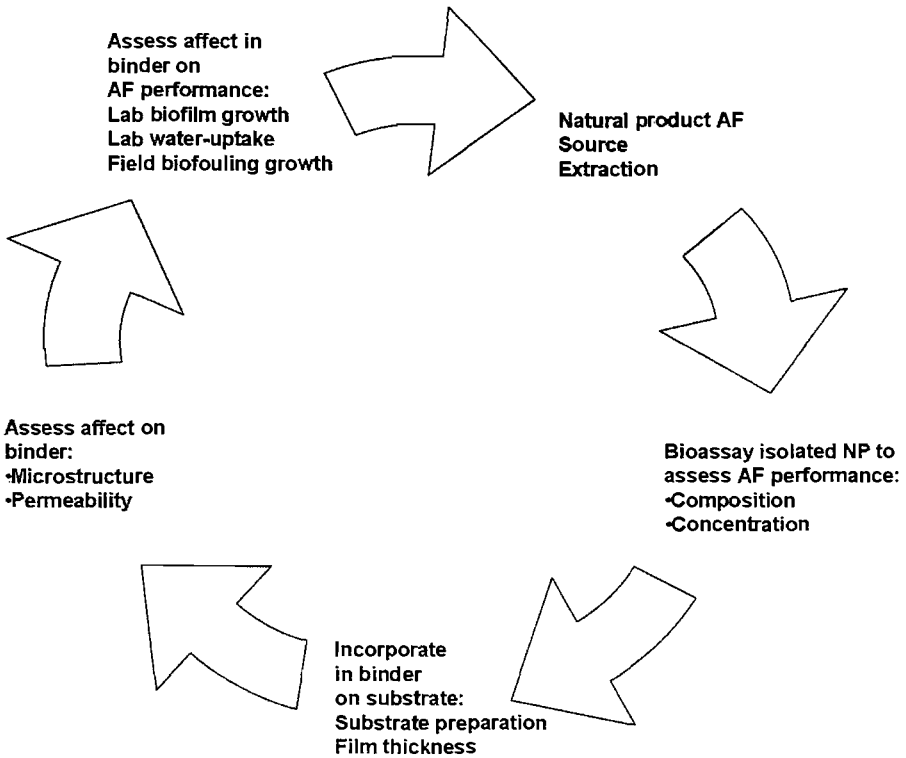

Figure 8.1 Tests used in thesis to optimise an NP based antifoulant solution

Figure 8.1 outlines an optimisation cycle for the development of an NP based antifoulant system and describes the parameters used in this thesis to address the issue. This thesis provides a unifying framework, by using a multidisciplinary approach, for the development of a natural product based antifoulant.

8.1 Conclusions

This project is a multidisciplinary one encompassing, engineering, biology and chemistry. Over 100 papers were reviewed to assess past, present and future trends within the discipline of antifouling research. From this review the main challenge facing antifouling technology was determined to be the present and future legislative restrictions. This requires not only an increased environmental awareness but also innovative approaches that attempt to address this through their engineering design. Many approaches were considered but the chosen inventive method used was biomimetics. Biomimetics utilises a marine biology basis for the engineering of a functional, environmentally acceptable solution to prevent marine biofouling on large ship hulls. In this project it was the chemical defence mechanisms or natural products of marine organisms that were the conceptual basis for the development of an environmentally acceptable antifouling system.

The approaches undertaken are unique and represent a new strategy for safe antifouling coating development using natural products.

An extensive review of the natural product literature has shown that there is a research gap in the use of marine extracts and their delivery in a paint system. Few reports have characterised their incorporation into a paint system. For those natural products that have been incorporated, limited engineering tests have been made to assess their performance or to investigate any disturbances to the paint system. Conversely the complexity of the biofouling community and the possible interactive effects with the surface coating is often underestimated in the coating literature. The novelty of this project lies in applying a biomimetics approach, sourcing a potential marine organism, extracting, incorporating and finally characterising natural products in a coating system using surface engineering and biological techniques. Surface engineering techniques and analysis, as applied in this project, investigated two main aspects of the antifouling system the (i) substrate/coating interface and (ii) coating/environment interface (Fig. 1.2) as well as the coating functionality.

The natural product used throughout this project was from *Chondrus crispus* (Rhodophycae) which was sourced locally as well as purchased dried from a commercial source to help assess the potential of a less exotic source. The antifouling efficacies of these two differently sourced algae were tested, the 'commercial off-the-shelf' dried algae (extract A) and coastal algae from Calshot UK (extract B) (Chapter 4). Bioassays of the two ethanol extracts indicated good antifouling activity for extract A at concentrations of 10 $\mu g\ mL^{-1}$ for 6 out of ten bacterial and microalgae species. Due to its potential, extract A was directly compared to a booster biocide (Chlorothalonil) and both were incorporated into the proprietary control depletion polymer using a high shear mixer at 1 % wet w/w (Chapter 5).

The thesis examined the effect that a natural product antifoulant had on both coating quality and integrity as well as performance. Surface profilometry, optical microscopy and electrochemistry were used initially to determine the optimal substrate condition and successful keying of the coating to the steel substrate (Chapter 5). No obvious difference in the control blank coating and the natural product incorporated coating were noted through SEM and optical microscope transverse sections and planar views. The substrate/coating interface was further characterised regarding its performance by using a

variety of electrochemical techniques (Chapter 6). Thin coatings (12 μm dft) to accelerate defects in the coating were deposited for characterisation through ZRA electrochemistry. Although this technique was a beneficial learning tool to understand coupled and decoupled potentials with corrosion rates, the coatings were too thin and the defects quickly (500 minutes) controlled the electrochemistry at the coating/substrate interface. The three coatings (blank, algal extract and biocide) coupled OCP dropped to -650 mV *vs.* Ag/AgCl within 16 hrs which is nearing the OCP of the underlying steel at -700 to -750 mV *vs.* Ag/AgCl.

Thicker coatings (30 μm dft) were successfully investigated using electrochemical impedance spectroscopy and an appropriate equivalent circuit was determined to model the physicochemical parameters dominating the coating. The use of EIS qualitatively described a degrading coating and highlighted the rate of water ingress, with and without natural products in the coating. After 4 days EIS measurements of the algal extract coating showed an increase in the water uptake of the coating compared to the blank coating.

Using an undercoat of primer beneath the experimental topcoat (80 μm dft total) the OCP was measured over a longer time scale of 60 days in fresh seawater. As with EIS this technique was proven to be sensitive enough to detect differences. Experiments (OCP and ZRA in fresh seawater) proved that the incorporation of an antifouling component (natural product or biocide) causes the system to be more electronegative by approximately 50 mV *vs.* Ag/AgCl than the control (blank topcoat) within the first 5 days. However, the algal extract coating after 30 days shown by the OCPs in seawater had a higher OCP than both the blank base and biocide coatings. The algal extract coating also showed a higher OCP than the biocide in the ZRA experiments when coupled with a similar coating and with bare steel. Results for OCP trials in seawater of 40 μm dft on primer over 60 days in the laboratory and 105 days in the field showed that the algal NP coating functions as a barrier system in a similar manner to the blank coating with marginally more positive OCPs (+30 mV *vs.* Ag/AgCl). This indicates that the coating protection of the steel substrate has not been disturbed by the incorporation of the algal NP. OCP steady state was achieved for all experimental coatings in 3-5 days, showing a time dependence on electrolyte ingress.

NP incorporation was not seen to affect the rate that the water reached the steel when compared with the blank topcoat as measured by OCP but it did indicate that it affected the water volume fraction in the coating as measured by EIS. This increased water volume

uptake was attributed to the solubility of the natural product and its possible increased leaching rate from the matrix. With the antifoulant leaving the coating there would be increased voids for the water to replace. That is to say that the NP could have leached out independently from the controlled depletion front. This coupling of OCP and EIS techniques has proven that it is a sensitive tool to analyse the experimental antifouling coating differences, it also may help to infer challenges faced with the controlled delivery of the natural product. This is further backed up by the limited 10 week activity.

Microbiological assessment of the surface (section 7.1) using EDIC microscopy allowed a quantitative analysis of biofilm viability and formation on the NP-coating surface. This double nucleic acid staining technique was extremely useful coupled with fluorescence microscopy, as a rapid means to estimate *in situ* biofilm coverage and bacterial viability. Both the algal coating and base rosin had final live bacterial coverage's of 40 % mm^{-2}, however, the final biofilm thickness after 4 weeks immersion on the algal coating (4 ± 1.1 μm) was half that of the base rosin (9.4 ± 4.3 μm). This technique overcame the issues of the more conventional plate counting techniques requiring microbiological facilities for incubation. The coating pigment did not autoflouresce and so the technique has potential as a bacterial bioassay technique directly for the surface of antifouling coatings. The detection of bacterial biofilm was verified with FTIR studies.

An immersion trial (section 7.2) was conducted over the peak fouling season (April to August 2006). After 10 weeks the natural product antifouling coating was seen to outperform all other coatings, showing limited fouling. However, after 13 weeks the antifouling extract was ineffective and heavy biofouling had covered the working surface of the algal extract coating. This possibly indicates that the antifoulant leached too quickly (as suggested earlier from the electrochemical measurements), or that release was hindered through the paint film, or that the thickness used was not great enough. Further field trials (summer 2007) tested the performance for coatings with increased dft (50, 100, 150 μm) and increased NP antifoulant concentrations (1, 5, 10 % wet w/w). Due to fish scarring of the surfaces the variable thickness data set was lost. To remedy this, a further trial was caged. The cage established a niche for sea-squirts and lowered the overall biofouling assemblage rendering all the coatings foul free including the negative control surfaces.

Over the entire 4 months of that first sea trial the biocide loaded paint system was comparable to the NP based coating, indicating great promise for the NP. However, field

tests with increased concentration of natural product and an increase in the coating dry film thickness have both shown not to increase the working life of the antifouling coatings system. Further optimisation is required and the affect of aged paints investigated. Cross-sections of the coatings and surface biofouling from the exposure trial were analysed and initial SEM-EDX studies showed leached layers. The SEM-EDX was used to explain degradation through mechanisms such as the cohesive failure by crack propagation in the 10 % w/w algal natural product topcoat.

The approach used to span a wide range of disciplines and incorporate multiple techniques which needed pulling together to tackle this issue has been proven to be successful. Although the antifoulant and its deployment in a control depletion polymer was unrefined, the approach brought together a unique natural product based antifoulant system. Biological and surface engineering procedures were adapted and developed through this project. The issues and benefits of each technique have been discussed and provide a useful platform for future investigations into complex coating-NP additive interactions. In this thesis the crude algal NP in a controlled depletion polymer was investigated. One complete cycle of Figure 8.1 was completed towards the development of an NP based antifouling system through the sourcing, extraction, incorporation, and characterisation both electrochemically of the coating integrity and the antifouling performance of the NP in isolation in bioassays and as an agent within coatings in field trials.

This work demonstrates that the direct incorporation of the biomaterial into a coating matrix is a useful testing platform of compounds. In particular, the use of a controlled depletion polymer was a useful vehicle for natural products as an experimental platform. Testing both the electrochemical and the antifouling performance provides an effective means for better understanding novel antifouling coatings and to better inform further development of natural product based coatings. Through innovation and practical problem solving it is the authors opinion that natural products have been shown here to have potential in coated systems and future use on ship hulls. From surface growth bioassays to substrate corrosion and from seaweed to ship hulls this thesis has successfully bridged a range of disciplines and techniques to further this exciting new research area of natural products as antifoulants.

8.2 Further work

Electrochemical techniques provided knowledge on the physical and chemical phenomena occurring at the interfaces between the steel and coating as well as the coating and environment. The limitations of accelerating testing through coating thickness variation were noted in Chapter 6. Very thin (< 15 μm) coatings resulted in the electrochemistry being defect dominated within 24 h. Too thick a coating (> 80 μm) and the resistances were too high to be measured using electrochemical impedance techniques in the first 24 h. To assess the incorporated compounds in the coating dry film thickness it is necessary to insure that the electrochemical measurements are related to an intact coating. Both the biofilm and field trial functionality over time is further correlated by the electrochemical experiments and in particular the EIS data which indicates that increased water uptake by the NP-coating occurs. Increased water uptake would affect the leaching rate and concentration of antifoulant at the coating surface. The rate of hydration is linked to the erosion mode and the release of a biocide from an antifouling coating is 'greatly dependant on the macromolecular matrix and the erosion mode' [8.1]. This could explain the lack of algal NP antifouling functionality after 6 weeks in the field. Further leaching tests could verify this.

Characterisation of the natural product using bioassays was an important and beneficial test. It provided a clear indication of the extracts antifouling efficacy against a range of key fouling micro-organisms and macro algae. The chemistry of the natural product extract investigated in this project was very complex as it was a whole cell ethanol extract. It would be useful to assess natural products where the chemical structure was better controlled, in this manner the binder and subsequent electrochemical measurements could be more accurately modelled and possibly used to predict product lifetimes more effectively. It is important with the antifoulant natural product that the economics of extraction/synthesis is taken into consideration. For this reason the whole cell extraction was a good starting point as it was simple and was made on dry preserved algae which would allow for a longer shelf life and sourced from algae which is already an industrially aquacultured species. It also allowed for the testing of a natural ratio of metabolites i.e. a 'cocktail' approach as highlighted in Chapter 4. It is suggested here that this could be an effective means of overcoming the challenge of finding natural products with broad spectrum activity.

Figure 8.2 highlights the technical aspects of furthering this development. In simple terms the antifouling system is composed of a binder and a biocide. Regarding the binder, electrochemical techniques informed this project about permittivity but the equally important aspect of depletion needs further analysis e.g. leaching rate experiments. The use of a crude natural product (biocide) was shown to be a good antifoulant in isolation, and initial GC-MS looked at its composition, it is an important future work aspect to consider what its active fractions are. The free association incorporation method of the NP in the CDP used in this project could be furthered by considering control mechanisms. Finally a continuation of the bioassays and field trails should be maintained.

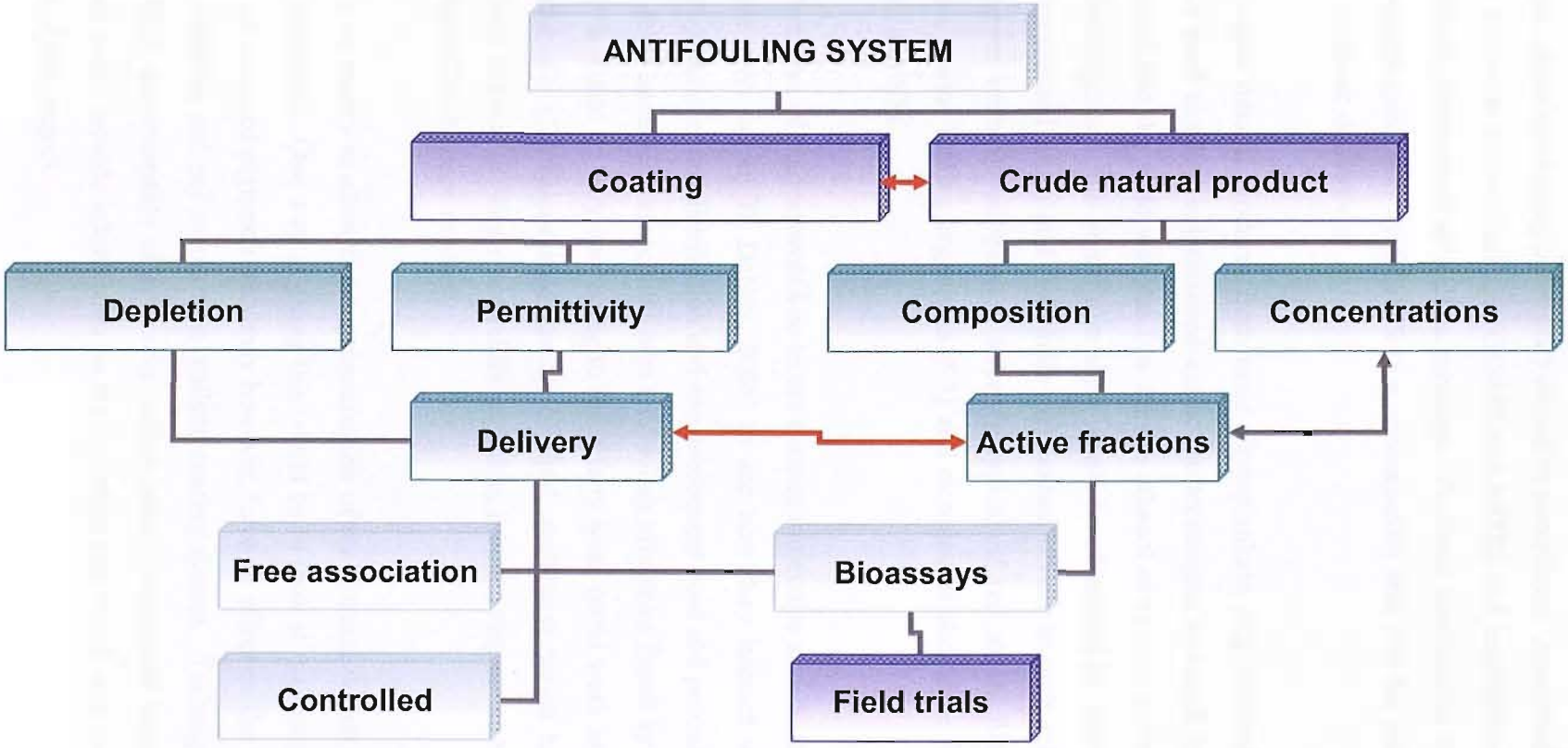

Figure 8.2 Outline of the project considering further work goals

8.2.1 Natural products

Further studies into the local marine algae chemical defence mechanisms like *Chondrus crispus* (fresh and locally harvested) should be completed. Analytical chemistry should be used to isolate active fractions (GC-MS and NMR) and test their antifouling activity as individual components as well as mixtures. Purchase commercial NPs as indicated from the spectra generated by GC-MS (e.g. eicosanoids) and test for antifouling affect along with synthetic derivatives.

Investigate natural products from toxic phytoplankton (e.g *Alexandrium sp*). First one would need to adapt volumisation extraction techniques as initial tests on phytoplankton indicated that the yield was too low for the ethanol extraction technique. Further whole cell investigations into unicellular algae would be of interest as they are not differentiated into specialised tissue and the whole metabolism occurs in each cell [8.2]. Specific NP categories such as halogenated terpenes typical of red algae, function as antifoulants against marine fouling organisms [8.3] and eicosanoids should be further investigated as antifoulant NPs.

Another area of interest would be to use dummy molecules such as known fatty acid chain lengths (pers comm R. DeNys, 2006) to see how they interact with coating systems. Investigate their size distribution and any subsequent void and porosity formation. Certain fatty acids have been associated with antifouling affects as found by Gaquerel et al., 2007 [8.4]. It would be very interesting to see if fatty acids could work as specific antifoulants, for example C20 (eicosanoid family of lipid mediators) which has been noted to be involved in the regulation of cell differentiation, immune responses, homeostasis as well as C18 and C16 (defence related).

Stains or tracers to allow for the visualisation of the extracts within the coating system is also necessary. One way of doing this would be to look at the extracts in binder systems with no coloured pigments, this may however, have an affect on the total pigment volume concentration and not represent a realistic coating system. Techniques such as the SEM and EDX are incapable of detecting carbon based compounds accurately. Locating the extract could provide information on the depletion rate which was unattainable in the time scale of this project.

8.2.2 Delivery mechanism

Natural products are easily degraded in the marine environment and if used in a coating system must be active at the working surface for the entirety of the application lifespan a challenge that was highlighted in this thesis. A key design goal of this technology is to control the delivery of the natural product. To do this one method could be to incorporate unique bio-nanocomposite materials to produce advanced surface coatings that immobilise and control the delivery of natural product antifoulants. Few authors (see Table 2.3) have tackled the issue of incorporating natural products into a delivery system.

The use of clay minerals as monolithic drug delivery devices has received attention in forming biocompatible polymer nanocomposite systems [8.5]. The use of halloysite for use as a drug delivery system was successfully shown by Levis and Deasy (2002) [8.6]. The mineral works as a host lattice to which the compound to be released can be intercalated or tethered [8.5]. Layered Double Hydroxide (LDH) materials are structures that are made up of metal hydroxide layers with an alternating interlayer which can be manipulated [www.ambafrance-dk.org]. The layers of the clay can form nano-clay/polymer composites in three different ways as shown in the schematic Figure 8.3.

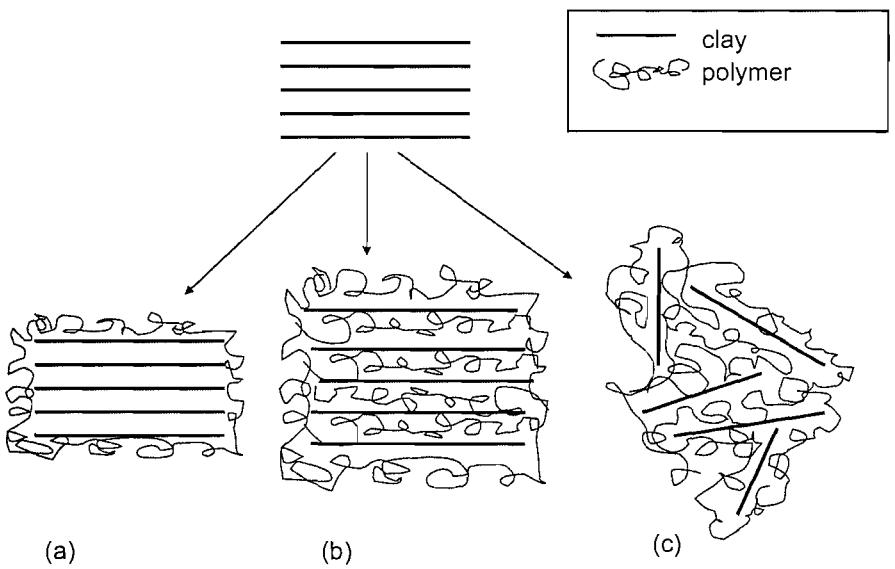

Figure 8.3 Dispersion of clays in polymer, after [8.7], (a) clay dispersed in clumps, (b) retention of layered shape but allows some polymer between layers and (c) fully exfoliated into individual layers through out polymer

Charged and neutral molecules can be incorporated into the interlayer of the clay [8.7]. The aim of using the clay would be to see if the tethering of a natural product to the surface or between the layers of the clay lattice structure would be possible. The next step would be to incorporate this into the polymer coating and characterise its dispersion and release

rate. An outline of the experimental steps to evaluate this delivery mechanism was determined with C. Greenwell (pers com 2006) as a potential collaborative effort:

1) Preparation of LDH-isolate hybrid system (2 weeks)
2) Characterisation of LDH-isolate system (2 weeks)
3) Computer simulation of structure of LDH-isolate (optional, to be done in conjunction with other steps).
4) Testing of efficacy of LDH-isolate vs. isolate in bioassays (5 months)

8.2.3 Leaching rates

Using detection equipment such as electrophoresis or HP-LC, leaching rates of the natural product should be measured for both the paint vehicle investigated in this thesis as well as new delivery mechanisms. As well as the leaching rate the environmental fate and risk of both crude and isolated extracts should be investigated. The physical and chemical properties of the NP compounds should be further investigated such as the light and seawater degradation. There is a need to further understand the environmental fate of the marine antifoulants through such pathways as UV degradation, bioaccumulation, biodegradation, hydrolysis speciation, and sorption to particulate matter. Other processes include sediment settling, partitioning and finally burial. This would be to increase control over the system components as well as to begin the important process of preparing for the registration of an NP as an antifoulant and prevent a repeat of the issues associated with the ban on TBT.

An electrochemical H-cell configuration could be used for the analysis of coating porosity and leach rate. The coating film can be created by using the drawbar to apply the wet paint over a glass or plastic surface from which the dry film can later be peeled. Platinum meshes are to be used as the anode and cathode as they are low cost and inert. A voltage is passed between the anode and the cathode and the impedance of the system by the presence of the coating film can be determined. Cyclic voltamograms can be used to detect species that diffuse through the membrane. Further tests beyond the raft trials and electrochemical techniques would be useful to prove that antifouling activity of the natural product is occurring even when immobilised in the coating matrix.

8.3 References

[8.1] F. Fay, I. Linossier, V. Langlois, and K. Vallée –Rehel, *Biodegradable poly(ester-anhydride) for new antifouling coating*, Biomacromolecules 8 (2007) 1751-1758.

[8.2] G. Jacobi, Enzyme Systems, Physiology and Biochemistry of Algae (Ed) R.A. Lewin, Academic Press (1962) p.126.

[8.3] P. Bhadbury and P.C. Wright, *Exploitation of marine algae: biogenic compounds for potential antifouling applications*, Planta 219 (2004) 561-578.

[8.4] E. Gaquerel, C. Hervé, C. Labrière, C. Boyen, P. Potin, J-P. Salaün, *Evidence for oxylipin synthesis and induction of a new polyunsaturated fatty acid hydroxylase activity in Chondrus crispus in response to methyljasmonate*, Biochimica et Biophysica Acta 1771 (2007) 565-575.

[8.5] R. Toth, M. Ferrone, S. Miertus, E. Chiellini, M. Fermeglia and S. Pricl, *Structure and energetics of biocompatible polymer systems: a molecular dynamics study*, Biomacromolecules, 7 (2006) 1714 - .

[8.6] S.R. Levis and P.B. Deasy, *Characterisation of halloysite for use as a microtubular drug delivery system*, Int. J. Pharm., 243 (2002) 125-134.

[8.7] C. Greenwell (2005) Source http://www.exclaim.org.uk/CP_Group.htm accessed [04-10-06].

Appendix I

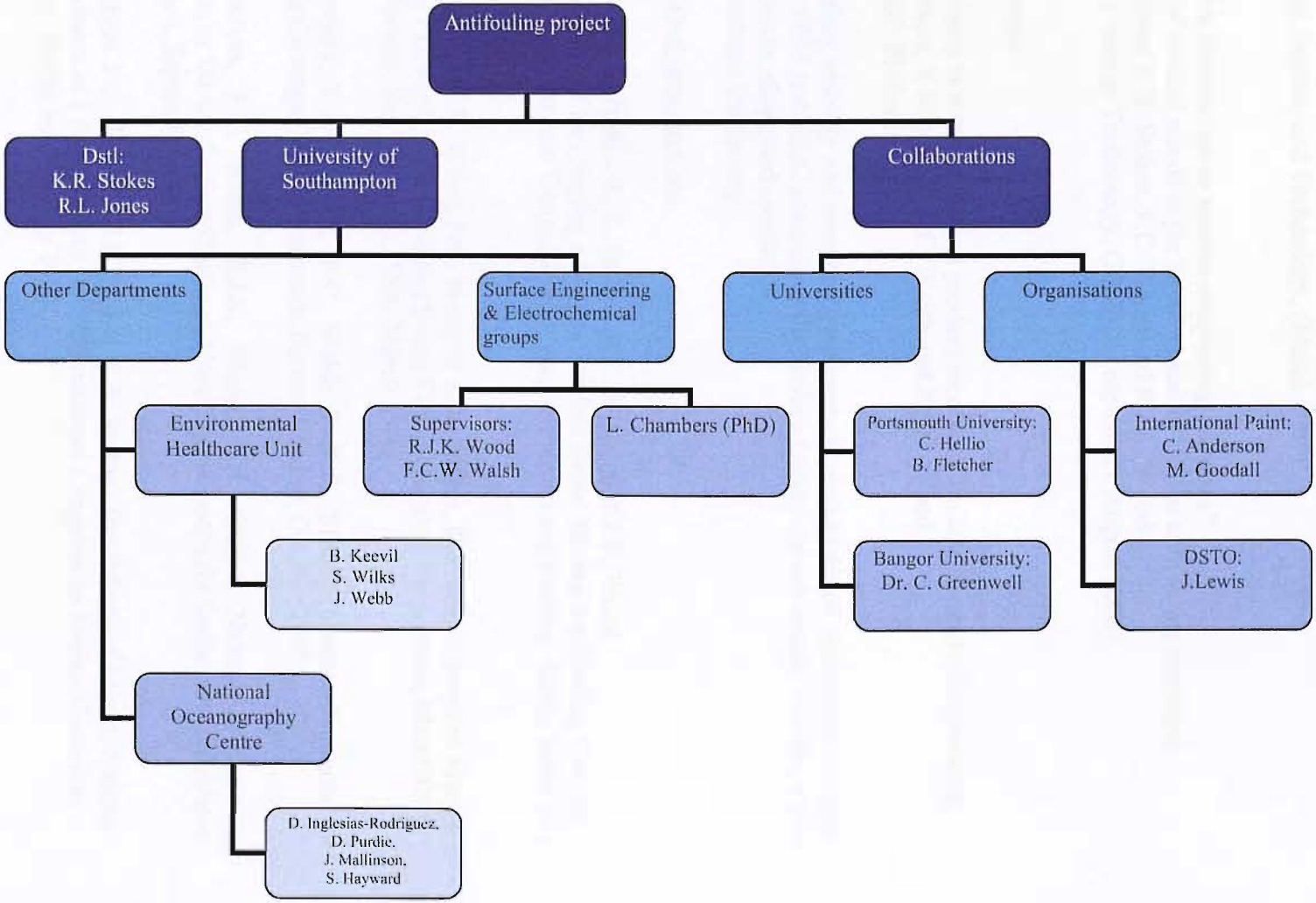
Antifouling project
Dstl:
K.R. Stokes
R.L. Jones
University of Southampton
Collaborations
Other Departments
Surface Engineering & Electrochemical groups
Universities
Organisations
Environmental Healthcare Unit
Supervisors:
R.J.K. Wood
F.C.W. Walsh
L. Chambers (PhD)
Portsmouth University:
C. Hellio
B. Fletcher
International Paint:
C. Anderson
M. Goodall
B. Keevil
S. Wilks
J. Webb
Bangor University:
Dr. C. Greenwell
DSTO:
J.Lewis
National Oceanography Centre
D. Inglesias-Rodriguez,
D. Purdie,
J. Mallinson,
S. Hayward

Appendix II

Conference and journal papers:

(1) ***"Biomimetic approach to the design of the marine antifouling coatings"***

L.D. Chambers, F.C. Walsh, R.J.K. Wood, and K.R. Stokes
World Maritime Technology Conference, ICMES Proceedings, The Institute of Marine Engineering, Science and Technology, (March 2006)
Published

(2) ***"Modern approaches to marine antifouling coatings"***
(A review of modern trends in the development of marine antifouling coatings)
L.D. Chambers, K.R. Stokes, F.C. Walsh and R.J.K. Wood
Surface & Coatings Technology, (2006), Accepted (21 August 2006)
Published

Proposed papers:

(3) 'Techniques to measure natural product incorporation into an antifouling coating'
L.D. Chambers, K.R. Stokes, F.C. Walsh and R.J.K. Wood
Draft journal: Biofouling

(4) 'Biofouling viability and morphology on natural product based antifouling coatings'
(Confocal, SEM and EDIC analysis of the surface features of the aquatic biofilm, a time series in growth, shape and species)
Proposed journal: Biofouling

Poster and Oral presentations:

L.D. Chambers, C. Hellio, K. R. Stokes, F.C. Walsh, & R.J.K. Wood
Practical Aspects of Developing a Natural Product Based Marine Antifouling Coating System, 14th International Congress on Marine Corrosion and Fouling, Kobe, Japan July 2008

L.D. Chambers, R.J.K. Wood, F.C. Walsh & K.R. Stokes, Biomimetic Inspired Marine Antifouling Coating System Assessed Using Electrochemical Techniques, Materials Research Society, San Francisco, USA, March 2008

L.D. Chambers, R.J.K. Wood, F.C. Walsh & K.R. Stokes, Natural Products for Antifouling Coatings, Marine Corrosion Forum, London, October 2007.

L.D. Chambers, F.C. Walsh, R.J.K. Wood, K.R. Stokes, Natural Products as Antifoulants in Marine Surface Coatings, Novel Applications for Surface Modifications, Southampton, September 2007.

L.D. Chambers, F.C. Walsh, R.J.K. Wood, K.R. Stokes, The Effects of Marine Natural Product Extracts in a Paint System, 13th International Congress on Marine Corrosion and Fouling, Rio de Janeiro, July 2006

Appendix III

Dock Fouling Species adapted from Collins & Mallison

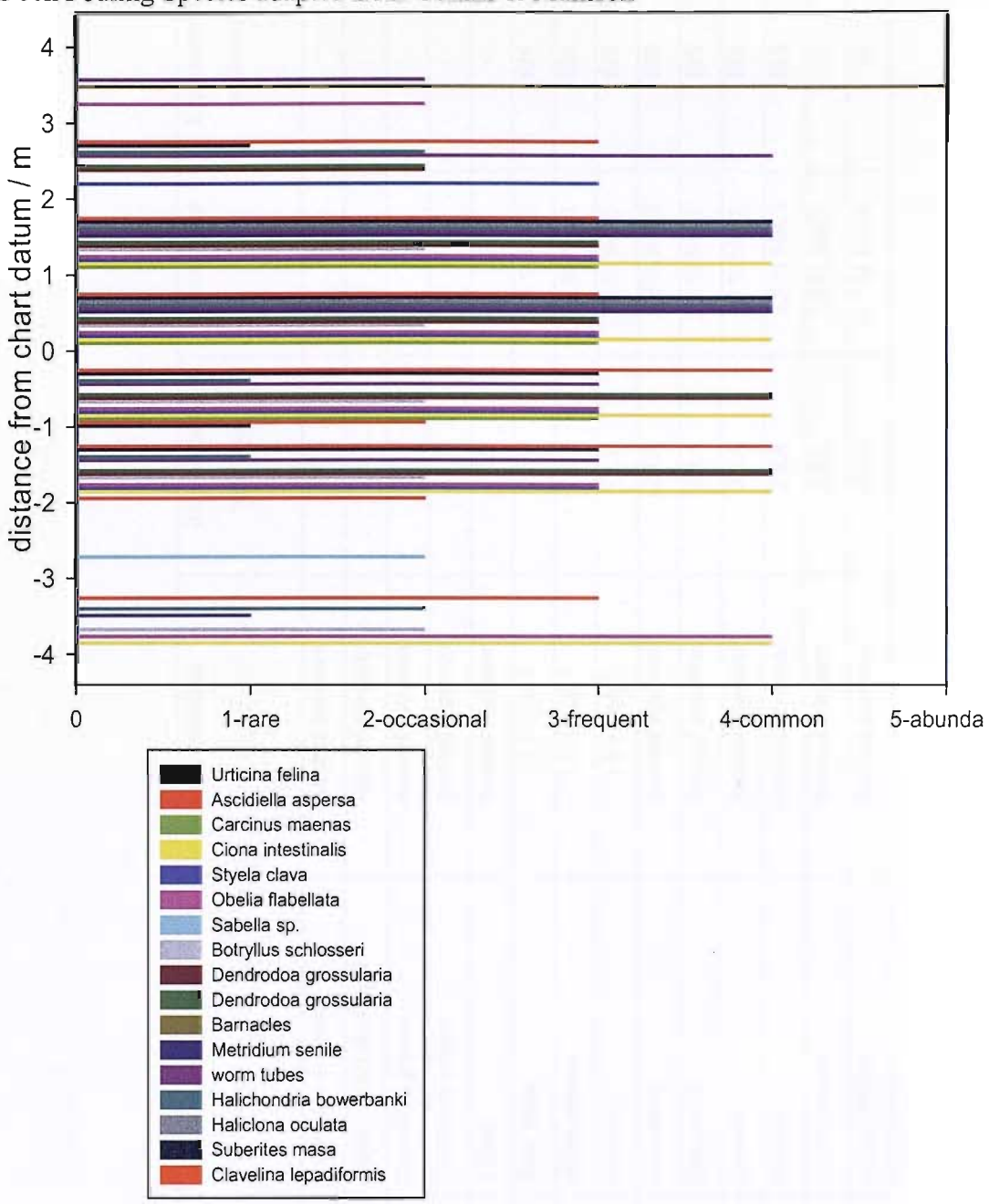

K.J. Collins and J.J. Mallinson, Marine flora and fauna of Southampton docks, Report to the Nature Conservancy Council February p. 26 (1987).

Appendix IV

Sample no.	Mean coating dft µm (n=10)	Standard deviation µm (n=10)	Coating type	Environment	Experimental technique	Environment	Experimental technique
1	78.0	10.1	Base rosin & primer	Aerated seawater	OCP	-	-
2	85.2	12.3	Algae extract & primer	Aerated seawater	OCP	-	-
3	72.8	17.5	Biocide & primer	Aerated seawater	OCP	-	-
4	64.4	8.27	Control & primer	Aerated seawater	OCP	-	-
5	37	11.4	Primer	Aerated seawater	OCP	-	-
6	31	2.13	Base rosin	3.5 % NaCl	OCP	3.5 % NaCl	EIS
7	30.4	3.18	Algae extract	3.5 % NaCl	OCP	3.5 % NaCl	EIS
8	29.1	3.74	Biocide	3.5 % NaCl	OCP	3.5 % NaCl	EIS
9	10.8	1.62	Base rosin	Aerated seawater	ZRA	3.5 % NaCl	EIS
10	9.4	1.25	Base rosin	Aerated seawater	ZRA	3.5 % NaCl	EIS
11	10.9	2.64	Biocide	Aerated seawater	ZRA	3.5 % NaCl	EIS
12	8.2	1.54	Biocide	Aerated seawater	ZRA	3.5 % NaCl	EIS
13	18	2.6	Algae extract	Aerated seawater	ZRA	3.5 % NaCl	EIS
14	5.9	1.23	Algae extract	Aerated seawater	ZRA	3.5 % NaCl	EIS

15	0	0	Raw steel	Aerated seawater	ZRA	3.5 % NaCl	EIS
16	0	0	Raw steel	Aerated seawater	ZRA	3.5 % NaCl	EIS
17	0	0	Raw steel	Aerated seawater	ZRA	3.5 % NaCl	EIS
18	12.7	2.86	Base rosin	Aerated seawater	ZRA	3.5 % NaCl	EIS
19	12.8	1.01	Biocide	Aerated seawater	ZRA	3.5 % NaCl	EIS
20	13.5	2.81	Algae extract	Aerated seawater	ZRA	3.5 % NaCl	EIS

Table 4.2 Samples used in electrochemistry

GLOSSARY

Biological term	Definition
Allelochemicals:	Chemicals produced by a species to inhibit the growth of a different species.
Byssus:	Tuft of silky filaments used by mussels to adhere to objects.
EPS	Extracellular polymeric substances
Flagella:	Projecting propulsive organelles.
Furanone:	Five-membered ring lactone natural product with the ability to disrupt the acylated homoserine lactone regulatory systems in organisms.
Moiety	The specific part of a molecule i.e. the functional group
Photic:	Layers of the ocean reached by sufficient sunlight to allow plant growth.
Quebracho:	Tanning substance from a family of hardwood evergreen trees.
Spicules:	Spines characteristic of the surface of sea-urchins
Antifeedant	Chemicals used to deter feeding
Phylum	Taxonomic grouping of organisms with the same body plan